ANALYTICAL STUDIES OF BODY WAVE PROPAGATION AND ATTENUATION

by

Ignacio Sánchez-Salinero, José M. Roesset
and Kenneth H. Stokoe, II

a report on research
sponsored by
United States Air Force
Office of Scientific Research
Bolling Air Force Base

UNCLASSIFIED

SECURITY CLASSIFICATION OF THIS PAGE

REPORT DOCUMENTATION PAGE

AD-A179 480

1a. REPORT SECURITY CLASSIFICATION: UNCLASSIFIED	1b. RESTRICTIVE MARKINGS
2a. SECURITY CLASSIFICATION AUTHORITY	3. DISTRIBUTION/AVAILABILITY OF REPORT: Approved for Public Release; Distribution Unlimited.
2b. DECLASSIFICATION/DOWNGRADING SCHEDULE	
4. PERFORMING ORGANIZATION REPORT NUMBER(S)	5. MONITORING ORGANIZATION REPORT NUMBER(S): AFOSR-TR- 87-0442
6a. NAME OF PERFORMING ORGANIZATION: UNIVERSITY OF TEXAS AT AUSTIN; 6b. OFFICE SYMBOL (If applicable)	7a. NAME OF MONITORING ORGANIZATION: AFOSR/NA
6c. ADDRESS (City, State and ZIP Code): DEPARTMENT OF CIVIL ENGINEERING AUSTIN, TX 78712	7b. ADDRESS (City, State and ZIP Code): Bldg 410 Bolling AFB, DC 2033-6448
8a. NAME OF FUNDING/SPONSORING ORGANIZATION: AIR FORCE OFFICE OF SCIENTIFIC RESEARCH; 8b. OFFICE SYMBOL (If applicable): AFOSR/NA	9. PROCUREMENT INSTRUMENT IDENTIFICATION NUMBER: AFOSR-83-0062
8c. ADDRESS (City, State and ZIP Code): Bldg 410 BOLLING AFB, DC 20332-6448	10. SOURCE OF FUNDING NOS.

PROGRAM ELEMENT NO.	PROJECT NO.	TASK NO.	WORK UNIT NO.
61102F	2307	C1	

11. TITLE (Include Security Classification): ANALYTICAL STUDIES OF BODY WAVE PROPAGATION AND ATTENUATION

12. PERSONAL AUTHOR(S): IGNACIO SANCHEZ-SALINERO, JOSE M. ROESSET AND KENNETH H. STOKOE, II

13a. TYPE OF REPORT	13b. TIME COVERED	14. DATE OF REPORT (Yr., Mo., Day)	15. PAGE COUNT
TECHNICAL	FROM 2/1/83 TO 6/15/86	SEPTEMBER, 1986	296

16. SUPPLEMENTARY NOTATION

17. COSATI CODES		
FIELD	GROUP	SUB. GR.

18. SUBJECT TERMS (Continue on reverse if necessary and identify by block number): ANALYTICAL STUDY, ATTENUATION, BODY WAVES, COMPRESSION WAVES CROSS CORRELATION, DAMPED WAVE VELOCITY, DISPERSION, FAR-FIELD WAVES, FREQUENCY-DOMAIN ANALYSIS, GREEN'S FUNCTIONS, (cont.)

19. ABSTRACT (Continue on reverse if necessary and identify by block number)

In situ seismic methods are becoming widely used as a means of nondestructively evaluating the elastic properties of geotechnical systems. The crosshole and downhole seismic methods are most often used. Elastic constants are calculated from the records of body waves (longitudinal and transverse) traveling through the media. Measurements are made by generating a seismic disturbance at one point and measuring the time required for the disturbance to travel to one or more seismic receivers. Several simplifying assumptions are made in the traditional analysis of seismic measurements for engineering purposes. These assumptions include assuming plane wave propagation, measurement of only far-field waves, and independence of the measurements on the source-receiver configuration and on the amount of material damping. An analytical study of the effects and the validity of the different assumptions is presented. A review of existing techniques to evaluate seismic data based on time domain analysis is performed, and new techniques based on correlation and spectral analyses are presented. Emphasis is placed on determination of wave velocities and

(continued on reverse)

20. DISTRIBUTION/AVAILABILITY OF ABSTRACT	21. ABSTRACT SECURITY CLASSIFICATION
UNCLASSIFIED/UNLIMITED ☒ SAME AS RPT. ☐ DTIC USERS ☐	UNCLASSIFIED

22a. NAME OF RESPONSIBLE INDIVIDUAL	22b. TELEPHONE NUMBER (Include Area Code)	22c. OFFICE SYMBOL
DR. SPENCER T. WU	(202) 767-4935	AFOSR/NA

DD FORM 1473, 83 APR EDITION OF 1 JAN 73 IS OBSOLETE.

SECURITY CLASSIFICATION OF THIS PAGE

UNCLASSIFIED

18. (cont.) HYSTERETIC DAMPING, LINE SOURCES, LONGITUDINAL MOTION, MATERIAL DAMPING, NEAR-FIELD EFFECTS, NEAR-FIELD WAVES, PLANE WAVE PROPAGATION, POINT SOURCES, SHEAR WAVES, SEISMIC WAVES, SPECTRAL ANALYSIS, SPHERICAL WAVE FRONT, SOURCE-RECEIVER CONFIGURATION, TIME-DOMAIN ANALYSIS, TRANSVERSE MOTION, VELOCITY, WHOLE SPACE

19. (cont.)
attenuation parameters from which elastic properties and material damping can be calculated.

It is found that, for the range of distances and frequencies typically used in engineering applications, body wave fronts generated by point sources cannot be considered plane and that near-field effects associated with spherical wave fronts can be very important. The near-field effects are caused by coupling between waves which exhibit the same particle motion but which propagate at different velocities and attenuate at different rates. To minimize the detrimental effects of near-field waves in those methods based on spectral analysis techniques, it is recommended that, in the field setup, the ratio of distances from the source to the second and first receivers be of the order of two or greater. For typical setups in which the distance from the source to the first receiver is equal to the distance between the receivers, near-field effects can be neglected if measurements are made at frequencies such that the distance from the source to the closest receiver is at least one wavelength. Additional recommendations regarding body wave techniques are presented.

ANALYTICAL STUDIES OF BODY WAVE PROPAGATION AND ATTENUATION

by

Ignacio Sánchez-Salinero, José M. Roesset and Kenneth H. Stokoe, II

a report on research
sponsored by
United States Air Force
Office of Scientific Research
Bolling Air Force Base

September, 1986

Geotechnical Engineering Report GR86-15
Geotechnical Engineering Center
Civil Engineering Department
The University of Texas at Austin

ACKNOWLEDGEMENTS

The authors wish to express their gratitude to:

- Linda M. Iverson for her assistance in typing this report, and to
- The United States Air Force Office of Scientific Research (AFOSR), Bolling Air Force Base, Washington, D.C., for supporting this research under grant AFOSR 83-0062, Major John J. Allen was the initial project manager, after which Lt. Col. Dale Hokanson became the project manager.

ABSTRACT

In situ seismic methods are becoming widely used as a means of nondestructively evaluating the elastic properties of geotechnical systems. The crosshole and downhole seismic methods are most often used. The elastic constants are calculated from the records of body waves (longitudinal and transverse waves) traveling through the media. Measurements are made by generating a seismic disturbance at one point and measuring the time required for the disturbance to travel to one or more seismic receivers. Several simplifying assumptions are made in the traditional analysis of seismic measurements for engineering purposes. These assumptions include assuming plane wave propagation, measurement of only far-field waves, and independence of the measurements on the source-receiver configuration and on the amount of material damping. An analytical study of the effects and the validity of the different assumptions is presented. A review of existing techniques to evaluate seismic data based on time domain analysis is performed, and new techniques based on correlation and spectral analyses are presented. Emphasis is placed on determination of wave velocities and attenuation parameters from which elastic properties and material damping can be calculated.

It is found that, for the range of distances and frequencies typically used in engineering applications, body wave fronts generated by point sources cannot be considered plane, and that near-field effects associated with spherical wave fronts can be very important. The near-field effects are caused by coupling between waves which exhibit the same particle motion but which propagate at different velocities and attenuate at different rates. To minimize the detrimental effects of near-field waves in those methods based on spectral analysis techniques, it is recommended that, in the field setup, the ratio of distances from the source to the second and first receivers be of the order of two or greater. For typical setups in which the distance from the source to the first receiver is equal to the distance between the receivers, near-field effects can be neglected if measurements are made at frequencies such that the distance from the source to the closest receiver is at least one wavelength. Additional recommendations regarding body wave techniques are presented.

TABLE OF CONTENTS

Page

ACKNOWLEDGEMENTS....iii

ABSTRACT....iv

LIST OF FIGURES....vii

LIST OF SYMBOLS....xxi

CHAPTER ONE
INTRODUCTION....1
1.1 Seismic methods in civil engineering....1
1.1.1 Uses and benefits of seismic methods....2
1.2 Seismic methods based on body waves....6
1.3 Organization and objectives of this report....8

CHAPTER TWO
ANALYTICAL FORMULATION FOR BODY WAVES IN A FULL SPACE....13
2.1 Introduction....13
2.2 Theoretical background....14
2.2.1 Two-dimensional antiplane motion....17
2.2.2 Two-dimensional in-plane motions....19
2.2.3 Three-dimensional motions....20
2.3 Time and frequency domain parameters....22
2.4 Summary....31

CHAPTER THREE
CHARACTERISTICS OF BODY WAVE SIGNATURES....33
3.1 Introduction....33
3.2 Analysis of time records....33
3.2.1 Medium with no material damping....34
3.2.2 Medium with material damping....43
3.2.3 Effect of Poisson's ratio....44
3.3 Near-field effects....50
3.4 Polarity reversals upon reversing the impulse....52
3.5 Wave amplitude decay....57
3.6 Summary....76

CHAPTER FOUR
TECHNIQUES OF EVALUATING BODY WAVE VELOCITIES....79
4.1 Introduction....79
4.2 Wave velocities from direct times of arrival....79
4.3 Wave velocities from interval times of arrival....80
4.4 Wave velocities from cross-correlation records....92
4.4.1 Cross-correlation function....92
4.4.2 Analysis of cross-correlation records....94
4.5 Wave velocities using spectral analysis techniques....106
4.5.1 Theoretical background....106
4.5.2 Dispersion curves from cross spectrum function....110
4.5.3 Dispersion curves from transfer functions....129
4.6 Summary....137

Page

CHAPTER FIVE
EVALUATION OF BODY WAVE ATTENUATION.....141
5.1 Introduction.....141
5.2 Theoretical background.....141
5.3 Material damping calculated from seismic records.....144
5.4 Curves of apparent damping ratio.....149
5.5 Summary.....160

CHAPTER SIX
SUMMARY, CONCLUSIONS AND RECOMMENDATIONS.....173
6.1 Introduction.....173
6.2 Body wave characteristics.....174
6.3 Body wave velocities.....176
6.4 Wave attenuation and material damping.....177

APPENDIX A
TIME DOMAIN RECORDS.....179

APPENDIX B
RELATIONSHIP BETWEEN ELASTIC AND DAMPED BODY WAVE VELOCITIES AND MODULI...209

APPENDIX C
CROSS-CORRELATION RECORDS.....215

APPENDIX D
BODY WAVE DISPERSION CURVES.....237

BIBLIOGRAPHY.....269

LIST OF FIGURES

Figure		Page
1.1	Crosshole seismic method (after Stokoe and Hoar, 1978)	9
1.2	Downhole seismic method (After Stokoe and Hoar, 1978)	10
2.1	Particle motion for antiplane and inplane loading	18
2.2	Particle motion in three-dimensional case	21
2.3	Loading function and fast Fourier transform parameters	23
2.4	Displacement, velocity and acceleration records for two-dimensional longtudinal-motion	26
2.5	Displacement, velocity and acceleration records for two-dimensional in-plane shear-motion	27
2.6	Displacement, velocity and acceleration records for two-dimensional antiplane shear-motion	28
2.7	Displacement, velocity and acceleration records for three-dimensional longitudinal-motion	29
2.8	Displacement, velocity and acceleration records for three-dimensional shear-motion	30
3.1	Two-dimensional in-plane longitudinal motion. Effect of different damping ratios	35
3.2	Two-dimensional in-plane shear motion. Effect of different damping ratios	37
3.3	Two-dimensional anitplane shear motion. Effect of different damping ratios	39
3.4	Three-dimansional longitudinal motion. Effect of different damping ratios	41
3.5	Three-dimensional shear motion. Effect of different damping ratios	42
3.6	Two-dimensional in-plane longitudinal motion. Effect of Poisson's ratio	45
3.7	Two-dimensional in-plane shear motion. Effect of Poisson's ratio	46
3.8	Two-dimensional antiplane shear motion. Effect of Poisson's ratio	47

Figure		Page
3.9	Three-dimensional longitudinal motion. Effect of Poisson's ratio	48
3.10	Three-dimensional shear motion. Effect of Poisson's ratio	49
3.11	Longitudinal- and transverse-motion records as monitored by a perfect vertical receiver	54
3.12	Transverse-motion records produced by reversed impulses as monitored by a perfect vertical receiver	55
3.13	"Transverse-motion" records produced by reversed impulses as monitored by a receiver with a 30 degree inclination	56
3.14	Wave amplitude decay due to radiational damping. Two-dimensional in-plane longitudinal motion	60
3.15	Wave amplitude decay due to radiational damping. Two-dimensional in-plane shear motion	61
3.16	Wave amplitude decay due to radiational damping. Two-dimensional antiplane shear motion	62
3.17	Wave amplitude decay due to radiational damping. Three-dimensional longitudinal motion	63
3.18	Wave amplitude decay due to radiational damping. Three-dimensional shear motion	64
3.19	Wave amplitude decay due to radiational damping and two percent material damping. Two-dimensional in-plane longitudinal motion	66
3.20	Wave amplitude decay due to radiational damping and two percent material damping. Two-dimensional in-plane shear motion	67
3.21	Wave amplitude decay due to radiational damping and two percent material damping. Two-dimensional antiplane shear motion	68
3.22	Wave amplitude decay due to radiational damping and two percent material damping. Three-dimensional longitudinal motion	69
3.23	Wave amplitude decay due to radiational damping and two percent material damping. Three-dimensional shear motion	70
3.24	Wave amplitude decay due to radiational damping and five percent material damping. Two-dimensional in-plane longitudinal motion	71

Figure		Page
3.25	Wave amplitude decay due to radiational damping and five percent material damping. Two-dimensional in-plane shear motion	72
3.26	Wave amplitude decay due to radiational damping and five percent material damping. Two-dimensional antiplane shear motion	73
3.27	Wave amplitude decay due to radiational damping and five percent material damping. Three-dimensional longitudinal motion	74
3.28	Wave amplitude decay due to radiational damping and five percent material damping. Three-dimensional shear motion	75
4.1	Two-dimensional in-plane longitudinal motion at two different points in a medium with no damping	81
4.2	Two-dimensional in-plane shear motion at two different points in a medium with no damping	82
4.3	Two-dimensional antiplane shear motion at two different points in a medium with no damping. Illustration of interval travel time determination	83
4.4	Three-dimensional longitudinal motion at two different points in a medium with no damping	84
4.5	Three-dimensional shear motion at two different points in a medium with no damping	85
4.6	Two-dimensional in-plane longitudinal motion at two different points in a medium with five percent damping	86
4.7	Two-dimensional in-plane shear motion at two different points in a medium with five percent damping	87
4.8	Two-dimensional antiplane shear motion at two different points in a medium with five percent damping. Illustration of interval travel time determination	88
4.9	Three-dimensional longitudinal motion at two different points in a medium with five percent damping	89
4.10	Three-dimensional shear motion at two different points in a medium with five percent damping	90
4.11	Cross-correlation function of two-dimensional P-motion records obtained in the near field. Poisson's ratio = 0.25 and damping = 0%	91

Figure		Page
4.12	Cross-correlation function of two-dimensional SV-motion records obtained in the near field. Poisson's ratio = 0.25 and damping = 0%	96
4.13	Cross-correlation function of two-dimensional SH-motion records obtained in the near field. Poisson's ratio = 0.25 and damping = 0%	97
4.14	Cross-correlation function of three-dimensional P-motion records obtained in the near field. Poisson's ratio = 0.25 and damping = 0%	98
4.15	Cross-correlation function of three-dimensional S-motion records obtained in the near field. Poisson's ratio = 0.25 and damping = 0%	99
4.16	Cross-correlation function of two-dimensional P-motion records obtained in the far field. Poisson's ratio = 0.25 and damping = 0%	100
4.17	Cross-correlation function of two-dimensional SV-motion records obtained in the far field. Poisson's ratio = 0.25 and damping = 0%	101
4.18	Cross-correlation function of two-dimensional SH-motion records obtained in the far field. Poisson's ratio = 0.25 and damping = 0%	102
4.19	Cross-correlation function of three-dimensional P-motion records obtained in the far field. Poisson's ratio = 0.25 and damping = 0%	103
4.20	Cross-correlation function of three-dimensional S-motion records obtained in the far field. Poisson's ratio = 0.25 and damping = 0%	104
4.21	Dispersion curves for two-dimensional in-plane longitudinal motion in a medium with no damping and Poisson's ratio = 0.25. Small spacing between receivers	111
4.22	Dispersion curves for two-dimensional in-plane longitudinal motion in a medium with no damping and Poisson's ratio = 0.25. Large spacing between receivers	112
4.23	Dispersion curves for two-dimensional in-plane shear motion in a medium with no damping and Poisson's ratio = 0.25. Small spacing between receivers	113
4.24	Dispersion curves for two-dimensional in-plane shear motion in a medium with no damping and Poisson's ratio = 0.25. Large spacing between receivers	114

Figure		Page
4.25	Dispersion curves for two-dimensional antiplane shear motion in a medium with no damping and Poisson's ratio = 0.25. Small spacing between receivers	115
4.26	Dispersion curves for two-dimensional antiplane shear motion in a medium with no damping and Poisson's ratio = 0.25. Large spacing between receivers	116
4.27	Dispersion curves for three-dimensional longitudinal motion in a medium with no damping and Poisson's ratio = 0.25. Small spacing between receivers	117
4.28	Dispersion curves for three-dimensional longitudinal motion in a medium with no damping and Poisson's ratio = 0.25. Large spacing between receivers	118
4.29	Dispersion curves for three-dimensional shear motion in a medium with no damping and Poisson's ratio = 0.25. Small spacing between receivers	119
4.30	Dispersion curves for three-dimensional shear motion in a medium with no damping and Poisson's ratio = 0.25. Large spacing between receivers	120
4.31	Dispersion curves for three-dimensional longitudinal motion normalized with respect to wavelength. Small spacing between receivers	125
4.32	Dispersion curves for three-dimensional longitudinal motion normalized with respect to wavelength. Large spacing between receivers	126
4.33	Dispersion curves for three-dimensional shear motion normalized with respect to wavelength. Small spacing between receivers	127
4.34	Dispersion curves for three-dimensional shear motion normalized with respect to wavelength. Large spacing between receivers	128
4.35	Dispersion curve obtained from ths phase of the transfer function for two-dimensional longitudinal motion in a medium with no damping and Poisson's ratio = 0.25	131
4.36	Dispersion curve obtained from the phase of the transfer function for two-dimensional in-plane shear motion in a medium with no damping and Poisson's ratio = 0.25	132
4.37	Dispersion curve obtained from the phase of the transfer function for two-dimensional antiplane shear motion in a medium with no damping and Poisson's ratio = 0.25	133

Figure		Page
4.38	Dispersion curve obtained from the phase of the transfer function for three-dimensional longitudinal motion in a medium with no damping and Poisson's ratio = 0.25	134
4.39	Dispersion curve obtained from the phase of the transfer function for three-dimensional shear motion in a medium with no damping and Poisson's ratio = 0.25	135
5.1	Apparent damping ratio for in-plane longitudinal motion in a medium with no damping and Poisson's ratio = 0.25. Small spacing between receivers	150
5.2	Apparent damping ratio for in-plane longitudinal motion in a medium with no damping and Poisson's ratio = 0.25. Large spacing between receivers	151
5.3	Apparent damping ratio for in-plane shear motion in a medium with no damping and Poisson's ratio = 0.25. Small spacing between receivers	152
5.4	Apparent damping ratio for in-plane shear motion in a medium with no damping and Poisson's ratio = 0.25. Large spacing between receivers	153
5.5	Apparent damping ratio for antiplane shear motion in a medium with no damping and Poisson's ratio = 0.25. Small spacing between receivers	154
5.6	Apparent damping ratio for antiplane shear motion in a medium with no damping and Poisson's ratio = 0.25. Large spacing between receivers	155
5.7	Apparent damping ratio for three-dimensional longitudinal motion in a medium with no damping and Poisson's ratio = 0.25. Small spacing between receivers	156
5.8	Apparent damping ratio for three-dimensional longitudinal motion in a medium with no damping and Poisson's ratio = 0.25. Large spacing between receivers	157
5.9	Apparent damping ratio for three-dimensional shear motion in a medium with no damping and Poisson's ratio = 0.25. Small spacing between receivers	158
5.10	Apparent damping ratio for three-dimensional shear motion in a medium with no damping and Poisson's ratio = 0.25. Large spacing between receivers	159
5.11	Apparent damping ratio for in-plane longitudinal motion in a medium with five percent damping and Poisson's ratio = 0.25. Small spacing between receivers	161

Figure | Page

5.12 Apparent damping ratio for in-plane longitudinal motion in a medium with five percent damping and Poisson's ratio = 0.25. Large spacing between receivers.....162

5.13 Apparent damping ratio for in-plane shear motion in a medium with five percent damping and Poisson's ratio = 0.25. Small spacing between receivers.....163

5.14 Apparent damping ratio for in-plane shear motion in a medium with five percent damping and Poisson's ratio = 0.25. Large spacing between receivers.....164

5.15 Apparent damping ratio for antiplane shear motion in a medium with five percent damping and Poisson's ratio = 0.25. Small spacing between receivers.....165

5.16 Apparent damping ratio for antiplane shear motion in a medium with five percent damping and Poisson's ratio = 0.25. Large spacing between receivers.....166

5.17 Apparent damping ratio for three-dimensional longitudinal motion in a medium with five percent damping and Poisson's ratio = 0.25. Small spacing between receivers.....167

5.18 Apparent damping ratio for three-dimensional longitudinal motion in a medium with five percent damping and Poisson's ratio = 0.25. Large spacing between receivers.....168

5.19 Apparent damping ratio for three-dimensional shear motion in a medium with five percent damping and Poisson's ratio = 0.25. Small spacing between receivers.....169

5.20 Apparent damping ratio for three-dimensional shear motion in a medium with five percent damping and Poisson's ratio = 0.25. Large spacing between receivers.....170

A.1 Amplitude decay with distance (short distances) for two-dimensional longitudinal motion in a medium with no damping and Poisson's ratio = 0.25.....180

A.2 Amplitude decay with distance (long distances) for two-dimensional longitudinal motion in a medium with no damping and Poisson's ratio = 0.25.....181

A.3 Amplitude decay with distance (short distances) for in-plane shear motion in a medium with no damping and Poisson's ratio = 0.25.....182

A.4 Amplitude decay with distance (long distances) for in-plane shear motion in a medium with no damping and Poisson's ratio = 0.25.....183

Figure		Page
A.5	Amplitude decay with distance (short distances) for antiplane shear motion in a medium with no damping and Poisson's ratio = 0.25	184
A.6	Amplitude decay with distance (long distances) for antiplane shear motion in a medium with no damping and Poisson's ratio = 0.25	185
A.7	Amplitude decay with distance (short distances) for three-dimensional longitudinal motion in a medium with no damping and Poisson's ratio = 0.25	186
A.8	Amplitude decay with distance (long distances) for three-dimensional longitudinal motion in a medium with no damping and Poisson's ratio = 0.25	187
A.9	Amplitude decay with distance (short distances) for three-dimensional shear motion in a medium with no damping and Poisson's ratio = 0.25	188
A.10	Amplitude decay with distance (long distances) for three-dimensional shear motion in a medium with no damping and Poisson's ratio = 0.25	189
A.11	Amplitude decay with distance (short distances) for two-dimensional longitudinal motion in a medium with five percent damping and Poisson's ratio = 0.25	190
A.12	Amplitude decay with distance (long distances) for two-dimensional longitudinal motion in a medium with five percent damping and Poisson's ratio = 0.25	191
A.13	Amplitude decay with distance (short distances) for in-plane shear motion in a medium with five percent damping and Poisson's ratio = 0.25	192
A.14	Amplitude decay with distance (long distances) for in-plane shear motion in a medium with five percent damping and Poisson's ratio = 0.25	193
A.15	Amplitude decay with distance (short distances) for antiplane shear motion in a medium with five percent damping and Poisson's ratio = 0.25	194
A.16	Amplitude decay with distance (long distances) for antiplane shear motion in a medium with five percent damping and Poisson's ratio = 0.25	195
A.17	Amplitude decay with distance (short distances) for three-dimensional longitudinal motion in a medium with five percent damping and Poisson's ratio = 0.25	196

Figure | Page

A.18 Amplitude decay with distance (long distances) for three-dimensional longitudinal motion in a medium with five percent damping and Poisson's ratio = 0.25.....197

A.19 Amplitude decay with distance (short distances) for three-dimensional shear motion in a medium with five percent damping and Poisson's ratio = 0.25.....198

A.20 Amplitude decay with distance (long distances) for three-dimensional shear motion in a medium with five percent damping and Poisson's ratio = 0.25.....199

A.21 Amplitude decay with distance (short distances) for two-dimensional longitudinal motion in a medium with no damping and Poisson's ratio = 0.4.....200

A.22 Amplitude decay with distance (long distances) for two-dimensional longitudinal motion in a medium with no damping and Poisson's ratio = 0.4.....201

A.23 Amplitude decay with distance (short distances) for in-plane shear motion in a medium with no damping and Poisson's ratio = 0.4.....202

A.24 Amplitude decay with distance (long distances) for in-plane shear motion in a medium with no damping and Poisson's ratio = 0.4.....203

A.25 Amplitude decay with distance (short distances) for three-dimensional longitudinal motion in a medium with no damping and Poisson's ratio = 0.4.....204

A.26 Amplitude decay with distance (long distances) for three-dimensional longitudinal motion in a medium with no damping and Poisson's ratio = 0.4.....205

A.27 Amplitude decay with distance (short distances) for three-dimensional shear motion in a medium with no damping and Poisson's ratio = 0.4.....206

A.28 Amplitude decay with distance (long distances) for three-dimensional shear motion in a medium with no damping and Poisson's ratio = 0.4.....207

C.1 Cross-correlation function of two-dimensional P-motion records obtained in the near field. Poisson's ratio = 0.25 and damping = 5%.....216

C.2 Cross-correlation function of two-dimensional SV-motion records obtained in the near field. Poisson's ratio = 0.25 and damping = 5%.....217

Figure		Page
C.3	Cross-correlation function of two-dimensional SH-motion records obtained in the near field. Poisson's ratio = 0.25 and damping = 5%	218
C.4	Cross-correlation function of three-dimensional P-motion records obtained in the near field. Poisson's ratio = 0.25 and damping = 5%	219
C.5	Cross-correlation function of three-dimensional S-motion records obtained in the near field. Poisson's ratio = 0.25 and damping = 5%	220
C.6	Cross-correlation function of two-dimensional P-motion records obtained in the near field. Poisson's ratio = 0.4, Damping = 0%	221
C.7	Cross-correlation function of two-dimensional SV-motion records obtained in the near field. Poisson's ratio = 0.4, Damping = 0%	222
C.8	Cross-correlation function of two-dimensional SH-motion records obtained in the near field. Poisson's ratio = 0.4, Damping = 0%	223
C.9	Cross-correlation function of three-dimensional P-motion records obtained in the near field. Poisson's ratio = 0.4, Damping = 0%	224
C.10	Cross-correlation function of three-dimensional S-motion records obtained in the near field. Poisson's ratio = 0.4, Damping = 0%	225
C.11	Cross-correlation function of two-dimensional P-motion records obtained in the far field. Poisson's ratio = 0.25 and damping = 5%	226
C.12	Cross-correlation function of two-dimensional SV-motion records obtained in the far field. Poisson's ratio = 0.25 and damping = 5%	227
C.13	Cross-correlation function of two-dimensional SH-motion records obtained in the far field. Poisson's ratio = 0.25 and damping = 5%	228
C.14	Cross-correlation function of three-dimensional P-motion records obtained in the far field. Poisson's ratio = 0.25 and damping = 5%	229
C.15	Cross-correlation function of three-dimensional S-motion records obtained in the far field. Poisson's ratio = 0.25 and damping = 5%	230

Figure		Page
C.16	Cross-correlation function of two-dimensional P-motion records obtained in the far field. Poisson's ratio = 0.4 and damping = 0%	231
C.17	Cross-correlation function of two-dimensional SV-motion records obtained in the far field. Poisson's ratio = 0.4 and damping = 0%	232
C.18	Cross-correlation function of two-dimensional SH-motion records obtained in the far field. Poisson's ratio = 0.4 and damping = 0%	233
C.19	Cross-correlation function of three-dimensional P-motion records obtained in the far field. Poisson's ratio = 0.4 and damping = 0%	234
C.20	Cross-correlation function of three-dimensional S-motion records obtained in the far field. Poisson's ratio = 0.4 and damping = 0%	235
D.1	Dispersion curves for two-dimensional in-plane longitudinal motion in a medium with five percent damping and Poisson's ratio = 0.25. Small spacing between receivers	238
D.2	Dispersion curves for two-dimensional in-plane longitudinal motion in a medium with five percent damping and Poisson's ratio = 0.25. Large spacing between receivers	239
D.3	Dispersion curves for two-dimensional in-plane shear motion in a medium with five percent damping and Poisson's ratio = 0.25. Small spacing between receivers	240
D.4	Dispersion curves for two-dimensional in-plane shear motion in a medium with five percent damping and Poisson's ratio = 0.25. Large spacing between receivers	241
D.5	Dispersion curves for two-dimensional antiplane shear motion in a medium with five percent damping and Poisson's ratio = 0.25. Small spacing between receivers	242
D.6	Dispersion curves for two-dimensional antiplane shear motion in a medium with five percent damping and Poisson's ratio = 0.25. Large spacing between receivers	243
D.7	Dispersion curves for three-dimensional longitudinal motion in a medium with five percent damping and Poisson's ratio = 0.25. Small spacing between receivers	244
D.8	Dispersion curves for three-dimensional longitudinal motion in a medium with five percent damping and Poisson's ratio = 0.25. Large spacing between receivers	245

Figure		Page
D.9	Dispersion curves for three-dimensional shear motion in a medium with five percent damping and Poisson's ratio = 0.25. Small spacing between receivers	246
D.10	Dispersion curves for three-dimensional shear motion in a medium with five percent damping and Poisson's ratio = 0.25. Large spacing between receivers	247
D.11	Dispersion curves for two-dimensional in-plane longitudinal motion in a medium with no damping and Poisson's ratio = 0.4. Small spacing between receivers	248
D.12	Dispersion curves for two-dimensional in-plane longitudinal motion in a medium with no damping and Poisson's ratio = 0.4. Large spacing between receivers	249
D.13	Dispersion curves for two-dimensional in-plane shear motion in a medium with no damping and Poisson's ratio = 0.4. Small spacing between receivers	250
D.14	Dispersion curves for two-dimensional in-plane shear motion in a medium with no damping and Poisson's ratio = 0.4. Large spacing between receivers	251
D.15	Dispersion curves for two-dimensional antiplane shear motion in a medium with no damping and Poisson's ratio = 0.4. Small spacing between receivers	252
D.16	Dispersion curves for two-dimensional antiplane shear motion in a medium with no damping and Poisson's ratio = 0.4. Large spacing between receivers	253
D.17	Dispersion curves for three-dimensional longitudinal motion in a medium with no damping and Poisson's ratio = 0.4. Small spacing between receivers	254
D.18	Dispersion curves for three-dimensional longitudinal motion in a medium with no damping and Poisson's ratio = 0.4. Large spacing between receivers	255
D.19	Dispersion curves for three-dimensional shear motion in a medium with no damping and Poisson's ratio = 0.4. Small spacing between receivers	256
D.20	Dispersion curves for three-dimensional shear motion in a medium with no damping and Poisson's ratio = 0.4. Large spacing between receivers	257
D.21	Dispersion curves obtained from the phase of the transfer function for two-dimensional longitudinal motion in a medium with five percent damping and Poisson's ratio = 0.25	258

Figure | Page

D.22 Dispersion curves obtained from the phase of the transfer function for two-dimensional inplane shear motion in a medium with five percent damping and Poisson's ratio = 0.25.....259

D.23 Dispersion curves obtained from the phase of the transfer function for two-dimensional antiplane shear motion in a medium with five percent damping and Poisson's ratio = 0.25.....260

D.24 Dispersion curves obtained from the phase of the transfer function for Three-dimensional longitudinal motion in a medium with five percent damping and Poisson's ratio = 0.25.....261

D.25 Dispersion curves obtained from the phase of the transfer function for three-dimensional shear motion in a medium with five percent damping and Poisson's ratio = 0.25.....262

D.26 Dispersion curves obtained from the phase of the transfer function for two-dimensional longitudinal motion in a medium with no damping and Poisson's ratio = 0.4.....263

D.27 Dispersion curves obtained from the phase of the transfer function for two-dimensional inplane shear motion in a medium with no damping and Poisson's ratio = 0.4.....264

D.28 Dispersion curves obtained from the phase of the transfer function for two-dimensional antiplane shear motion in a medium with no damping and Poisson's ratio = 0.4.....265

D.29 Dispersion curves obtained from the phase of the transfer function for Three-dimensional longitudinal motion in a medium with no damping and Poisson's ratio = 0.4.....266

D.30 Dispersion curves obtained from the phase of the transfer function for three-dimensional shear motion in a medium with no damping and Poisson's ratio = 0.4.....267

LIST OF SYMBOLS

A = auto spectrum of displacement

$a_o = \frac{\omega r}{c_s}$

$b_o = \frac{\omega r}{c_p}$

c = phase velocity

c_p = compressional wave velocity

c_p^D = damped compressional wave velocity

$c_{pI} = D_p \cdot c_p$, imaginary part of complex compressional wave velocity

$c_p^* = c_p + ic_{pI}$

c_s = shear wave velocity

c_s^D = damped shear wave velocity

$c_{sI} = D_S \cdot c_S$, imaginary part of complex shear wave velocity

$c_s^* = c_s + ic_{sI}$

$CR(\tau)$ = cross correlation function

$CS(f)$ = cross spectrum function

d = distance

d_1 = distance from source to first receiver

d_2 = distance from source to second receiver

D = hysteretic damping ratio

D_p = damping ratio in compression-extension

D_S = damping ratio in shear

e = base of natural logarithmics

E = Young's modulus of elasticity

f = frequency in Hz

f_{max} = maximum frequency of the FFT

F = amplitude of loading function

FFT = fast Fourier transform

G = shear modulus of elasticity

G_I = $2GD_S$, imaginary part of complex shear modulus

G^* = $G(1+2iD_S)$, complex shear modulus

$H(\omega)$ = Green's function or transfer function

$H_o^{(2)}$ = zero order Hankel function of the second kind

i = $\sqrt{-1}$

k = wave number

K_o, K_1, K_2 = modified Bessel functions of the second kind and orders zero, one, and two, respectively

L = wavelength

L_p = primary wave in a record of longitudinal-motion (far-field wave)

L_S = secondary wave in a record of longitudinal-motion (near-field wave)

L_{SV} = secondary wave in a record of in-plane longitudinal-motion (near-field wave)

M = constrained modulus of elasticity

M_I = $2MD_p$, imaginary part of constrained modulus

M^* = $M(1+2iD_p)$, complex constrained modulus

N = number of points of FFT

r = distance from source to receiver

t = time variable

T = $1/f$, time period

T_p = total duration of function to transform with the FFT

T_P = primary wave in a record of transverse-motion (near-field wave)

T_s = period of loading function

T_S = secondary wave in a record of transverse-motion (far-field wave)

T_{SH} = secondary wave in a record of transverse antiplane motion

T_{SV} = secondary wave in a record of transverse in-plane motion (far-field wave)

u = displacement

u = displacement in x-direction

U = linear spectrum of displacement

v = velocity

v = displacement in y-direction

V = apparent velocity

w = displacement in z-direction

W = elastic strain energy stored when the strain is a maximum

α = attenuation coefficient

δ = logarithmic decrement

Δt = sampling rate for the FFT

ΔW = energy dissipated per stress cycle

λ = Lame's constant of elasticity

λ = wavelength of shear wave

ν = Poisson's ratio

π = 3.14159...

ρ = mass density

Φ = inclination of geophone with respect to a vertical line

τ = time delay

ϕ = phase of cross spectrum or phase of transfer function

Ψ = damping capacity factor

ω = frequency in rad/sec

CHAPTER ONE

INTRODUCTION

1.1 SEISMIC METHODS IN CIVIL ENGINEERING

Steel, concrete, soil, rock, pavement and other engineering materials behave like elastic bodies at small strains. For soil, rock and pavement materials, small strains can be considered any strains on the order of o.oo1 percent or less. The small-strain range in steel and concrete is considerably higher. Stresses produced by a source releasing energy into the medium which creates small strains will propagate away from the source as elastic waves. The velocities at which these waves propagate depend mainly on the elastic moduli of the materials that compose the medium. Therefore, if one generates small-strain stress waves and measures propagation velocities, elastic material properties can be calculated. Such measurements are typically categorized as seismic measurements.

It is the purpose of this study to understand more completely seismic measurements as used for engineering applications. Most applications of seismic methods, to date, have been by exploration geophycisists, seismologists and petroleum engineers. The main efforts of these groups have been directed toward determining abrupt and broad geological changes in the interior of the earth, generally at great depths within rock formations. Estimation of the structure of the earth or location of the position of natural resources was typically the goal of those measurements. This

information was generally obtained by studying the arrivals of waves (usually compression waves) that were reflected or refracted at the interfaces of layers with very different elastic properties.

Engineers have also been interested in locating abrupt structural changes in earth materials. In addition to interpretation of the structural bedding surfaces, engineers have been attempting to determine the physical properties and stratigraphy of the uppermost zone of the earth. In certain cases near the surface of the earth, conventional sampling techniques can be used. In other cases, at greater depths or under circumstances where conventional sampling techniques and laboratory testing are not feasible or do not provide an adequate evaluation of the physical properties of the materials being tested, seismic methods offer the engineer a viable tool for evaluating engineering materials.

The emphasis in this research is placed on developing analytical formulations with which synthetic seismic records can be generated. These synthetic records are then processed following standard field procedures used in engineering applications. The applicability and limitations of the uses and processing of seismic records are studied. The thrust of this work is placed on wave velocity measurements (hence elastic stiffnesses), but attenuation measurements (material damping) are also addressed.

1.1.1 Uses and benefits of seismic methods

As analytical techniques to analyze physical problems are becoming more and more sophisticated, so are the laboratory testing methods used to determine the properties of the materials involved

in these problems. There are, however, several difficulties inherent with laboratory testing of sampled materials that do not exist with in situ methods. One of these difficulties is trying to minimize the disturbance caused by sampling methods in testing materials (especially in geotechnical materials). This complication is almost completely avoided by most seismic field methods since there is no need to obtain any physical samples. Another shortcoming of laboratory techniques is caused by the inability to simulate properly in situ stress conditions. With field testing techniques, in situ stress conditions do not need to be simulated since they are, in most cases, the stresses acting in the materials at the time the tests are performed. A further obstacle in laboratory testing occurs when one tries to obtain representative samples of the zone of interest. Many times the specimens tested are only characteristic of a small area within a larger zone having some irregularities (like in most jointed rock and in soils with primary and secondary structure). With most of the seismic methods, however, the areas sampled by the propagating waves are large enough so that the properties obtained are representative of the zone of concern.

When compared with other in situ testing methods, such as the standard penetration test and the cone penetration test (in soils), seismic methods have the advantages that: 1) they can be tailored to sample small or large zones of materials; 2) they have a strong theoretical basis (the theory of elasticity) and are not dependent on empirical correlations; and 3) measured wave velocities are independent of equipment used and do not need correction factors like many of the other in situ testing methods.

The most important properties usually obtained from seismic tests are the elastic shear modulus (G), which is obtained from the

propagation velocity of shear waves, the constrained modulus (M), which is obtained from the propagation velocity of longitudinal waves, and Poisson's ratio (ν) which can be calculated if shear and longitudinal wave velocities are known. Other properties like mass density (ρ), material damping (D), strain amplitudes and strain rates can be inferred or estimated from the analysis of wave propagation records. One of the main objectives of this study is to understand better what and how variables affect wave velocities calculated from various propagation measurements as outlined in Section 1.3.

Elastic properties obtained from seismic methods are those corresponding to very low-amplitude strains (strains less than o.oo1 percent for most geotechnical materials). Elastic moduli at these small strains are usually called initial tangent moduli. Initial tangent moduli are used directly as the stiffness of engineering materials in vibration problems where the amplitudes of the vibrations are kept very small (as is the case of most problems concerning vibrations of soils and foundations). For larger-amplitude straining, initial tangent moduli represent key parameters needed to fit nonlinear material models.

For anisotropic materials like soils, it is possible to determine the small-strain elastic properties in different directions by generating waves whose motions are polarized in different planes. In fact, one of the possible future uses of seismic methods in soils is to evaluate the state of stress from a three-dimensional picture of the seismic wave velocities (Lee and Stokoe, 1986).

In the same way that geophysicists are interested in determining structural changes and discontinuities in subsurface

materials, so are engineers interested in locating anomalies of engineering materials. In this respect seismic methods can be used to determine layering and properties of pavement systems; to detect cracks and other anomalies like voids in structural members, rock formations or pavement systems; to locate tunnels; in the integrity testing of piles and piers and other structures where construction specifications are difficult to check; and for many other purposes.

In Geotechnical Engineering, one of the major areas for the use of seismic methods and the area of focus in this study, shear and constrained moduli and their variation with strain are essential in characterizing soil behavior under dynamic loadings such as those created by earthquakes and blasting, in determining dynamic stiffnesses of foundations for soil-structure interaction analyses, and in evaluating the liquefaction susceptibility of cohesionless soils by the strain approach. Seismic methods often used to determine the variation of initial shear and constrained moduli with depth include the crosshole, downhole, surface refraction, surface reflection, steady-state Rayleigh-wave method and the spectral-analysis-of-surface-waves (SASW) method. Of these techniques the crosshole and the downhole methods (body wave methods) are the most widely used methods today for engineering applications and the ones that provide the most reliable results. The SASW method, a variation of the steady-state Rayleigh-wave method, is a promising new technique that has all of the advantages of the steady-state method without having its disadvantages. The surface refraction and surface reflection techniques are not suitable for most engineering applications since one is not able to obtain detailed moduli profiles with these methods.

1.2 SEISMIC METHODS BASED ON BODY WAVES

Body wave methods are based on the fact that the velocity at which seismic waves travel through the interior of materials depends on the elastic properties of the materials. Measurements are made by generating a seismic disturbance at one point in the medium and measuring the time required for the disturbance to travel to one or more seismic receivers. If the distances travelled by the measured waves are known, body wave velocities can be calculated by dividing the distances by the corresponding travel times.

From the theory of plane wave propagation in a homogeneous isotropic elastic body, it can be shown that two types of body waves propagate. The first type, usually called the compressional-, primary- or P-wave, propagates at a velocity c_p (or v_p; both notations are used in this study) which is given by

$$c_p^2 = M/\rho \tag{1.1a}$$

or

$$c_p^2 = (\lambda + 2G)/\rho \tag{1.1b}$$

or

$$c_p^2 = \frac{E(1 - \nu)}{\rho(1 + \nu)(1 - 2\nu)} \tag{1.1c}$$

where,

M is constrained modulus of elasticity,
ρ is mass density,
λ is Lame's constant of elasticity,
G is shear modulus of elasticity,
E is Young's modulus of elasticity, and
ν is Poisson's ratio.

The second kind of body wave is called the shear-, transverse-, secondary- or S-wave and propagates at a velocity c_s (or v_s) given by

$$c_s^2 = G/\rho \tag{1.2}$$

For plane wave propagation, P-waves are characterized by particle motion along the line of the wave advance, while S-waves are distinguished by having particle motion perpendicular to the direction of wave propagation. A look at Eqs. 1.1 and 1.2 shows that, in the same material, P-waves propagate at a much faster speed than S-waves, with the difference in velocities depending on the value of Poisson's ratio.

The most common methods to determine wave propagation velocities in the field for engineering applications are the crosshole and downhole (or uphole) methods. In the crosshole method, the time required for body waves to travel horizontally between several points located at the same depth is measured. By repeating the process at different depths, a profile of shear and compressional wave velocities with depth can be obtained. In the downhole method, a seismic disturbance is generated at a point on the surface, and the waves are monitored at several points in the interior of the soil mass. By measuring the travel times, wave

velocities can be calculated after travel distances have been determined.

Elements required in downhole and crosshole seismic surveys are boreholes, sources, receivers and recording and triggering systems. Typical field procedures are shown schematically in Figs. 1.1 and 1.2. A detailed analysis of the field processes and data analysis can be obtained in Woods (1978), Stokoe and Hoar (1978), Corps of Engineers EM 1110-1-1802 (1979), Patel (1981) and Hoar (1982).

1.3 ORGANIZATION AND OBJECTIVES OF THIS REPORT

If increasingly broader and more accurate conclusions and information are to be drawn from seismic records, it is essential to understand better the wave propagation signatures and the methods to analyze these signatures. Geophysical applications usually involve analysis of seismic waves that are recorded at far distances from the source. At these long distances, body waves are usually considered plane waves (plane fronts). The fact that these waves were generated by a point source and therefore are propagating with a spherical wave front is usually neglected without incurring serious errors. For engineering applications, however, seismic waves are recorded at short distances from the source and should not be considered plane if a precise evaluation of elastic velocities is necessary. An analytical formulation to generate wave propagation records produced by a point source in a full space (and therefore spreading in a spherical pattern) is explained in Chapter Two. It is not intended in this chapter to give a general overview of the theory of wave propagation in a linearly elastic, homogeneous and isotropic body. However, by

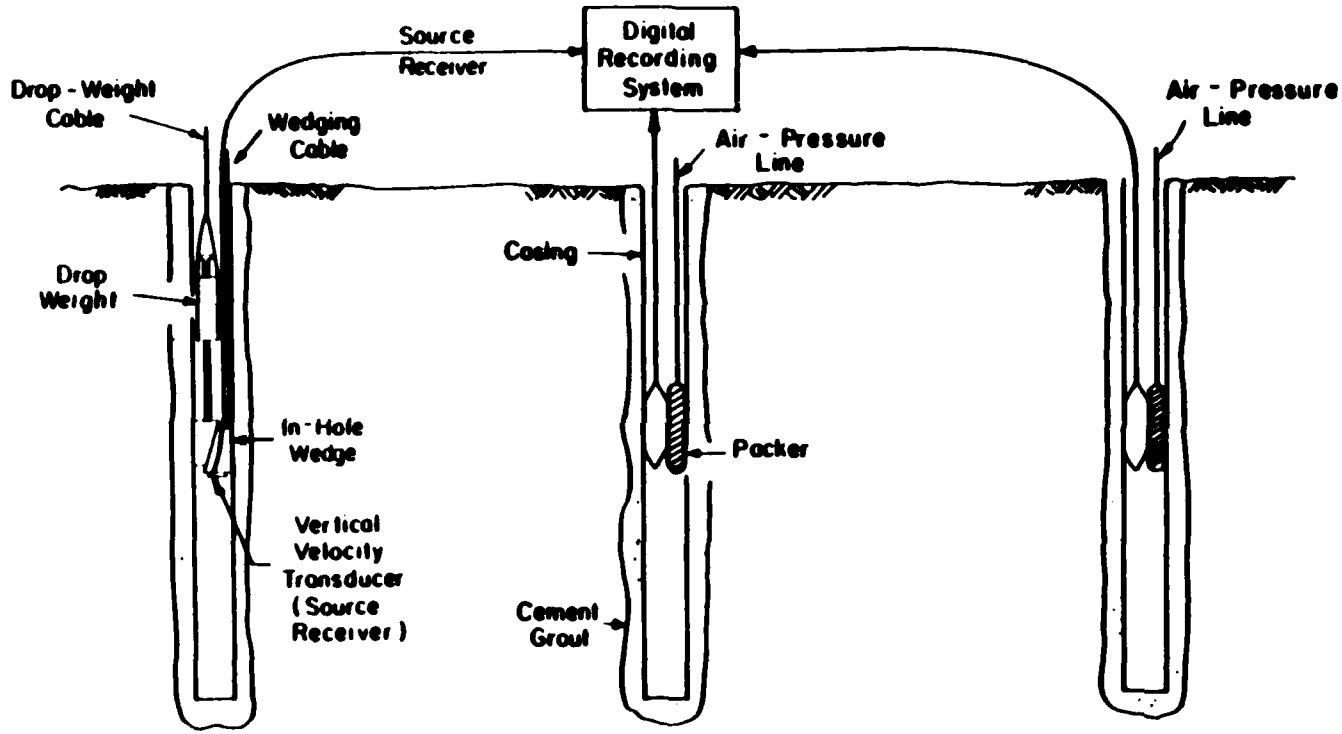

Fig. 1.1 - Crosshole seismic method (after Stokoe and Hoar, 1978).

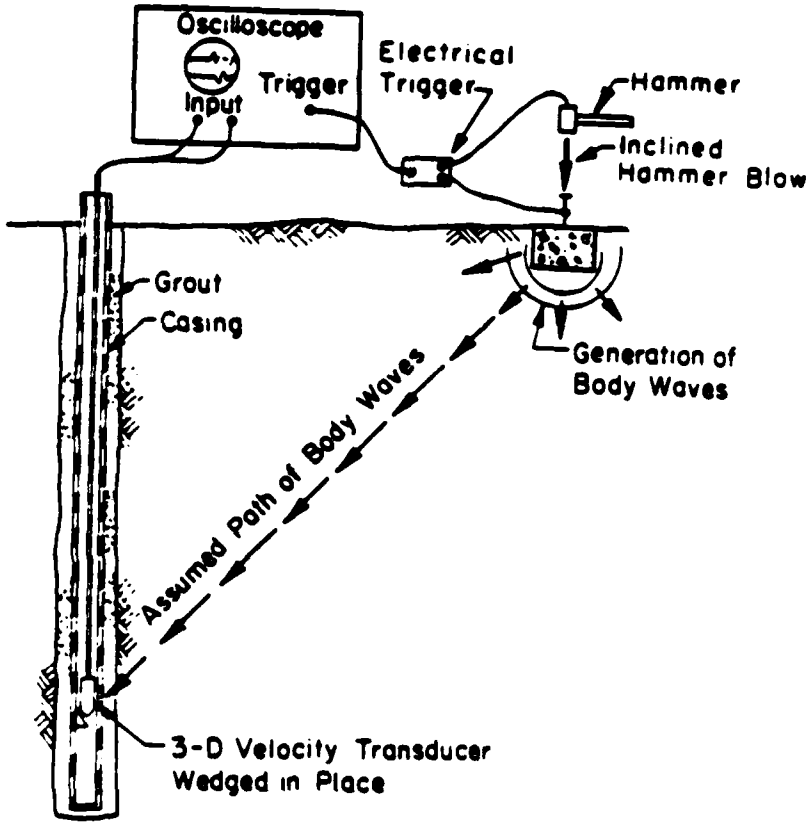

Fig. 1.2 - Downhole seismic method (after Stokoe and Hoar, 1978).

making use of the Green's functions formulation of displacements produced by a point load in the interior of a full-space (for which case closed-form solutions exist), a set of synthetic wave propagation records is generated. Typical features of these synthetic records are studied in Chapter Three.

It is also necessary to develop new methods of analysis of the field data that make better use of all the information contained in the wave propagation records of body waves. In this respect, Chapter Four is devoted to the analysis of existing and new techniques to evaluate propagation velocities from which the elastic properties of the propagating medium can be determined. The subjective nature of visual identifications of times of arrivals is demonstrated, especially for wave propagation in a medium with material damping. The cross-correlation function is shown to be an excellent method for determining elastic constants. Finally spectral analysis techniques based in cross spectrum and transfer functions are shown to be excellent tools to determine elastic wave propagation velocities if properly applied. Care must be taken not to use in the near field.

A technique to estimate material damping is presented in Chapter Five. The technique is based in spectral analysis methods and although is at a preliminary phase of development seems to hold promise in the field determination of material damping.

A summary of this work, conclusions and recommendations are then presented in Chapter Six.

CHAPTER TWO

ANALYTICAL FORMULATION FOR BODY WAVES IN A FULL SPACE

2.1 INTRODUCTION

In the crosshole and downhole seismic methods, body waves (longitudinal and shear waves) are generated by a source at one point and monitored at one or more other points as the waves pass these points. Direct as well as reflected and refracted waves are recorded by the receivers. It is assumed, however, in most of the analyses performed of the wave propagation records that only direct waves arrive at the receivers or that the effect of the reflected and refracted waves is negligible (compared to the effect of the direct waves). It can be assumed under these conditions that the waves behave as propagating in a full space. Although the validity of this assumption is questionable, it is intended (as a first step in the process of understanding the behavior of the waves generated by seismic sources) to analyze wave propagation records produced by point and line loads in the interior of a three-dimensional space. The mathematical formulation that leads to the analytical generation of wave propagation records in a full space is explained in this chapter.

2.2 THEORETICAL BACKGROUND

One of several methods to study wave propagation phenomena in a linearly elastic medium is by superposition of the response to steady-state (or harmonic) excitations. The method, known as Fourier superposition, Fourier synthesis or frequency domain analysis, provides an easy way to study complicated transient events when the solution to the steady-state problem is known. Assume, for instance, that the solution to a harmonically vibrating point load is known for all frequencies of vibration. Then, the response of the medium to any transient point load excitation can be calculated by expressing the load in terms of its harmonic components, evaluating the response of the system to each component, and superposing the harmonic solutions to obtain the final results. If the solution to the point load is known, the solution to loads over any area can also be obtained by integrating the point load solutions over the area.

Superposition techniques are limited to linear systems. Internal dissipation of energy in a truly nonlinear system is simulated in a linear system by assuming a complex stiffness, G^*, of the form $G^* = G(1 + 2iD)$ in which G is the elastic shear modulus of the material, $i = \sqrt{-1}$, and D is the hysteretic damping ratio. In the following, the asterisk will be dropped from G^* for simplicity, and G will be used as a complex number when the material exhibits a hysteretic type of damping. The notation will be clarified at each point in the text when confusion might arise.

A hysteretic type of damping is considered, in a frequency domain analysis, to be frequency and strain independent. While the

first assumption is usually true for most geotechnical materials in the frequency ranges of interest herein (1 to 1ooo Hz), the second assumption is not. It has been experimentally observed that the energy dissipated per vibration cycle can generally be considered independent of frequency but depends on the amplitude of the vibration. For low-strain amplitudes such as those associated with seismic waves, however, damping can be considered to be independent of strain (Johnston et al, 1979; Toksöz et al, 1979). The Fourier superposition technique is, thus, an approximate method to study waves propagating through a dissipative medium. Even for a material with true strain and frequency independent hysteretic damping, the solution would be approximate due to some mathematical problems created by the fact that hysteretic damping does not satisfy the principle of causality. The method offers, however, a very good approximation, particularly for materials with low damping.

Assume that the response of a medium to an excitation of the form p(t) is desired. As a first step in the Fourier superposition method, the function p(t) is decomposed in its different frequency components by means of a Fourier transform, $P(\omega)$, as

$$P(\omega) = \int_{-\infty}^{\infty} p(t) e^{-i\omega t} dt \qquad (2.1)$$

where

$$p(t) = \frac{1}{2\pi} \int_{-\infty}^{\infty} P(\omega) \cdot e^{i\omega t} d\omega \qquad (2.2)$$

and

t is the time variable in seconds,

ω is frequency in rad/sec,
e is the base of the natural logarithmics,
$i = \sqrt{-1}$, and
$\pi = 3.14159...$

The two integrals in Eqs. 2.1 and 2.2 are known as a Fourier transform pair. $P(\omega)$ represents the harmonic components of the loading function $p(t)$.

The response of the medium to an excitation of the form $e^{i\omega t}$ is defined by the Green's function or fundamental solution. The fundamental solution gives the displacement at one point of the medium due to a unit harmonic force applied at any other point of the medium. If the Green's function of the problem under consideration, $H(\omega)$, is known and the superposition principle is applied, the response of the system, $u(t)$, to the loading function, $p(t)$, defined in Eq. 2.2 is then given by

$$u(t) = \frac{1}{2\pi} \int_{-\infty}^{\infty} P(\omega) \cdot H(\omega) \cdot e^{i\omega t} d\omega \qquad (2.3)$$

This means that the response of the system to any excitation is given by the inverse Fourier transform of the product of the fundamental solution by the Fourier transform of the excitation. In other words, the Fourier transform of the response, $U(\omega)$, is the product of the Fourier transform of the excitation and the Green's function and can be written as

$$U(\omega) = P(\omega) \cdot H(\omega) \qquad (2.4)$$

Forward and inverse Fourier transforms can be efficiently calculated in a digital computer by means of a Fast Fourier

Transform (FFT) algorithm. Details on Fourier Transform theory and FFT algorithms are explained in references such as Bracewell, R.N., 1965; Brigham, E.O., 1974; and Newland, D.E., 1975.

Two- and three-dimensional wave propagation in a homogeneous, isotropic, linearly elastic medium with or without linear hysteretic damping is considered in this and the following two chapters. Fundamental solutions for two-dimensional plane strain (in-plane) and out-of-plane (antiplane) elastodynamic motion as well as three-dimensional elastodynamic motion are presented in the following sections.

2.2.1 Two-dimensional antiplane motion

Antiplane shear motion is illustrated in Fig. 2.1a. This type of transverse motion (SH-motion) is characterized by particle movement perpendicular to the plane of propagation of the wave. The displacement caused by a unit concentrated harmonic force at a distance r is (Achenbach, 1973)

$$w(\omega) = \frac{-i}{4G} H_o^{(2)}(\frac{\omega r}{c_s}) \qquad (2.5)$$

where

w is the value of the displacement,
ω is the circular frequency of the vibration,
G is the complex shear modulus,
r is the distance from the source to the target point,
$c_s = \sqrt{G/\rho}$, is the shear wave velocity of the material (complex value),

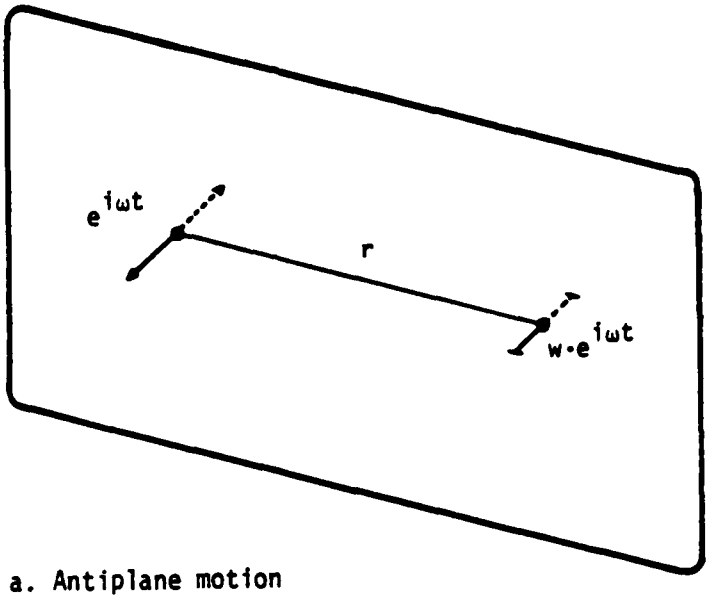

a. Antiplane motion

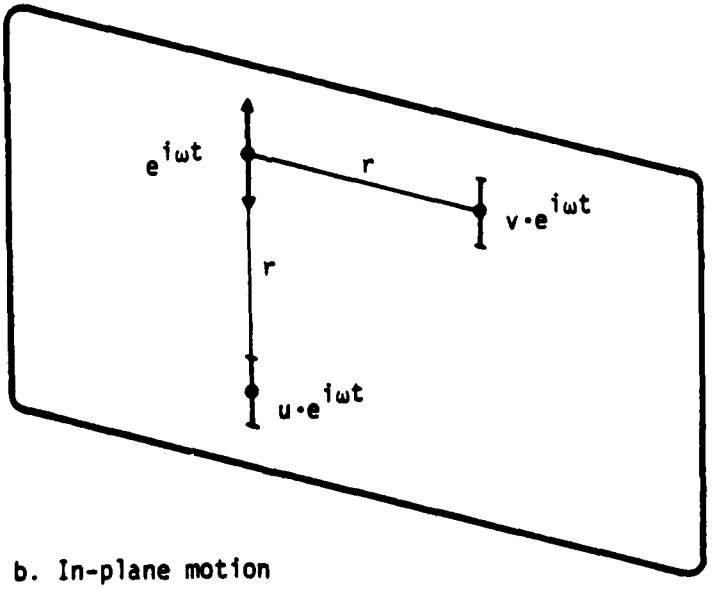

b. In-plane motion

Fig. 2.1 - Particle motion for antiplane and inplane loading.

ρ is the density of the material, and
$H_o^{(2)}$ is the zero order Hankel function of the second kind.

It should be noticed that the displacement, w, is a complex value. Since this displacement is the response of the medium to a steady-state excitation, the magnitude of the complex number represents the amplitude of the steady-state displacement, and the phase gives the phase difference between the excitation and the response.

2.2.2 Two-dimensional in-plane motions

In-plane excitation leads to two kinds of motions, a longitudinal motion and a transverse or shear motion. The longitudinal motion (P-motion) is characterized by particle displacement in the direction of propagation of the wave. In the shear motion (SV-motion), particle movement is perpendicular to the direction of wave propagation (Fig. 2.1b). These motions cause a compression (or extension) and a shear distortion, respectively.

The displacement in the direction of the load at a point along the line of excitation (P-motion) caused by a unit concentrated harmonic force at a distance r is (Cruse and Rizzo, 1968)

$$u(\omega) = [1/(2\pi\rho c_s^2)]\ [\psi-\chi] \qquad (2.6)$$

where,
u is the value of the displacement,
ρ is the density of the material, and
ψ and χ are given by the formulas:

$$\psi = K_o(ia_o) + (1/ia_o)\,[K_1(ia_o) - (c_s/c_p)K_1(ib_o)] \qquad (2.7)$$

$$\chi = K_2(ia_o) - (c_s/c_p)^2\, K_2(ib_o) \qquad (2.8)$$

where,

$a_o = \omega r/c_s$,

$b_o = \omega r/c_p$,

$c_p = [(\lambda+2G)/\rho]^{1/2}$, is the compression wave velocity of the material (complex value),

λ is the complex Lame's constant, and

K_o, K_1 and K_2 are the modified Bessel functions of the second kind and orders zero, one and two, respectively.

The displacement in the direction of the load at a point on a line perpendicular to the direction of excitation and passing by the point of impact (SV-motion), caused by a unit concentrated harmonic force at a distance r is (Cruse and Rizzo, 1968)

$$v(\omega) = [1/(2\pi\rho c_s^{\,2})] \cdot \psi \qquad (2.9)$$

where,

v is the value of the displacement, and

ψ is defined in Eq. 2.7.

2.2.3 Three-dimensional motions

The three-dimensional notation is illustrated in Fig. 2.2. The fundamental solution for longitudinal motion (P-motion) is defined by

$$u(\omega) = [1/(4\pi\rho c_s^{\,2}][\Gamma-\Xi] \qquad (2.10)$$

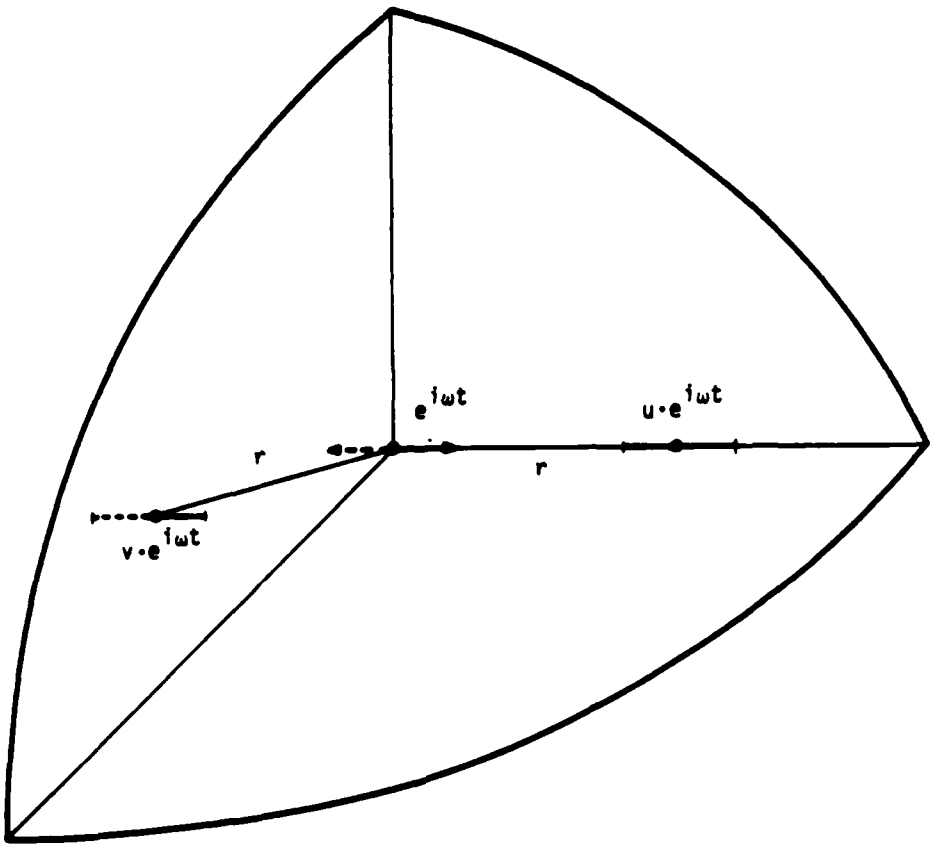

Fig. 2.2 - Particle motion in three-dimensional case.

and the fundamental solution for shear motion (S-motion) is

$$v(\omega) = [1/(4\pi\rho c_s^2)] \cdot \Gamma \tag{2.11}$$

where Γ and Ξ are given by

$$\Gamma = \{[1+(1/ia_o) - (1/a_o)^2]/r\}\ e^{-ia_o} - (c_s/c_p)^2\ \{[(1/ib_o) - (1/b_o)^2]/r\}\ e^{-ib_o} \tag{2.12}$$

$$\Xi = \{[1 + 3(1/ia_o) - 3(1/a_o)^2]/r\}\ e^{-ia_o} - (c_s/c_p)^2\ \{[1 + 3(1/ib_o) -3(1/b_o)^2]/r\}\ e^{-ib_o} \tag{2.13}$$

2.3 TIME AND FREQUENCY DOMAIN PARAMETERS

The loading function considered in this study is one cycle of a sine wave of amplitude F and period T_s as illustrated in Fig. 2.3. The amplitude F has a value of one unit and the duration of the impulse, T_s, is one second. The material considered as the medium of propagation has a shear wave velocity of 100 units and a mass density of 3.1 units. Note that no specific units are needed (except for the time). If a specific set of units was to be used, then all units would have to be compatible. For instance if forces are expressed in lbs, and the wave velocities in ft/sec, then the mass density should be in lb-sec^2/ft^4 and so on. If the density was set in kg/m^3, then velocities should be in m/sec and forces in Newtons. The results are presented in dimensionless form, in most of the cases. Therefore, the actual magnitude of the force used,

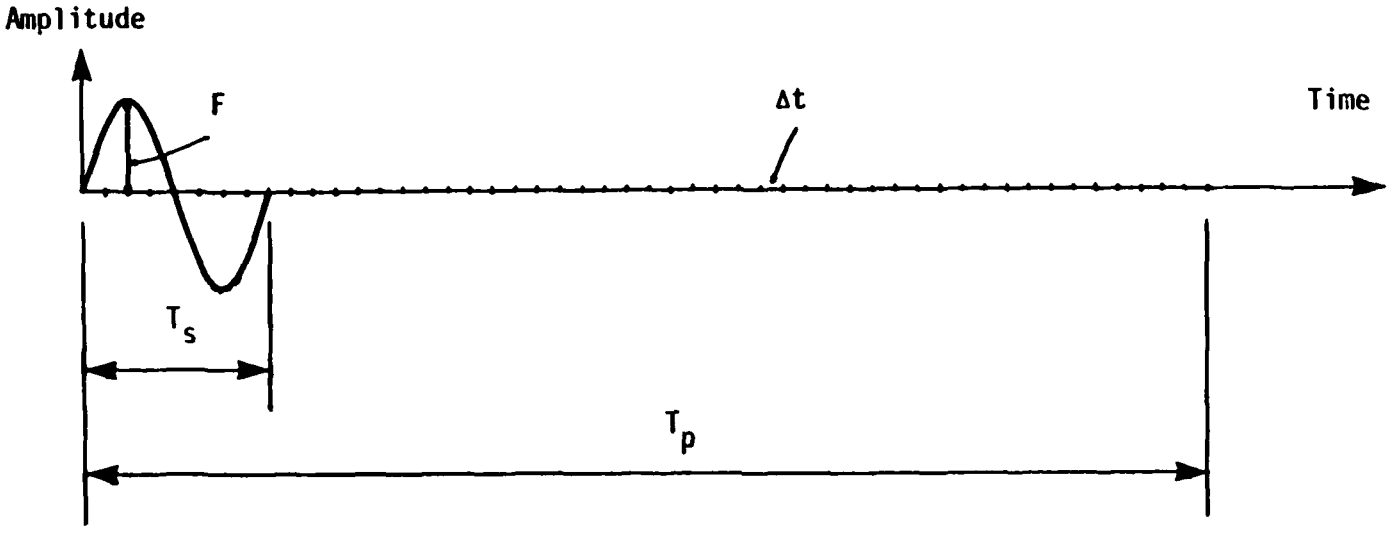

$$T_p = N \cdot \Delta t$$

$$\Delta f = \frac{1}{T_p}$$

$$f_{max} = \frac{1}{2 \cdot \Delta T}$$

Fig. 2.3 - Loading function and fast Fourier transform parameters.

the value of the shear wave velocity or the duration of the impulse are irrelevant when presenting the results.

The fast Fourier transform parameters used in this study are a sampling rate, $\Delta t = 0.01$ sec, and a total number of sampling points, $N = 1024$. (A few studies were done with, $\Delta t = 0.05$ sec and $N = 512$, when the target point was far from the source). In choosing these parameters, the following conditions were considered:

a) The sampling time, Δt, should be small enough: 1. to reproduce accurately the loading and response functions, and 2. to allow a sufficiently high maximum frequency, f_{max} to be obtained.

b) The total duration of the function to transform, T_p, should be long enough: 1. to minimize the effects of the periodicity inherent in the FFT algorithm, 2. to cover the time range of interest, and 3. to produce a small frequency domain sampling rate, Δf.

A singularity occurs in the fundamental solutions at zero frequency (Eqs. 2.5 through 2.13). In the present study, this singularity was avoided using the fundamental solution at a frequency equal to $\Delta f/10$ as the solution for the static case.

The studies presented in this chapter and in the following chapters have been conducted from records of particle displacement with time. Similar studies could have been performed from time histories of particle velocity or acceleration, but trends are easier to identify from waveforms of particle displacement than from records of particle velocity or acceleration. As an illustration, displacement, velocity and acceleration records for the five cases of motion considered in this report (two-dimensional P-, SV- and SH-motions and three-dimensional P- and S-motions) are

presented in Figs. 2.4 through 2.8. The notation used in these figures is the following:

u is particle displacement,
v is particle velocity,
a is particle acceleration,
G is shear modulus of the material (real value),
F is amplitude of loading force,
c_s is shear wave velocity (real value),
t is time in seconds,
d is distance from the source to the target point,
$\lambda = c_s \cdot T_s$ ("wavelength of loading function", not to be confused with Lame's constant),
D is damping ratio in percent, and
ν is Poisson's ratio.

Velocity or acceleration records can be obtained from velocity or acceleration fundamental solutions, or by differentiating the displacement records. All velocity and acceleration records in this study were obtained by using fundamental solutions of velocity or acceleration.

It can be observed in Figs. 2.4 through 2.8 that the velocity and acceleration waveforms are more complex than the displacement records. Even the simple case of the two-dimensional (2-D) SH-motion in Fig. 2.6 seems easier to understand in terms of displacement than in terms of velocity or acceleration. A further study of the displacement waveforms is done in the following chapters.

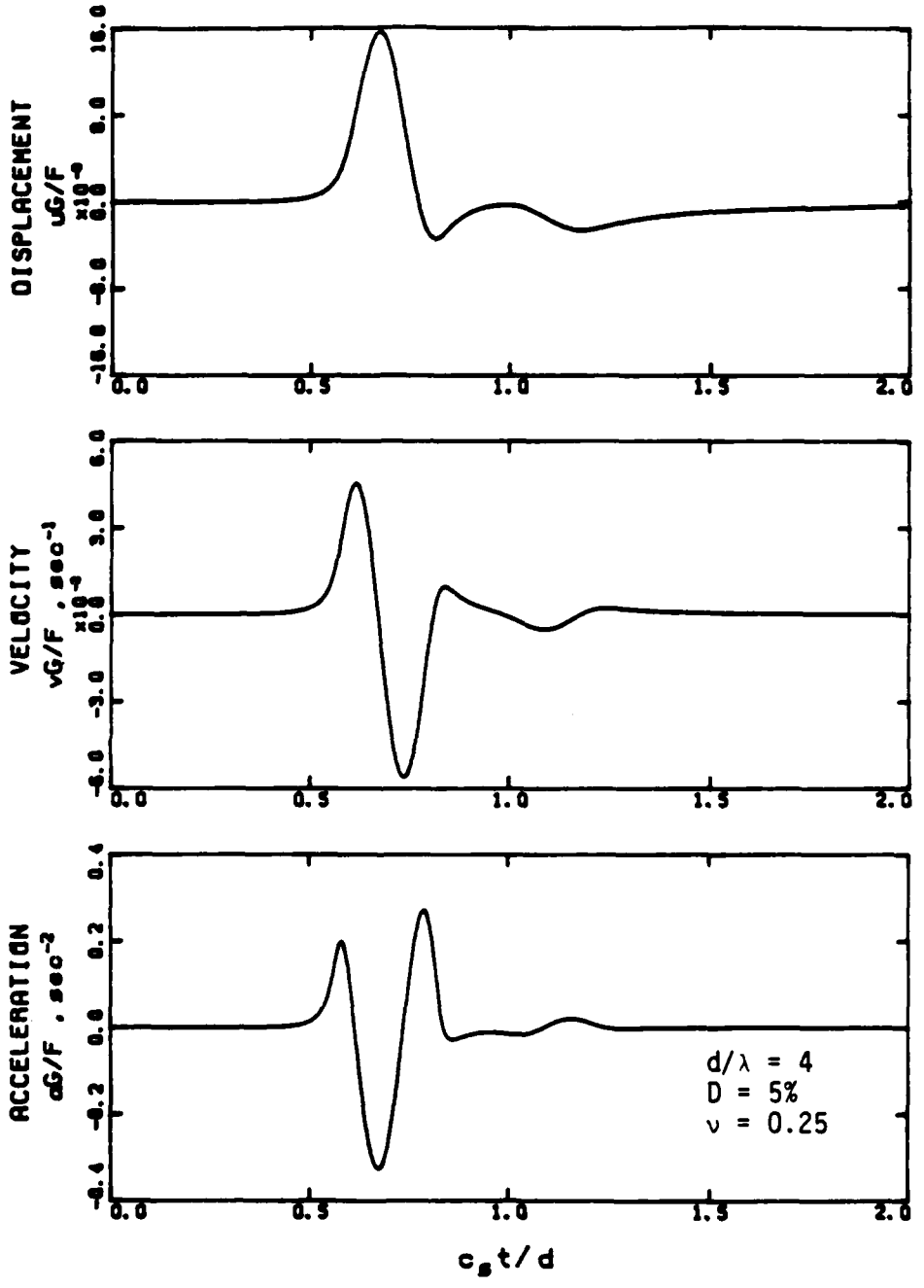

Fig. 2.4 - Displacement, velocity and acceleration records for two-dimensional longitudinal-motion.

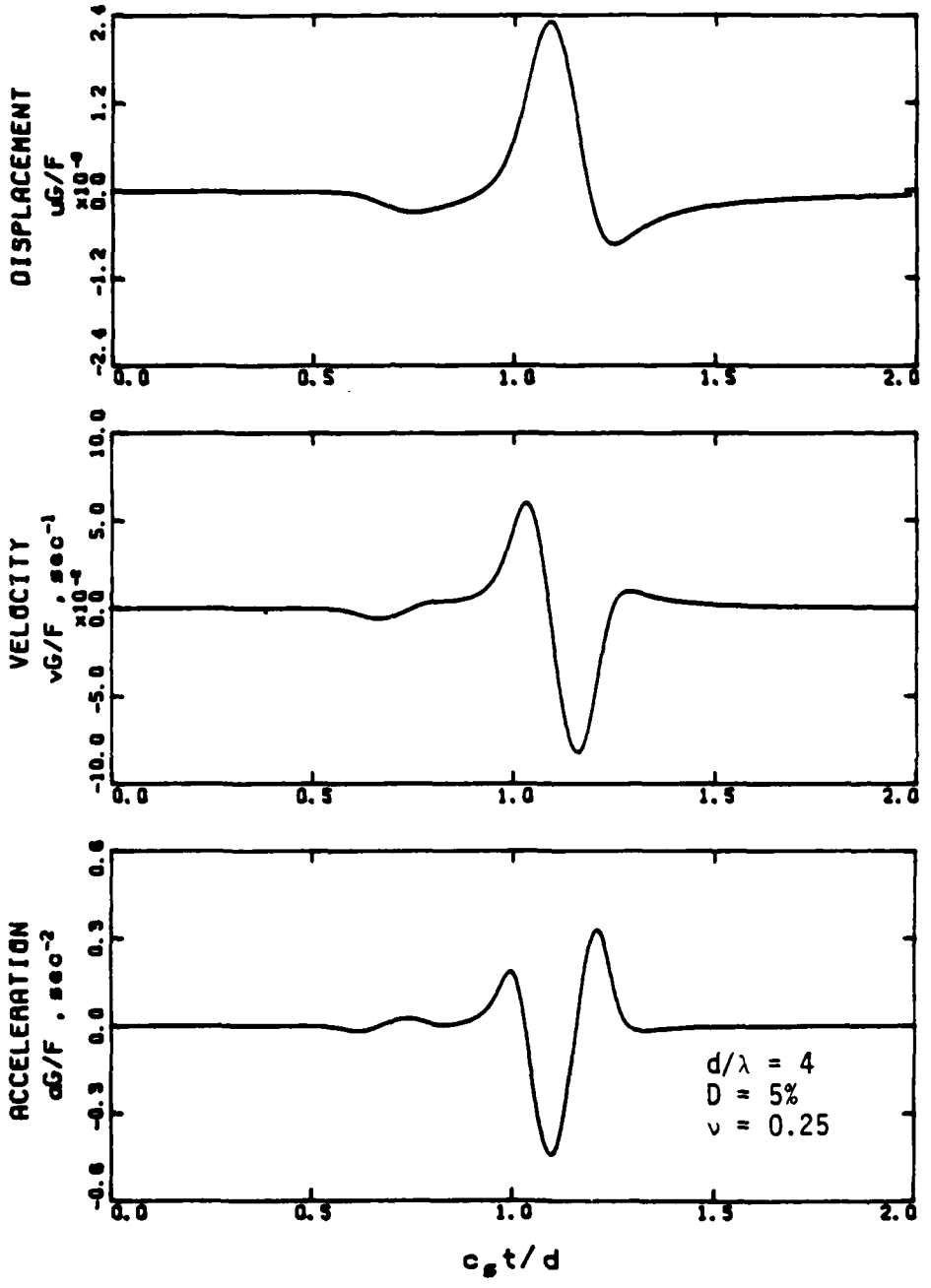

Fig. 2.5 - Displacement, velocity and acceleration records for two-dimensional in-plane shear-motion.

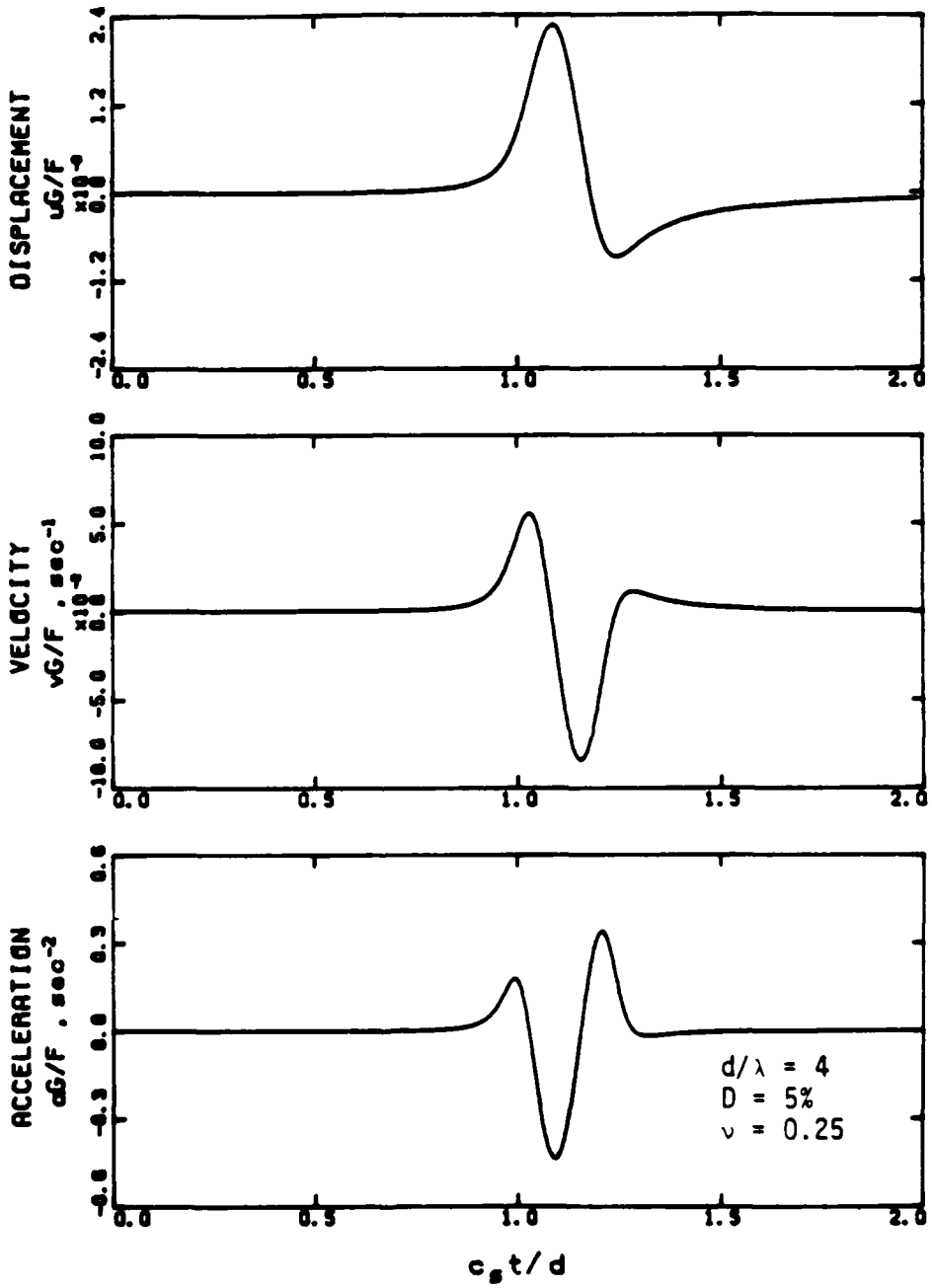

Fig. 2.6 - Displacement, velocity and acceleration records for two-dimensional antiplane shear-motion.

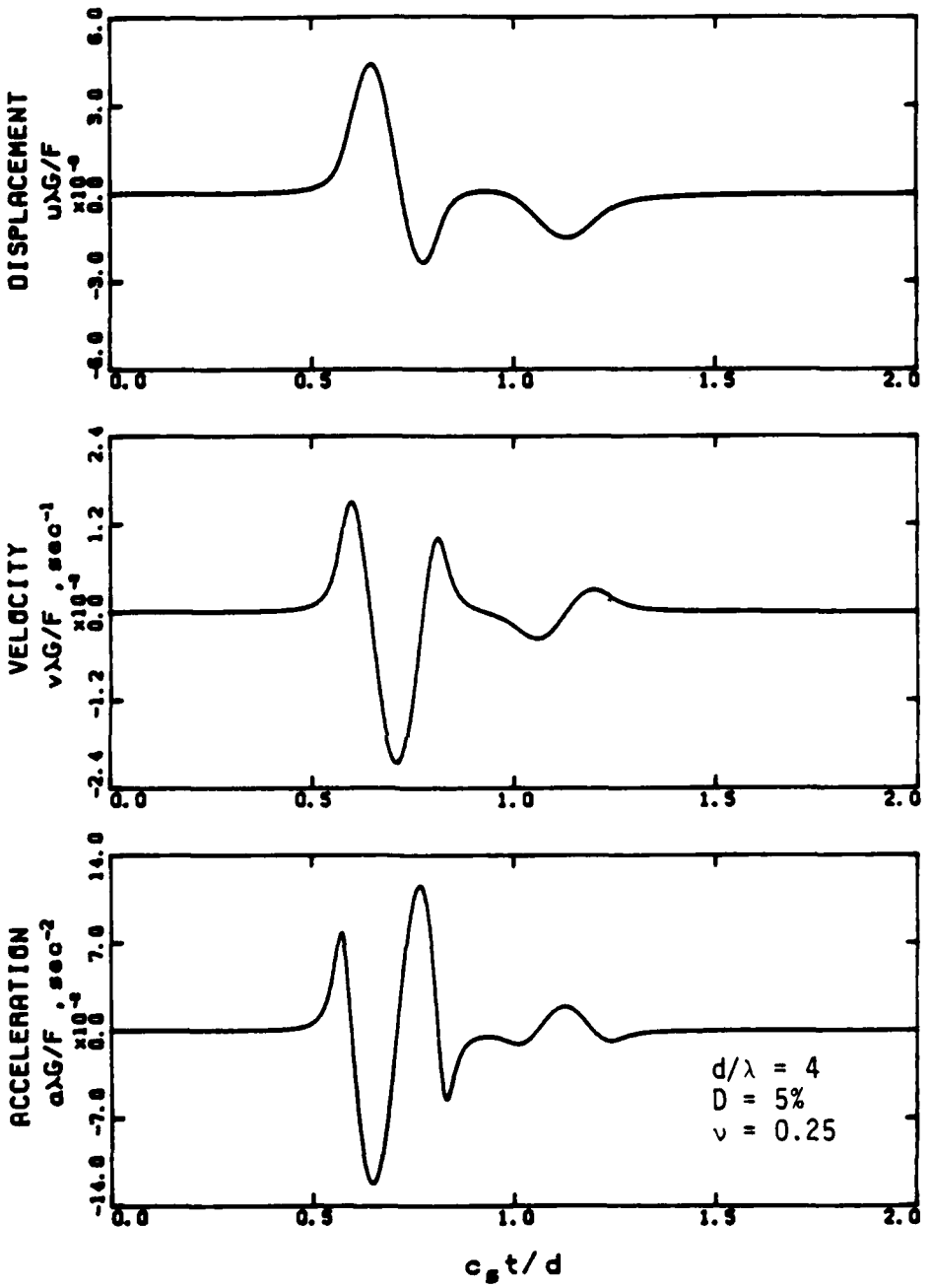

Fig. 2.7 - Displacement, velocity and acceleration records for three-dimensional longitudinal-motion.

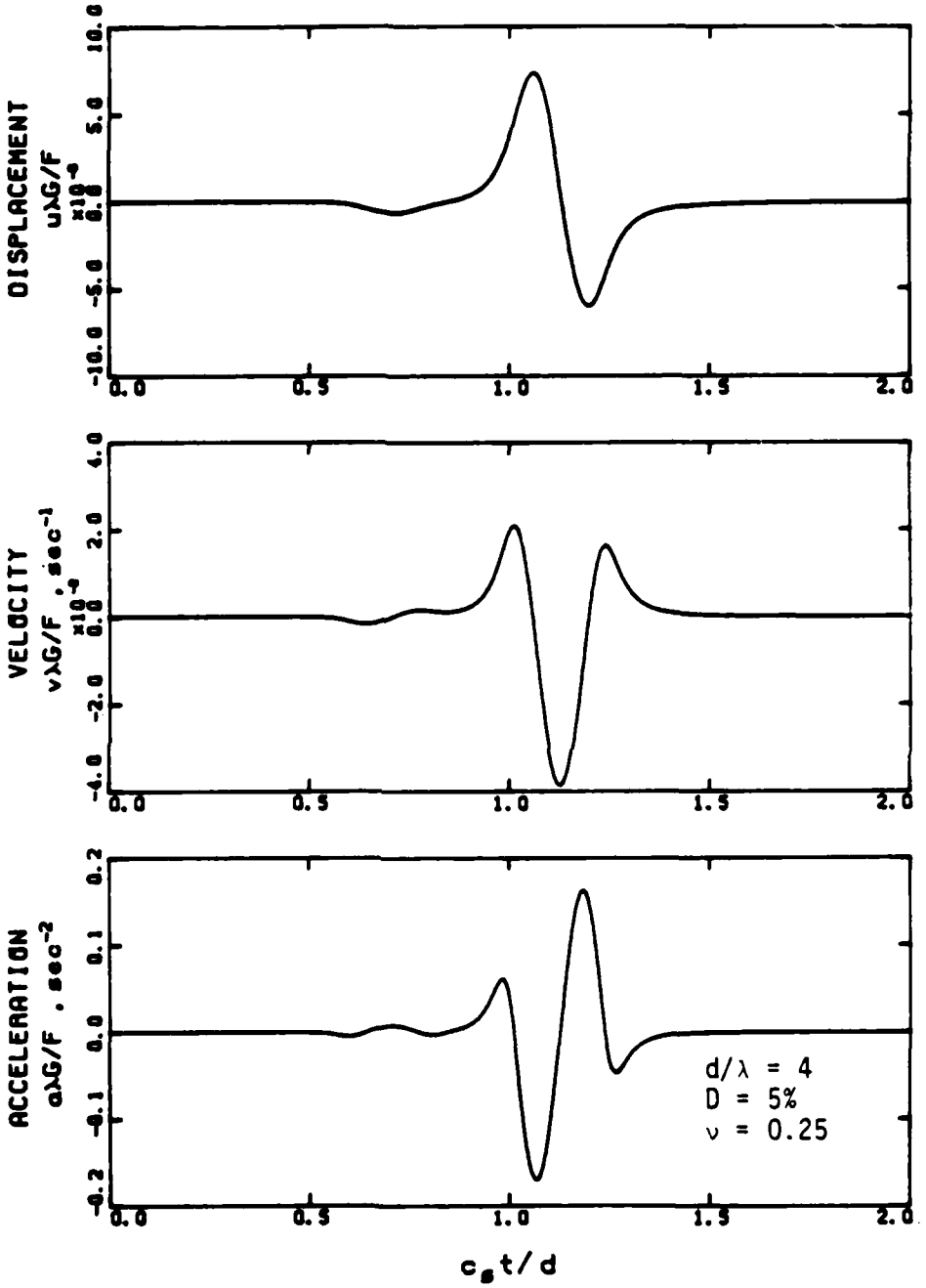

Fig. 2.8 - Displacement, velocity and acceleration records for three-dimensional shear-motion.

2.4 SUMMARY

Analytical formulations to compute wave propagation records of displacement, velocity or acceleration generated by a point load in the interior of two- or three-dimensional, isotropic, homogeneous, elastic full-spaces has been presented in this chapter. The formulations are based on Fourier synthesis of the Green's functions. The loading conditions and fast Fourier transform parameters used in the computations for the examples shown in the next two chapters are given in Section 2.3.

CHAPTER THREE

CHARACTERISTICS OF BODY WAVE SIGNATURES

3.1 INTRODUCTION

Evaluation of in situ soil properties and site characterization from wave propagation records is gaining acceptance in engineering practice. However, the level of use is very superficial because the understanding of the wave record is basically limited to "first-arrival" determinations. In some cases estimation of the "apparent" wave arrival may even lead to erroneous values of elastic moduli. A better understanding of the waveforms, the effect of different parameters on the time of arrival of the waves and a better use of all the information provided by the wave record is necessary for a more efficient use of seismic methods. A series of analytical studies on the time histories of body wave signatures is presented in the following sections.

3.2 ANALYSIS OF TIME RECORDS

Waveforms obtained in the time domain at a dimensionless distance, $d/\lambda = 2$ are presented in Figs. 3.1 through 3.10 for different kinds of body wave motion (where d is the distance from the point source to the receiver and $\lambda = c_s \cdot T_s$ is the "wavelength of the loading function"). All results are presented

in dimensionless form. The wave amplitude is presented as a dimensionless displacement uG/F for the two-dimensional cases (since the force F is per unit length), and as $u\lambda G/F$ for the three-dimensional cases (point forces). The time is presented in dimensionless form as $c_s t/d$. In this way, the theoretical time of arrival of the shear wave controlled by the elastic stiffness, $t_s = d/c_s$, always corresponds to a value of one, and the theoretical time of arrival of the longitudinal wave, $t_p = d/c_p$, corresponds to

$$c_s \cdot t_p/d = c_s/c_p = [(1-2\nu)/(2-2\nu)]^{1/2} \qquad (3.1)$$

which depends on the value of Poisson's ratio, ν. For most figures presented in this chapter, a value of 0.25 was used for Poisson's ratio. This ratio results in a theoretical arrival time of the P-wave of 0.577. Also, in these expressions and in all figures presented in this and other chapters, G, c_s and c_p represent the real values of the shear modulus, shear wave velocity and compressional wave velocity, respectively.

3.2.1 Medium with no material damping

The waveforms presented in Fig. 3.1 correspond to two-dimensional in-plane longitudinal motion. Consider the upper part of the figure which corresponds to a wave travelling in a medium with no material damping. The trace shown is composed of three basic parts. The first part on the left of the trace represents a quiet zone. This results from the fact that the impulse has been applied at the excitation point, but no energy has yet arrived at the target point. The second part, starting at the point indicated

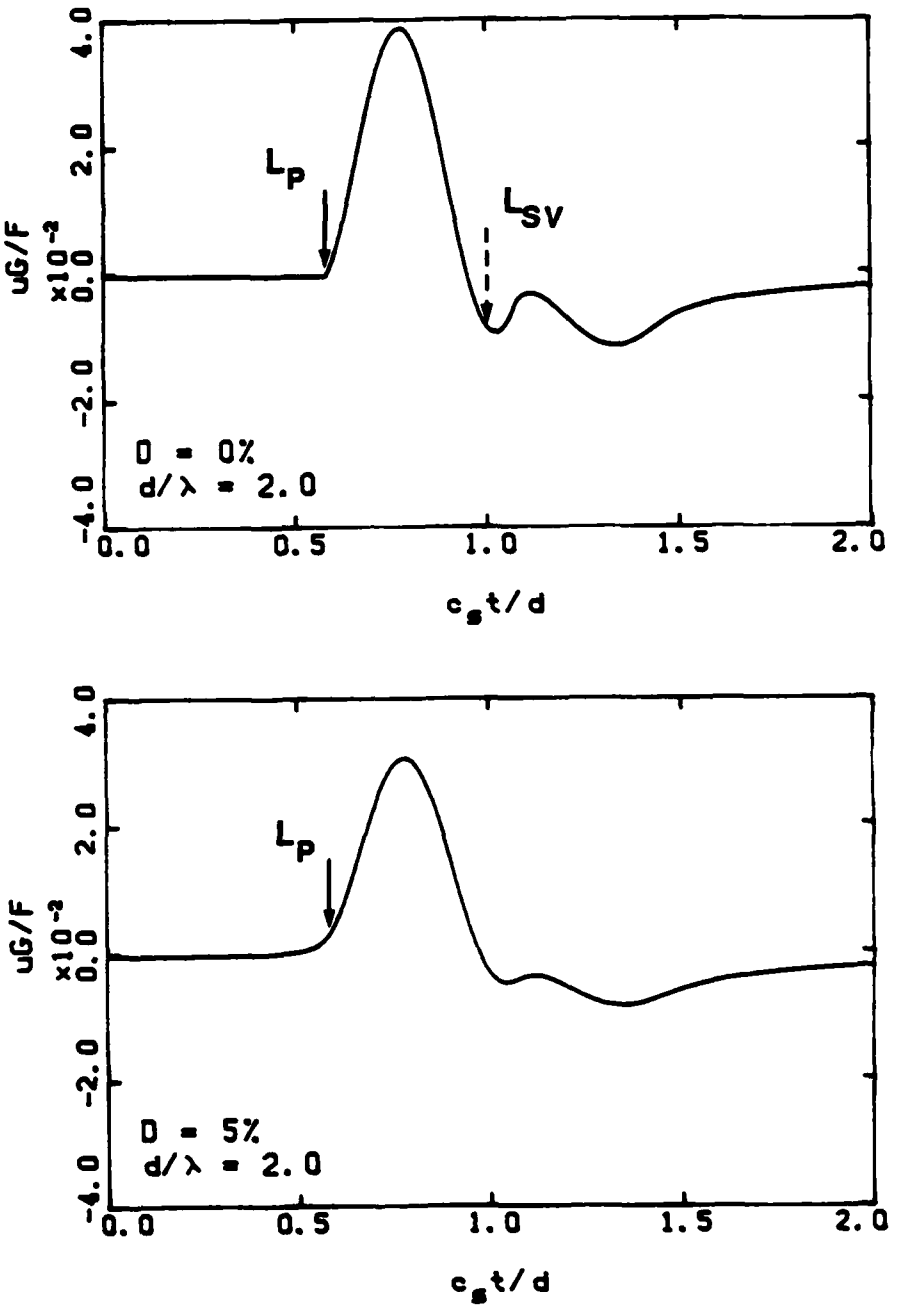

Fig. 3.1 - Two-dimensional in-plane longitudinal motion. Effect of different damping ratios.

by the solid arrow, includes a big excursion of the wave and lasts until a second excursion arrives at a dimensionless time of one, where the third part of the trace begins. The point where the wave arrives corresponds to a dimensionless time $c_s t/d = 0.577$. This time coincides precisely with the time of arrival of a wave traveling at the compressional wave velocity in a medium with Poisson's ratio equal to 0.25 (as used in this case). The second part of the wave (third part of the trace), starting at the point denoted by the dashed arrow, arrives at a dimensionless time equal to one, meaning that it is traveling at the shear wave velocity. Hence, the first part of the waveform is called the primary wave (P-wave), because it arrives first, and is denoted by the symbol L_p for reasons that will become obvious soon. The second part of the waveform is called the secondary wave, because it arrives second, and is denoted by L_{SV}. It should be noticed that even though the second part of the wave is traveling at the shear wave velocity, it does <u>not</u> represent a shear motion. This second part of the wave is actually a longitudinal motion (compression and extension) since the particle motion is in the direction of propagation of the wave. This second part of the waveform is called the near-field wave (or additional near-field wave) of the P-motion and is discussed in later sections.

A second set of records, similar to those presented in Fig. 3.1 for two-dimensional P-motion, is presented in Fig. 3.2 for two-dimensional SV-motion. Consider again the wave propagating in a medium with no material damping (upper trace). After a quiet period, a perturbation arrives at the target point. This arrival, indicated in the figure by the dotted arrow, comes at a time corresponding to the compressional wave velocity ($c_s t/d = 0.577$). The second and main part of the wave arrives at a dimensionless time equal to one (corresponding to the shear wave velocity).

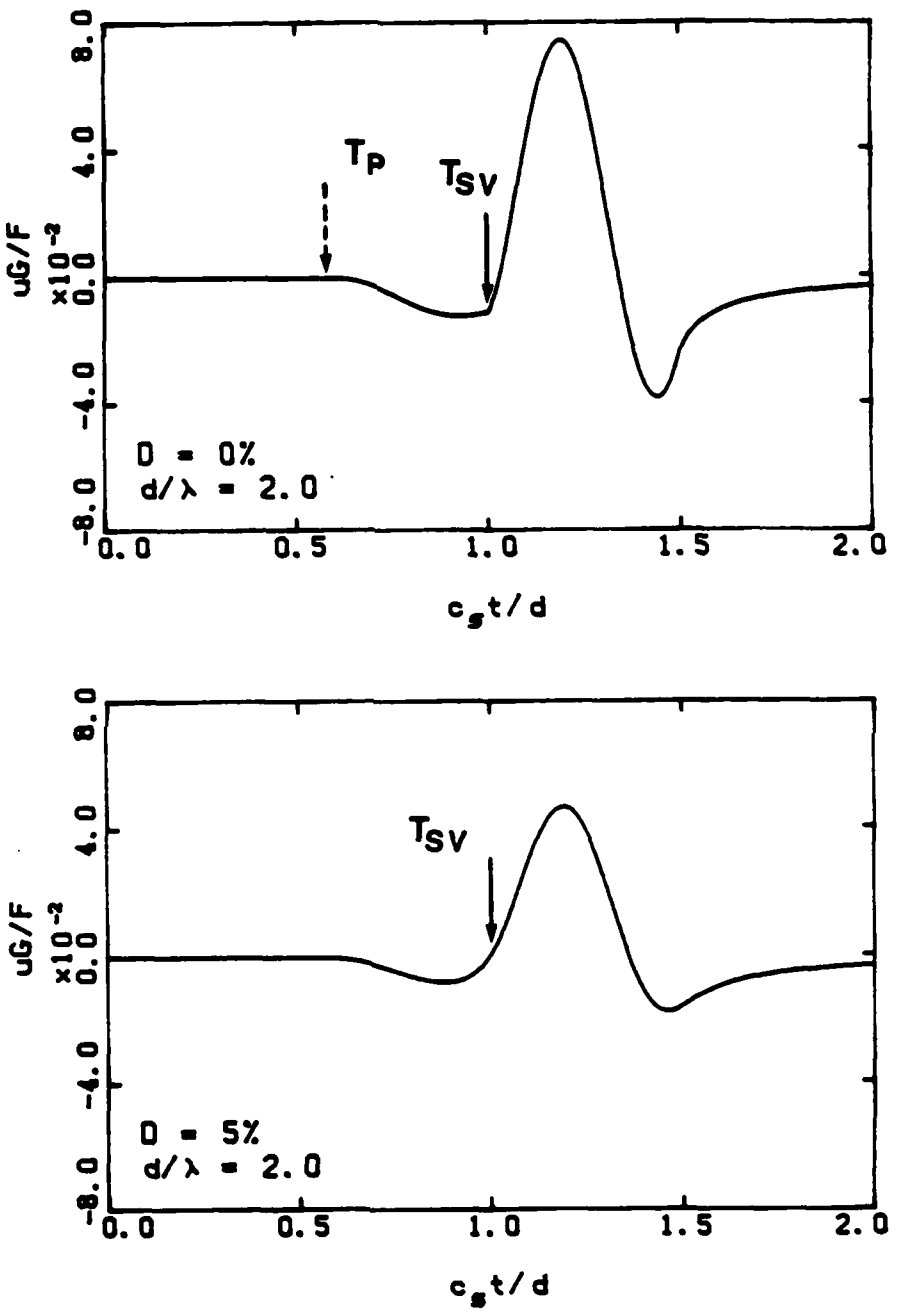

Fig. 3.2 - Two-dimensional in-plane shear motion. Effect of different damping ratios.

Again, the first wave arrival (between the two arrows) is called the P-wave, because it arrives first (primary), but is denoted by T_p, because it represents a transverse or shear motion. The second part (starting at the point indicated by the solid arrow) is called the S-wave (or SV-wave) and is denoted by T_{SV}. The P-wave (additional near-field in this case) represents that part of the energy transmitted at the compressional wave velocity, and the S-wave represents that part of the energy transmitted at the shear wave velocity (although in both cases the motion is in the same direction). Note that, in general, when P-motion (longitudinal motion) is being measured, as in the case in Fig. 3.1, most of the energy is carried by the P-wave, L_p, (indicated by the large amplitude excursion of this wave). On the other hand, when shear motion is being monitored, the bulk of the energy is transmitted by the shear wave, T_{SV} (Fig. 3.2). This is true at distances that are far from the source (which $d/\lambda = 2$ corresponds to). When the receiver is located near the source, the additional near-field wave may carry as much energy as the other wave. Records of waveforms monitored at other distances are presented in Figs. A.1 through A.4. Notice that, in these figures, the wavelength is constant from one graph to the next. Because the horizontal axis is normalized with respect to the distance from the source to the receiver and this distance varies from one graph to the other, the horizontal scale is changing giving the impression that the wavelength is varying.

Two-dimensional SH-motion at a point located at a distance $d/\lambda = 2$ from the source is shown in Fig. 3.3. This kind of motion is characterized by a pure shear wave. All energy is transmitted at the shear wave velocity as can be observed in the upper trace of Fig. 3.3. SH-motion will help clarify certain topics in the following sections. But for the moment, notice that there is no

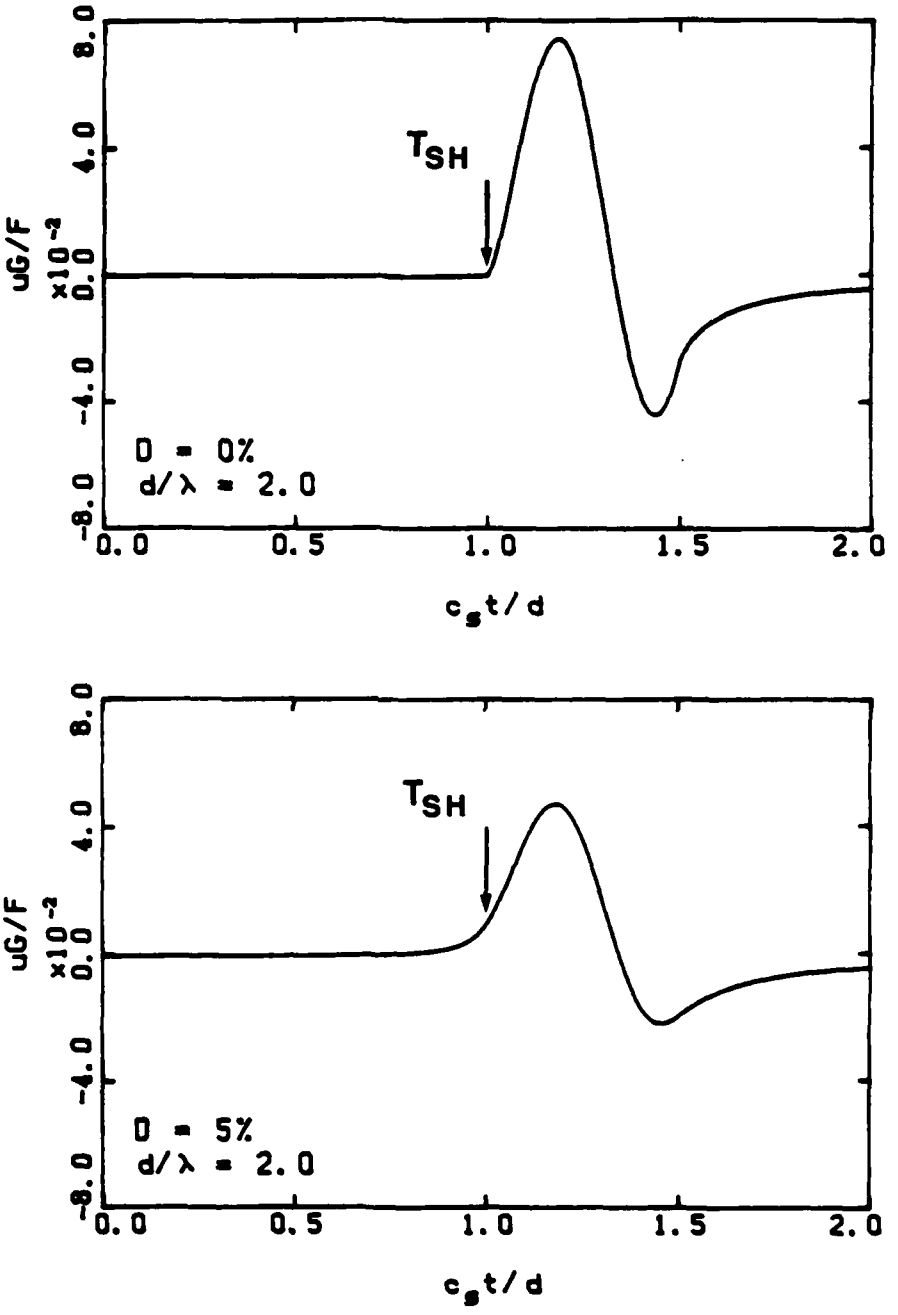

Fig. 3.3 - Two-dimensional antiplane shear motion. Effect of different damping ratios.

P-wave energy coupled with the SH-motion. Additional antiplane motion (SH-motion) records of wave propagation in a medium with no material damping are included in Figs. A.5 and A.6.

Three-dimensional motion is presented in Figs. 3.4 and 3.5. The same conclusions drawn for the two-dimensional motions apply to the three-dimensional case. The secondary wave arriving at a dimensionless time of one in Fig. 3.4 does not present a clear arrival. This is due to the coupling of the primary and secondary waves which distorts the shape of the waves. Actually the sharp angle in Fig. 3.4 is caused by the P-wave energy terminating at that point and not to the arrival of the S-wave energy. It should also be noticed that, in the three-dimensional case, there is no pure S-wave. This occurs because of the inherent coupling between P- and S-waves generated by the point source. Records of waveforms monitored at other distances are presented in Appendix A (Figs. A.7 through A.10). A look at these records further clarifies the topic.

A first conclusion can be reached at this point. If compression wave velocity is to be determined from wave propagation records, it is easier and more accurate to measure the time of arrival from records of P-motion than from records of S-motion. Similar conclusions can be made with respect to shear wave velocity. In terms of practical application, this conclusion means that three-dimensional sensors oriented along the directions of particle motions must be used in seismic testing to obtain the most precision.

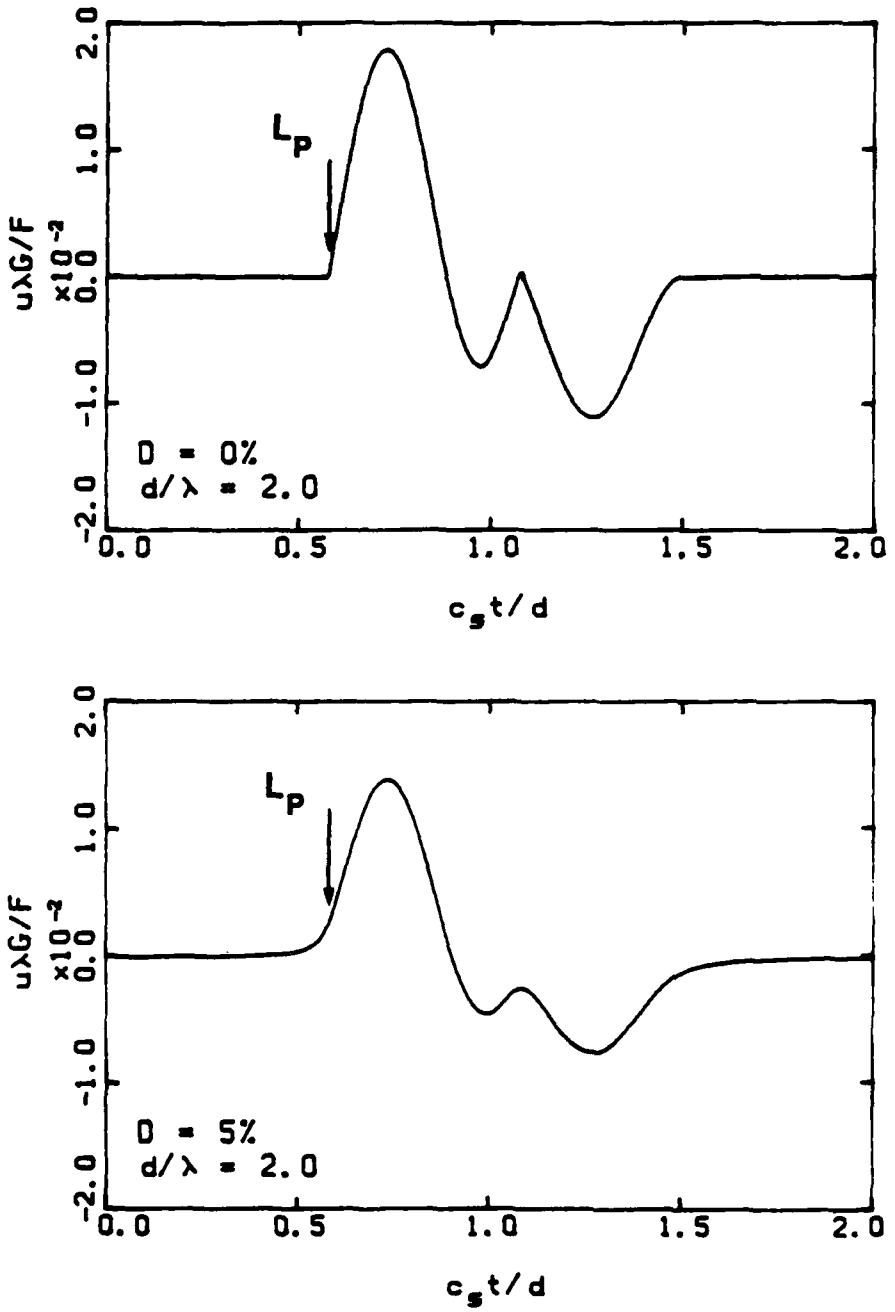

Fig. 3.4 - Three-dimensional longitudinal motion. Effect of different damping ratios.

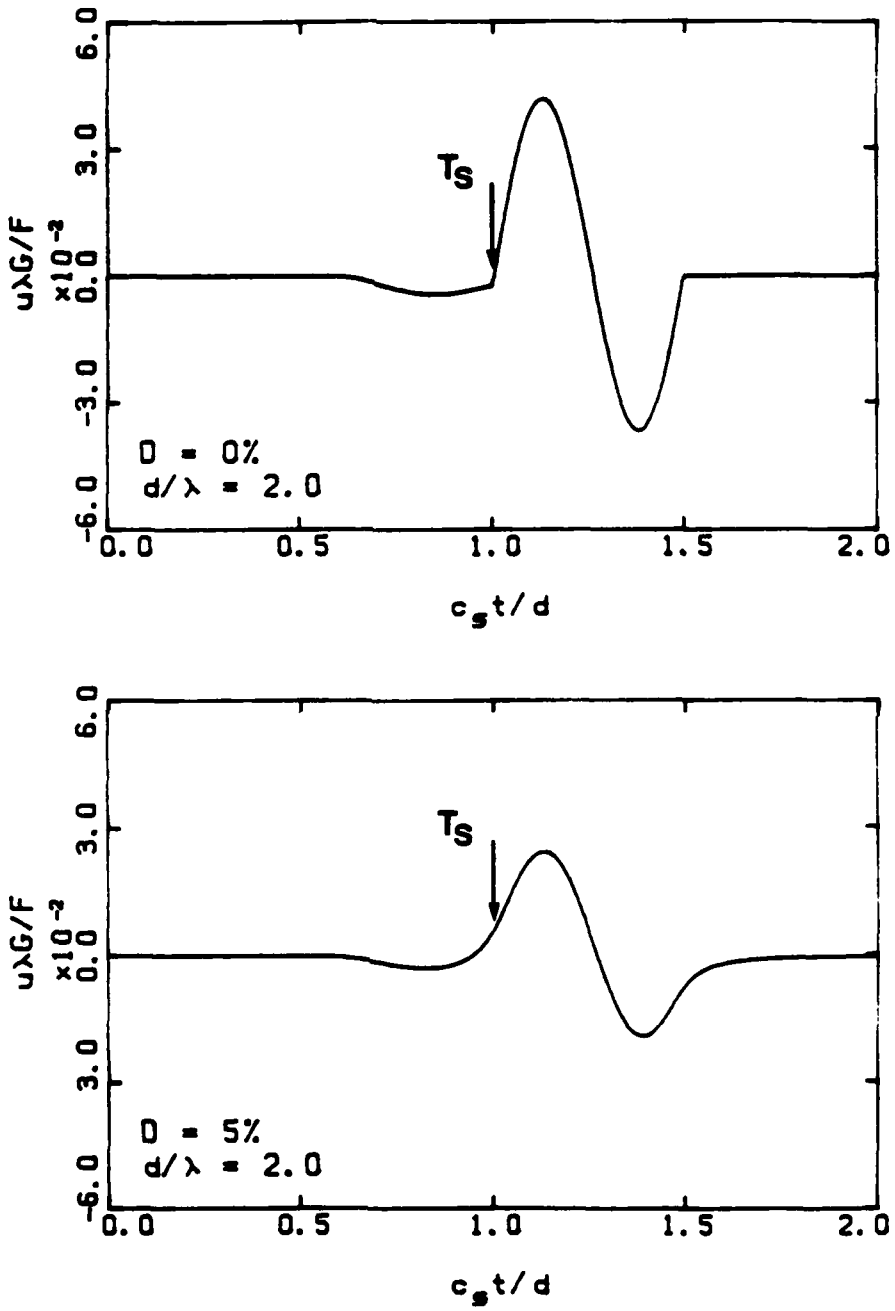

Fig. 3.5 - Three-dimensional shear motion. Effect of different damping ratios.

3.2.2 Medium with material damping

Records of wave propagation in a medium with no material damping have been considered so far. In the lower traces of Figs. 3.1 through 3.5 and in Figs. A.11 through A.20, synthetic records of waves propagating in a medium with five percent material damping are presented. It can be observed in these figures that the general shape of the waveforms remains the same as those for waves propagating in a medium with no damping. Both primary and secondary waves are encountered in two-dimensional P- and SV-motions as well as in three-dimensional motions; and a pure shear wave is encountered in only two-dimensional SH-motion. It is further observed that the amplitude of the waves has decreased compared to the amplitude of the waves in a material without damping; but the most important fact is that the time of arrival is no longer easy to identify. The arrival of the wave is not marked by a sudden change of slope, as in the case with no damping, but is represented by a smooth change.

It has been noted that for real materials, the time of arrival chosen depends many times on the amplification applied to the time history record (Ricker, 1953; Hoar and Stokoe, 1978). The higher the amplification, the sooner the waves seem to arrive. The synthetic records shown in Figs. 3.1 through 3.5 and A.11 through A.20 clearly exhibit this point. It is also observed in the synthetic records that the waves arrive earlier than the arrival times calculated from the theoretical velocities of propagation, c_s or c_p (c_s and c_p being the real values). The theoretical propagation velocities (c_s^D and c_p^D) caused by the use of complex shear and compressional wave velocities ($c_s^* = c_s + ic_{sI}$ and $c_p^* = c_p + ic_{pI}$) are

$$c_p^D = [c_p^2 + (c_{pI})^2]/c_p \tag{3.1}$$

and

$$c_s^D = [c_s^2 + (c_{sI})^2]/c_s \tag{3.2}$$

in which

c_{pI} and c_{sI} are the imaginary parts of the complex velocities, and

c_p^D and c_s^D are the damped propagation velocities.

The damped velocities, c_p^D and c_s^D, are practically identical to c_s and c_p, respectively (with differences smaller than 0.25 percent for values of the damping ratio smaller than five percent). A discussion and derivation of the relationships between elastic and damped body wave velocities and moduli is presented in Appendix B.

The theoretical times of arrival ($t = d/c_s$, or $t = d/c_p$) are marked with arrows in Figs. 3.1 through 3.5. Times obtained from the first arrival of the wave will lead to estimates of the shear or compression wave velocities of the medium which are slightly too high. This "sooner" arrival of the waves is a problem encountered in the field and should always be kept in mind when analyzing real time records. Other approaches that eliminate the uncertainty in the arrival-time estimation are presented in the next chapter.

3.2.3 Effect of Poisson's ratio

Finally the effect of Poisson's ratio, ν, is studied in Figs. 3.6 through 3.10. In the upper part of these figures are the records of waves propagating in a medium with a low Poisson's ratio

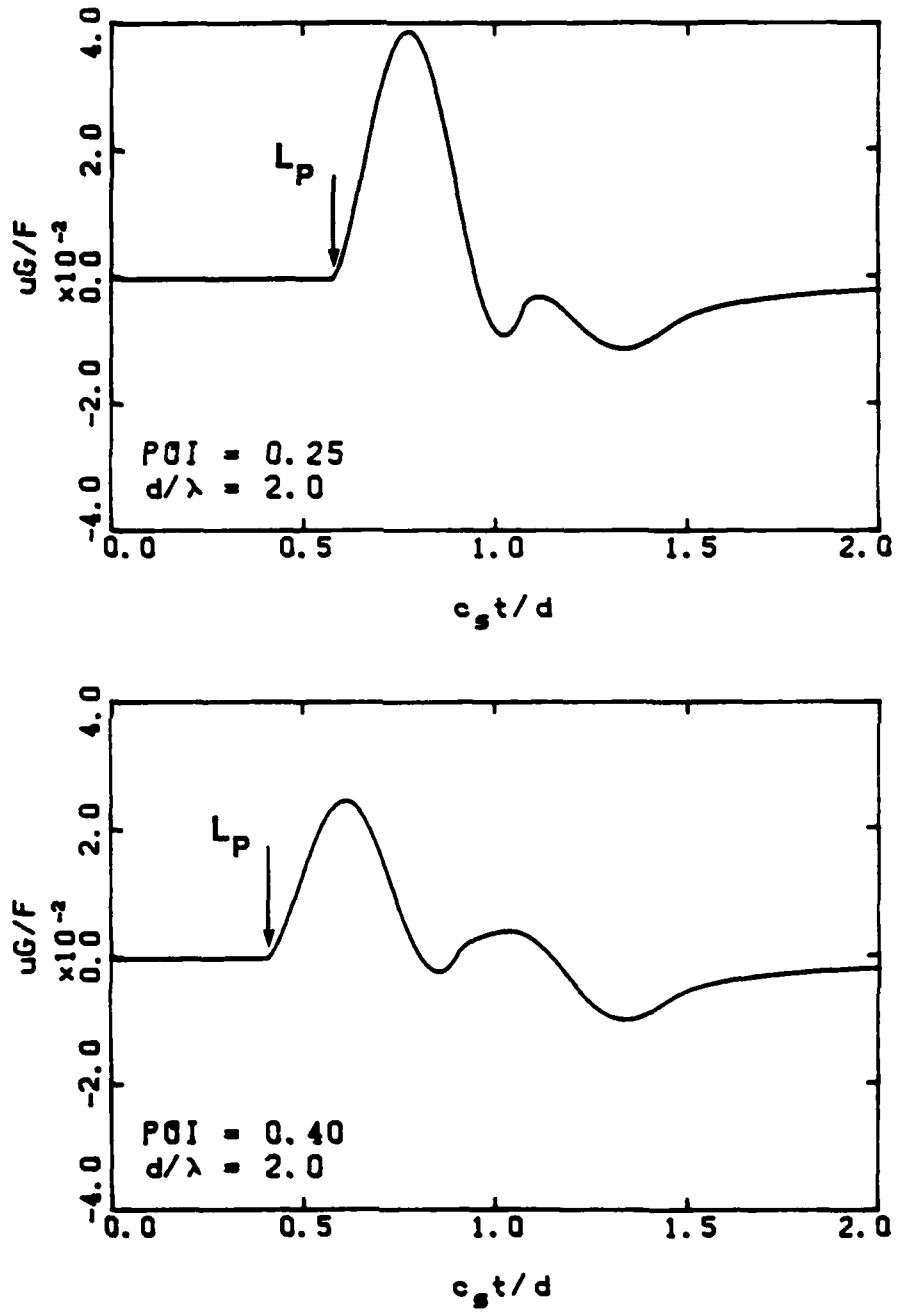

Fig. 3.6 - Two-dimensional in-plane longitudinal motion. Effect of Poisson's ratio.

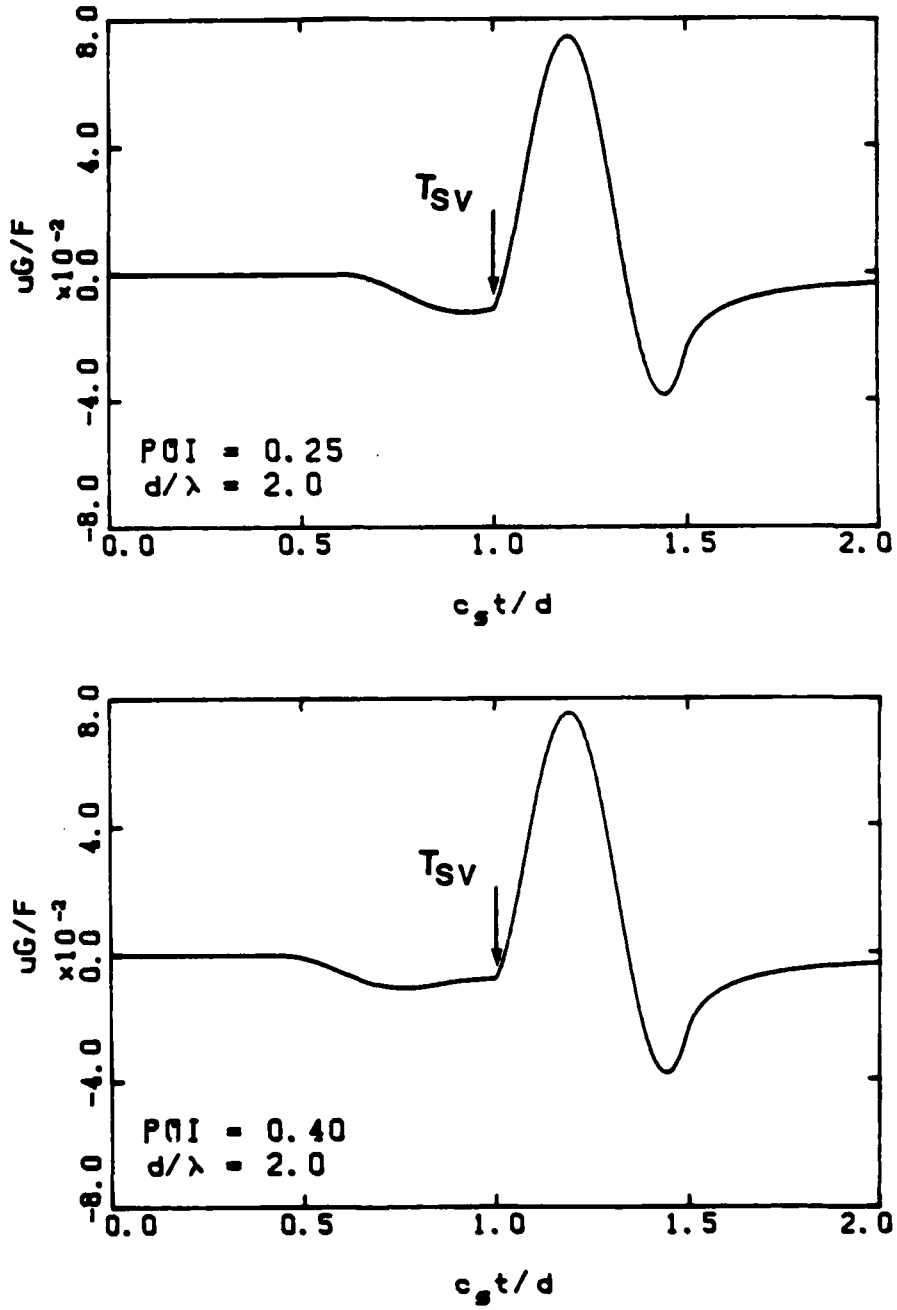

Fig. 3.7 - Two-dimensional in-plane shear motion. Effect of Poisson's ratio.

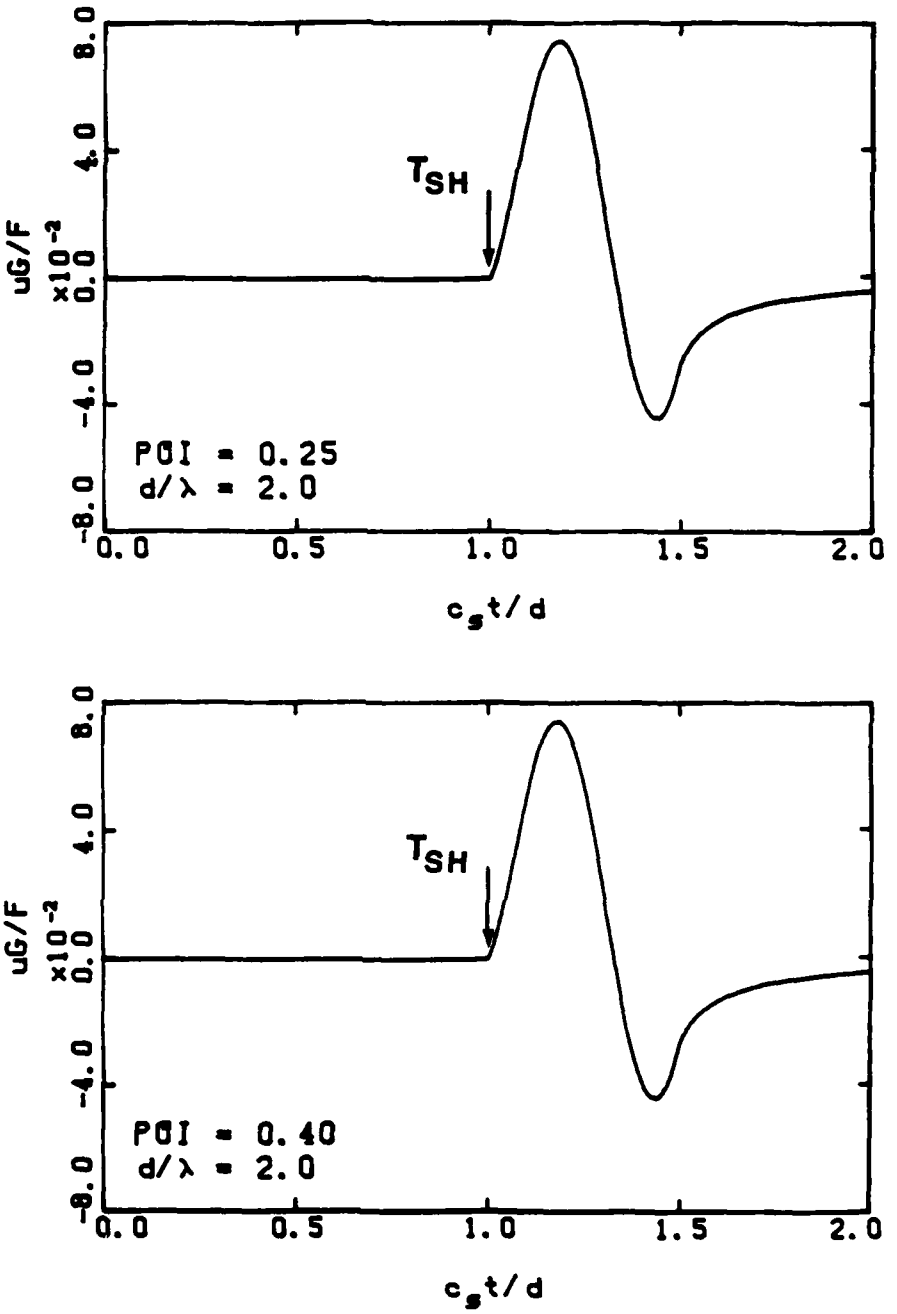

Fig. 3.8 - Two-dimensional antiplane shear motion. Effect of Poisson's ratio.

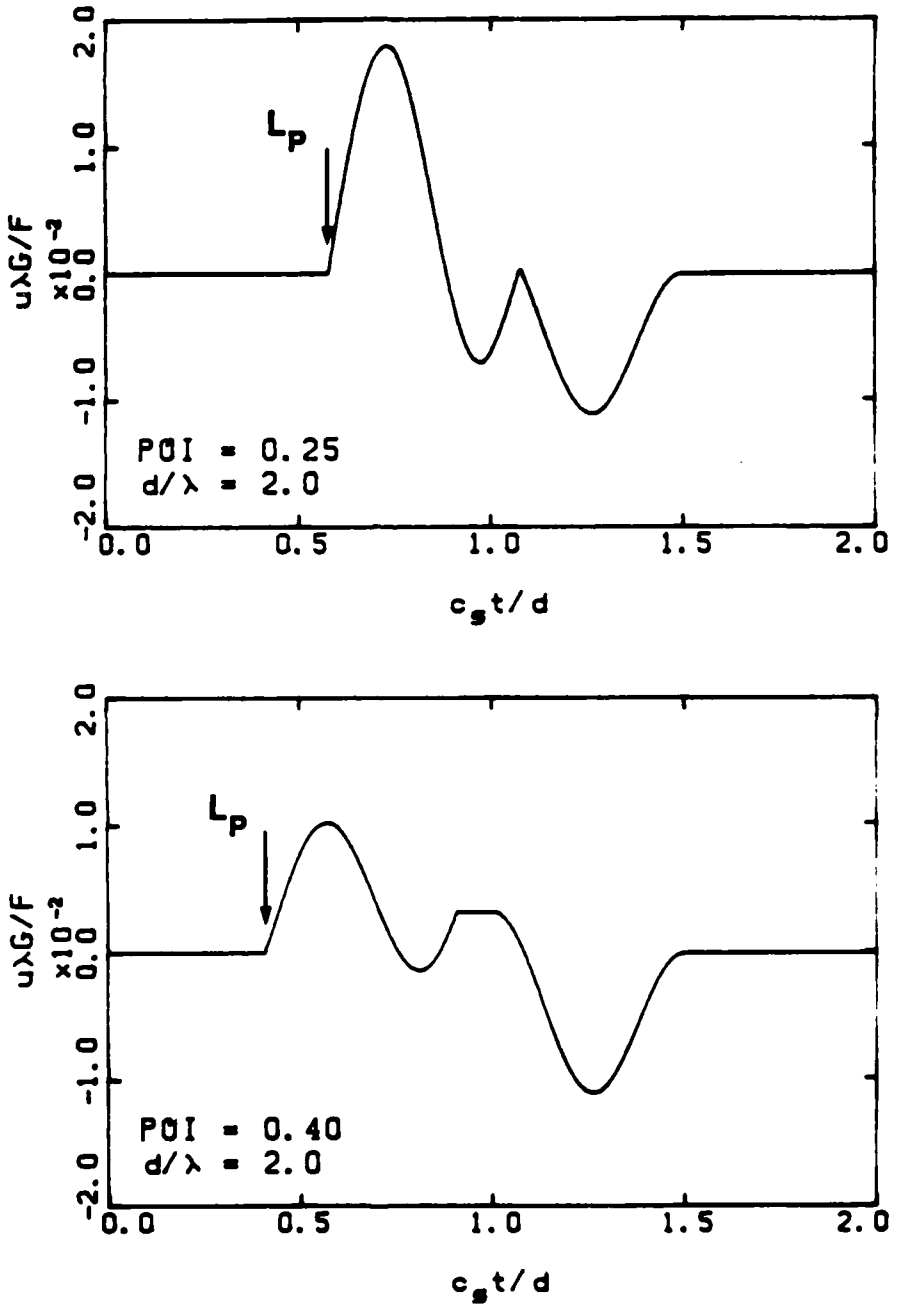

Fig. 3.9 - Three-dimensional longitudinal motion. Effect of Poisson's ratio.

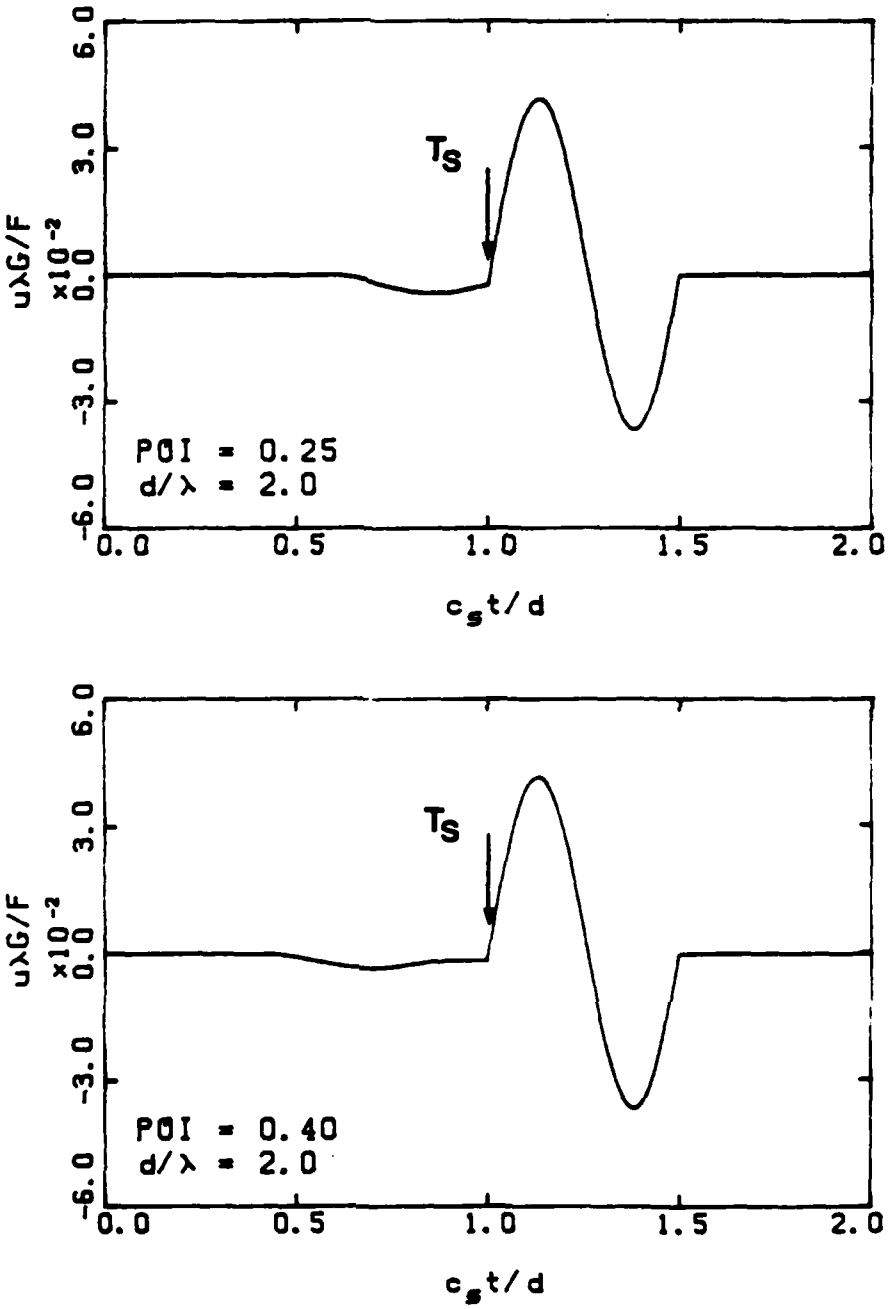

Fig. 3.10 - Three-dimensional shear motion. Effect of Poisson's ratio.

(ν = POI = 0.25) and in the lower part are corresponding waves in a medium with a higher Poisson's ratio (ν = POI = 0.4). All the results are for a material with no damping.

The first observation that can be made is that Poisson's ratio does not affect the secondary wave characteristics. Secondly, the P-wave velocity increases as ν increases. According to Eq. 3.1 the dimensionless time of arrival for a Poisson's ratio of 0.4 should be 0.408 as is the case. Finally it can be observed that, due to the higher stiffness, the amplitude of the P-waves decrease with increasing Poisson's ratio. A complete set of records at other distances from the source is given in Appendix A.

3.3 NEAR-FIELD EFFECTS

It was indicated in the previous section that, in all the motion records except for those of two-dimensional SH-motion, two types of waves appeared in the waveform, one travelling at the longitudinal wave velocity (P-wave) and the other travelling at the shear wave velocity (S-wave). If one inspects the time history records of longitudinal motion at different distances from the source (presented in Appendix A), it can be observed that the amplitude of the secondary wave (L_{SV}) in these P-motion records is attenuating at a much faster rate than the main event (the P-wave). At a certain distance from the source, the amplitude of the S-wave (L_{SV}-wave) becomes insignificant compared with the amplitude of the P-wave (L_P-wave). Therefore, the S-wave (L_{SV}-wave) in a pure longitudinal-motion (P-motion) record (no shear motion) only "exists" at distances that are close to the source and is commonly referred to as the additional near-field wave or near-field wave (Aki and Richards, 1980; White, 1983).

Similarly, in a shear motion (transverse motion) record, there are two events present: one travelling at the compressional wave velocity (a P-wave, T_p) and a second travelling at the shear wave velocity (T_{SV}). The first event (T_p) is, in this case, the one that decays at a faster rate and represents the additional near-field effect.

To illustrate this point, consider the case of three-dimensional shear-motion in Eqs. 2.11 and 2.12. The first exponential in Eq. 2.12 represents a wave that is propagating at the shear wave velocity, c_s, ($e^{-ia_o} \cdot e^{i\omega t} = e^{i\omega[(r/c_s)-t]}$), while the second exponential is a wave propagating at the compressional wave velocity, c_p. The amplitude of the wave travelling at the shear wave velocity is composed of terms that vary with $1/r$, $1/r^2$ and $1/r^3$, whereas the amplitude of the wave propagating at the compressional wave velocity has terms varying at $1/r^2$ and $1/r^3$. Therefore, at large distances from the source (large r's), the controlling term is that attenuating at a rate $1/r$. This term is usually called the far-field term, since it is the only one existing at far distances from the point of excitation. The other terms, those propagating at the shear and compression wave velocities are called the additional near-field terms (or near-field terms). Notice that the wave travelling at the shear wave velocity also has near-field terms. However, since these components are travelling with the far-field component, they are undistinguishable in the wave record, and the term near-field is usually applied only to the components of the P-wave. An analogous reasoning can be made for the three-dimensional longitudinal-motion and for the two-dimensional motions. Further illustrations are given in Section 3.5.

In summary, when monitoring a pure longitudinal-motion (P-motion), the P-wave represents the main event called the far-field effect, and the S-wave represents the near-field effect. When exciting a pure shear motion (S-motion), the S-wave is the main event (far-field effect) and the P-wave is composed only of near-field terms.

3.4 POLARITY REVERSALS UPON REVERSING THE IMPULSE

It should be noted that when the direction of the impulse is reversed, both near- and far-field terms change polarity. However, when measuring transverse motion in crosshole and downhole tests, it is frequently found that S-waves change polarity but P-waves keep the same polarity when the direction of the impulse is reversed. To explain this behavior, several conditions should be considered. First, to generate a shear motion (transverse motion) with a crosshole source, a vertical impulse is applied to the source. Since the source is of finite length and is usually wedged in a borehole when the vertical impulse is applied, a longitudinal motion is generated along with the shear motion. Second, when reversing the direction of the vertical impulse, the direction of the transverse motion is reversed, but the direction of the longitudinal motion remains the same.

For the conditions cited above, a receiver will only monitor the transverse motion and will not record any of the longitudinal motion if the receiver used to record the transverse motion is placed in a perfect vertical position (perpendicular to the direction of propagation) . Under these conditions, the P-wave recorded at the vertical receiver will be exclusively produced by near-field terms of the transverse motion. Therefore, when the

direction of the impulse is reversed, both P- and S-waves should reverse polarity. However, when placing "vertical" receivers in the field, the receivers are very seldom in a perfect vertical position, and they are most commonly imperfect receivers. (They exhibit some cross-sensitivity.) The small inclination of the receiver and/or the small cross-sensitivity present in receivers will allow the recording of a small component of the longitudinal motion. The waveform record will then be composed of both S- and P-motions with their corresponding near- and far-field terms. When the direction of the impulse is reversed, the transverse motion reverses but not the longitudinal motion. Therefore, unless the near-field wave associated with the transverse motion recorded is larger than the far-field component of the part of the longitudinal motion recorded by the receiver, the polarity of the P-wave will not change.

To illustrate this point, longitudinal- and transverse-motion records produced by horizontal and vertical point loads applied at a distance of two wavelengths from the source are presented in Fig. 3.11 as recorded by a perfect vertical receiver (zero cross-sensitivity and perfect vertical orientation, ϕ = 0 degrees). Time histories of forward and reversed vertical impulses as monitored by the perfect vertical receiver are shown in Fig. 3.12. It can be observed that the P-wave is exclusively composed of the near-field effect in the transverse-motion record and that both traces are opposite (reversed) but otherwise identical. The case of a receiver which is inclined 30 degrees (ϕ = 30 degrees, $\pi o\theta$ illustration purposes in which part of the inclination could correspond to cross-sensitivity effects) with the vertical is considered in Fig. 3.13. The lower trace in this figure is composed of seven-tenths of the shear motion produced by the direct impulse and by half of the longitudinal motion. In the upper

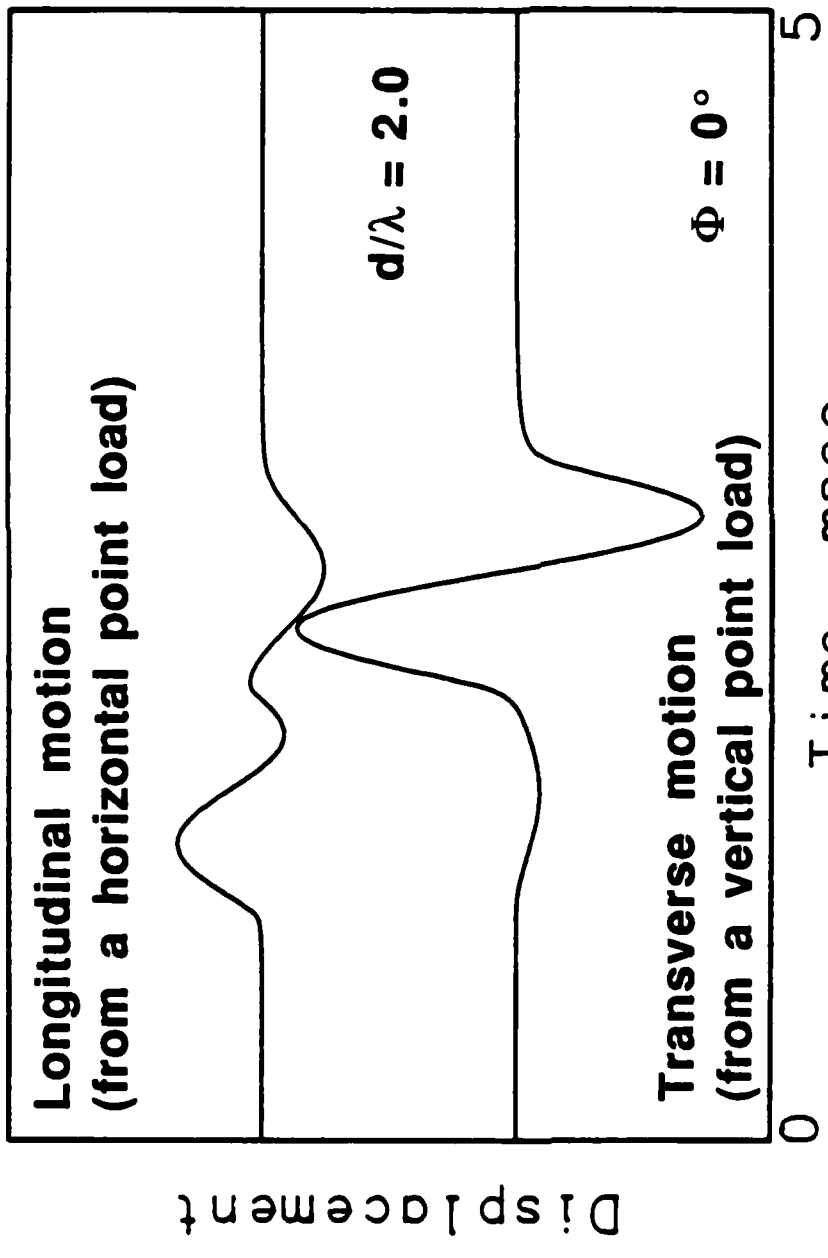

Fig. 3.11 - Longitudinal- and transverse-motion records as monitored by a perfect vertical receiver.

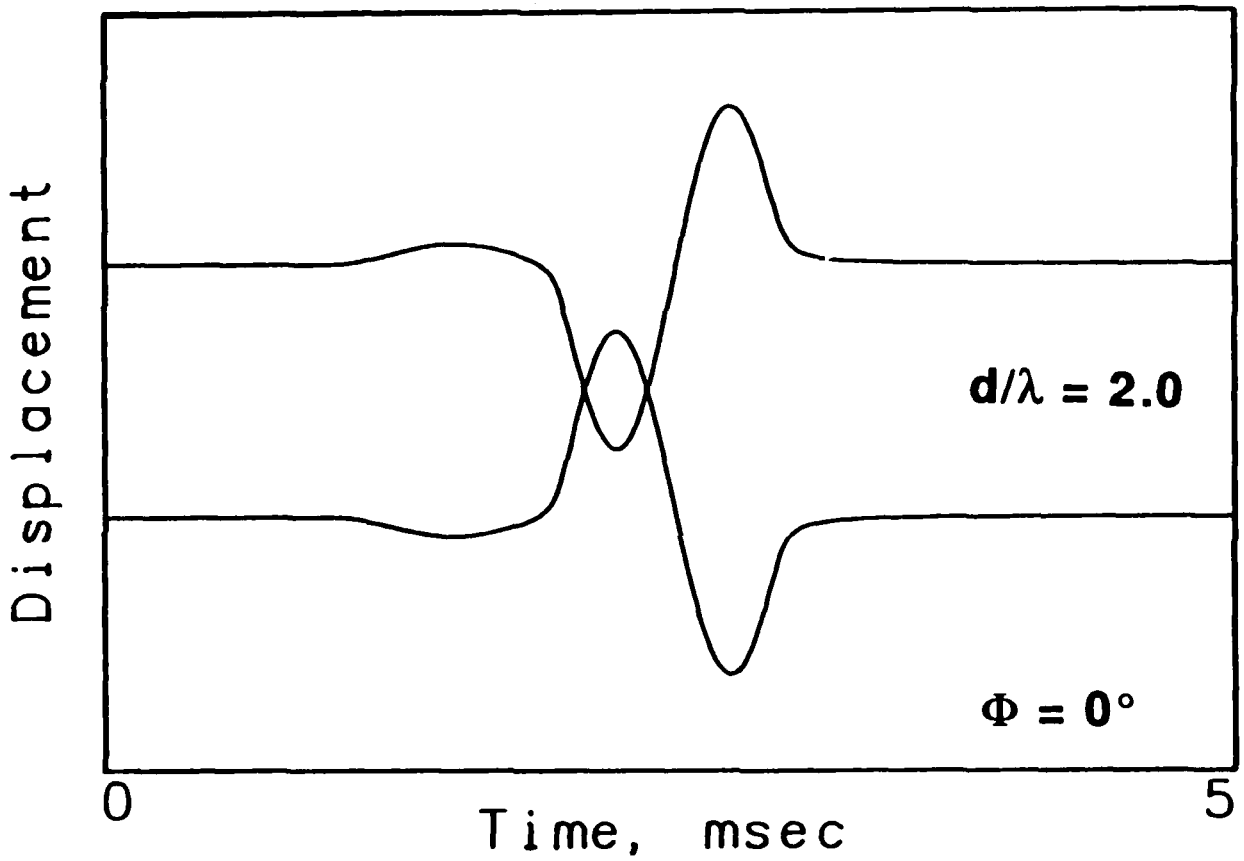

Fig. 3.12 - Transverse-motion records produced by reversed impulses as monitored by a perfect vertical receiver.

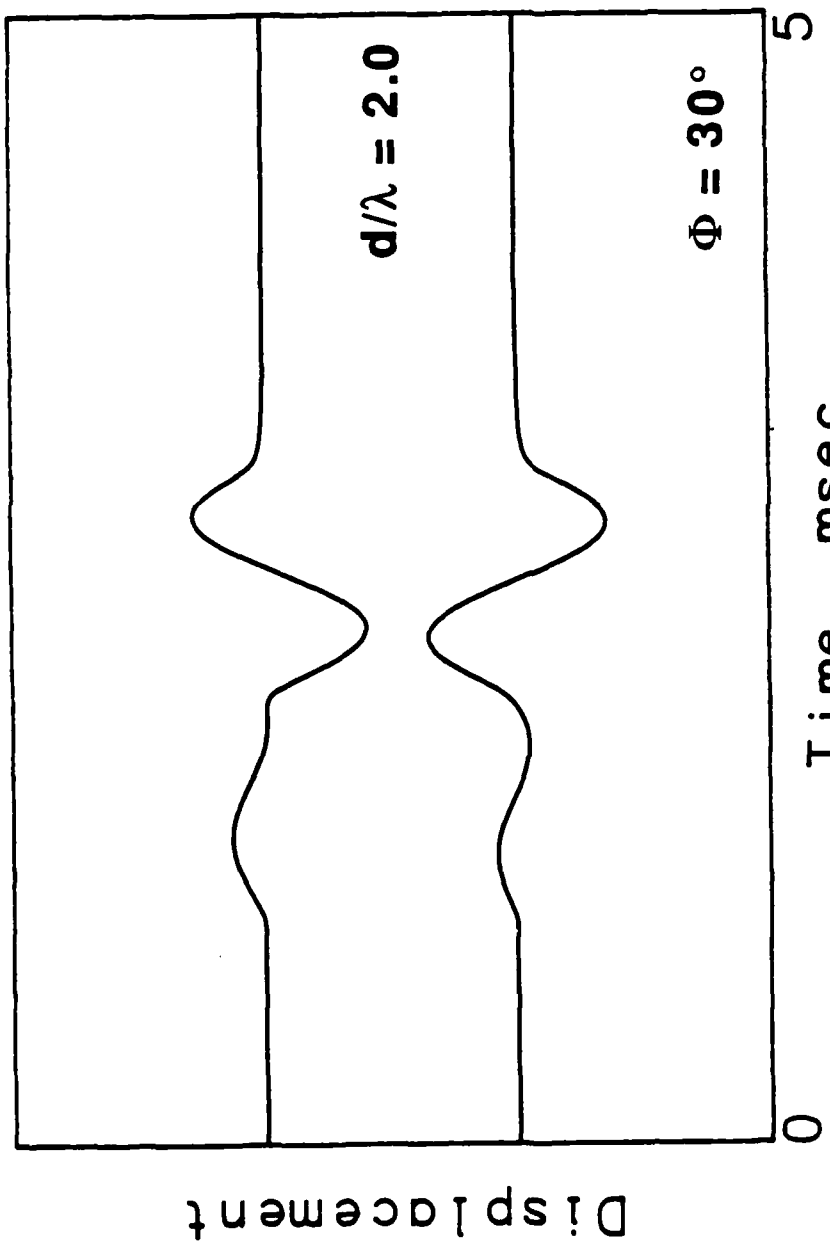

Fig. 3.13 - "Transverse-motion" records produced by reversed impulses as monitored by a receiver with a 30 degree inclination.

trace, that corresponds to the reverse impulse, the shear motion has reversed but the longitudinal motion has remained with the same sign. Since one half of the P-motion carried more P-wave energy than seven-tenths of the S-motion record, the combined waveform resulted in initial P-waves that did not reverse polarity when the direction of the impulse was reversed.

A similar line of reasoning can be used when the source and receiver are not at the same depth for a crosshole test, or for other cases in a downhole test.

3.5 WAVE AMPLITUDE DECAY

The amplitudes of seismic waves decrease as the waves propagate through a medium. This decay of wave amplitude is caused by two mechanisms: 1) spreading of wave energy from a source, generally called geometrical or radiational damping, and 2) dissipation of elastic energy due to primarily frictional losses in the material itself, commonly known as attenuation, material or internal damping.

Records of displacement with time at different distances from the source are presented in dimensionless form in Appendix A. The records are for two- and three-dimensional wave propagation in media with material damping of 0 or 5 percent and Poisson's ratio of 0.25 or 0.4. The input to the medium is one cycle of a sine wave, as described in Section 2.3, and the parameters used in these figures are the same as those described in Section 3.2.

Two-dimensional motion in a medium with no damping and Poisson's ratio of 0.25 is shown in Figs. A.1 through A.6. It can

be observed that for motions in which the primary and secondary waves are coupled, the coupling occurs mainly at short distances from the source ($d/\lambda < 2$). At larger distances, the P-wave has separated from the S-wave, and the two waves can be clearly distinguished from each other. The minor wave (S-wave in the case of P-motion and P-wave in the case of SV-motion) attenuates at a faster rate than the major wave. These minor waves, the additional near-field waves, only exist at short distances from the source. It should be noticed, however, that at short distances the energy carried by the near-field terms can be a substantial amount of the total energy in the waveform. Wave amplitude decay in these figures is due exclusively to radiation damping, since material damping, D, is zero.

A similar situation arises for motions in a three-dimensional full-space (Figs. A.7 through A.10). However, the amplitude of the waves decreases much faster than in the two-dimensional cases. This faster decay is due to the spreading of the energy from a point source in a spherical pattern while in the two-dimensional case the energy spreads in a cylindrical pattern from a line source.

Motion in a medium with five percent material damping is presented in Figs. A.11 through A.20. The behavior is similar to that in the medium with no material damping but amplitudes are decreasing with distance at a faster rate due to the energy lost in each cycle because of internal friction.

Finally a set of records corresponding to propagation in a medium with no damping and a Poisson's ratio of 0.4 is presented in Figs. A.21 through A.28. The behavior is similar to that described when Poisson's ratio was 0.25. The amplitude of the P-wave

component of the motion is, however, smaller when Poisson's ratio is 0.4. No records are included for SH-motion since they are the same as those when Poisson's ratio is 0.25.

To study the attenuation behavior of body wave amplitude with distance due to radiation damping, the variation of wave amplitude with distance for steady-state motion has been plotted in Figs. 3.14 through 3.18. In these figures the displacement amplitude is normalized as uG/F for two-dimensional motions and as $u\lambda G/F$ for three-dimensional motions (as in the figures in Appendix A), and the distance from the steady-state source to the receiver (d) is normalized by dividing by the wavelength of the shear wave ($\lambda = c_s/f$). The material considered as the propagating medium has a Poisson's ratio of 0.25 and no material damping. (The rest of the parameters are explained in Section 2.3). A frequency of 100 Hz was used for the computations.

The amplitude decay for a two-dimensional event is shown in Figs. 3.14, 3.15 and 3.16 for P-, SV- and SH-motions, respectively. It is observed that the general trend indicates that the amplitudes decay with the square root of the distance. This is particularly clear in Fig. 3.16 for SH-motion amplitude decay. For very small distances or very low frequencies ($d/\lambda < 0.2$), all wave amplitudes decay at a rate that is slightly smaller than with the square root of the distance. For P- and SV-motion the amplitude decrease is in proportion with the square root of the distance only at long distances. The value of this "long distance" seems to be of the order of two or three shear wavelengths (λ) for the shear motion and ten shear wavelengths for the longitudinal motion. (This distance translates to approximately five compression wavelengths). In the range of distances where the coupling of the P- and S-wave

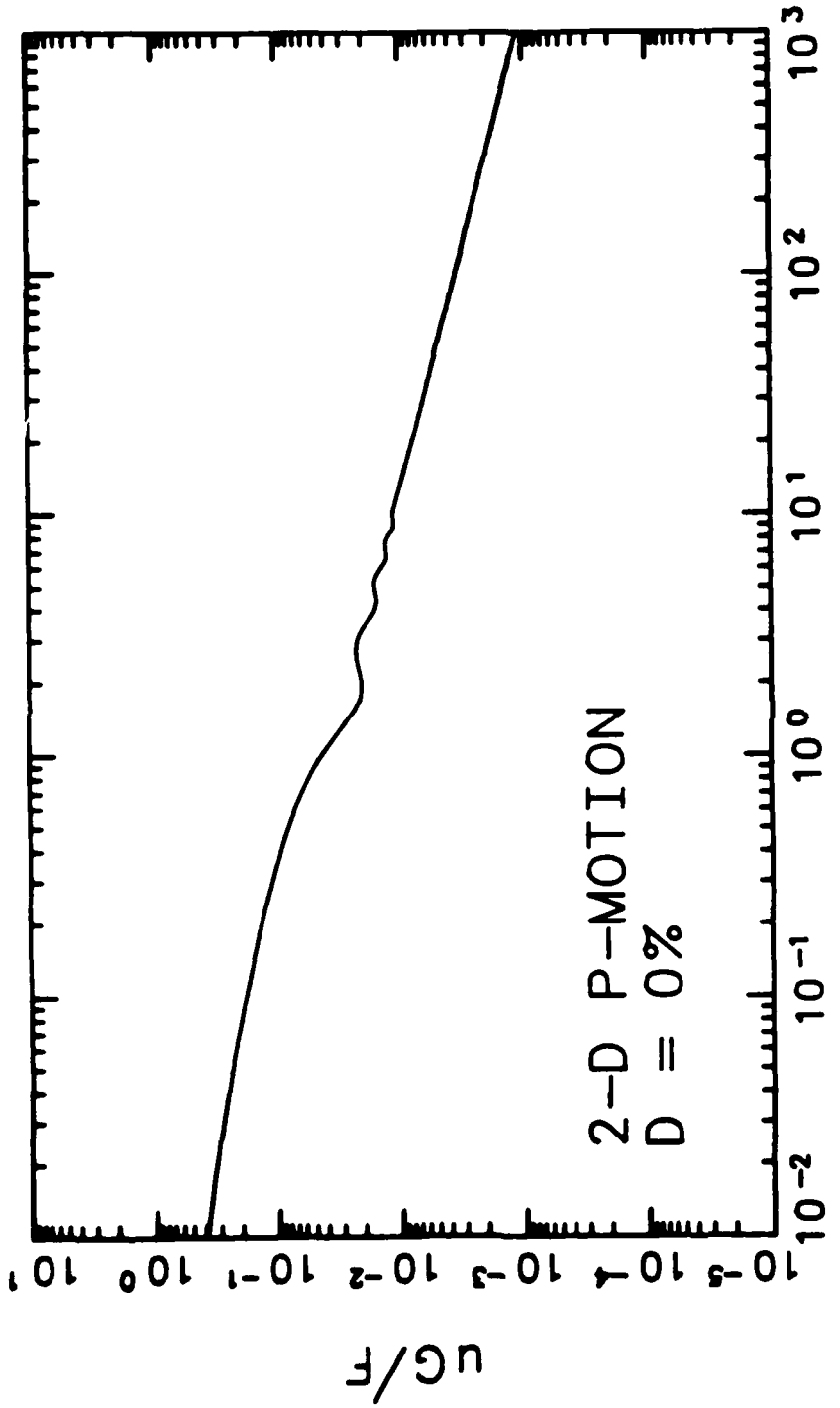

Fig. 3.14 - Wave amplitude decay due to radiational damping. Two-dimensional in-plane longitudinal motion.

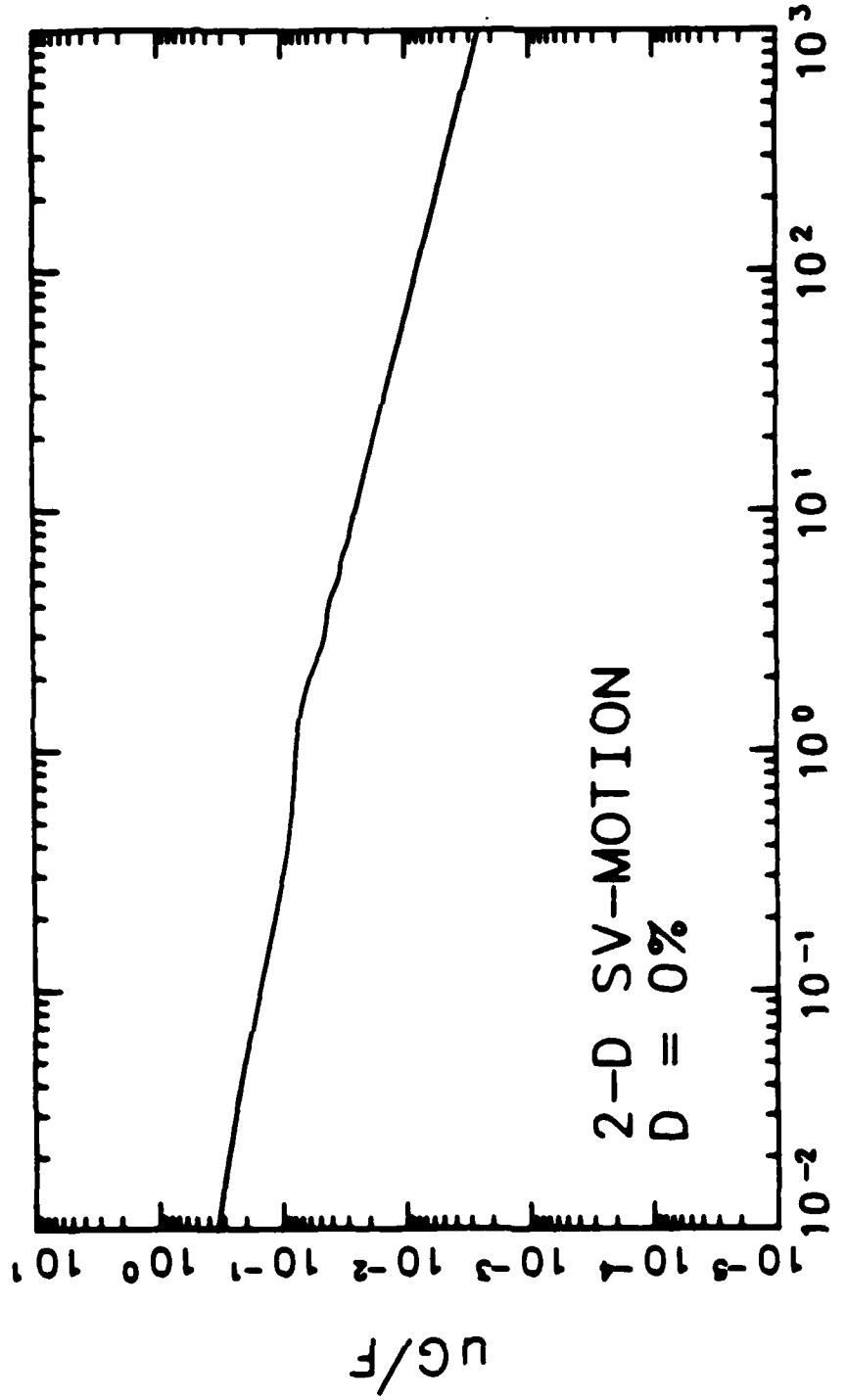

Fig. 3.15 - Wave amplitude decay due to radiational damping. Two-dimensional in-plane shear motion.

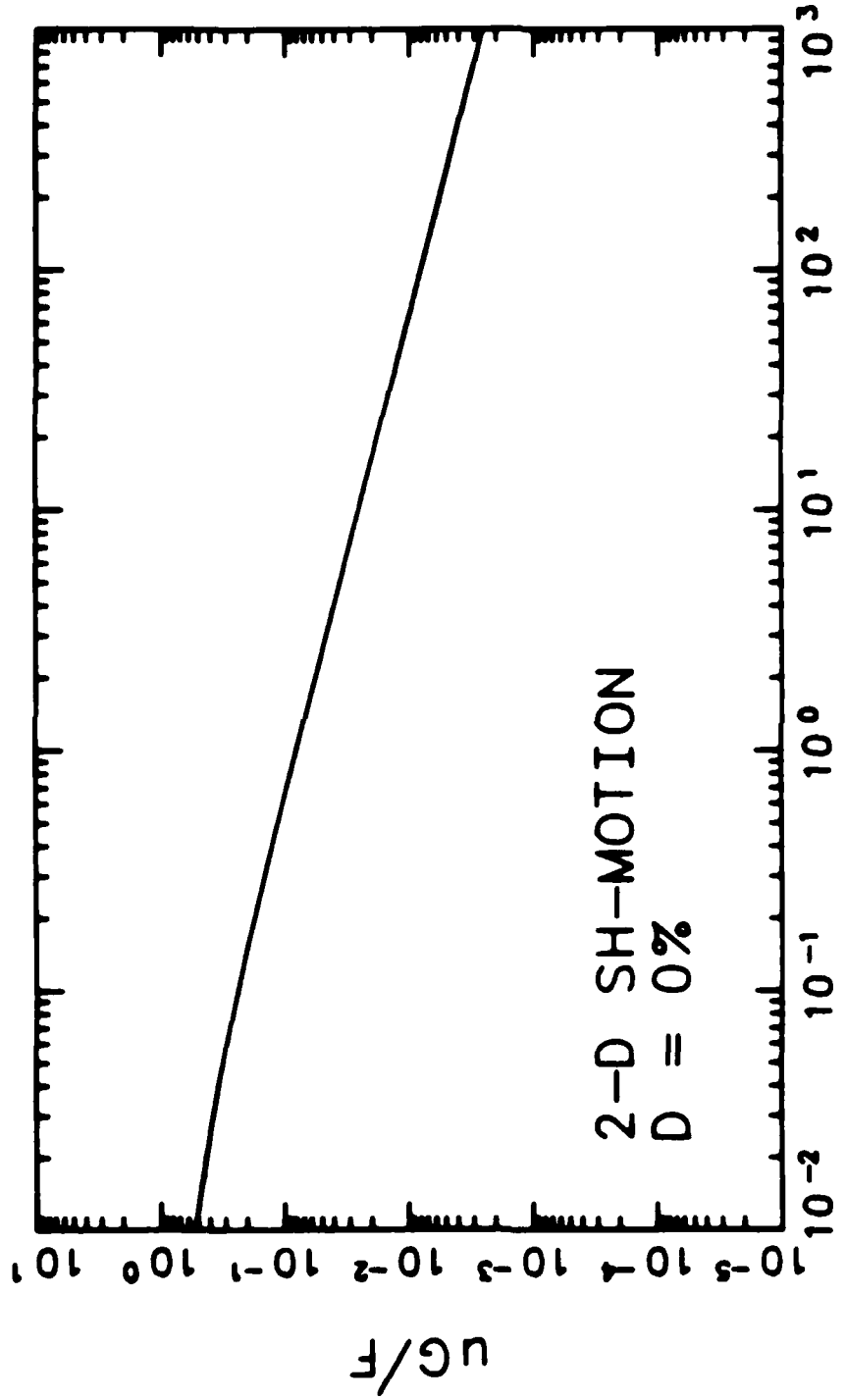

Fig. 3.16 - Wave amplitude decay due to radiational damping. Two-dimensional antiplane shear motion.

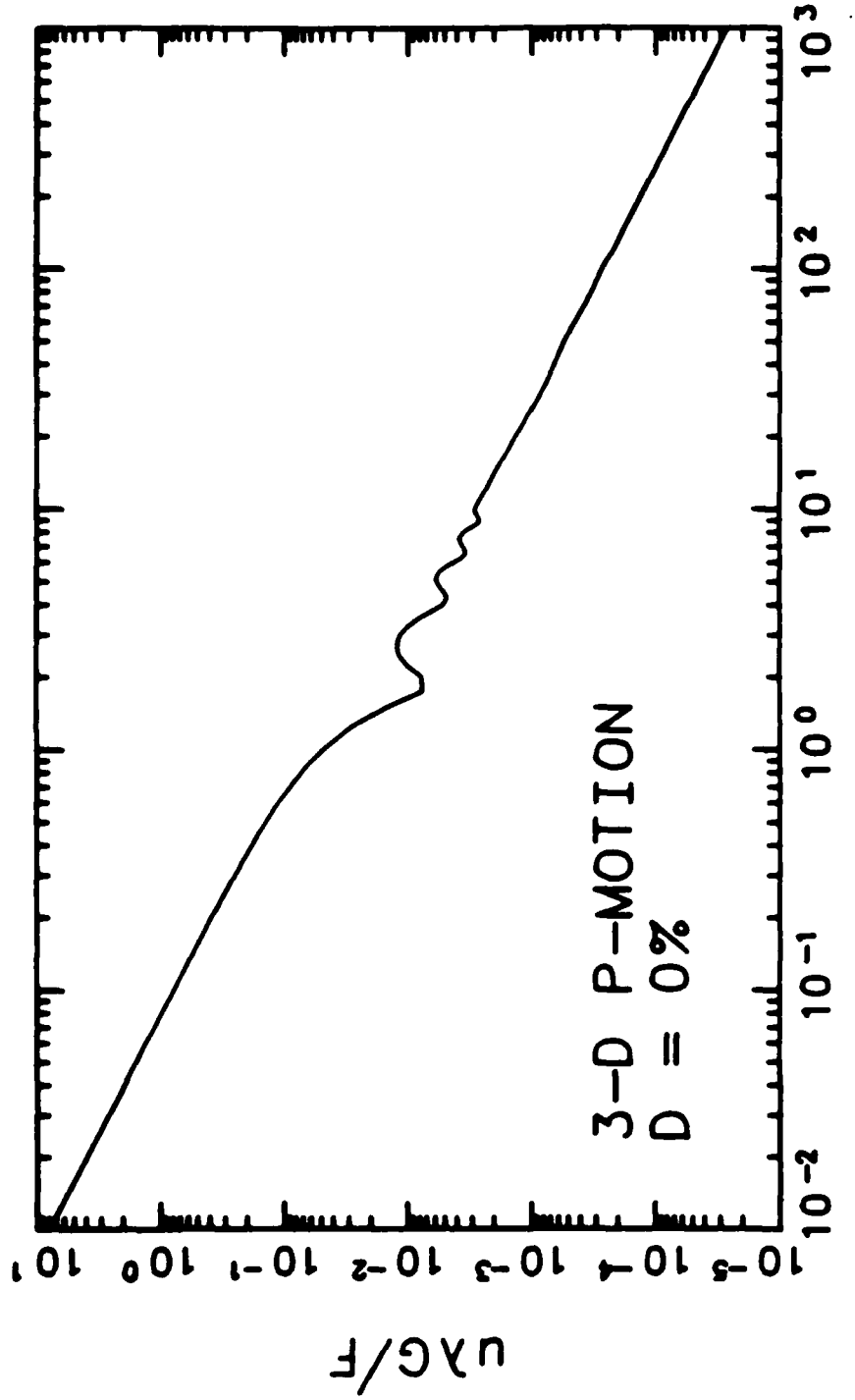

Fig. 3.17 - Wave amplitude decay due to radiational damping. Three-dimensional longitudinal motion.

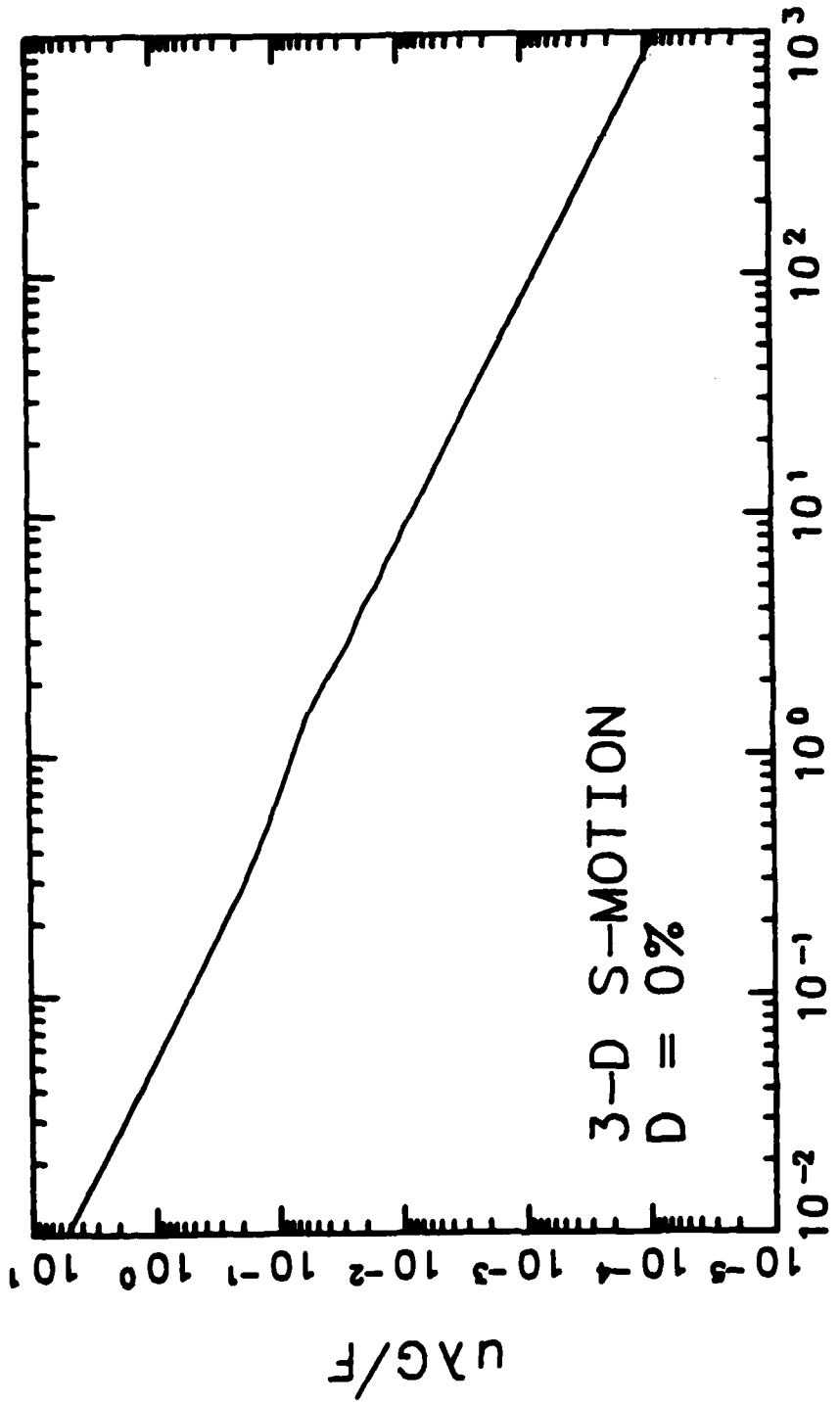

Fig. 3.18 - Wave amplitude decay due to radiational damping. Three-dimensional shear motion.

is important, the decay in amplitude is not proportional to the square root of the distance.

Three-dimensional wave-amplitude decay due to radiation is shown in Figs. 3.17 and 3.18. It can be observed that the general trend indicates that the amplitudes decay proportionally to the distance. The relation is valid, again, for long distances where the coupling of the P- and S-waves is almost insignificant. A further look at these figures indicates that at very short distances from the source, the decay is also proportional to the distance and that it is only in certain ranges of d/λ where the amplitudes of the waves do not decrease in proportion to the distance. A close inspection of Eqs. 2.10 through 2.13 indicates that the amplitude of the three-dimensional waves is formed by terms that decrease in proportion with the distance, the square of the distance and the cube of the distance. In the far field, the only significant terms are the far-field terms that decrease in proportion to the distance. In a mid-range of distances (say, $1 < d/\lambda < 10$), the decay is a combination of terms that decay in proportion to the distance, the square of the distance and the cube of the distance. Thus, the oscillating behavior of the decay curves in this mid-range of distances. Finally, in the very near field (d/λ on the order of tenths or less), the terms that decay in proportion with the square of the distance and the cube of distance essentially cancel, and amplitude decay is again nearly proportional to the distance.

Wave amplitude decay graphs for waves propagating in mediums with two and five percent material damping are presented in Figs. 3.19 through 3.23 and Figs. 3.24 through 3.28, respectively. It is noticeable in these figures that, at large distances (d/λ greater than about two), the amplitudes of the waves are decreasing at a

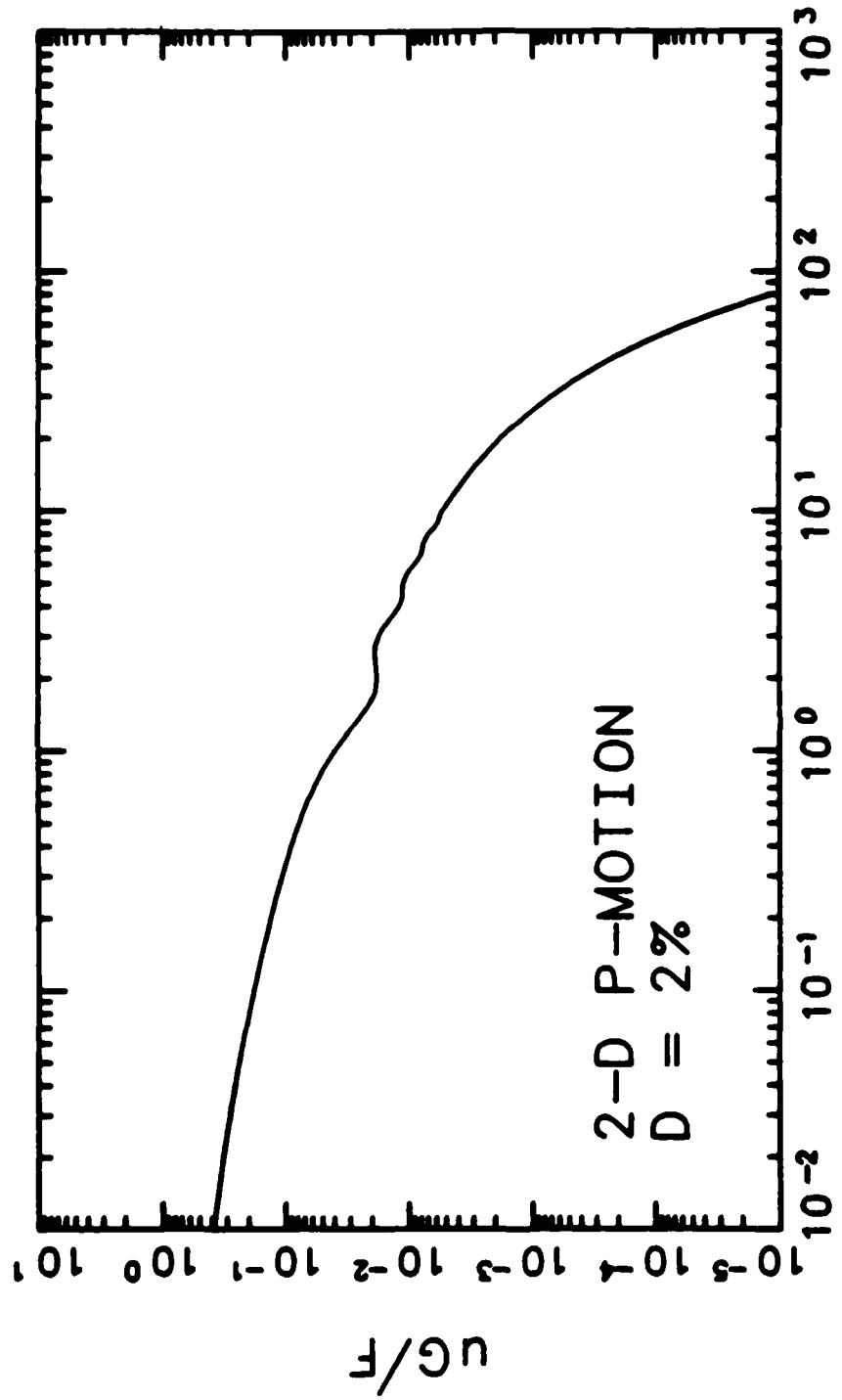

Fig. 3.19 - Wave amplitude decay due to radiational damping and two percent material damping. Two-dimensional in-plane longitudinal motion.

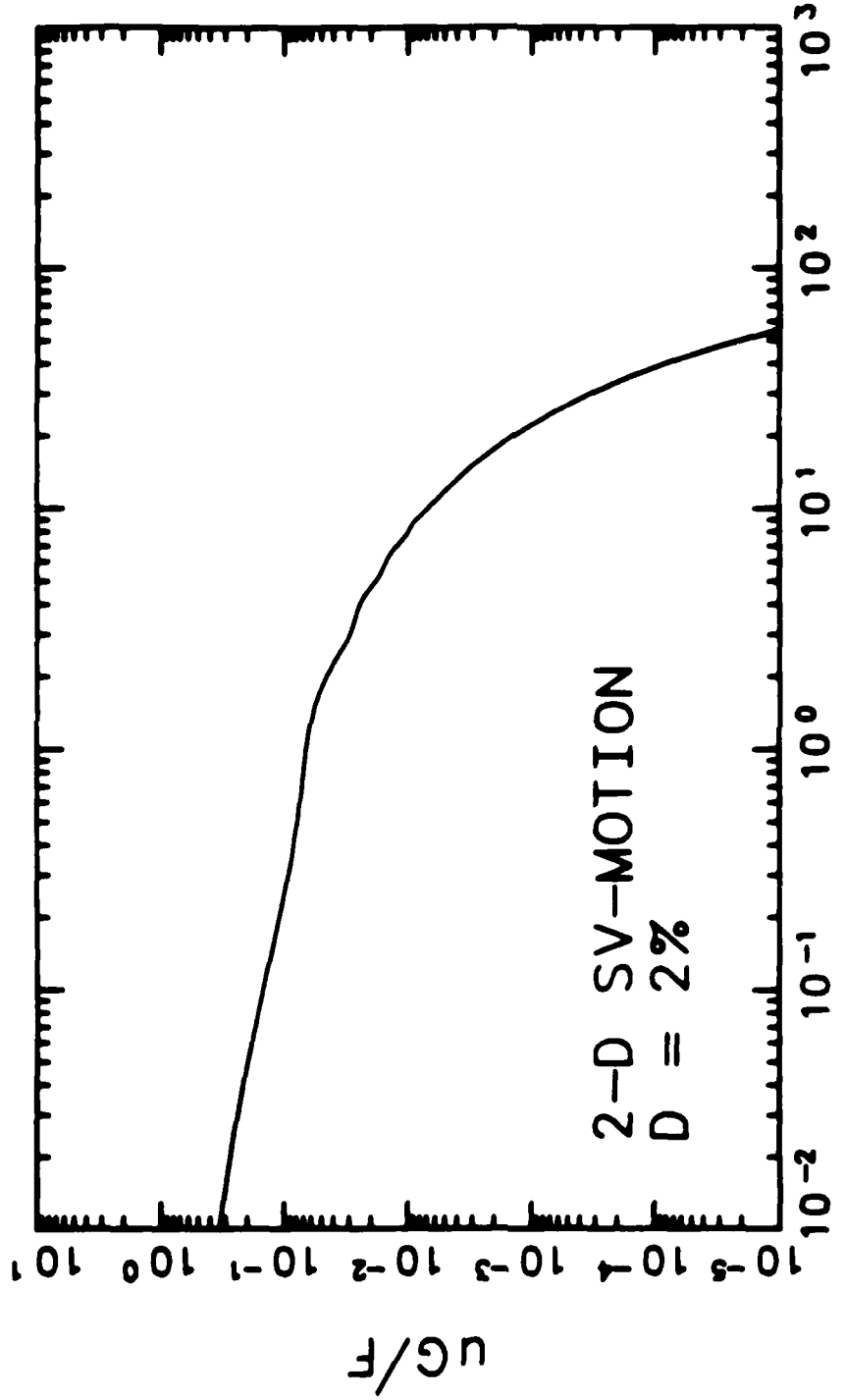

Fig. 3.20 - Wave amplitude decay due to radiational damping and two percent material damping. Two-dimensional in-plane shear motion.

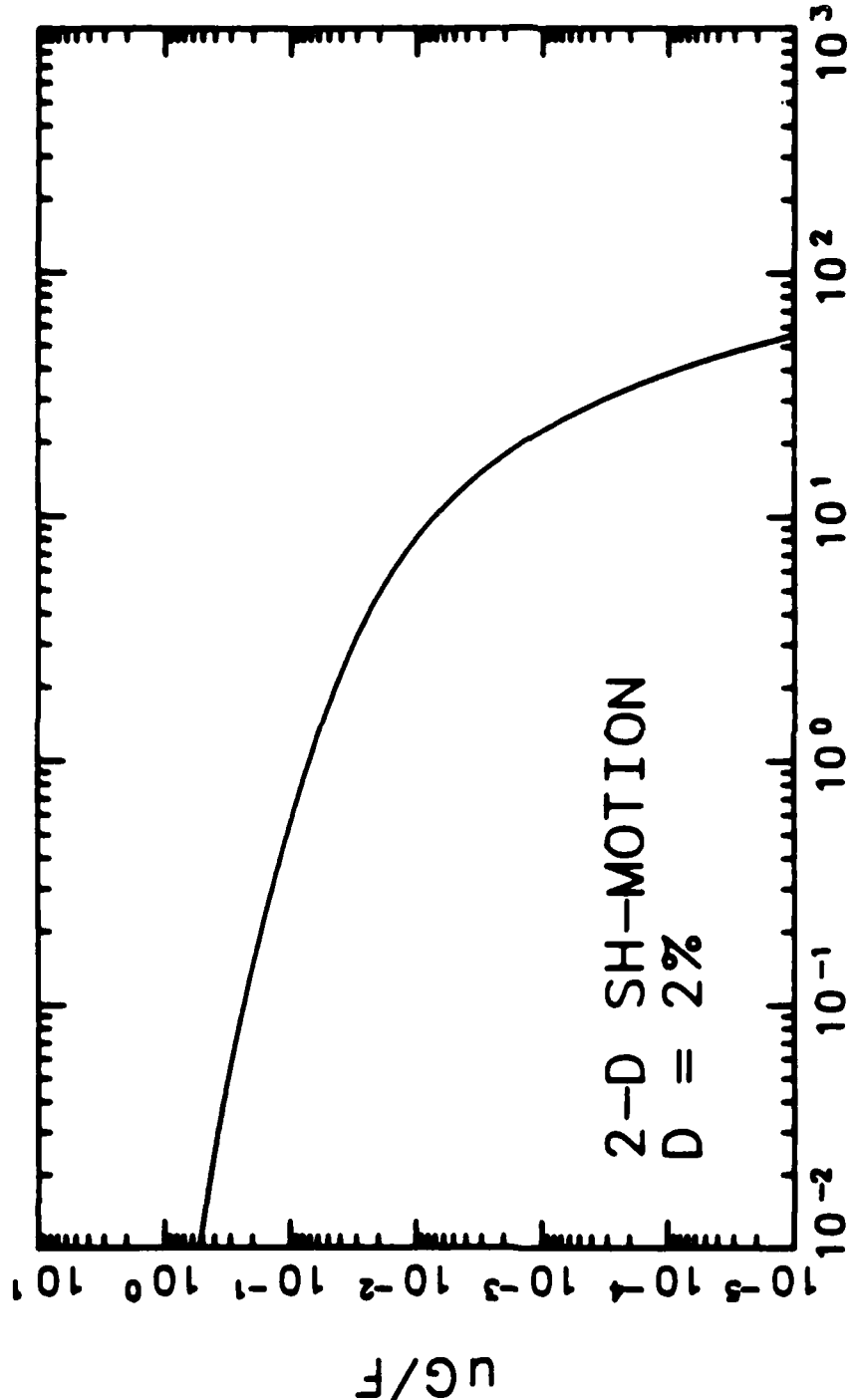

Fig. 3.21 - Wave amplitude decay due to radiational damping and two percent material damping. Two-dimensional antiplane shear motion.

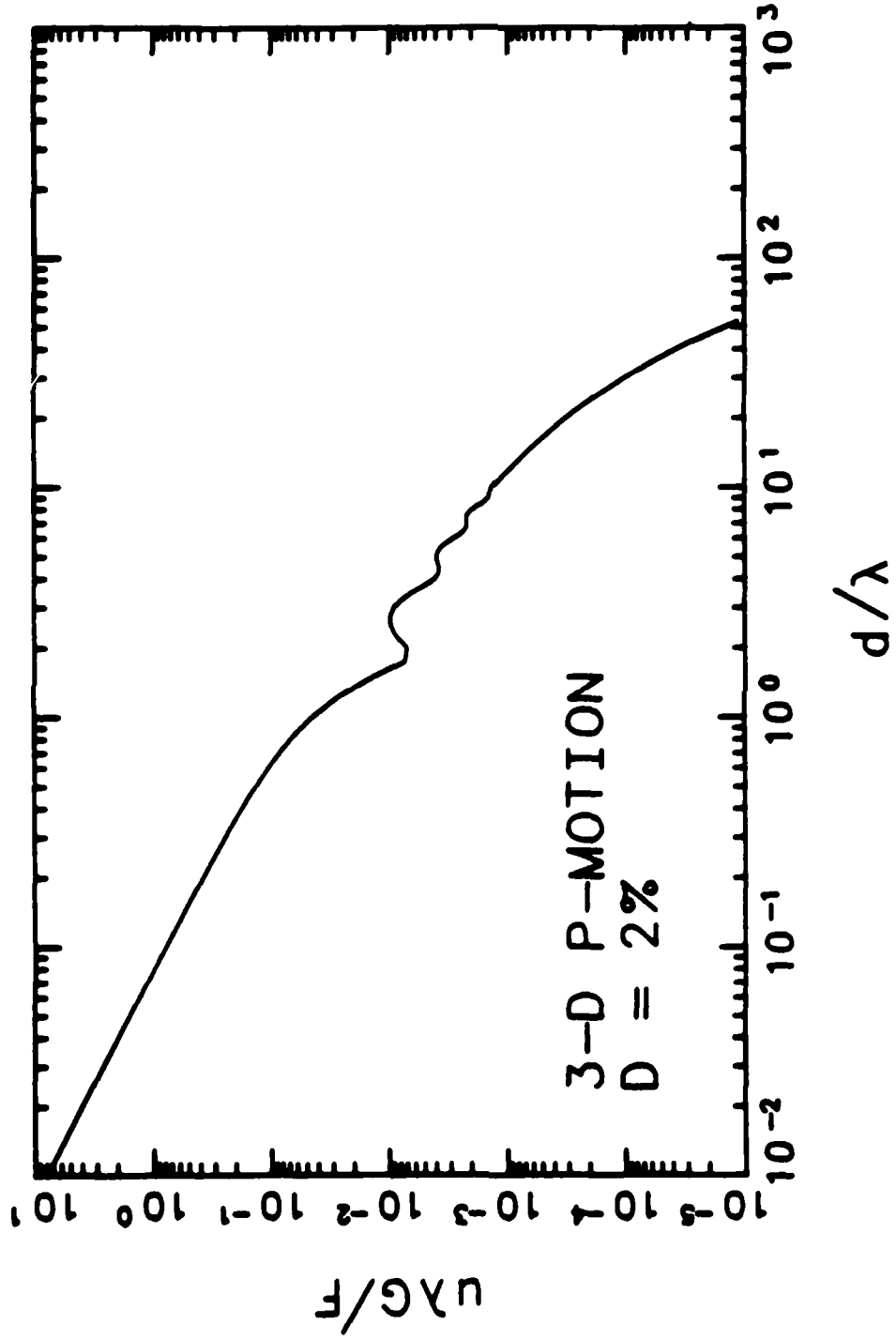

Fig. 3.22 - Wave amplitude decay due to radiational damping and two percent material damping. Three-dimensional longitudinal motion.

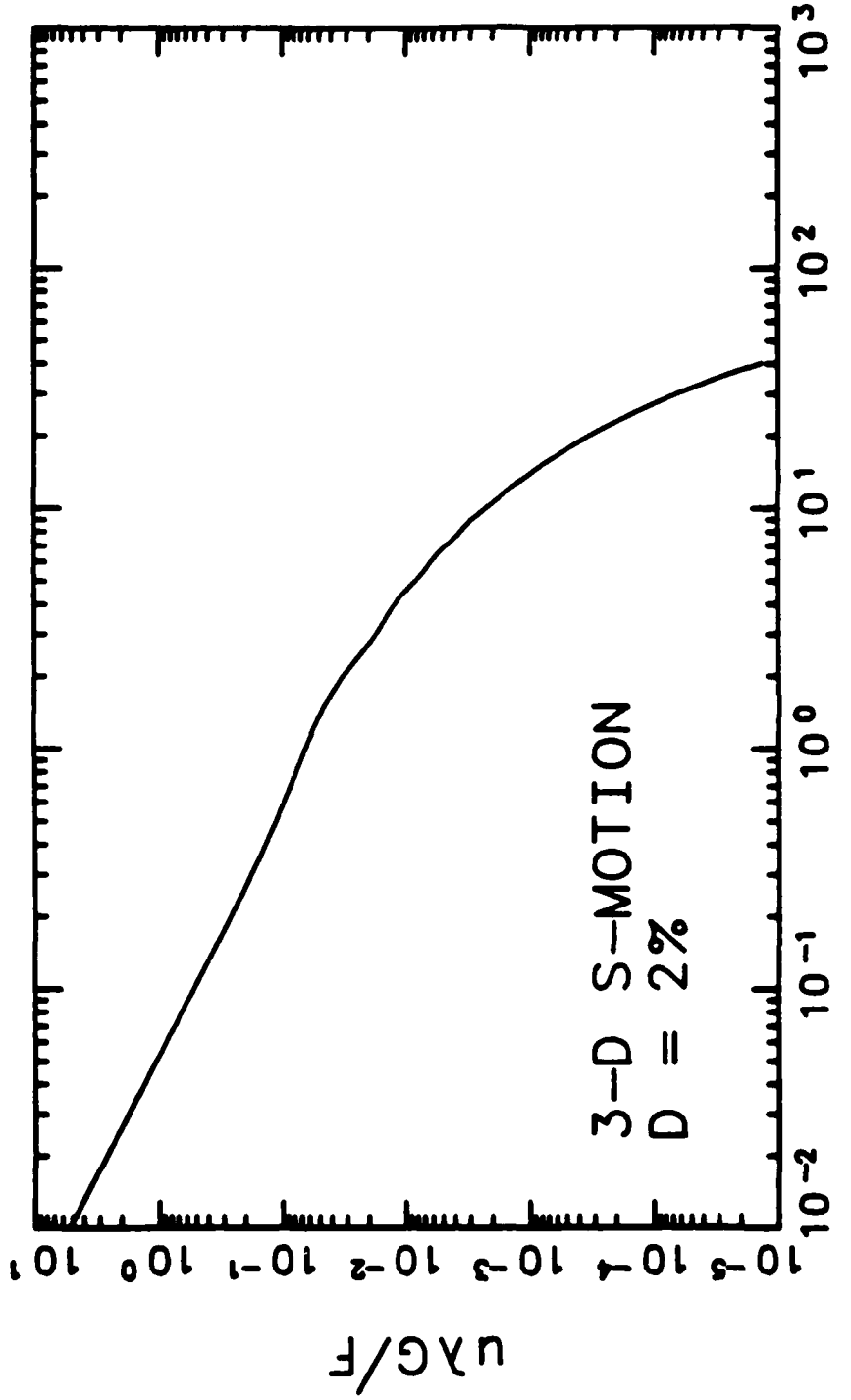

Fig. 3.23 - Wave amplitude decay due to radiational damping and two percent material damping. Three-dimensional shear motion.

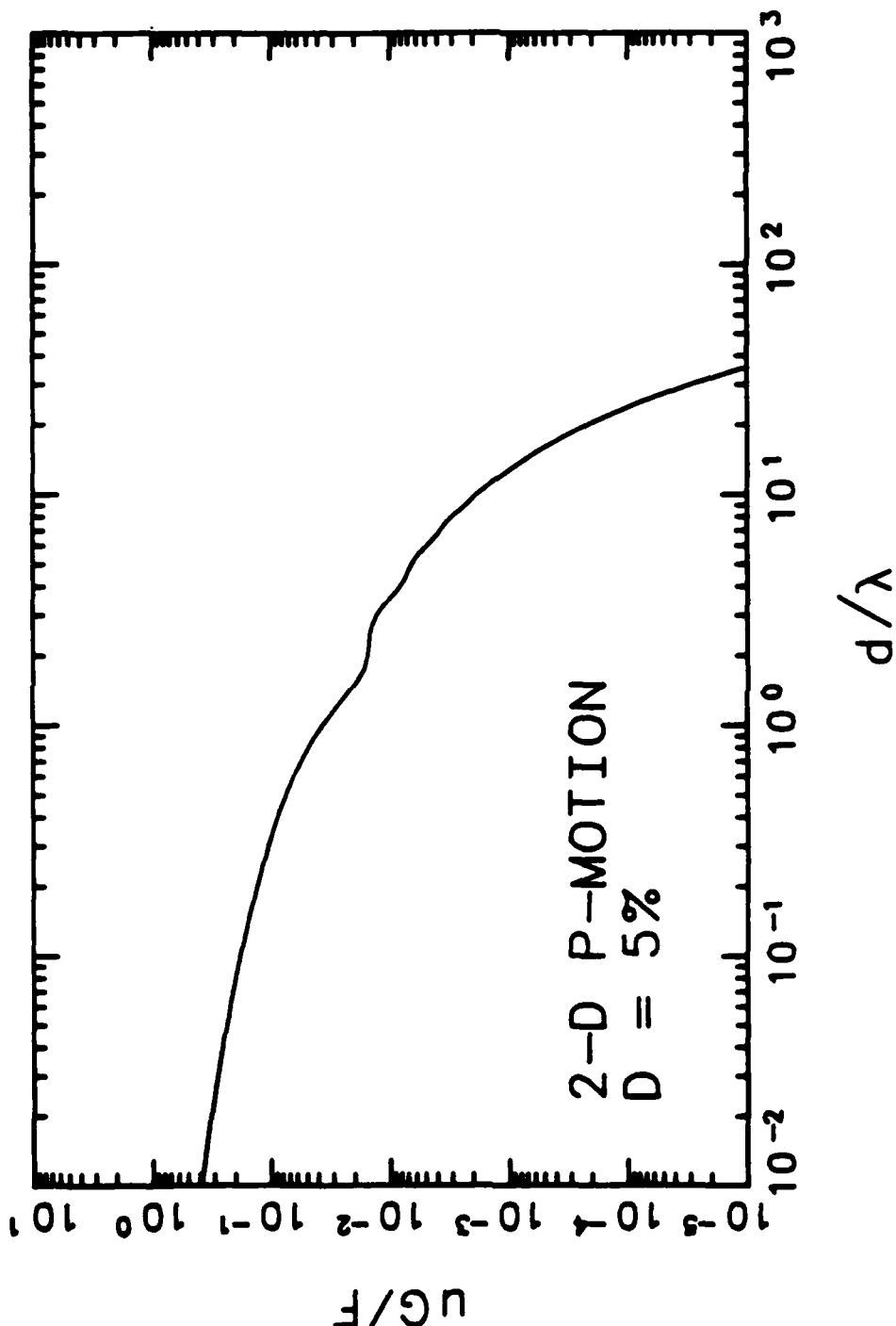

Fig. 3.24 - Wave amplitude decay due to radiational damping and five percent material damping. Two-dimensional in-plane longitudinal motion.

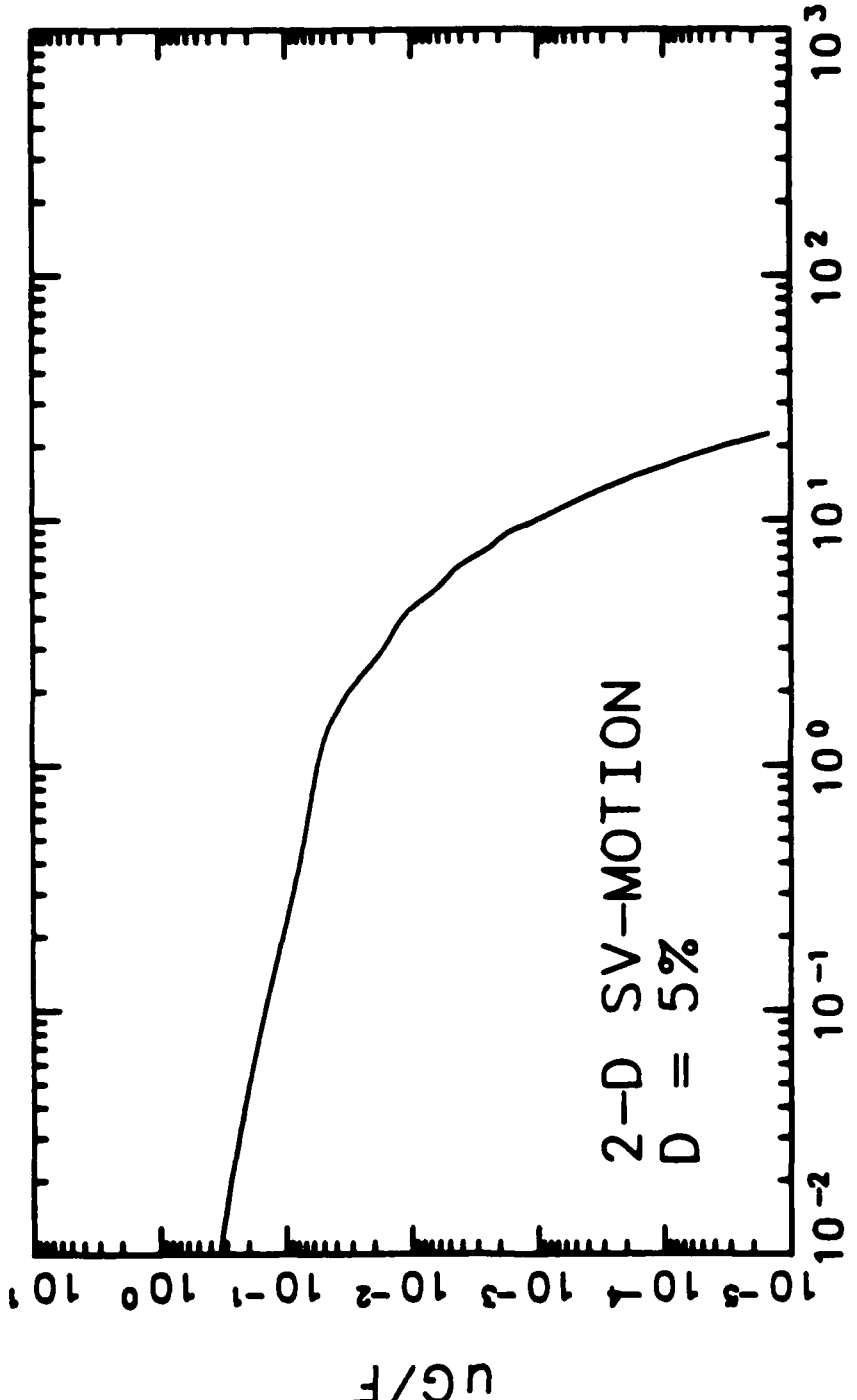

Fig. 3.25 - Wave amplitude decay due to radiational damping and five percent material damping. Two-dimensional in-plane shear motion.

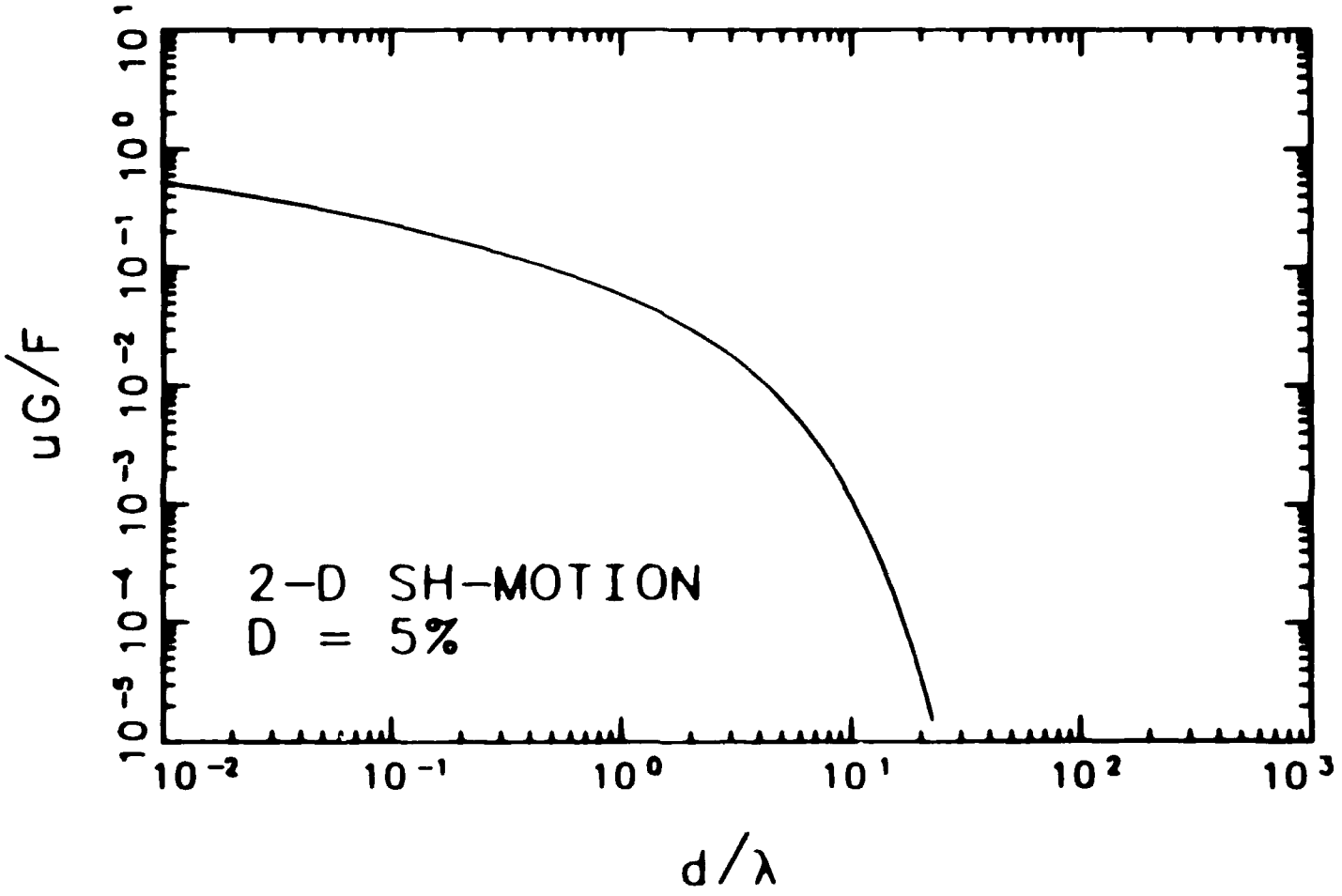

Fig. 3.26 - Wave amplitude decay due to radiational damping and five percent material damping. Two-dimensional antiplane shear motion.

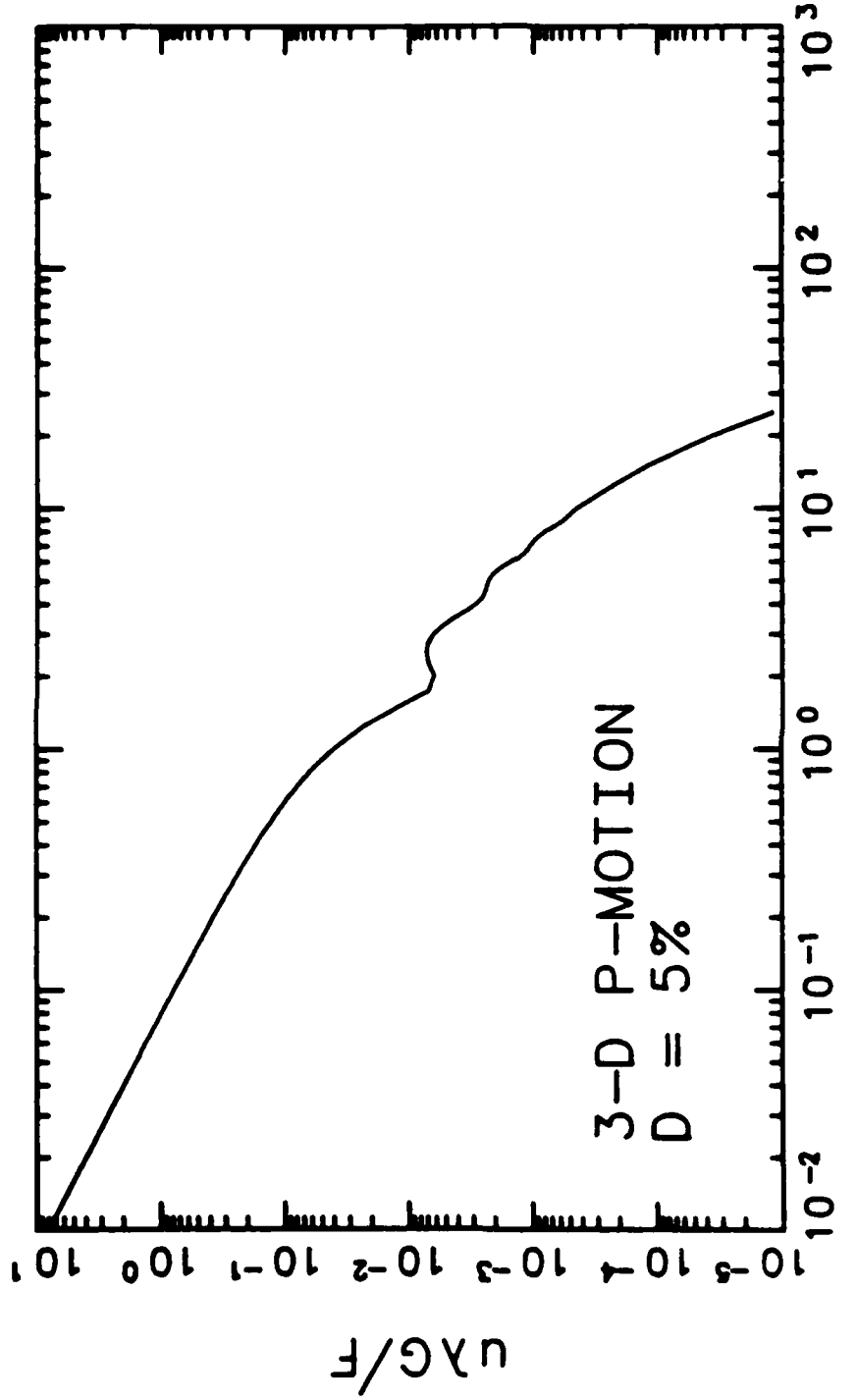

Wave amplitude decay due to radiational damping and five percent material damping. Three-dimensional longitudinal motion.

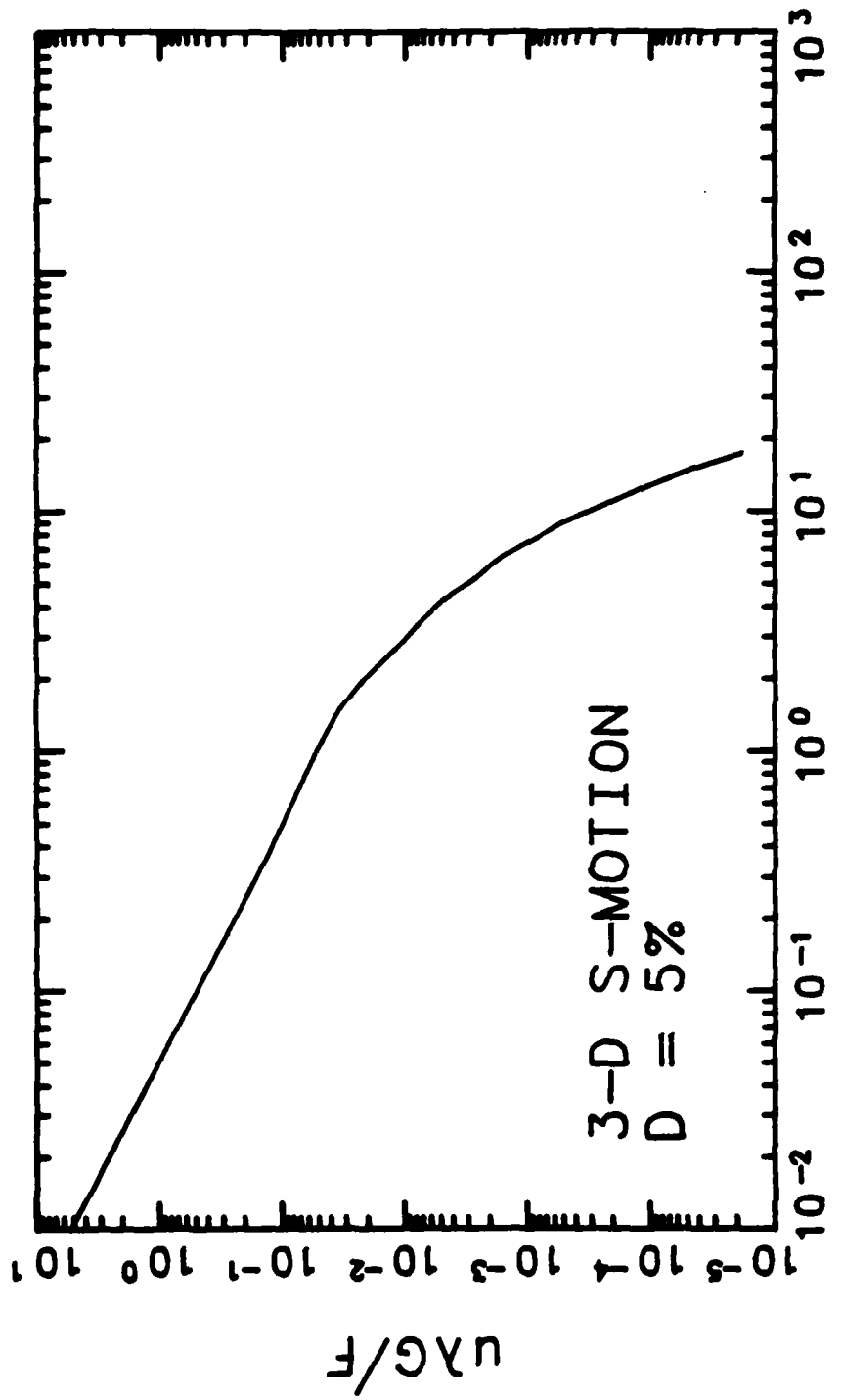

Fig. 3.28 - Wave amplitude decay due to radiational damping and five percent material damping. Three-dimensional shear motion.

much faster rate than when the waves were propagating in a medium with no material damping. At short distances, the waves have gone through very few cycles of motion (if any), and the effect of material damping has had a very minor influence. For this reason the amplitudes in the short range of distances are practically the same as when no damping was considered.

3.6 SUMMARY

Waveforms of particle displacement of body waves produced by line loads in a three-dimensional space (in-plane and antiplane point loads in two-dimensional notation) and by point loads also in a three-dimensional space have been analyzed in this chapter. From examination of these synthetic records, the following conclusions can be drawn.

1. The most precise evaluation of P- or S-wave velocities is obtained with receivers aligned parallel to the direction of particle motion. If the receivers are inclined, wave arrivals are more difficult to identify because of the additional coupling between waves. This conclusion is especially true for the S-wave, the one of most concern in geotechnical engineering applications.

2. When the material in which the body waves propagate presents a dissipative behavior (as represented by a hysteretic type of damping), it is more difficult to estimate the time of arrival of the waves than when the material is not dissipative. In those cases, the apparent time of arrival of the wave is very much influenced by the amplification applied to the wave record. The higher the amplification, the sooner the wave seems to arrive.

3. In all waveforms except in those for two-dimensional SH-motions, the waveforms are composed of two types of waves, P-waves travelling at the compressional wave velocity and S-waves travelling at the shear wave velocity. In a two-dimensional in-plane transverse-motion record, the P-wave (T_p wave) only exists at short distances from the source (distances smaller than approximately two shear wavelengths), but the secondary wave (T_{SV} wave) prevails at longer distances. It is for this reason that the T_{SV} wave is called the far-field wave while the T_p wave is called the additional near-field wave (or near-field wave). In records of two-dimensional in-plane longitudinal-motion, the far-field wave corresponds to the primary wave (L_p), and the near-field wave is the SV-wave (L_{SV}). In two-dimensional antiplane motion (SHmotion), there is only one wave (T_{SH}) which propagates at the shear wave velocity.

4. For waves generated by a point source in a three-dimensional space, the wave fronts spread in a spherical manner from the point source. There are, again, near- and far-field waves both in longitudinal- and transverse-motion records. The far-field wave in a longitudinal motion record (L_p) travels at the compressional wave velocity while the near-field wave (L_S) travels at the shear-wave velocity. In a transverse-motion record, the far-field wave (T_S) travels at the shear wave velocity while the near-field wave (T_p) propagates at the compressional wave velocity. The near- and far-field waves have components with amplitudes varying in proportion to $1/r^2$ and $1/r^3$. The far-field wave has, in addition, terms that diminish in proportion to the distance. Those terms with amplitudes decreasing with the square and the cube of the distance are called the near-field components (or near-field terms), while the terms decreasing with the distance are known as the far-field components. The expression "near-field term" or

"near-field component" is sometimes applied, however, to the near-field wave, while the expression "far-field term" or "far-field component" is sometimes applied to the far-field wave.

5. Near-field effects in longitudinal-motion (P-motion) records are more important than near-field effects in transverse-motion records. In addition, near-field effects in longitudinal-motion records last longer (to distances of about ten times the shear wavelength) than near-field effects in transverse-motion records (to distances of about two shear wavelengths).

6. Wave polarity reversals, which are frequently encountered in the field upon reversing the direction of the impulse, were explained in Section 3.4 by considering the effect of near-field waves.

7. For a medium in which energy dissipation occurs exclusively because of radiation damping (geometrical spreading of the energy), it was observed that wave amplitude decreases, in general, in proportion to the distance for point sources and in proportion to the square root of the distance for line sources. These general rules apply more precisely to the far-field range of distances which is defined as those distances (or frequencies) for which the ratio d/λ is greater than two for transverse motions and ten for longitudinal motions. For waveforms generated from a point source, this rule of energy dissipation (radiation damping) also applies correctly for values of d/λ that are smaller than about 1/2. When internal dissipation of energy is considered by the use of a hysteretic, frequency- and strain- independent, material damping, the amplitudes in the far-field decrease at a much faster rate.

CHAPTER FOUR

TECHNIQUES OF EVALUATING BODY WAVE VELOCITIES

4.1 INTRODUCTION

Many of the variables that can affect in situ seismic tests such as sources, receivers, recording equipment and triggering devices have been studied extensively in the literature (Stokoe and Woods, 1972; Stokoe and Hoar, 1978; Hoar, 1982; Patel, 1981) and do not require further extensive studies. However, techniques of determining wave velocities and attenuation have received little attention. With the advent of digital waveform processing in the field, several new techniques are available for velocity and attenuation measurements. In this chapter, new techniques for velocity measurements based on sophisticated waveform processing and data analysis are presented along with an extensive study of the traditional time-domain technique. Attenuation measurements are presented in Chapter Five.

4.2 WAVE VELOCITIES FROM DIRECT TIMES OF ARRIVAL

The cheapest and most commonly used method to calculate seismic wave velocities is by measuring the travel time of a wave from a source point to a target point. This time is usually called the direct travel time. By dividing the travel time into the distance between the two points, the propagation velocity of the

wave is obtained. Wave velocity calculations by measuring direct travel times have been analyzed in Chapter Three (Section 3.2) and will not be repeated herein. Suffice it to say that, even under ideal field conditions, some judgment is required when "picking" the wave arrival time.

4.3 WAVE VELOCITIES FROM INTERVAL TIMES OF ARRIVAL

It is common practice in the field to determine wave velocities by monitoring the waves passing by two or more different receivers. In such cases, the time for body waves to travel between several points within the soil mass is measured. Use of interval travel times between two or more receivers has the advantage that it eliminates possible triggering errors of the recording device and also minimizes other field errors that might occur when measuring direct travel times from the source to the first receiver (Hoar, 1982).

Records of wave trains monitored at dimensionless distances $d/\lambda = 2$ and $d/\lambda = 8$ from the source are presented in Figs. 4.1 through 4.10 (λ being the predominant shear wavelength, $\lambda = c_s \cdot T_s$). The dimensionless time is defined in these figures as $c_s t/\lambda$, to avoid the distortion of the waves produced by the distance (d) in the factor $c_s t/d$. All the records presented are for waves propagating in a medium with a Poisson's ratio of 0.25.

A first approach to calculating wave velocities is by identifying the interval time between first arrivals of the wave from the first to the second receivers. Similar approaches can be used when interval velocities are calculated in which the time it takes the wave to travel from the first to the second receiver is

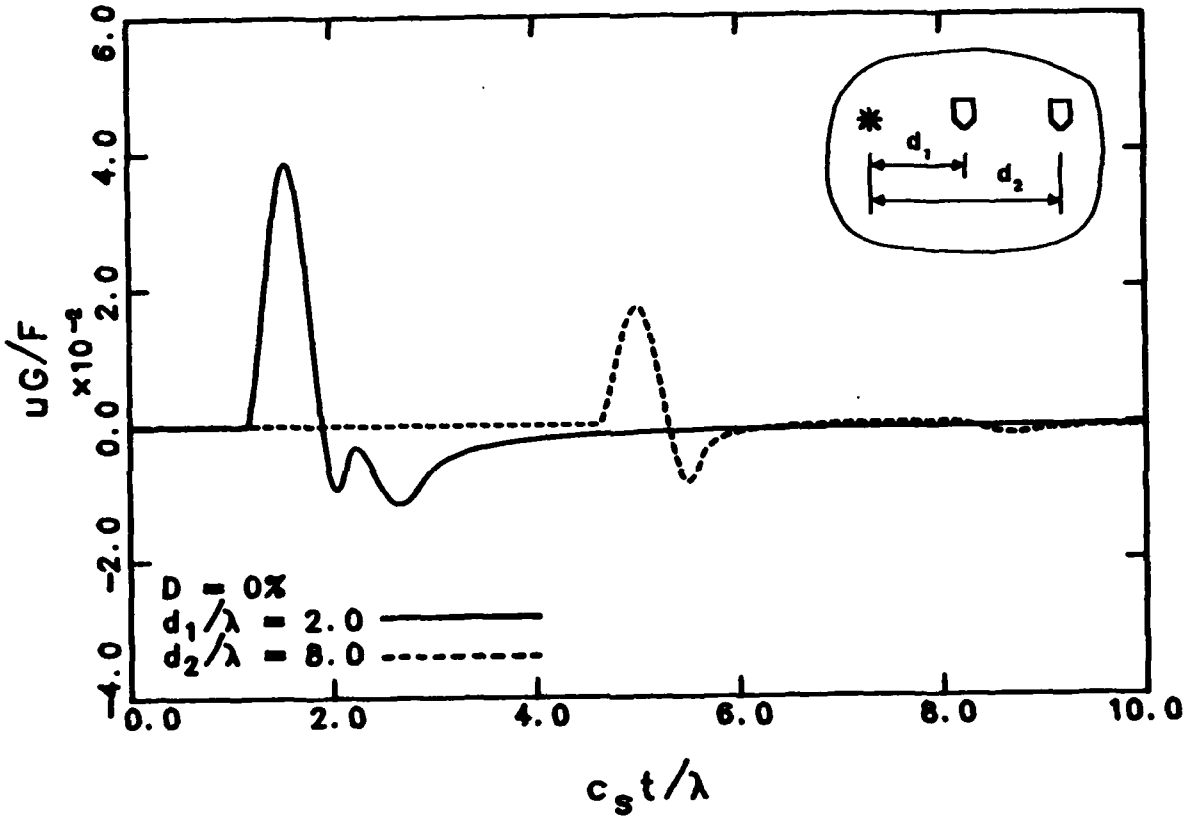

Fig. 4.1 - Two-dimensional in-plane longitudinal motion at two different points in a medium with no damping.

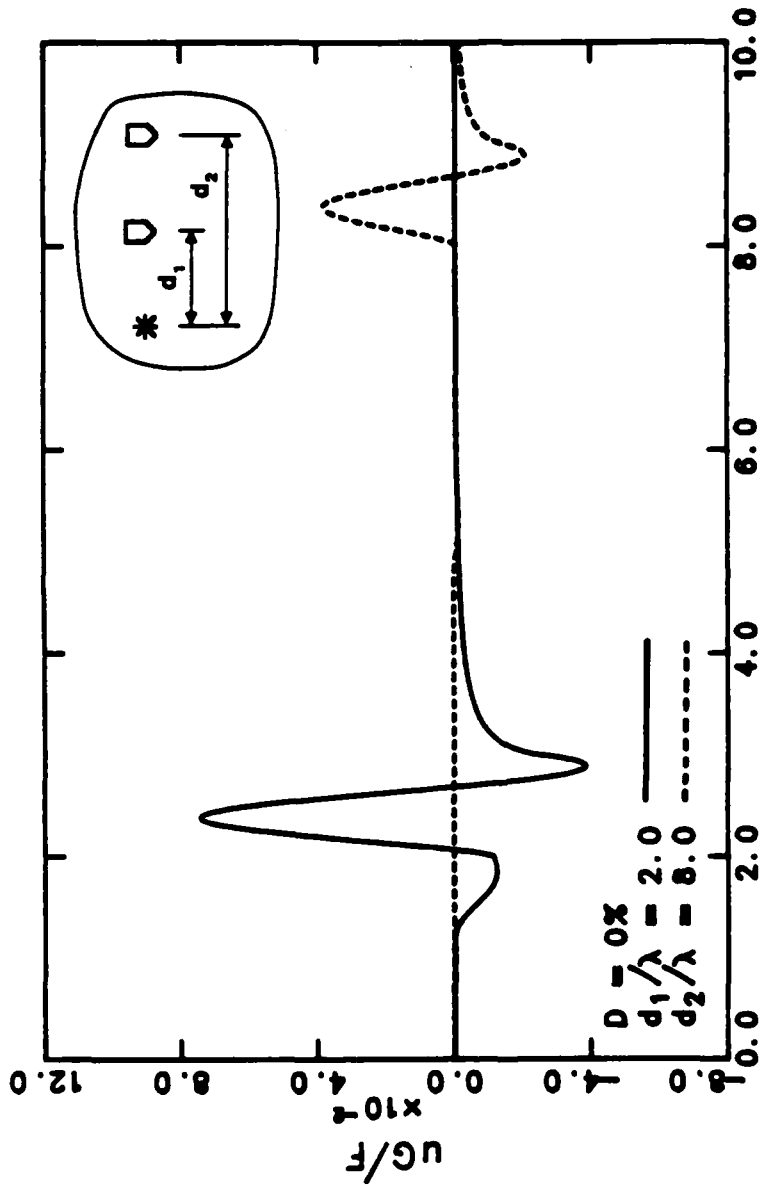

Fig. 4.2 - Two-dimensional in-plane shear motion at two different points in a medium with no damping.

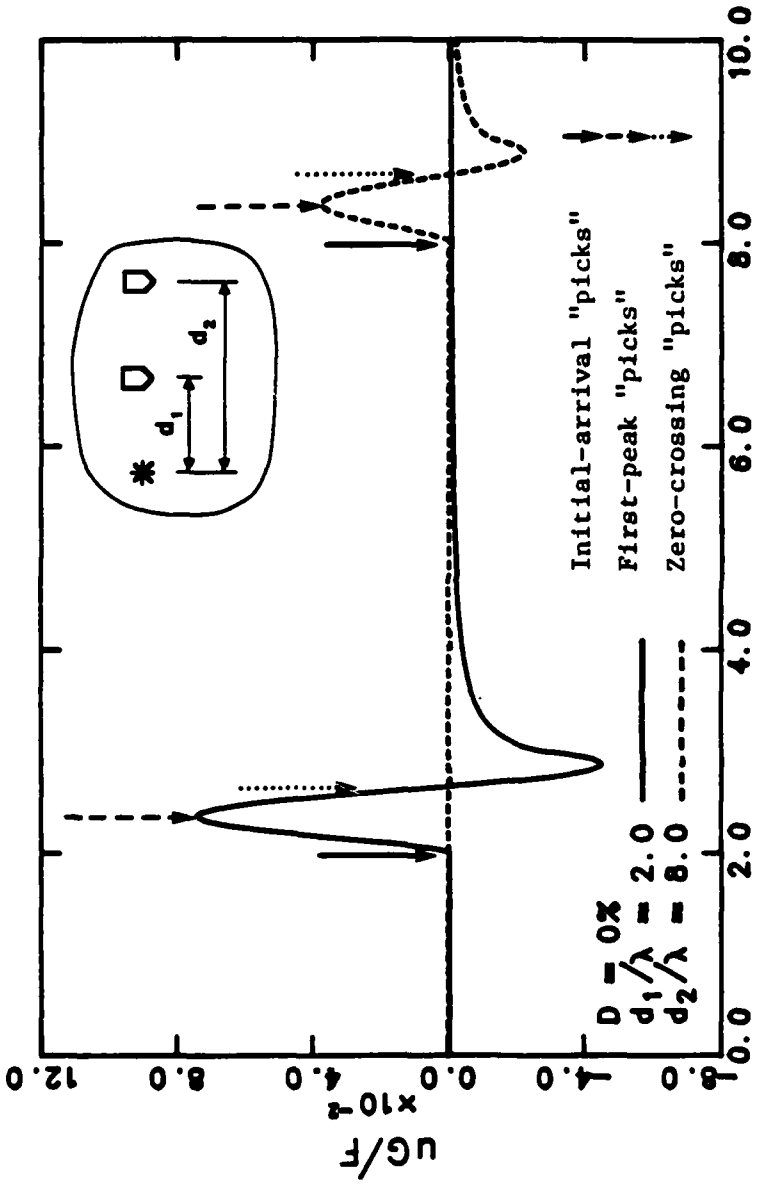

Fig. 4.3 - Two-dimensional antiplane shear motion at two different points in a medium with no damping. Illustration of interval travel time determination.

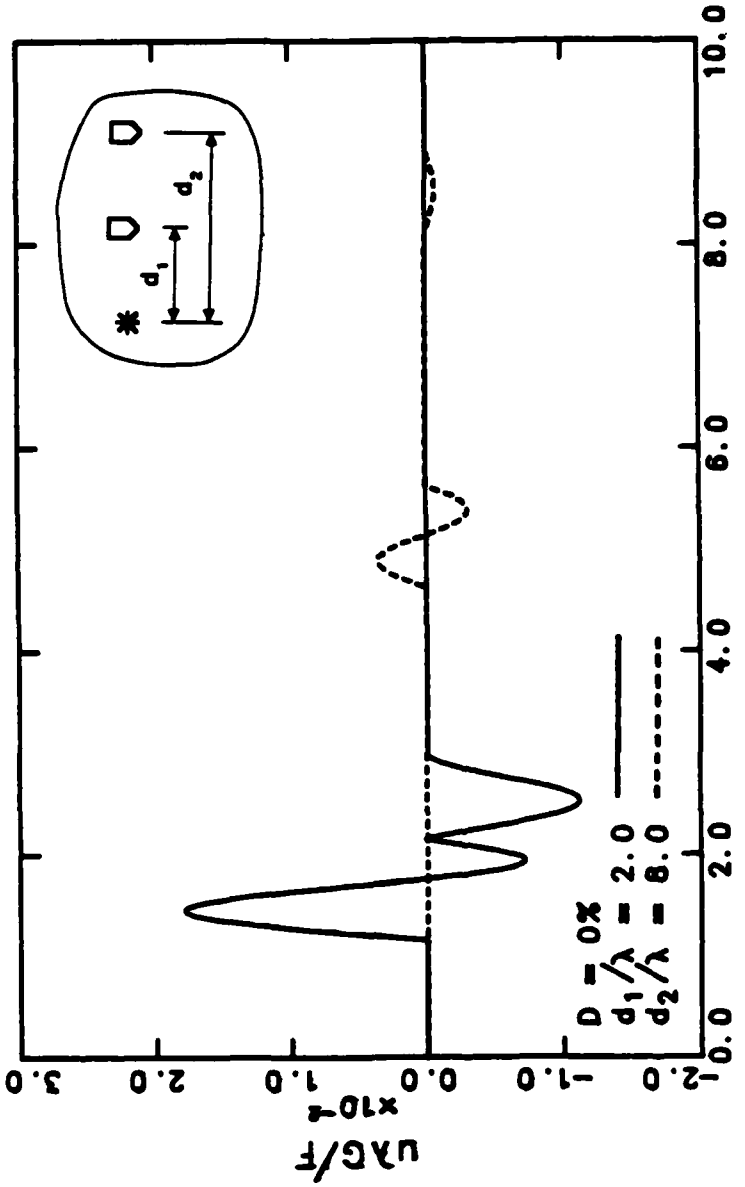

Fig. 4.4 - Three-dimensional longitudinal motion at two different points in a medium with no damping.

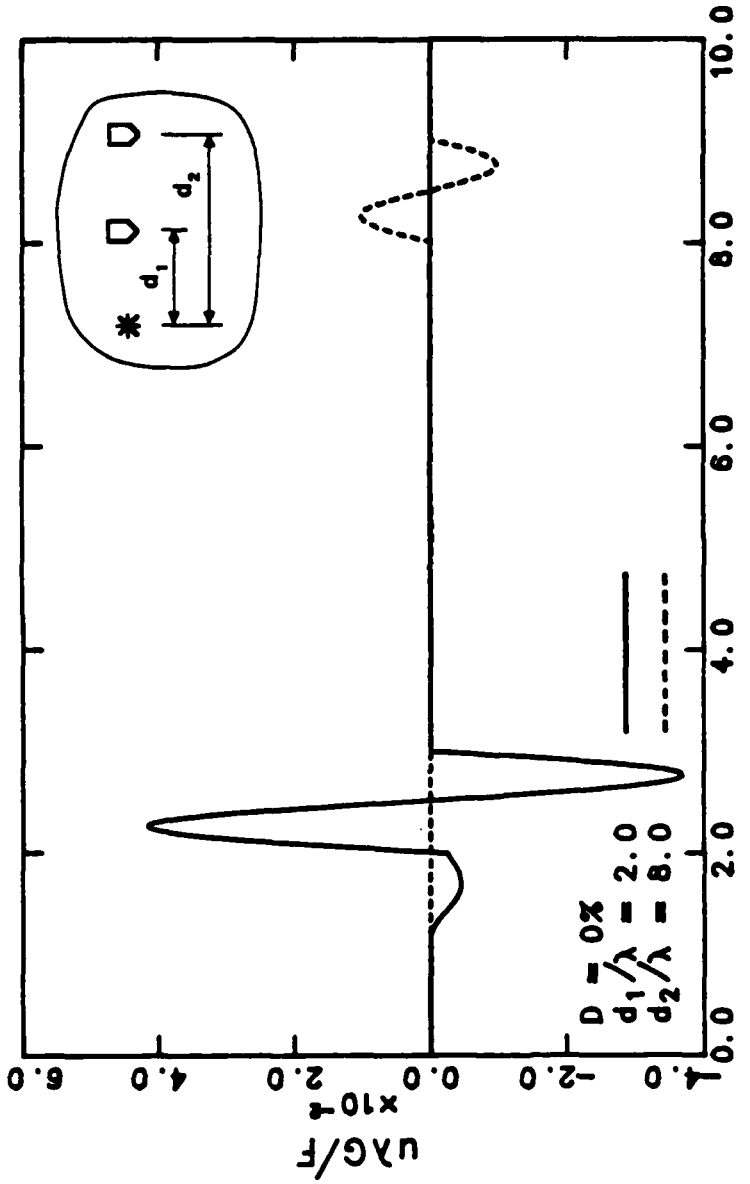

Fig. 4.5 - Three-dimensional shear motion at two different points in a medium with no damping.

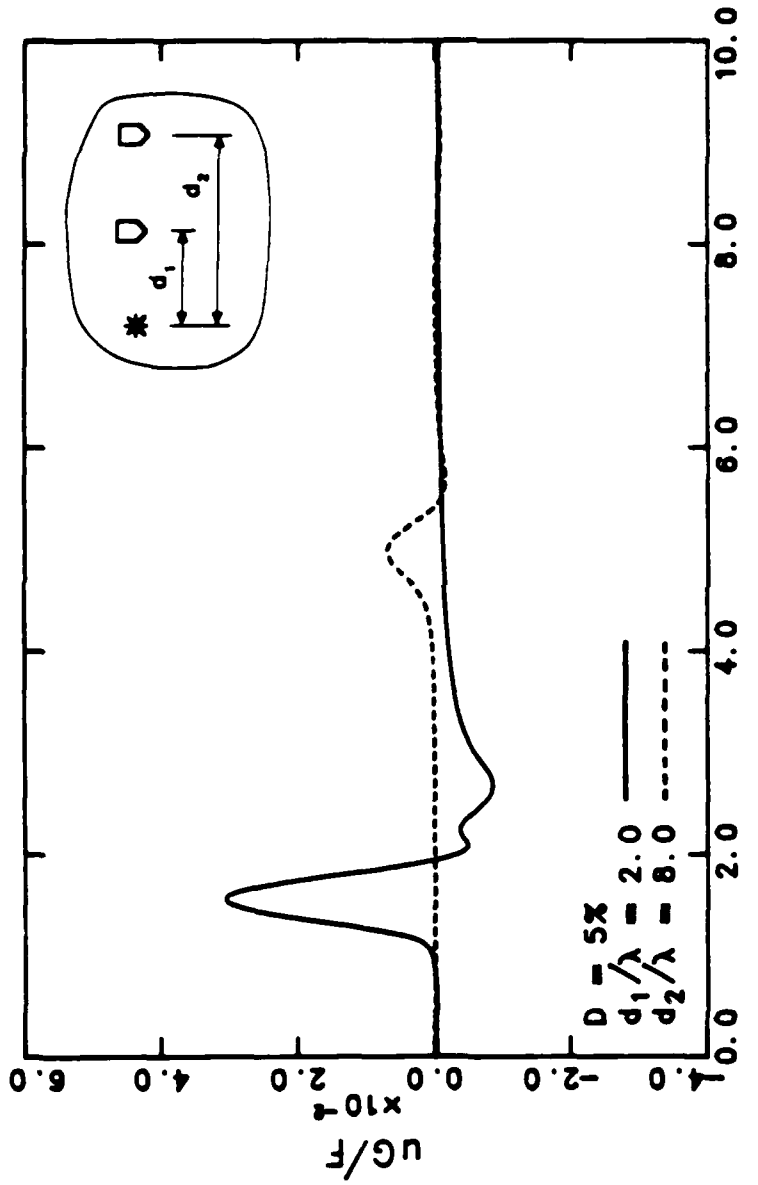

Fig. 4.6 - Two-dimensional in-plane longitudinal motion at two different points in a medium with five percent damping.

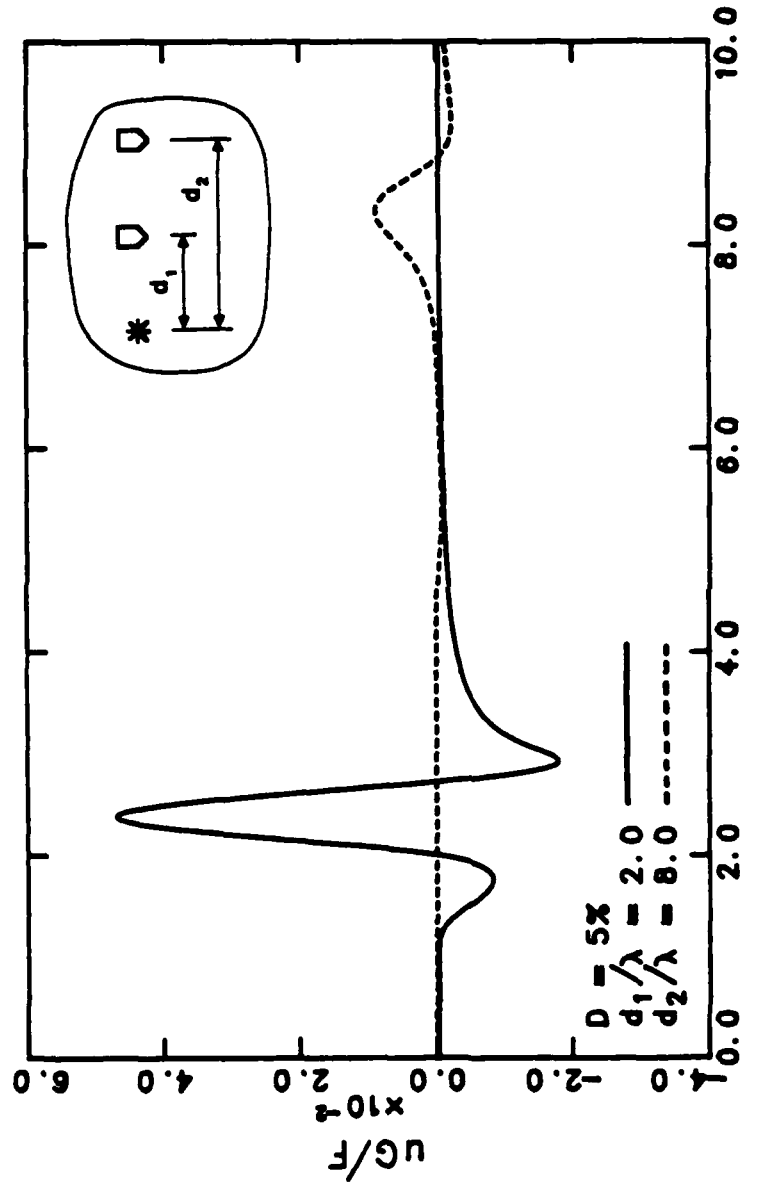

Fig. 4.7 - Two-dimensional in-plane shear motion at two different points in a medium with five percent damping.

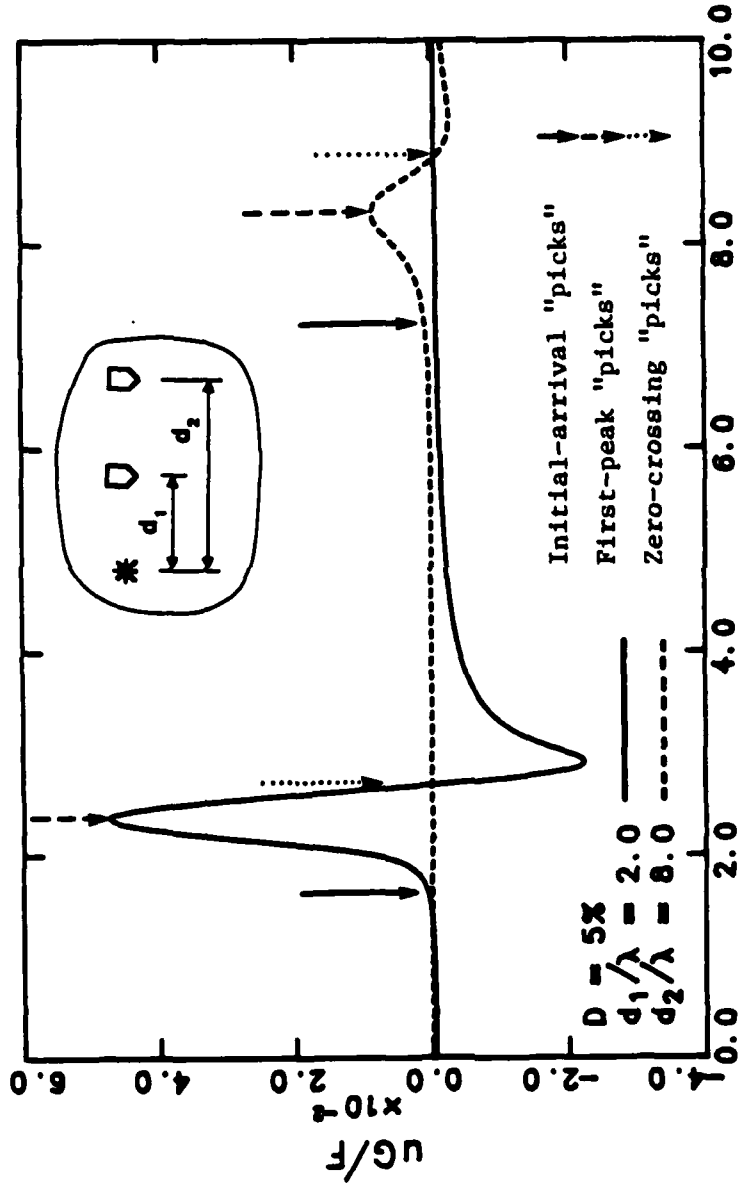

Fig. 4.8 - Two-dimensional antiplane shear motion at two different points in a medium with five percent damping. Illustration of interval travel time determination.

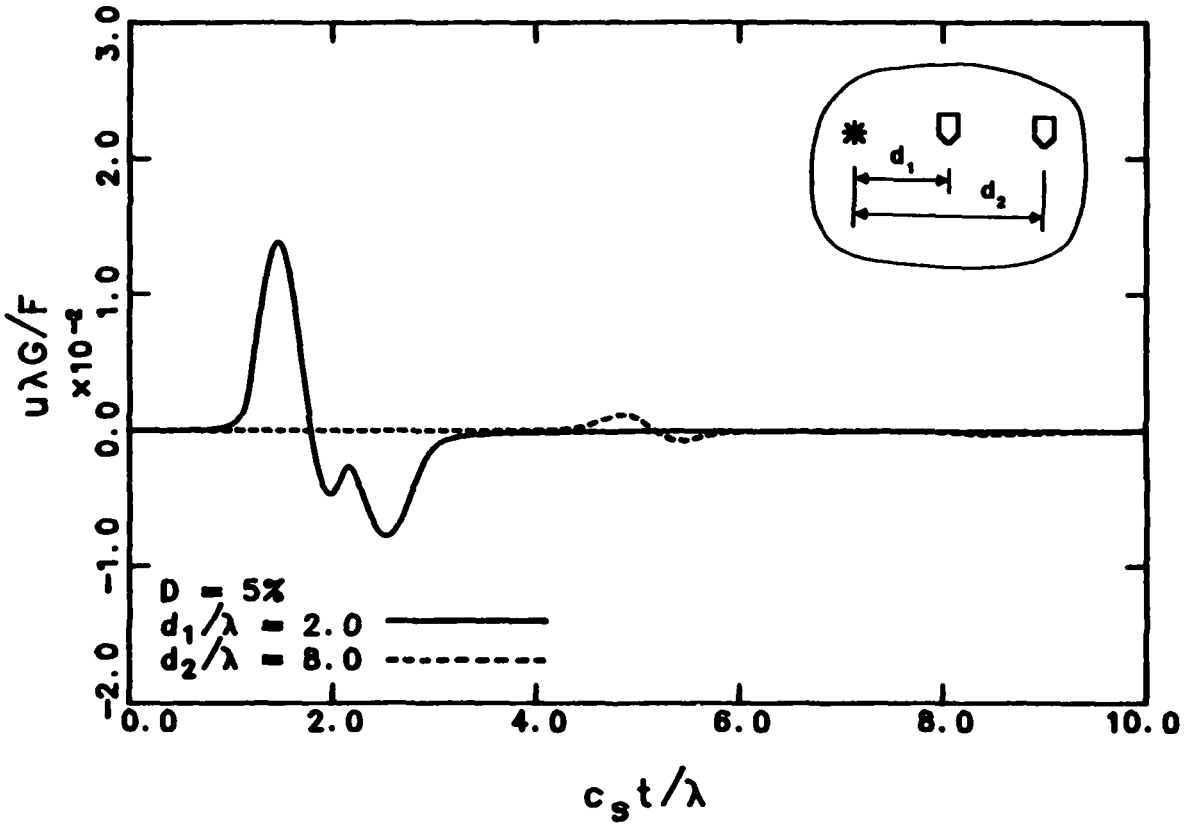

Fig. 4.9 - Three-dimensional longitudinal motion at two different points in a medium with five percent damping.

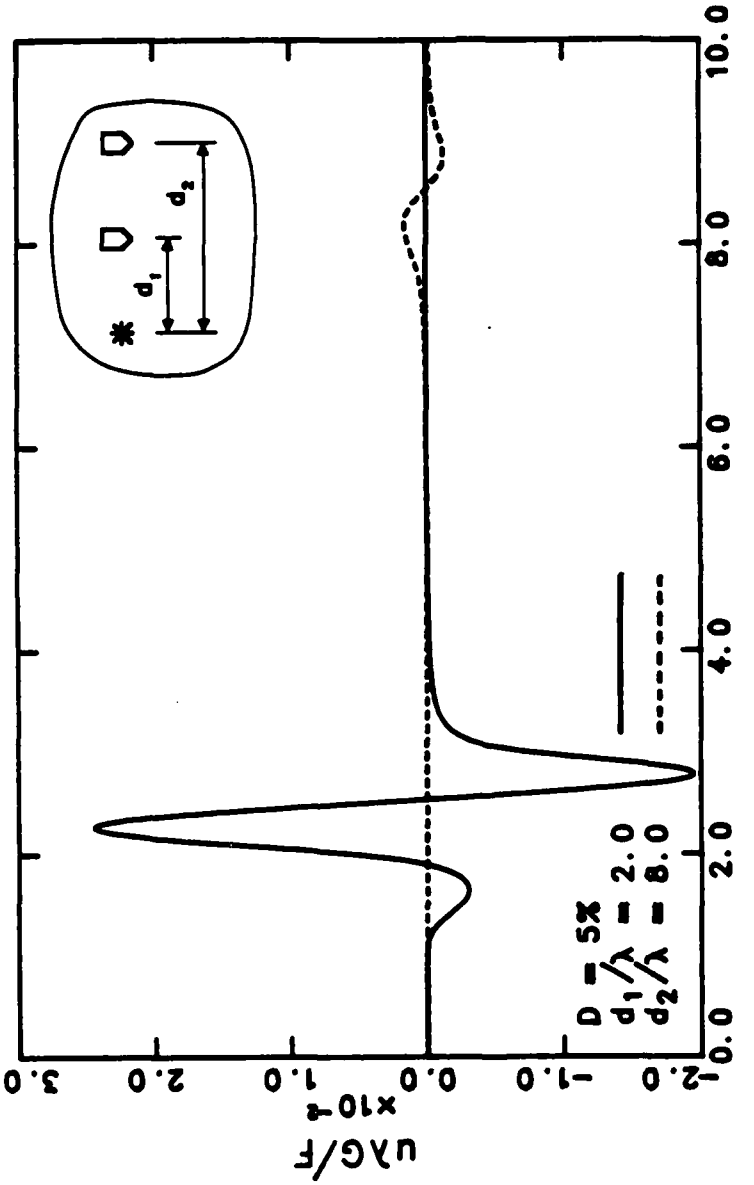

Fig. 4.10 - Three-dimensional shear motion at two different points in a medium with five percent damping.

determined by measuring the time difference between other reference points such as first troughs, first peaks or zero crossings. An example of these procedures is illustrated in Fig. 4.3, for the case of two-dimensional SH-motion in a material with no damping. It can be observed that, since the wave does not change its shape with distance in this case, all the approaches give the same interval times. Similar results would be obtained from the other records of waves propagating in a medium with no damping (Figs. 4.1, 4.2, 4.4 and 4.5). This conclusion is particularly true when the receivers are placed in the far field. If the receivers are located in the near field, then the coupling of near- and far-field waves can obscured the arrival of the waves.

When the medium in which propagation occurs is composed of a material with hysteretic damping, several problems arise. First, times of arrival of the waves are no longer easy to identify (as was previously noted in Section 3.2), and evaluation of interval times from first arrivals may lead to slightly erroneous results. In this regard, interval times from first peaks or zero crossings might be easier to estimate. The use of first troughs can be very troublesome for conditions in which the near-field and far-field waves are coupled together. The first trough attributed to the far-field wave might correspond or be obscured by the near-field wave, as could happen in cases similar to those in Figs. 4.6 and 4.9. A second problem arises from the fact that the shape of the waves vary with distance as shown in Figs. 4.6 through 4.10. This may lead to interval velocities that depend on the relative distance between the recording points. The change in shape is principally caused by the fact that the two components of the waveform (the P-wave and the S- wave) are traveling at different speeds. Therefore, short distances from the source (near field), the P- and S-waves are still coupled, and the combined wave can

have a very irregular shape. In the far field, the P-wave, which is traveling faster than the S-wave, arrives much earlier, and the displacements caused by both waves do not interfere with each other. In addition, in the far field, the near-field components have disappeared.

In Fig. 4.8, possible points to use for interval time measurements are indicated with arrows. It is clear that choosing the points is a subjective matter (especially the ones corresponding to times of the initial arrival). Even for a simple case like Fig. 4.8 (SH-motion), the choice is not clear. The dimensionless interval times obtained from first arrivals, first peaks and first zero crossings are 5.7, 5.9 and 6.1, respectively, compared to the theoretical value of 6.0. In his field research with the crosshole method, Hoar (1982) has experimentally shown a similar relationship between travel times.

It should be noted that the conclusions drawn here for the first peak of a wave whose first excursion goes up, will correspond to the first trough of a wave whose first excursion goes down.

4.4 WAVE VELOCITIES FROM CROSS-CORRELATION RECORDS

4.4.1 Cross-correlation function

A different technique to calculate wave velocities from seismic records is based on the cross-correlation function of waves traveling by two receivers. Cross-correlation, CR(t), of two functions, g(t) and h(t), is given by the integral:

$$CR(\tau) = \int_{-\infty}^{\infty} g(t)\ h(t+\tau)\ dt \qquad (4.1)$$

where g(t) and h(t) represent the time records of the waves passing by the first and second receivers, τ is the time delay and t is the variable of integration.

To interpret this integral, assume the second wave is shifted by a time τ. The sum of the products at each point of the shifted-second wave by the first wave will give one value of the cross-correlation function at time shift τ. If the process is repeated for other time shifts, the cross-correlation function is defined. Assume now that the two functions to be correlated are the same (in terms of the shape of the amplitude versus time function) but that one lags the other by a time t^*. Then the cross-correlation function will exhibit a maximum at a value of τ equal to t^*. If these two shifted but otherwise identical functions represent the waveforms recorded at two receivers of a seismic array, the time t^* where the peak of the cross-correlation occurs represents the time it takes the wave to travel between the two receivers. Unfortunately this idealization does not occur exactly in reality because body waves change shape as they travel in the medium. Nevertheless, when cross-correlating waves from two seismic records that contain energy from predominately one type of body wave, a maximum in the correlation function will occur at a time that corresponds approximately with the time it takes the predominate body wave to travel between the two receivers. If the distance between the two receivers is divided by this time, a shear or compression wave velocity is obtained.

4.4.2 Analysis of cross-correlation records

Cross-correlation functions of some of the records presented in Chapter Three are shown in Figs. 4.11 through 4.20 and in the figures in Appendix C. Two geophone spacings were considered. In the first case, the receivers were located in the near field ($d/\lambda \leq 2$), Figs. 4.11 through 4.15 and Figs. C.1 through C.10. In the second case, the receivers were located in the far field, Figs. 4.16 through 4.20 and Figs. C.11 through C.20. The ratio of the distance from the source to the first receiver to the distance from the source to the second receiver, d_2/d_1, was equal to 2, which is common practice for crosshole seismic measurements (ASTM, 1985). Values of Poisson's ratio (ν = POI.R. in the figures) of 0.25 and 0.4 were considered, and damping ratios (D) of 0 and 5 percent were used. The cross-correlation function is presented in dimensionless form by means of a normalized cross-correlation factor. The normalized cross-correlation is defined as the ratio of the value of the cross-correlation at any time delay to the maximum absolute cross-correlation value. The time delay is presented in dimensionless form as $c_s t/(d_2-d_1)$, where t represents the time delay. In this way the shear wave velocity of the material would correspond to a value of the abscissa equal to 1, while the compression wave velocity would correspond to values of 0.577 and 0.408 for Poisson's ratios of 0.25 and 0.4, respectively. The cross-correlation records are presented for two-dimensional, P-, SV- and SH-motions as well as three-dimensional, P- and S-motions.

From inspection of the cross-correlation records, the following conclusions can be made.

1. The cross-correlation function provides an easy and accurate method to calculate wave velocities from these synthetic seismic records. As such, the procedure represents a powerful tool

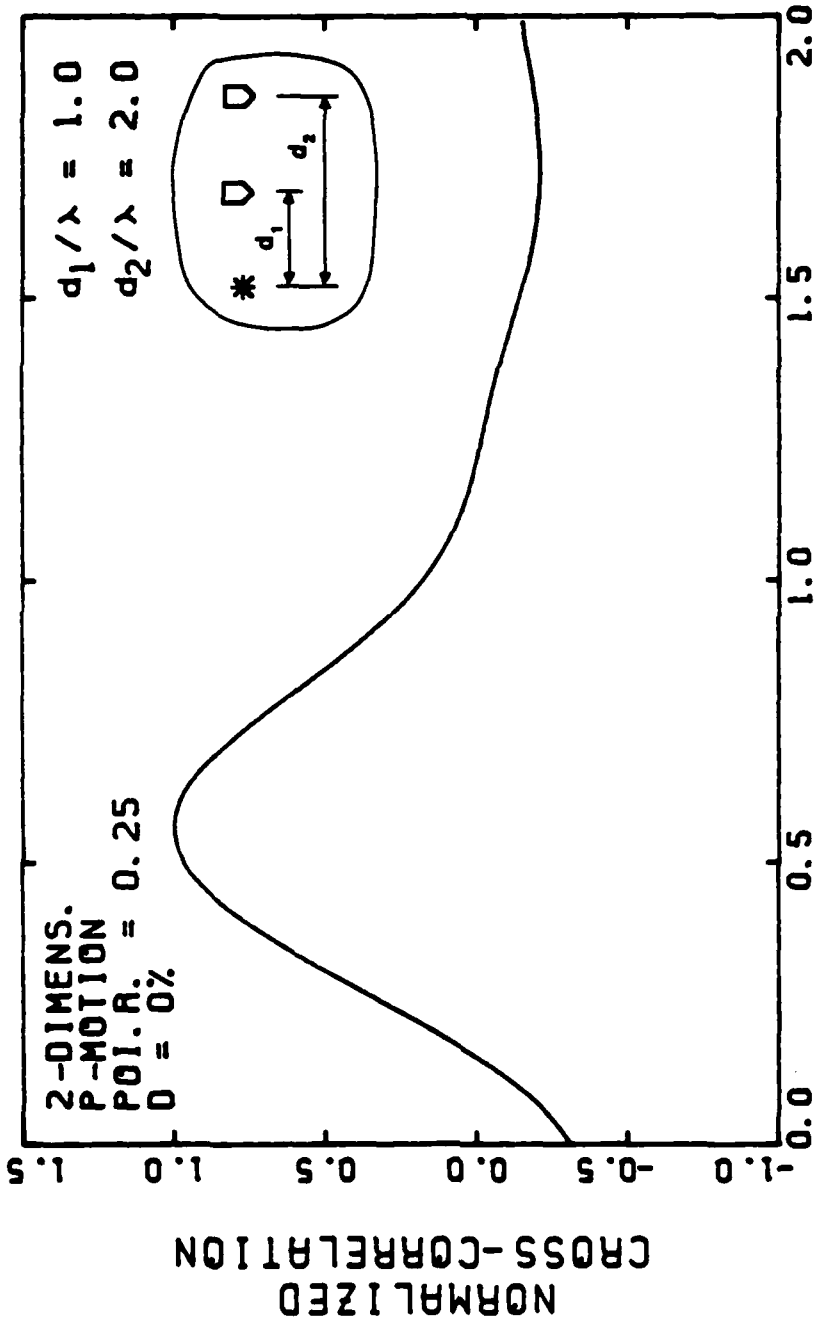

Fig. 4.11 - Cross-correlation function of two-dimensional P-motion records obtained in the near field. Poisson's ratio = 0.25 and damping = 0 %.

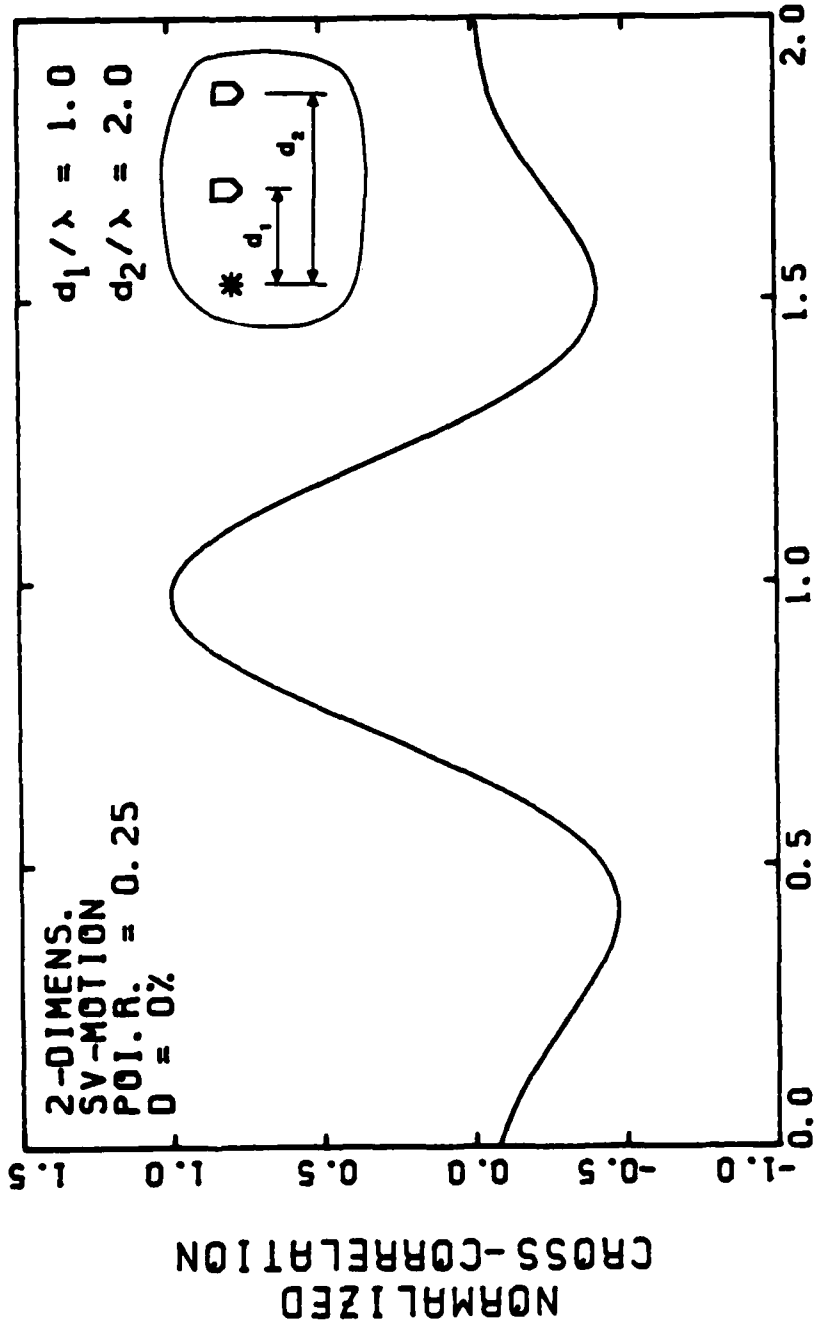

Fig. 4.12 - Cross-correlation function of two-dimensional SV-motion records obtained in the near field. Poisson's ratio = 0.25 and damping = 0 %.

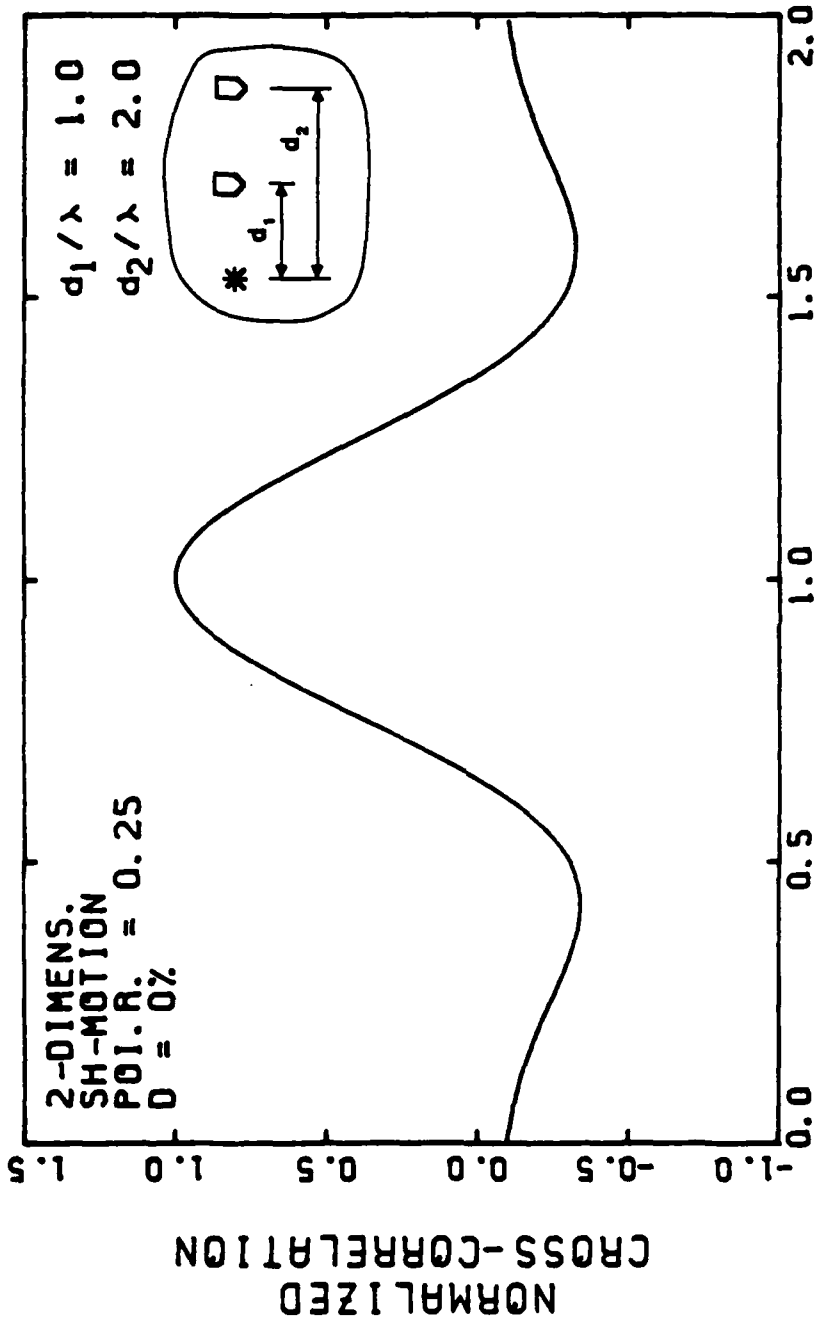

Fig. 4.13 - Cross-correlation function of two-dimensional SH-motion records obtained in the near field. Poisson's ratio = 0.25 and damping = 0 %.

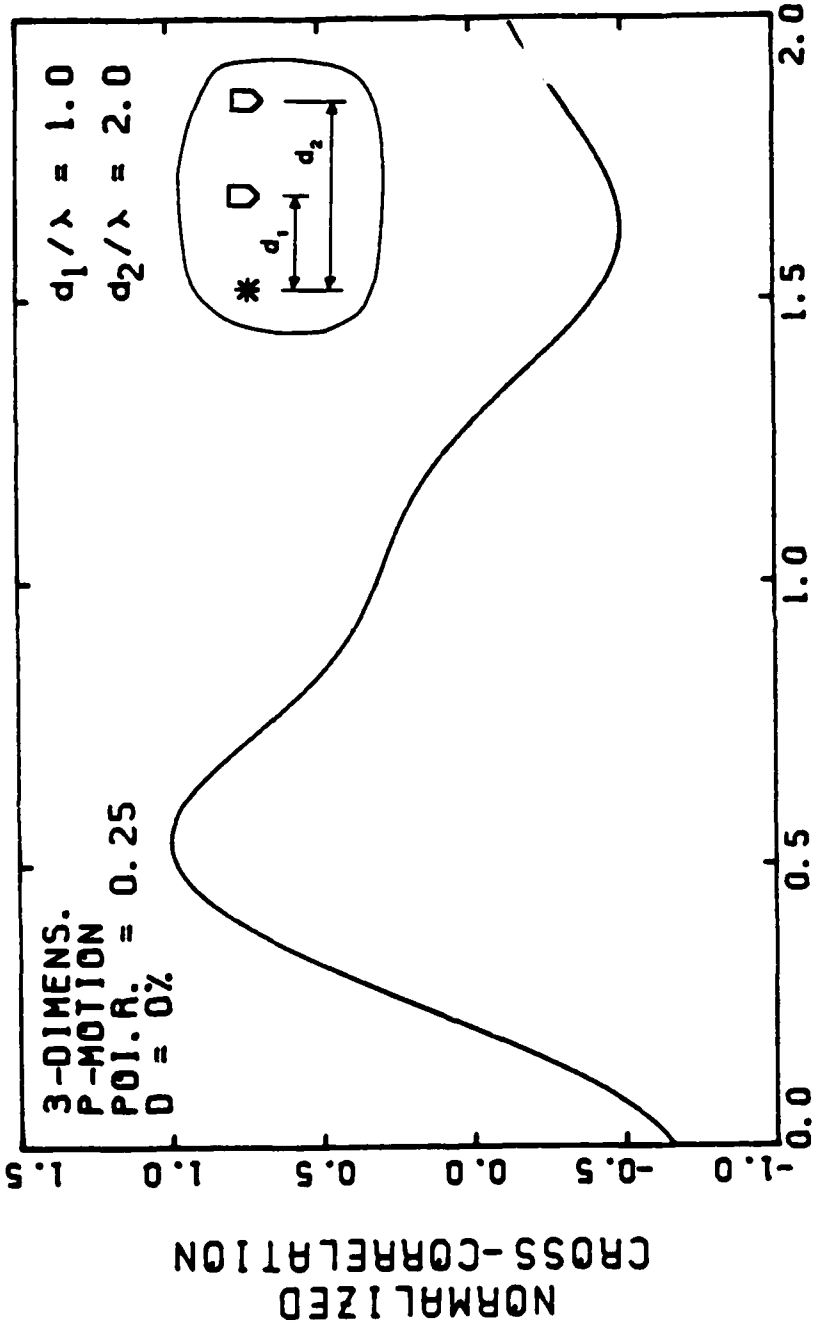

Fig. 4.14 - Cross-correlation function of three-dimensional P-motion records obtained in the near field. Poisson's ratio = 0.25 and damping = 0 %.

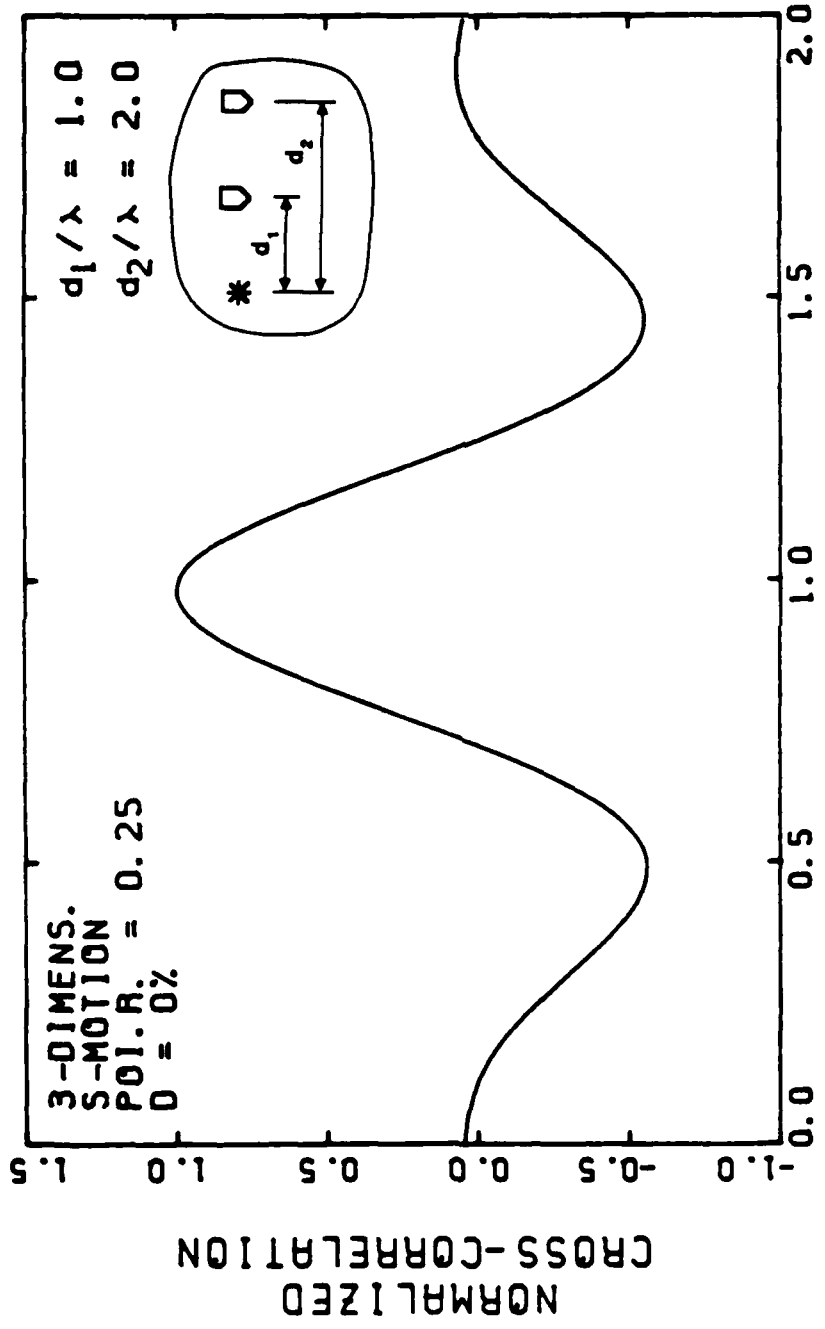

Fig. 4.15 - Cross-correlation function of three-dimensional S-motion records obtained in the near field. Poisson's ratio = 0.25 and damping = 0 %.

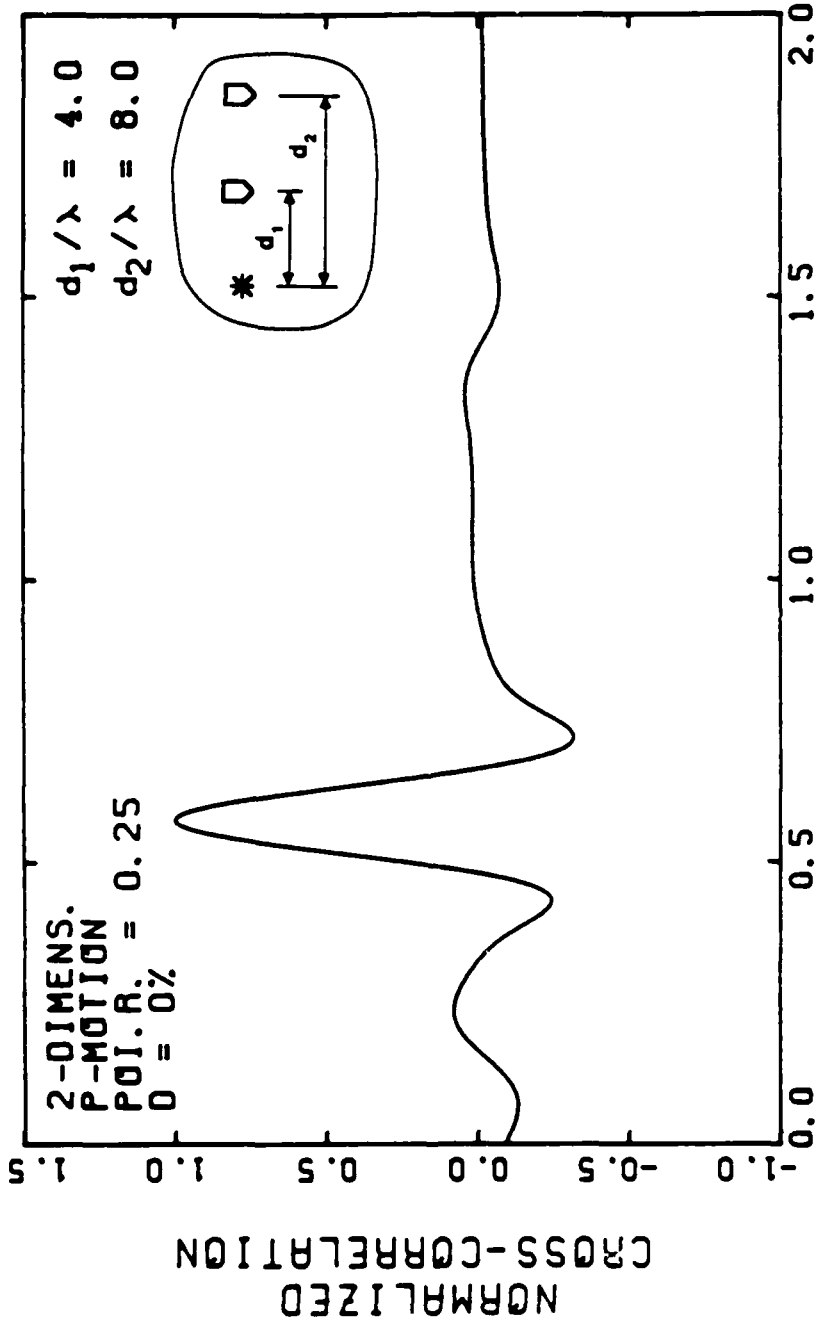

Fig. 4.16 - Cross-correlation function of two-dimensional P-motion records obtained in the far field. Poisson's ratio = 0.25 and damping = 0 %.

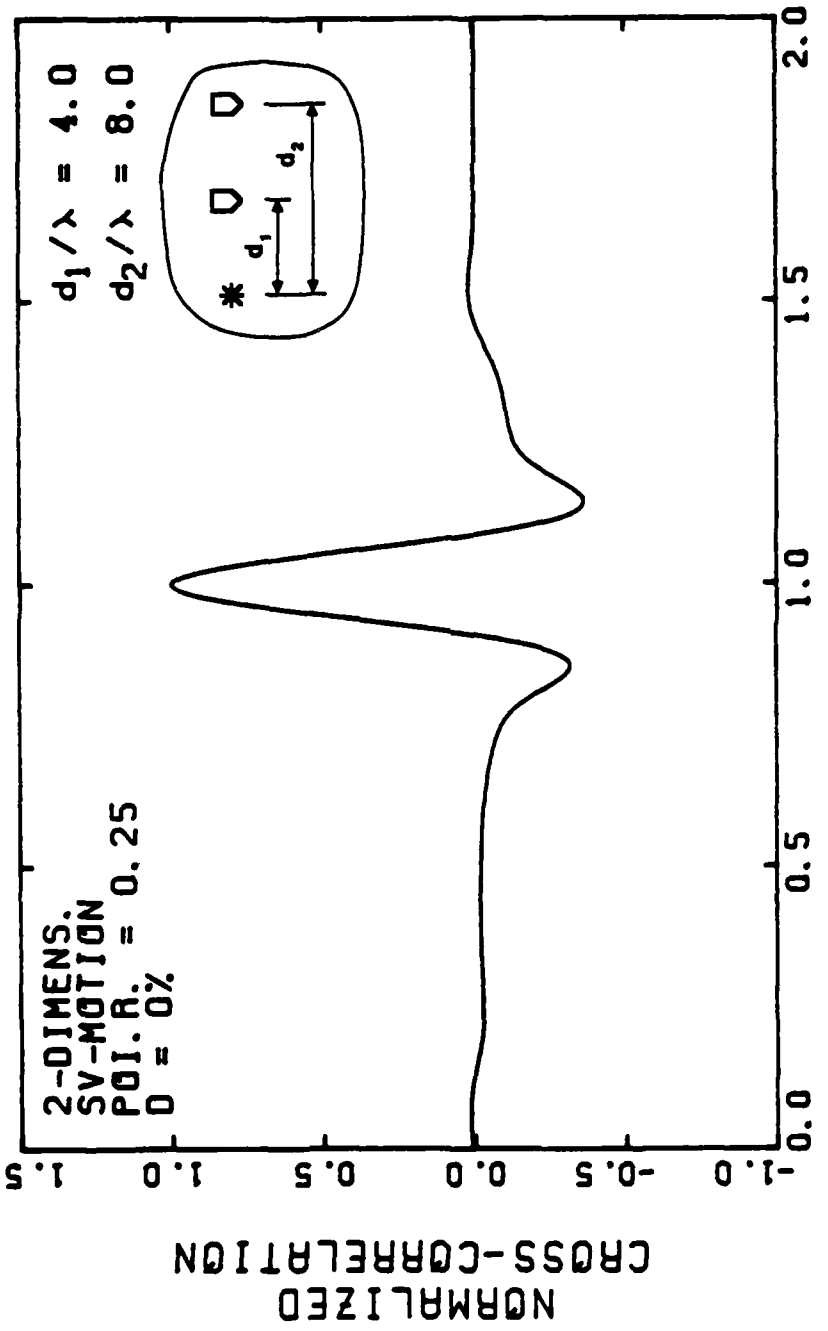

Fig. 4.17 - Cross-correlation function of two-dimensional SV-motion records obtained in the far field. Poisson's ratio = 0.25 and damping = 0 %.

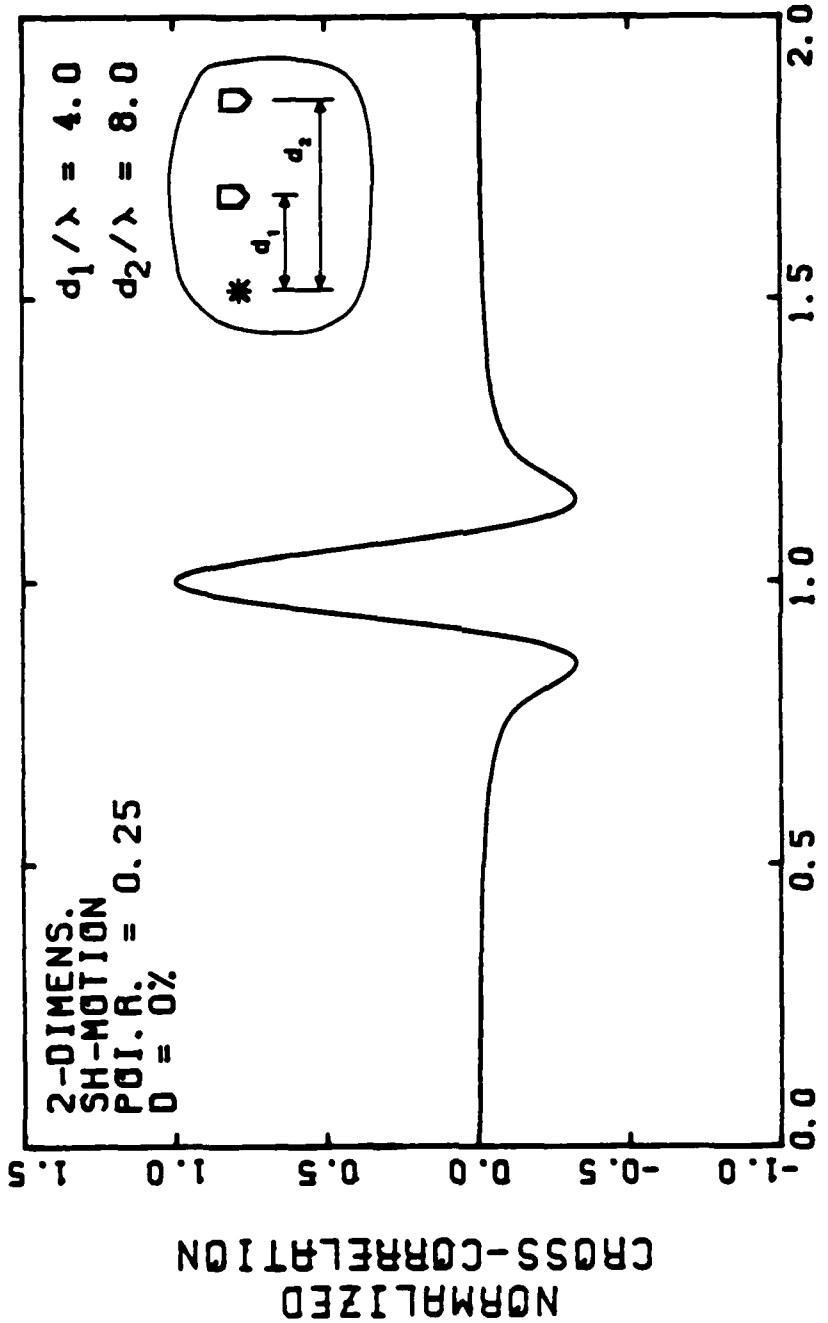

Fig. 4.18 - Cross-correlation function of two-dimensional SH-motion records obtained in the far field. Poisson's ratio = 0.25 and damping = 0 %.

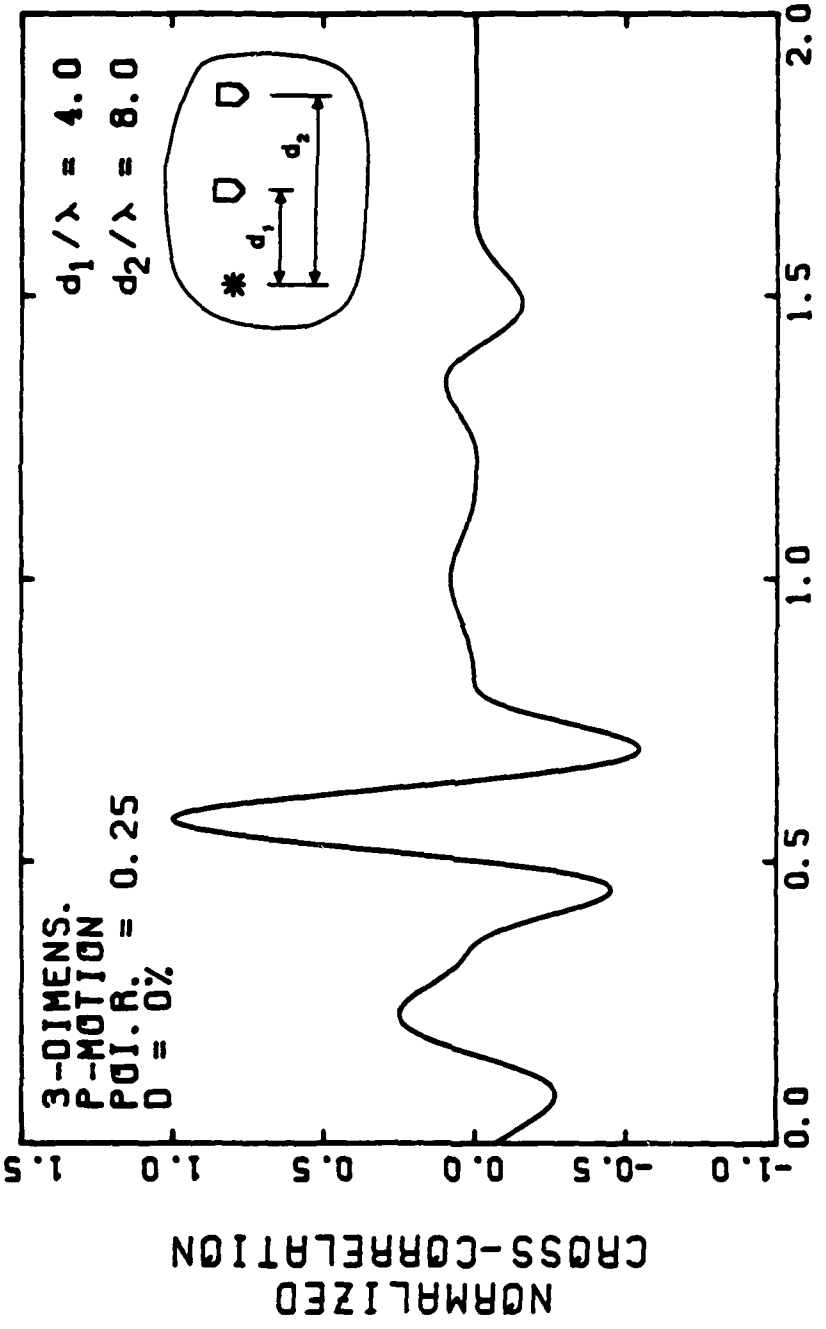

Fig. 4.19 - Cross-correlation function of three-dimensional P-motion records obtained in the far field. Poisson's ratio = 0.25 and damping = 0 %.

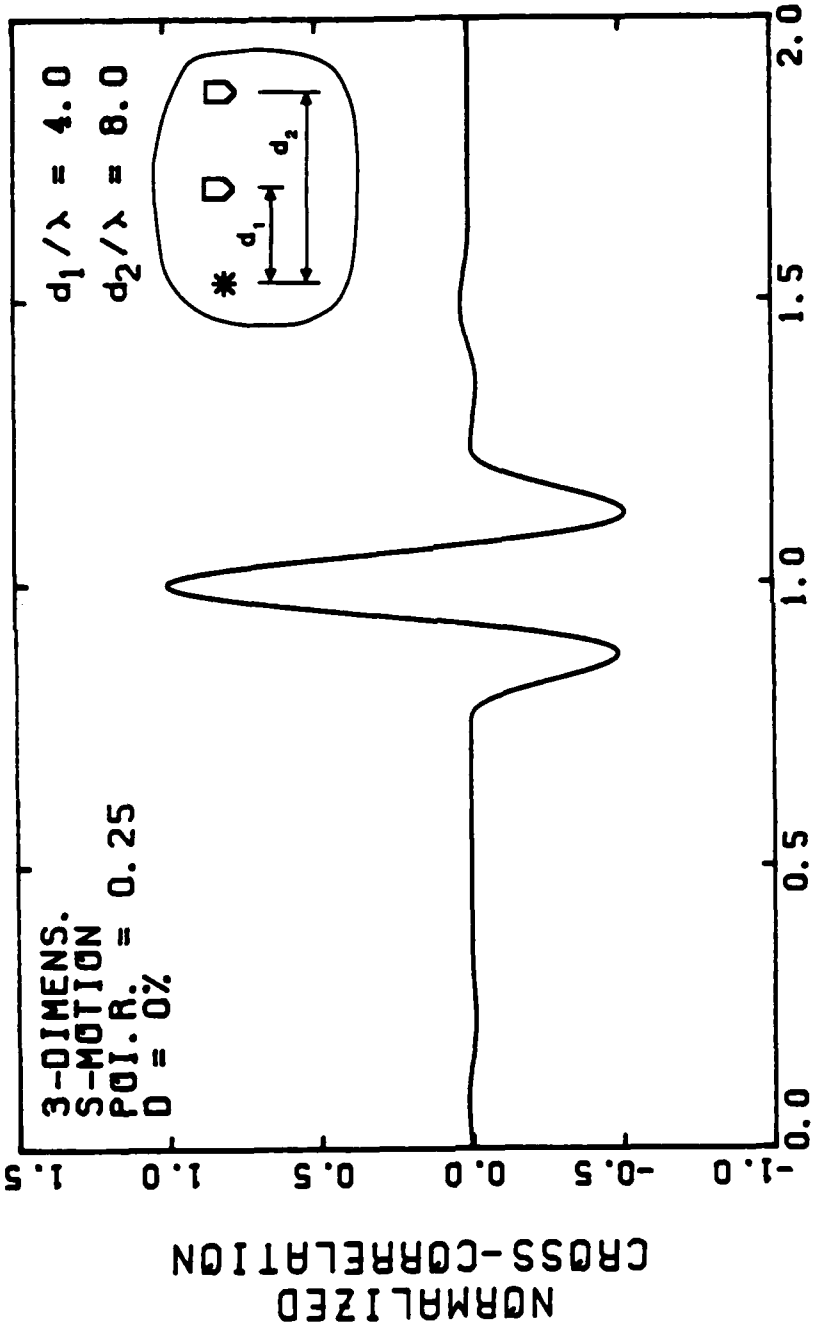

Fig. 4.20 - Cross-correlation function of three-dimensional S-motion records obtained in the far field. Poisson's ratio = 0.25 and damping = 0 %.

because it has the potential for full automation. However, a key aspect to application of this method is generation and recording of seismic waves of predominately one type (P or S).

2. Velocities calculated with the cross-correlation function are, in general, as accurate as (or more accurate than) those determined using times of arrival or interval times from time histories. Travel times obtained from the maximum of the cross-correlation function were in almost every case within one or two percent of the exact value. Interval travel times obtained in this manner have the following important characteristics: they are unique values; they are not subject to interpretation as are the times of arrival of the waves; and they are not affected or are only slightly affected by the value of the damping ratio.

3. The cross-correlation method can be used with confidence when the receivers are located in the far field. In the near field, the compression wave velocities obtained from longitudinal-motion records on materials with high values of Poisson's ratio require careful interpretation (as in the case in Fig. C.9 where the peak of the cross-correlation function corresponds to the value of the shear wave velocity instead of the value of the compression wave velocity as would be expected from a longitudinal-motion record).

These conclusions apply to the "clean" time histories shown in Appendix A. For actual seismic records obtained in the field, the cross-correlation curves may be not be as simple as those presented here. In those complicated cases, however, the time histories will be complex as well and the estimation of the times of arrival will also present some difficulties. A practical application of the cross-correlation technique to actual crosshole field tests can be found in Stokoe et al (1985).

4.5 WAVE VELOCITIES USING SPECTRAL ANALYSIS TECHNIQUES

4.5.1 Theoretical background

In recent years great improvements have been achieved in electronic equipment to monitor the response of dynamic systems. The development of microprocessors and computational algorithms has significantly increased the capability of the instrumentation for recording, measuring and analyzing systems in both time and frequency domains. Recording and analysis of signals can be easily and rapidly done in the field with modern spectral analyzers.

Frequency domain analyses have several advantages. First, trends that might be difficult to identify in the time domain can be easily studied in the frequency domain. Second, operations with signals in the time domain (such as integration or differentiation) can be greatly simplified if done in the frequency domain. Third, frequency domain techniques allow full automation of data reduction. Finally, averaging of signals, which requires extreme care in the time domain, is easily done in the frequency domain.

The spectrum of a signal is a representation of that signal in terms of its frequency components. The tool used to transform a signal from its time history to its frequency components is the Fourier transform. Forward and inverse Fourier transform formulas are given in Section 2.2, along with a brief introduction to the Fast Fourier Transform (FFT) algorithm to compute Fourier transforms. The FFT forms the basis for an additional method to calculate wave velocities (compared with those presented in the previous sections) based on the cross spectral density function (or cross spectrum).

The cross spectrum, CS(f), of two functions, $u_1(t)$ and $u_2(t)$, is defined as:

$$CS(f) = U_1(f) \cdot \underline{U_2}(f) \tag{4.2}$$

where,

$U_1(f)$ is the Fourier transform of $u_1(t)$,
$U_2(f)$ is the Fourier transform of $u_2(t)$,
t is the time variable,
f is the frequency in Hz, and
"_" indicates complex conjugate.

The cross spectrum is, therefore, a complex function of frequency.

Assume that the functions $u_1(t)$ and $u_2(t)$ are the time records at two sampling points. For each frequency the phase of the cross spectrum of $u_1(t)$ and $u_2(t)$ will give the phase difference in radians (or degrees) of the corresponding harmonic. Since the period (T) of that harmonic is known (T = 1/f), a travel time between target points can be obtained for each frequency, f, by:

$$t(f) = [T \cdot \phi(f)]/2\pi = \phi(f)/2\pi f \tag{4.3}$$

where,

t(f) is travel time for a given frequency, and
$\phi(f)$ is the phase in radians of the cross spectrum at each frequency.

The distance between the two receivers is a known parameter. Therefore the apparent wave velocity at a given frequency is simply calculated by:

$$V(f) = d/t(f) \tag{4.4}$$

where,

$d = d_2 - d_1$, is the distance between target points, and

d_1 and d_2 are the distances from the source to the first and second receiver respectively.

The term "apparent velocity" is used since it does not represent the phase velocity of a pure plane wave because of the interactions between near- and far-field components.

Using these formulas a curve of apparent wave velocity versus frequency can be calculated. Such a curve is called a velocity dispersion curve (or simply dispersion curve) in this study. Dispersion curves are also defined by other authors as relations of velocities with wavelengths, wave numbers or wave periods. Once one form of the dispersion curve is known, the others can be easily obtained since frequency, wavelength, wave number and period are related by:

$$\omega T = kL = 2\pi \tag{4.5}$$

$$\omega = 2\pi f \tag{4.6}$$

$$V(f) = Lf \tag{4.7}$$

where,

ω is the frequency of the harmonic in rad/sec,

T is the period in sec,

k is the wave number, and

L is the wavelength of the harmonic wave.

Variables that affect apparent wave velocity are: frequency (ω or f), distance from the source to the first receiver (d_1), and distance from the source to the second receiver (d_2), in addition to the elastic variables. The number of variables can be reduced if they are expressed in dimensionless form. In this study the distance from the source to the first receiver and the frequency are considered in dimensionless form as d_1/λ, where λ is the wavelength of the shear wave ($\lambda = c_s/f$). The distance between the two receivers is considered as d_2/d_1. The apparent velocity is presented in non-dimensional form as V/c_p for compressional (longitudinal) motions and as V/c_s for shear (transverse) motions. The other variables studied are Poisson's ratio and damping ratio.

Any impulse can be considered as the excitation force. However, since the only information that is needed to calculate the dispersion curves (for this theoretical study) is the phase of the cross spectrum, this relative phase can be calculated from the phases of the Green's functions at the two receivers. This calculation is very convenient because it can be done without performing any of the Fourier transforms. To illustrate this point, assume that the load applied at the source point is any arbitrary function p(t) and that the Green's functions (or transfer functions) at the two receivers (points 1 and 2) are $H_1(f)$ and $H_2(f)$. At each frequency the response at points 1 and 2 will be (see Eq. 2.4)

$$U_1(f) = P(f) \cdot H_1(f) \tag{4.8}$$

and

$$U_2(f) = P(f) \cdot H_2(f) \tag{4.9}$$

respectively. P(f) is the Fourier transform of p(t). The phase of the cross spectrum of $u_1(t)$ and $u_2(t)$ is then the phase of $U_1(f)$ minus the phase of $U_2(f)$, which in turn is the same as the phase of $H_1(f)$ minus the phase of $H_2(f)$.

4.5.2 Dispersion curves from cross spectrum function

A first set of dispersion curves for two- and three-dimensional motions are presented in Figs. 4.21 through 4.30 for a material with a Poisson's ratio of 0.25 and no material damping. It is first observed in Figs. 4.21 through 4.30 that the dispersion curves depend on the relative position of the source and receivers. For a constant ratio d_2/d_1, the apparent velocity fluctuates as d_1/λ varies (λ is the wavelength of the shear wave). This can be interpreted as the apparent velocity varying with frequency (or wavelength) for a given distance d_1, or as the apparent velocity varying with distance d_1, for a given frequency (or wavelength). The fluctuations are large in the near field (small distances, d_1, or low frequencies, f) and decrease as the distance d_1 increases (or the wavelength decreases).

The dispersive effect also decreases as the spacing between the receivers increases (or as d_2/d_1 increases). This can be observed in Figs. 4.21 and 4.22 for two-dimensional P-motion, Figs. 4.23 and 4.24 for two-dimensional SV-motion, Figs. 4.27 and 4.28 for three-dimensional P-motion and Figs. 4.29 and 4.30 for three-dimensional S-motion. The dispersive effect seems to be more important in longitudinal motions (P-motions) than in transverse motions (S-motions).

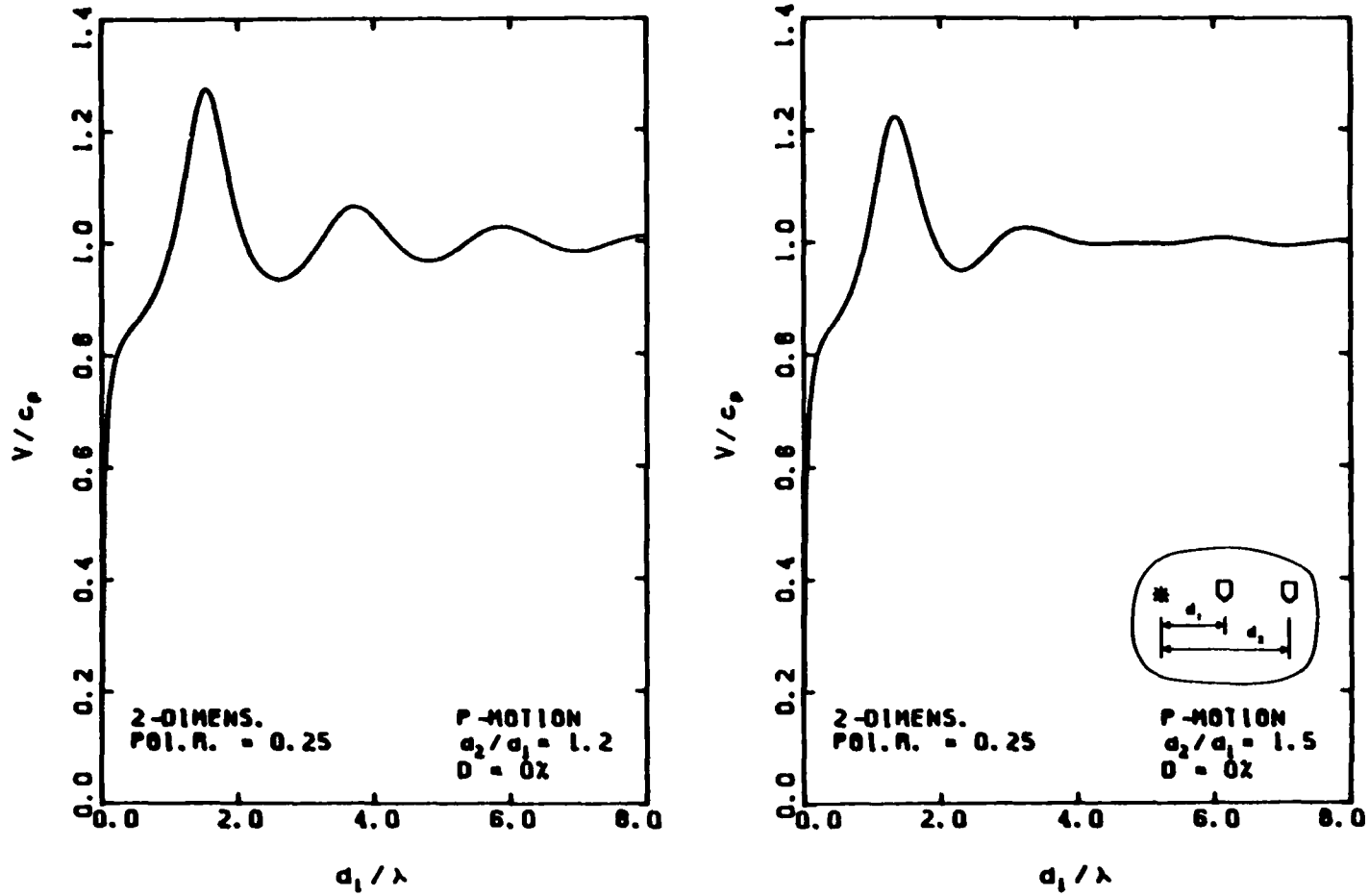

Fig. 4.21 - Dispersion curves for two-dimensional in-plane longitudinal motion in a medium with no damping and Poisson's ratio = 0.25. Small spacing between receivers.

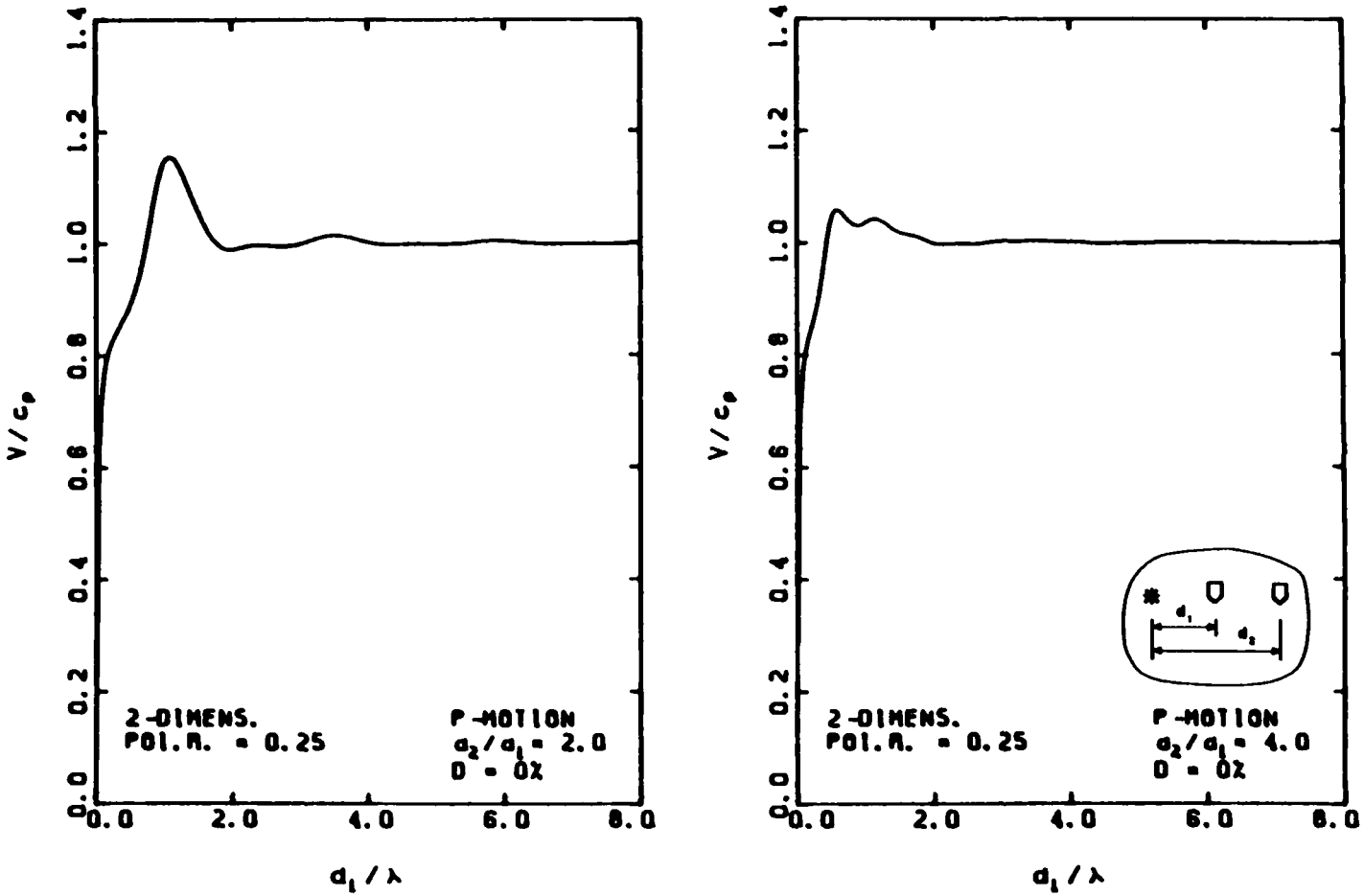

Fig. 4.22 - Dispersion curves for two-dimensional in-plane longitudinal motion in a medium with no damping and Poisson's ratio = 0.25. Large spacing between receivers.

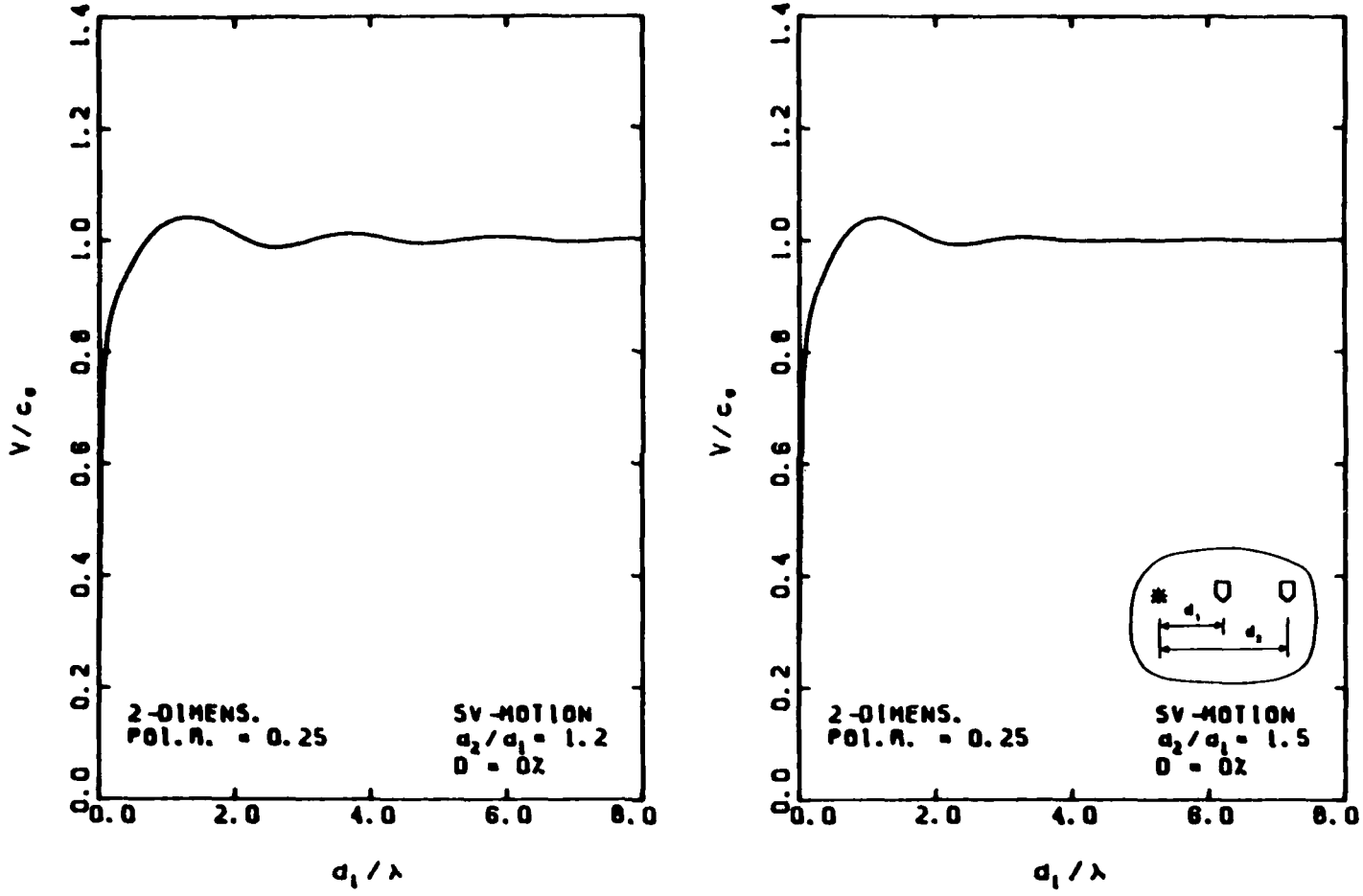

Fig. 4.23 - Dispersion curves for two-dimensional in-plane shear motion in a medium with no damping and Poisson's ratio = 0.25. Small spacing between receivers.

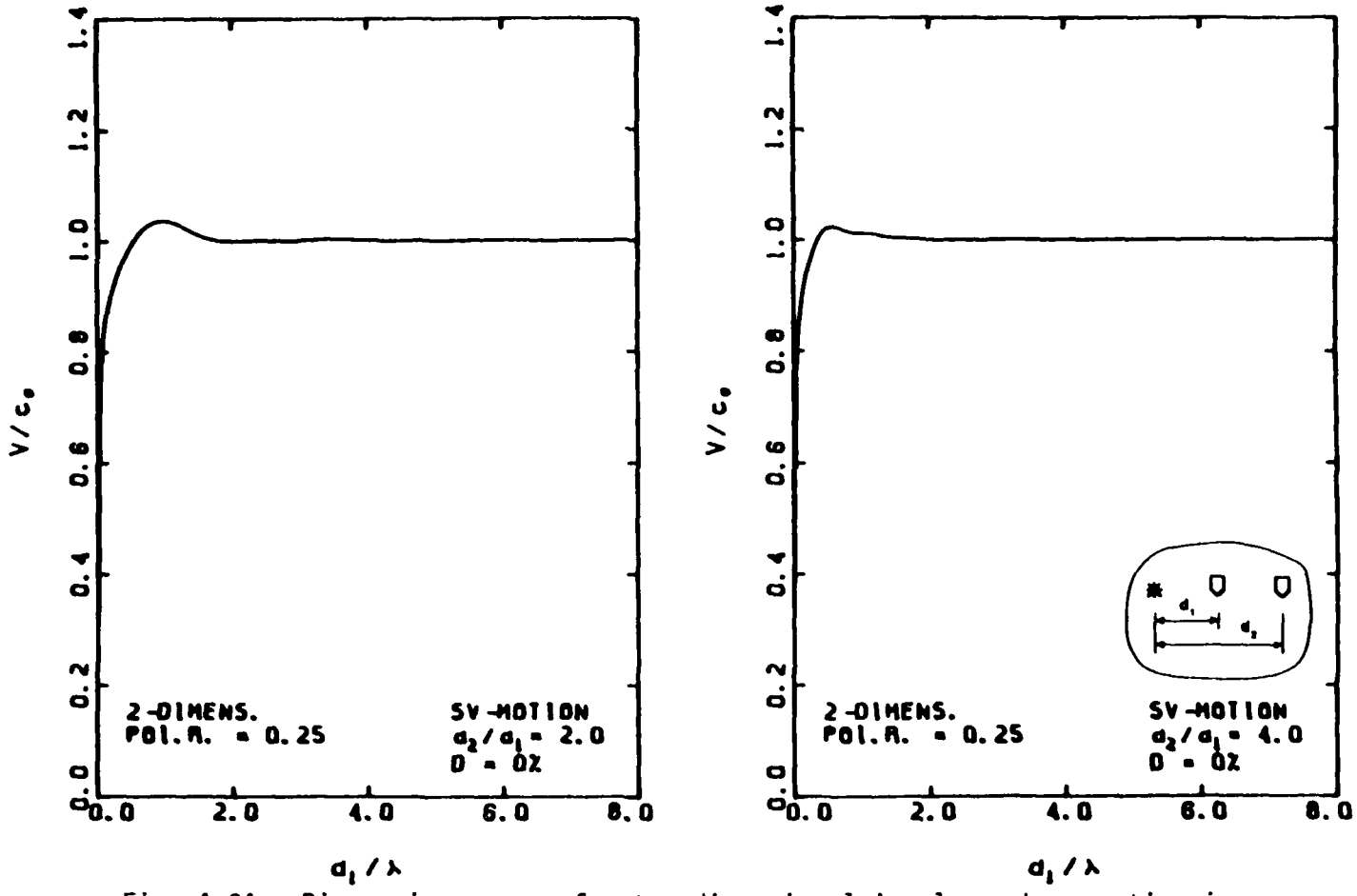

Fig. 4.24 - Dispersion curves for two-dimensional in-plane shear motion in a medium with no damping and Poisson's ratio = 0.25. Large spacing between receivers.

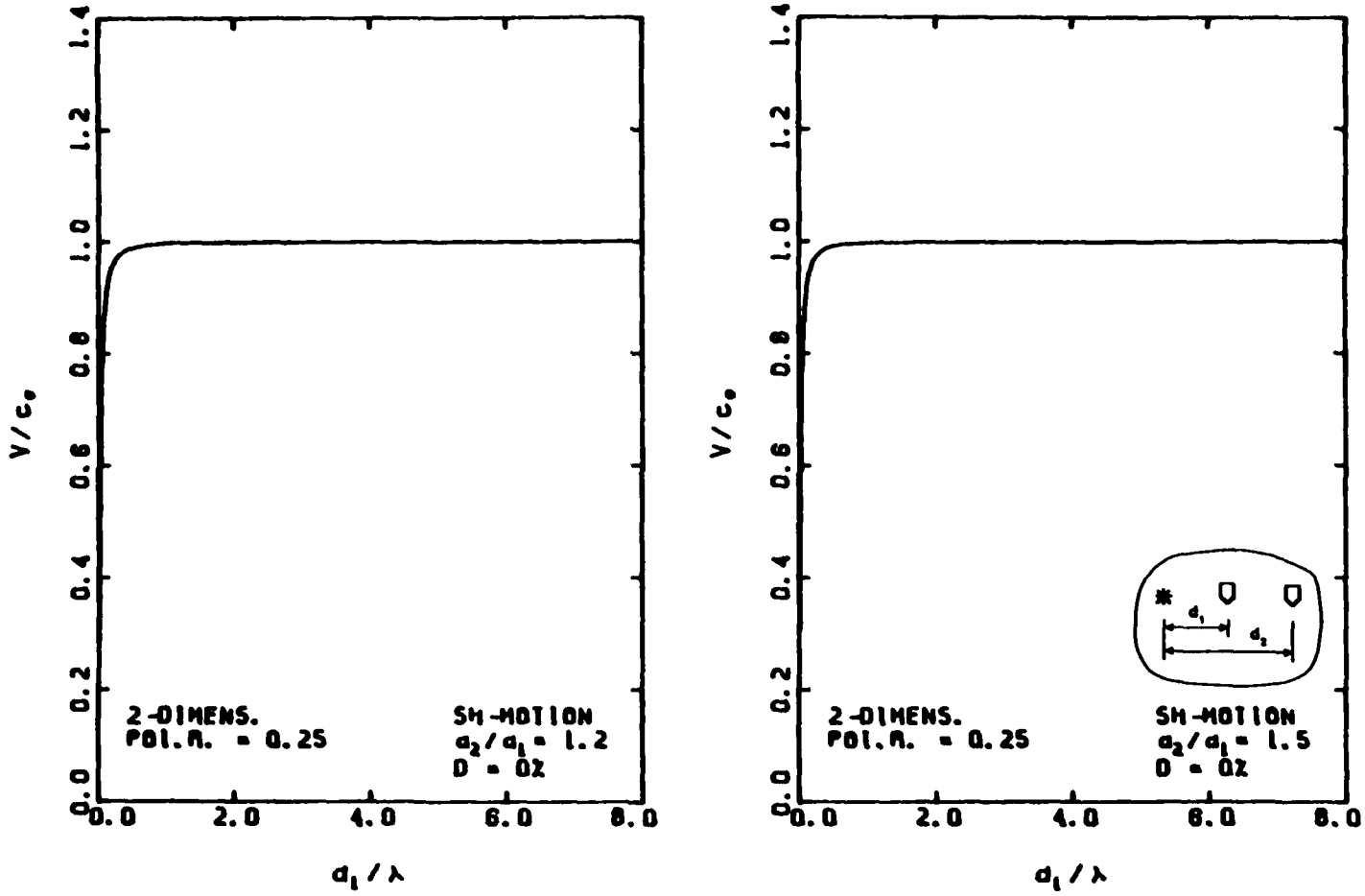

Fig. 4.25 - Dispersion curves for two-dimensional antiplane shear motion in a medium with no damping and Poisson's ratio = 0.25. Small spacing between receivers.

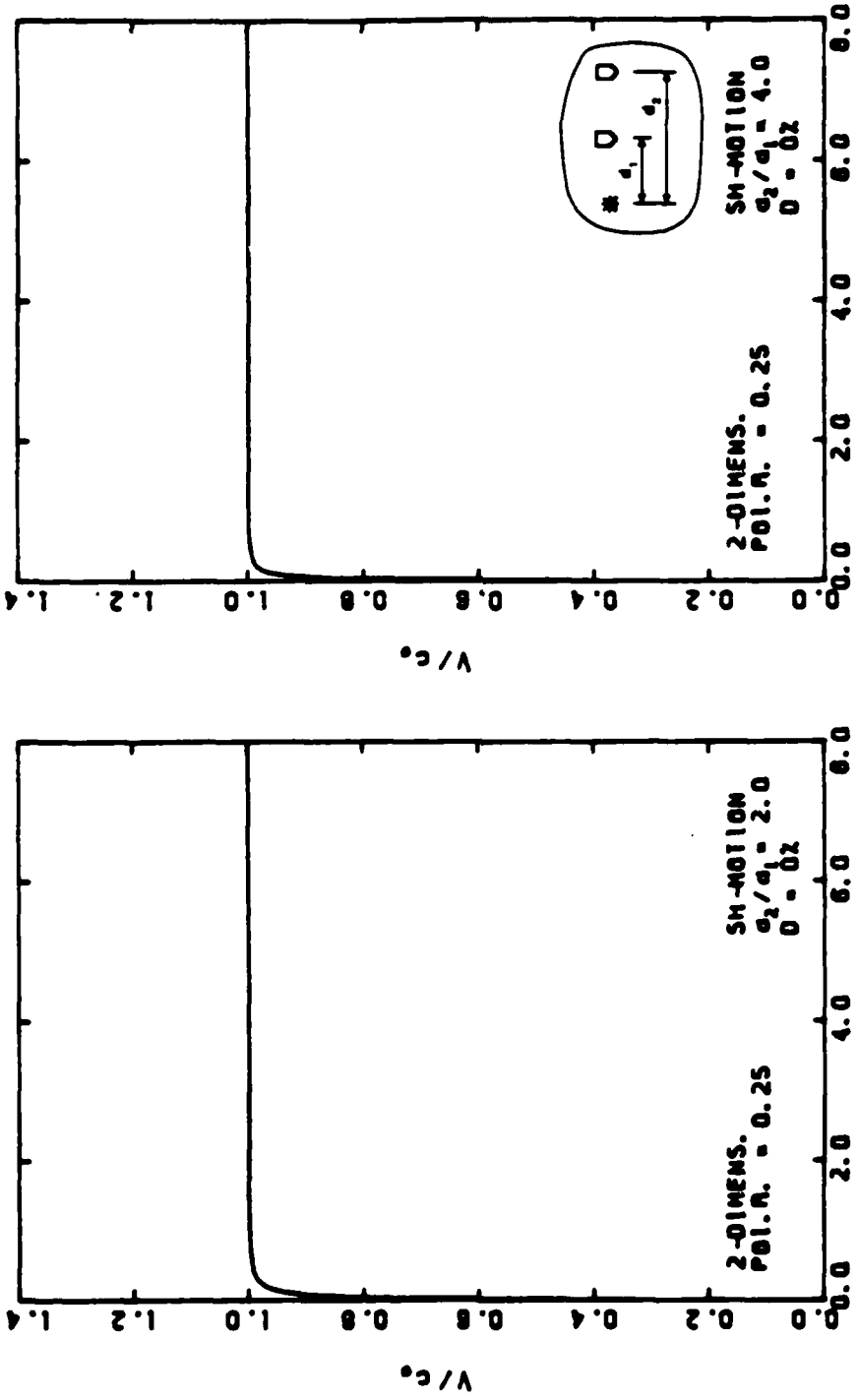

Fig. 4.26 - Dispersion curves for two-dimensional antiplane shear motion in a medium with no damping and Poisson's ratio = 0.25. Large spacing between receivers.

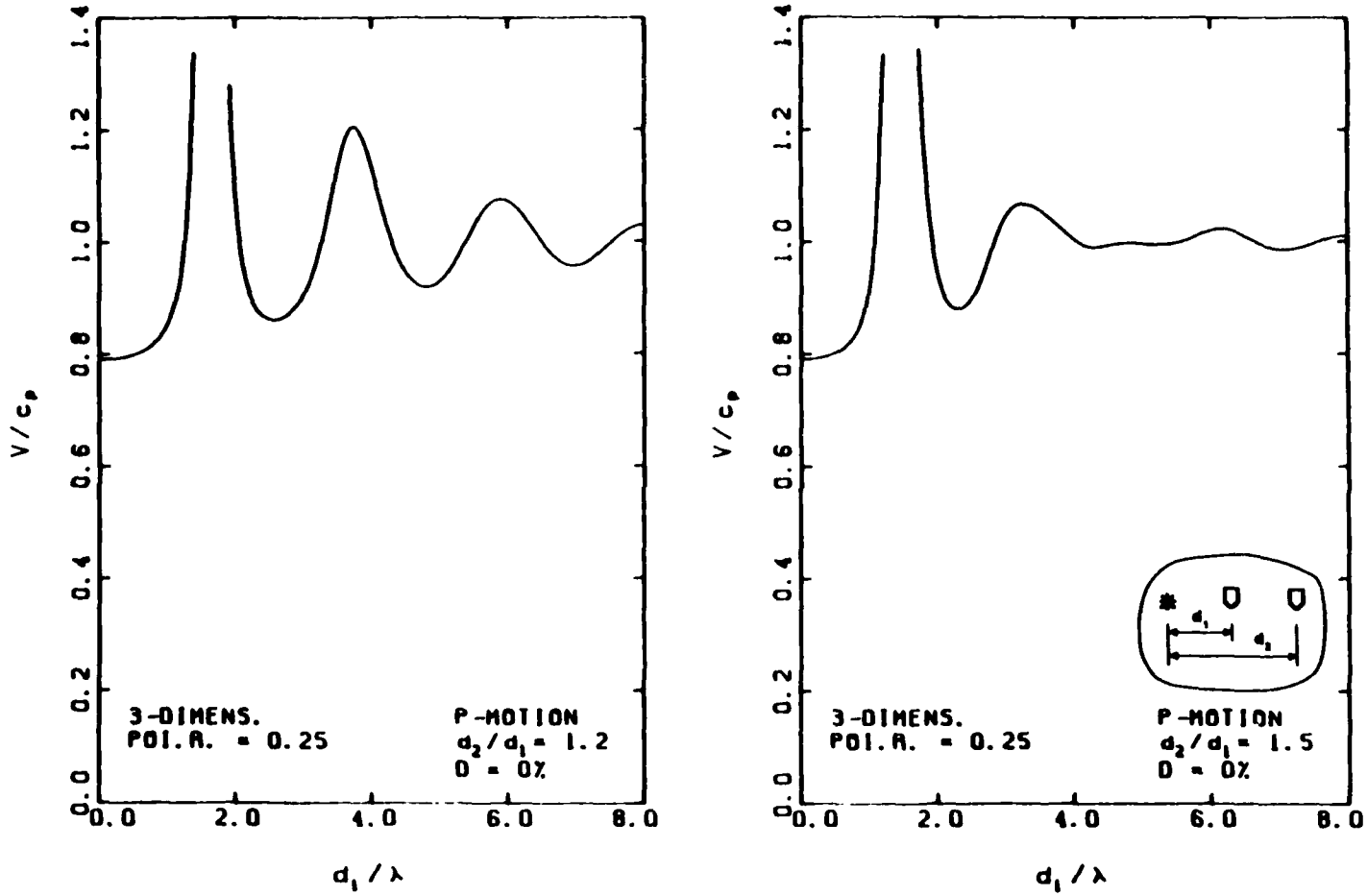

Fig. 4.27 - Dispersion curves for three-dimensional longitudinal motion in a medium with no damping and Poisson's ratio = 0.25. Small spacing between receivers.

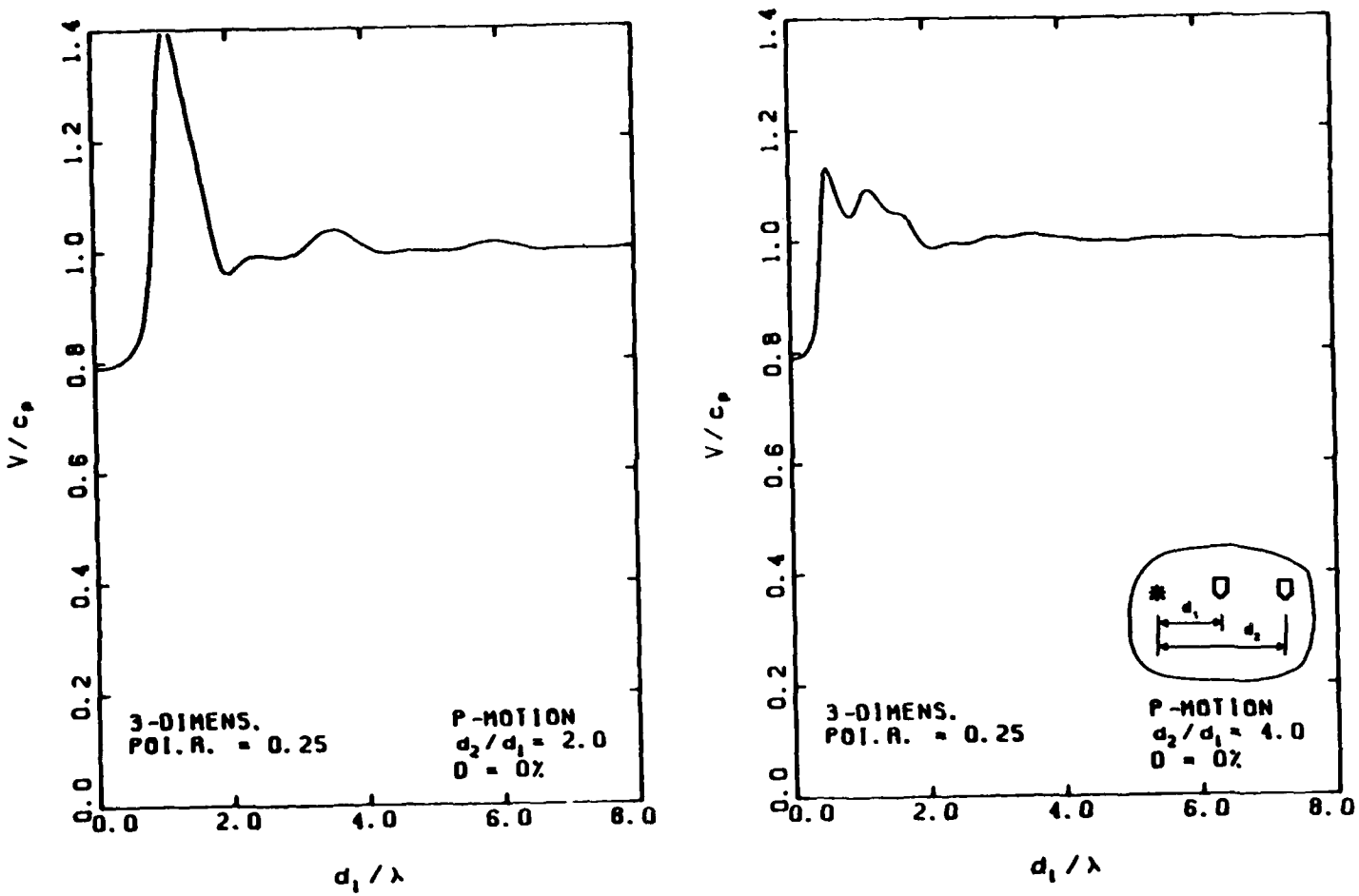

Fig. 4.28 - Dispersion curves for three-dimensional longitudinal motion in a medium with no damping and Poisson's ratio = 0.25. Large spacing between receivers.

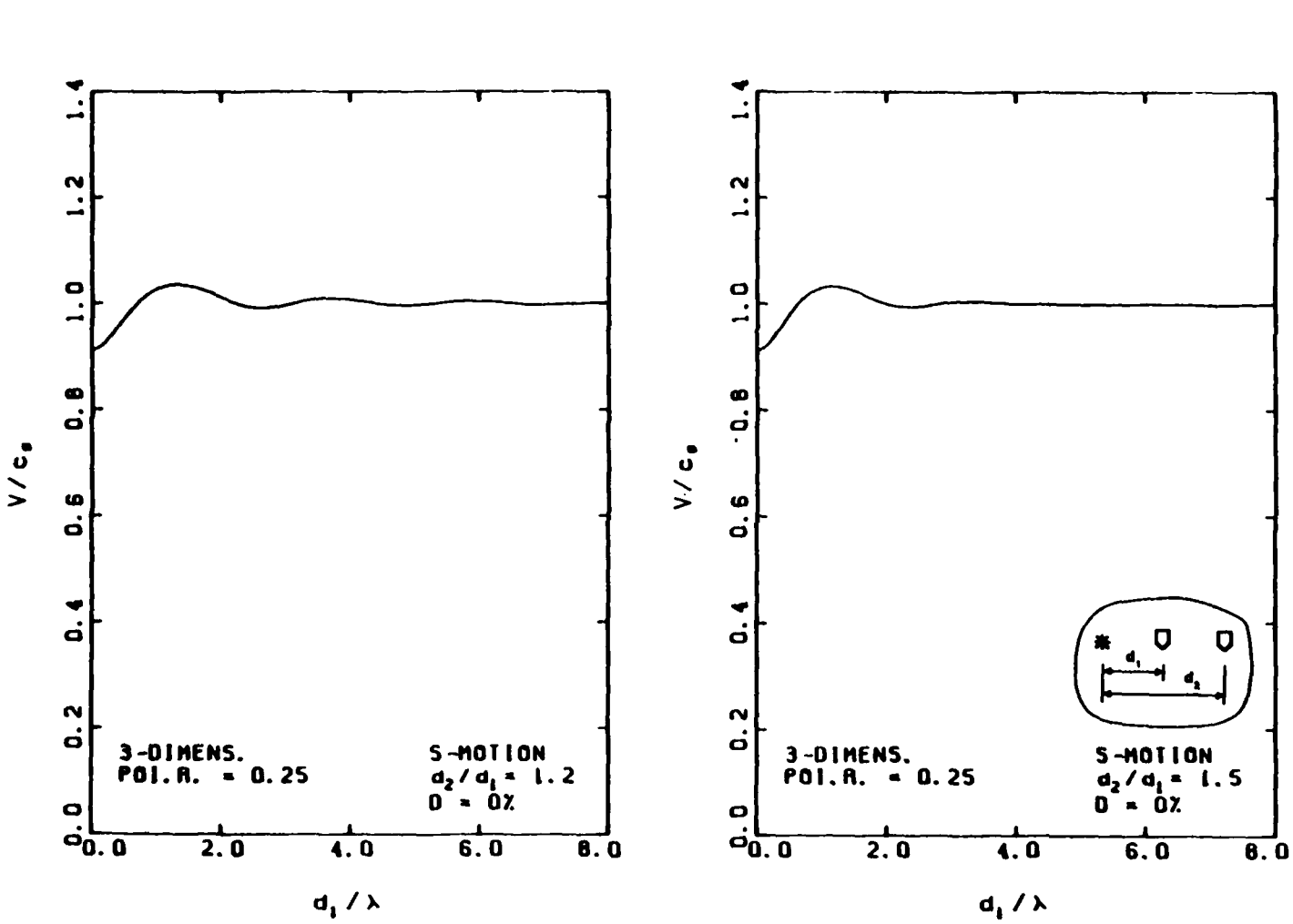

Fig. 4.29 - Dispersion curves for three-dimensional shear motion in a medium with no damping and Poisson's ratio = 0.25. Small spacing between receivers.

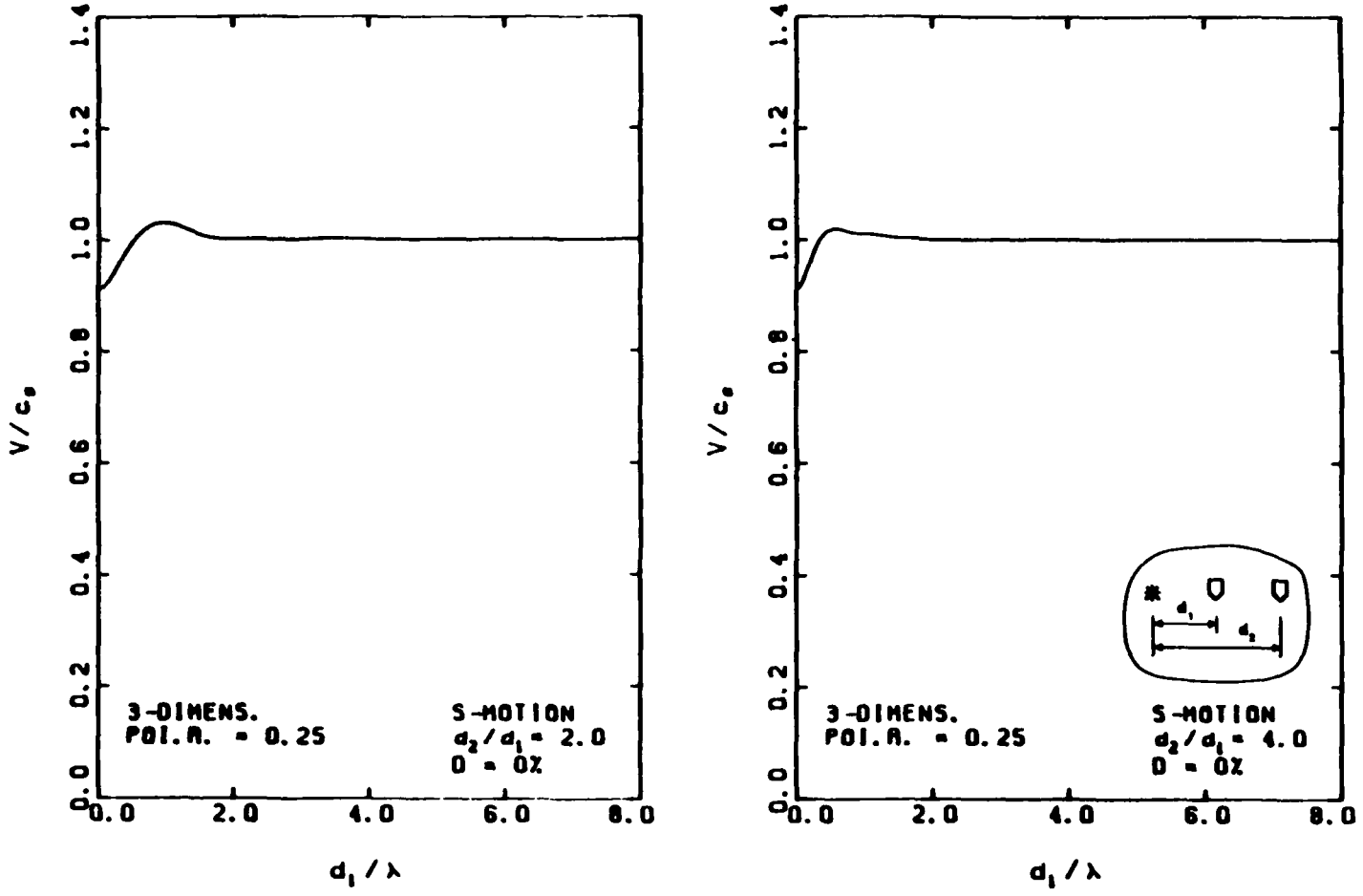

Fig. 4.30 - Dispersion curves for three-dimensional shear motion in a medium with no damping and Poisson's ratio = 0.25. Large spacing between receivers.

The nature of this dispersive behavior in the two-dimensional P- and SV-motions and in the three-dimensional, P- and S-motions, is due to the coupling between the additional near-field and the far-field waves. As was mentioned in Chapter Three, the coupling effect is more important in the near-field than in the far-field, and so is the dispersive behavior. This conclusion is further reinforced by looking at Figs. 4.25 and 4.26 in which dispersion curves for two-dimensional SH-motions are presented. The shear wave generated in 2-D, SH-motion is not coupled with any other type of wave; it is a "pure shear wave." It can be observed in these last two figures that the apparent shear wave velocity coincides exactly with the shear wave velocity of the medium except for very small values of d_1/λ. The reason why the apparent velocity at low values of d_1/λ (low frequencies) is not equal to the shear wave velocity of the medium is not entirely known. It should be noticed, however, that the dynamic solution for the Green's functions does not apply for the static case and that this solution is probably not accurate for small frequencies.

A second set of dispersion curves is shown in Appendix D (Figs. D.1 through D.10). This group of dispersion curves corresponds to waves propagating in a medium with 5 percent material damping. It is observed that the amplitudes of the fluctuations corresponding to P-motions have decreased slightly when compared to the respective curves for a medium with no material damping. This behavior is encountered in two-dimensional as well as three-dimensional motions. For the two-dimensional SV-motion and the three-dimensional S-motion, the fluctuations for the material with 5 percent damping are slightly larger than for the material with no damping. However these differences are so small that the corresponding dispersion curves can be considered almost identical.

The two-dimensional antiplane shear motion presents no dispersion whether the waves propagate in a medium with no damping (Figs. 4.25 and 4.26) or in a medium with material damping (Figs. D.5 and D.6). It becomes clear from Figs. D.5 and D.6 that strain and frequency independent material damping of the hysteretic type does not produce any dispersive effect on body waves propagating in a linearly elastic full space.

The effect of Poisson's ratio on dispersion curves is investigated in Figs. D.11 through D.20. In these figures are shown the dispersion curves of waves propagating in a medium with a Poisson's ratio of 0.4 and zero material damping. From comparison of these figures (Figs. D.11 through D.20) with the figures corresponding to waves propagating in a material with no damping and Poisson's ratio value of 0.25 (Figs. 4.21 through 4.30), the following conclusions can be drawn. First, for longitudinal motion (two- or three-dimensional) the dispersive effect is stronger for the waves propagating in the medium with higher Poisson's ratio. Second, for two-dimensional, SV-motion and three-dimensional, S-motion, the dispersive effect is more important for the waves propagating in the medium with Poisson's ratio of 0.4 than for those propagating in the medium with Poisson's ratio of 0.25. The difference is almost insignificant at high frequencies (or large values of d_1/λ), but at low frequencies, where the influence of the P-wave (near-field effect) is more important, the dispersive effect is greater when Poisson's ratio is 0.4. Third, Poisson's ratio does not affect the two-dimensional SH-motion dispersion curves. This result is expected since Poisson's ratio does not affect the two-dimensional SH-motion fundamental solution (Eq. 2.5). Finally it should be noticed that in some of the P-motion dispersion curves the apparent velocities fell out of the limits of the graphs and were not included in the plots. These high velocities were

obtained when the phase of the cross spectrum approached a value of zero. In some cases it was found that the phase of the cross spectrum became negative for a small range of frequencies and resulted in negative apparent velocities.

Two conclusions can be made at this point. 1. If elastic properties are to be back-calculated from dispersion curves it is better to space the receivers so as to obtain a large value of d_2/d_1. Of the configurations studied so far, that corresponding to a value of $d_2/d_1 = 4$ gives dispersion curves with apparent velocities closer to the velocities c_s and c_p from which the elastic properties can be calculated. 2. The agreement between apparent and phase velocities (c_s and c_p) is best for high values of d_1/λ.

It is important to notice that in the previous figures the horizontal axis, distance (or frequency), has been normalized with respect to the wavelength of the shear wave, since it was a known parameter for these theoretical studies. However for practical applications, it would probably be more convenient to normalize with respect to the wavelength of the propagating wave, $L = V/f$. In the field the parameters that are known are the distances (d_1 and d_2), the apparent velocities (V) and the frequency (f). It is interesting then to know at what value of d_1/L apparent velocities and the elastic velocities of plane waves (c_s and c_p) become equal so as to filter out any frequencies smaller than that corresponding to the critical value of d_1/L.

Dispersion curves that would be obtained if this new normalization were done would be, for the case of transverse motion, very similar to those previously presented (since in this case V and v_s are quite similar). However, curves obtained for

longitudinal motions would be shifted to the left by a factor of about two. (This factor depends on the value of Poisson's ratio and is about 1.7 for $\nu = 0.25$, about 2 for $\nu = 0.33$ and about 2.4 for $\nu = 0.4$.) To give an indication of how the new curves look, dispersion curves obtained for three-dimensional motion in a medium with a value of Poisson's ratio of 0.25 and no material damping have been plotted in Figs. 4.31 and 4.32 for longitudinal motion and Figs. 4.33 and 4.34 for shear motion.

As a practical application it can be concluded that for the measurement of body wave velocities in which the ratio of distances from the source to the second and to the first receivers (d_2/d_1) is larger or equal to 2, the apparent compression (or shear) wave velocity can be assumed equal to the compression (or shear) wave velocity of the elastic medium at values of d_1/L greater than 2. A value of d_1/L of one could be used without incurring any significant errors (errors greater than about five percent). However, when considering longitudinal-motion, dispersion curves produced by a point load in a medium with a high value of Poison's ratio (Fig. D.18) present large fluctuations and a higher value of d_1/L should be considered (of at least two). A similar problem occurred when analyzing cross-correlation functions for these material properties (Section 4.4.2 and Fig. C.9).

The ratio of $d_1/L > 1$ means that since wavelength can be expressed as

$$L = V/f \tag{4.10}$$

then

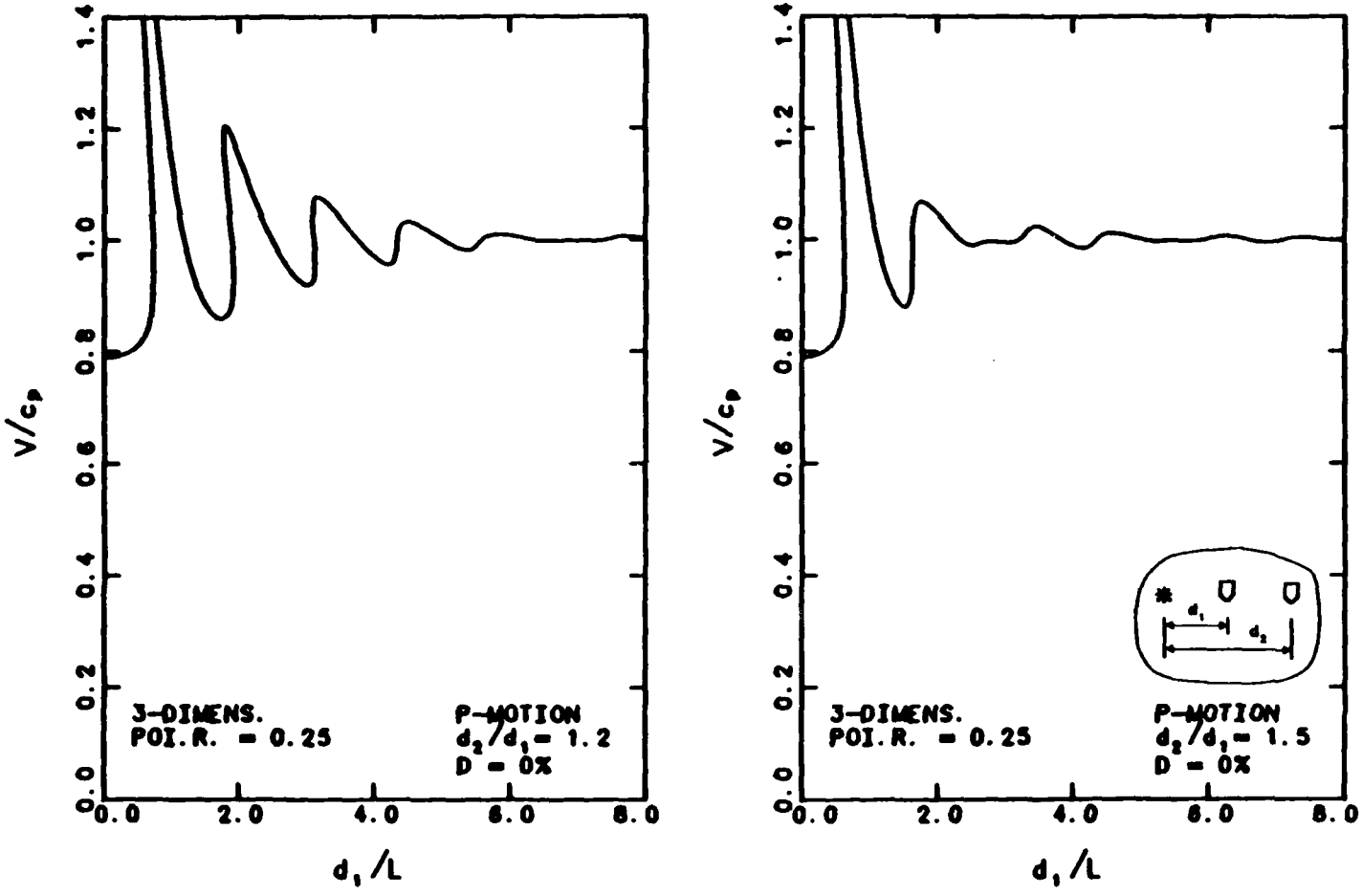

Fig. 4.31 - Dispersion curves for three-dimensional longitudinal motion normalized with respect to wavelength. Small spacing between receivers.

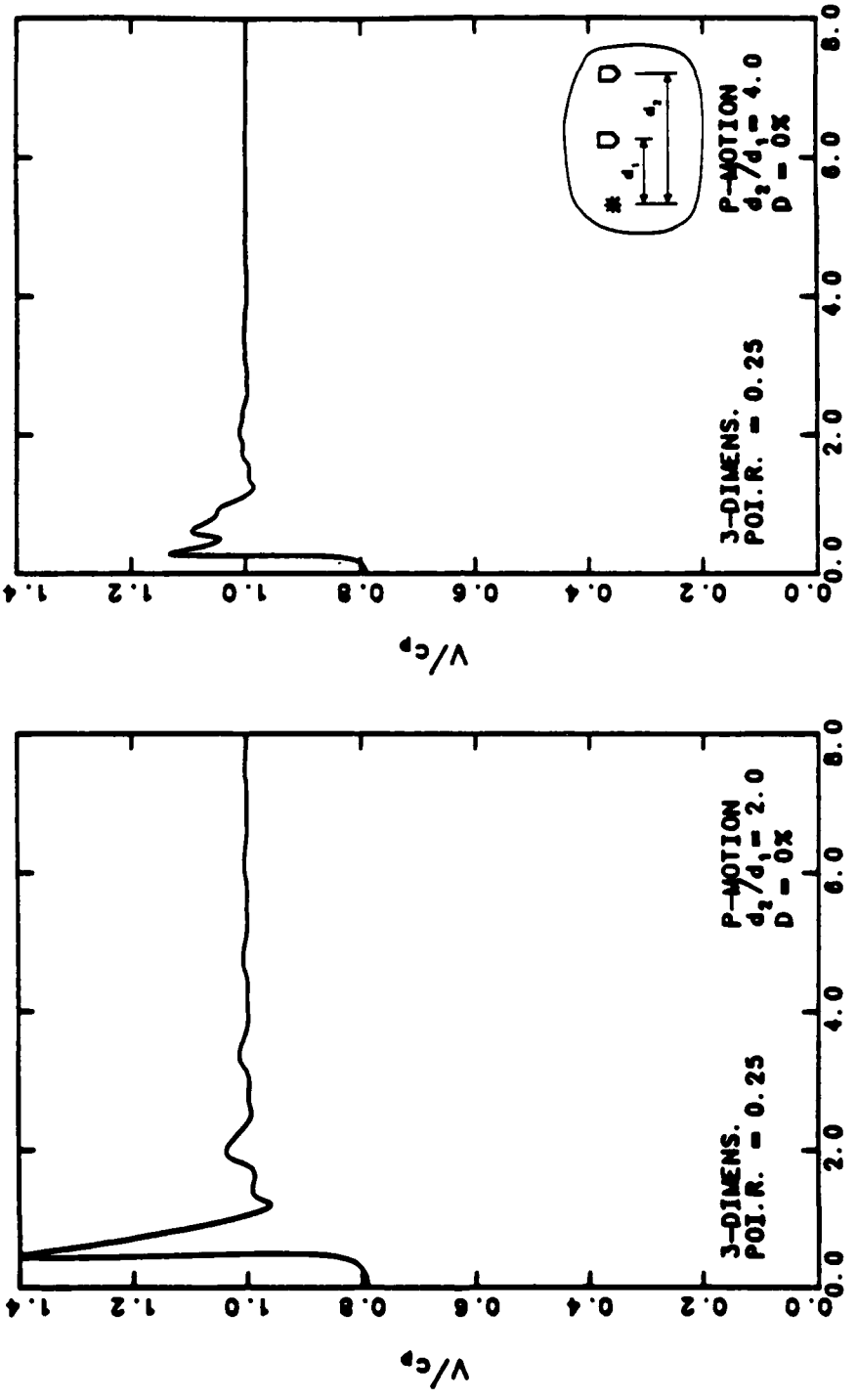

Fig. 4.32 - Dispersion curves for three-dimensional longitudinal motion normalized with respect to wavelength. Large spacing between receivers.

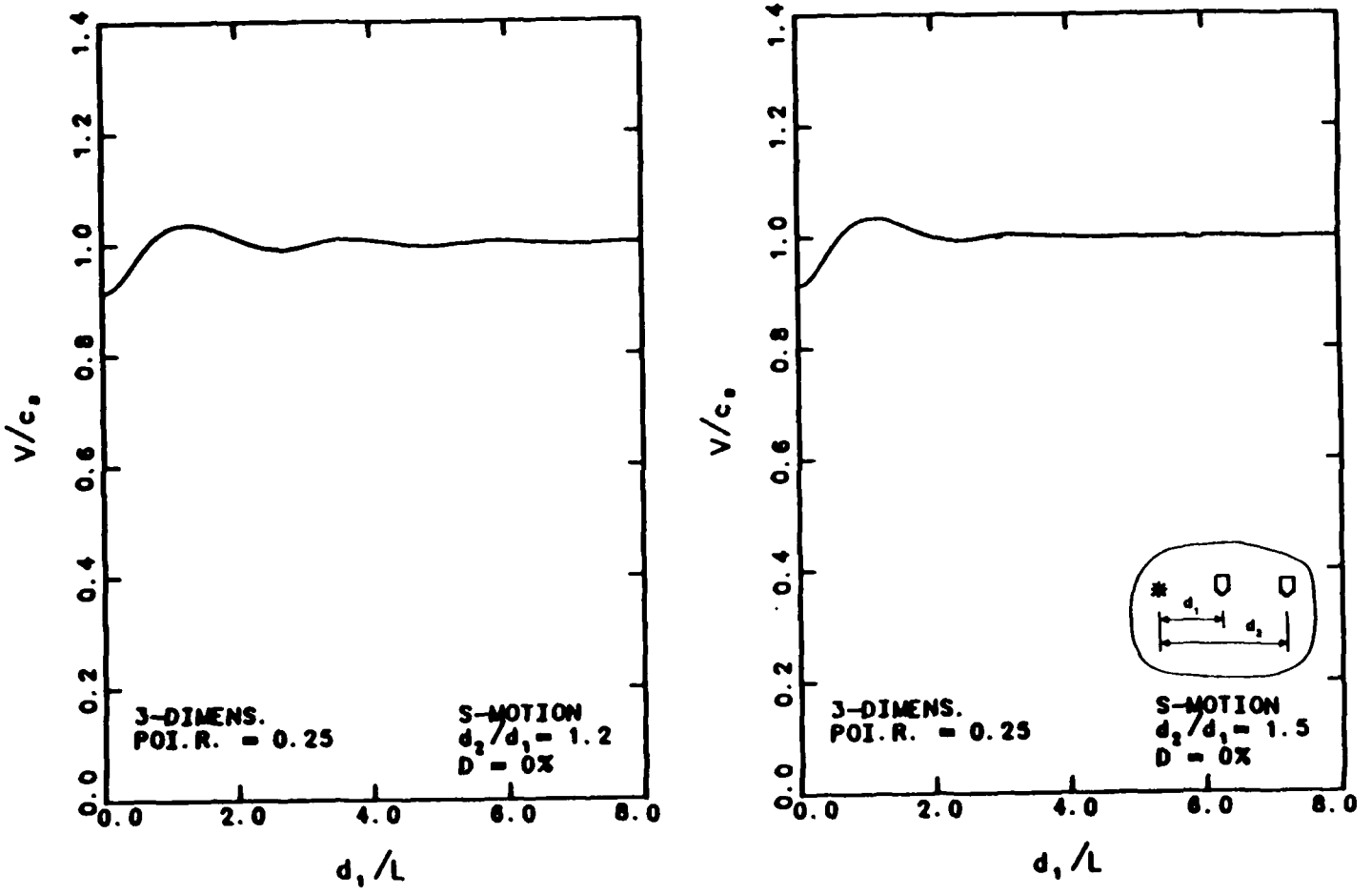

Fig. 4.33 - Dispersion curves for three-dimensional shear motion normalized with respect to wavelength. Small spacing between receivers.

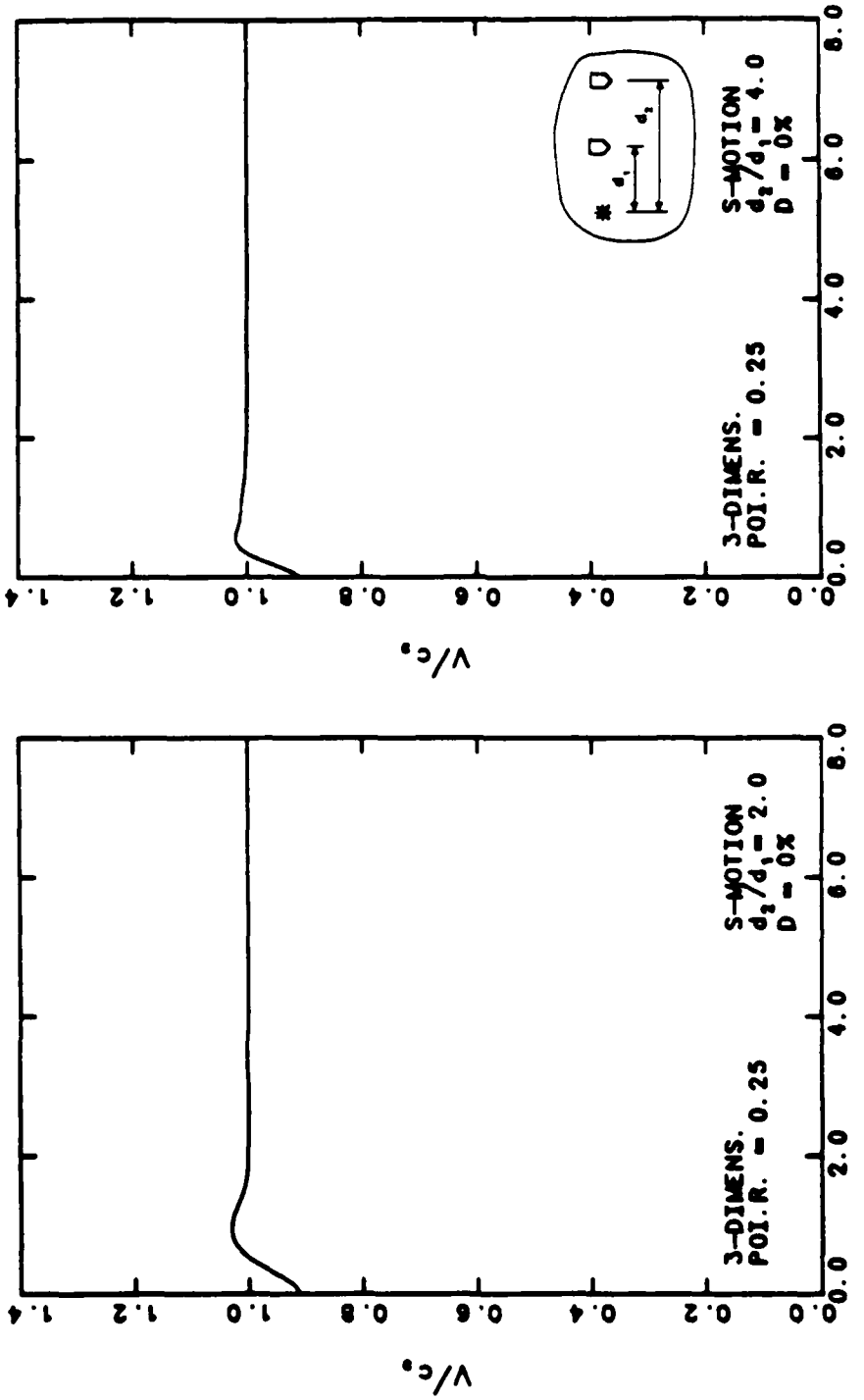

Fig. 4.34 - Dispersion curves for three-dimensional shear motion normalized with respect to wavelength. Large spacing between receivers.

$$d_1/L = d_1 \cdot f/V > 1 \qquad (4.11)$$

Since velocity can be expressed as

$$V = (d_2 - d_1) \cdot 360° \cdot f/\phi \qquad (4.12)$$

(with ϕ in degrees), then

$$d_1 \cdot \phi/360°(d_2 - d_1) > 1 \qquad (4.13)$$

or

$$\phi/360° > (d_2 - d_1)/d_1 \qquad (4.14)$$

For the case of $d_2/d_1 = 2$, The rule means that

$$\phi > 360° \qquad (4.15)$$

or the number of cycles has to be greater than one before the phase should be used to calculate apparent wave velocities. For cases where d_2/d_1 is greater than two, the limiting value of d_1/L would be smaller than one.

4.5.3 Dispersion curves from transfer functions

It is not always necessary to know the displacements (velocities or accelerations) at two different points in order to obtain a phase difference from which velocities can be calculated. If one knows the transfer function of the response at one point due

to an input force at other point, it is possible to calculate the phase difference between the source and receiver from the phase of the transfer function. If displacements are being used to monitor the response (as is the case in this theoretical study), then force and displacements are in phase at the source and one could use directly the phase of the transfer function of displacement due to a force to obtain the phase difference in between source and receiver. (For a material with damping there will be a small phase difference in between force and displacement). In the field it is common practice to use instrumented hammers that by means of an accelerometer (or a load cell) attached to the head of the hammer record the input to the system. In these cases it would be convenient then to use accelerometers to monitor the response at the target point so as to avoid any extraneous phase shifts produced by using different types of sensors. If velocity transducers are used at the target point and an accelerometer is attached to the hammer then a correction of 90 degrees would have to be made to account for the use of a transfer function of a velocity output due to an acceleration input.

Dispersion curves obtained from the phase of the transfer function of displacement due to a unit force (Green's function) are presented in Figs. 4.35 through 4.39 and in Appendix D, Figs. D.21 through D.30. Dispersion curves based on two-dimensional wave motions for a medium with no damping and Poisson's ratio of 0.25 are presented in Figs. 4.31, 4.32 and 4.33. When compared with the dispersion curves obtained from the phase difference at two receivers (Figs. 4.21 through 4.26), it can be observed that the apparent velocities in Figs. 4.31, 4.32 and 4.33 do not give as good an estimate of the elastic velocities, c_p or c_s, as the dispersion curves in Figs. 4.21 through 4.26 did (even at high values of $d_1/\cdot$). The apparent velocities always underestimate the

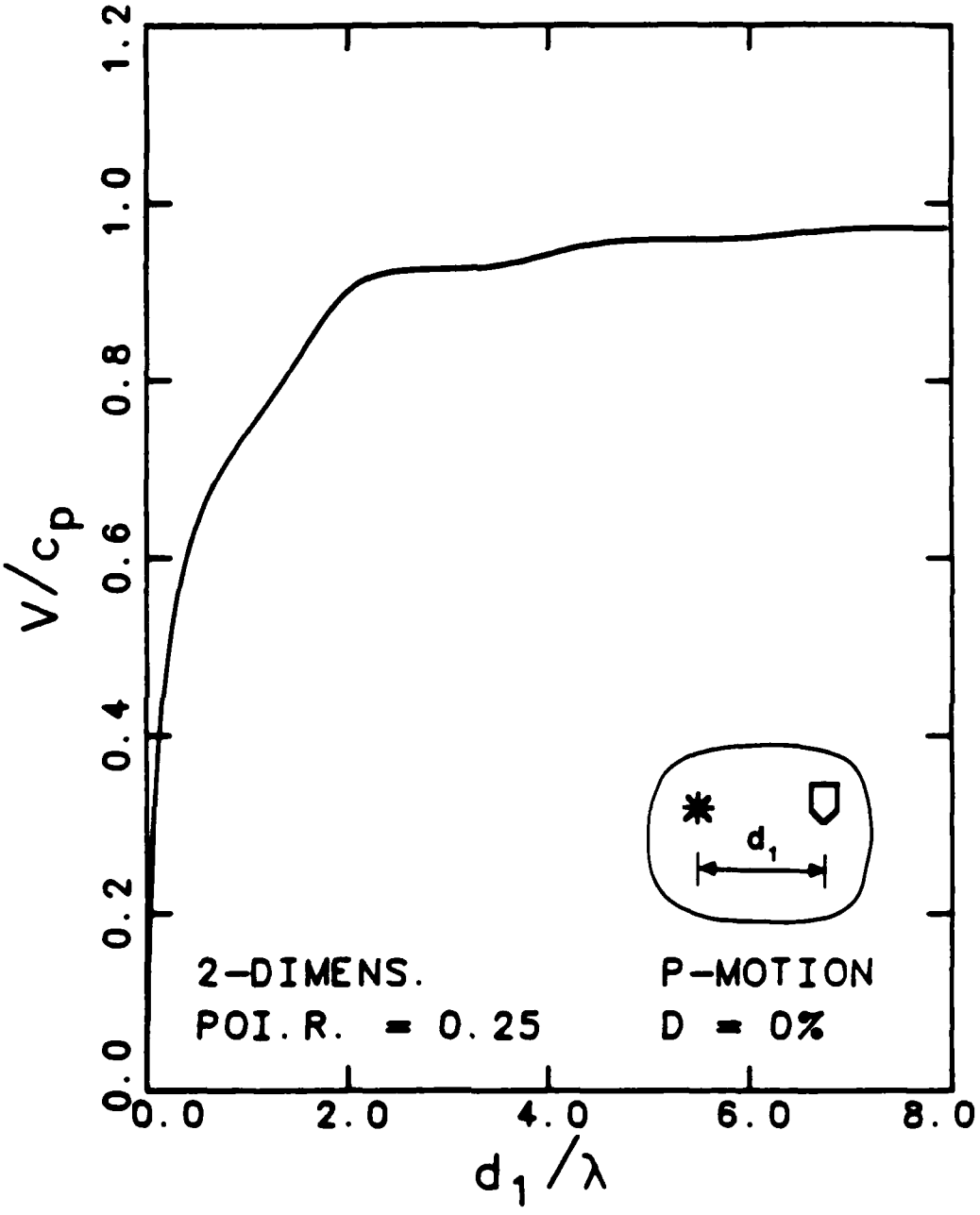

Fig. 4.35 - Dispersion curve obtained from the phase of the transfer function for two-dimensional longitudinal motion in a medium with no damping and Poisson's ratio = 0.25.

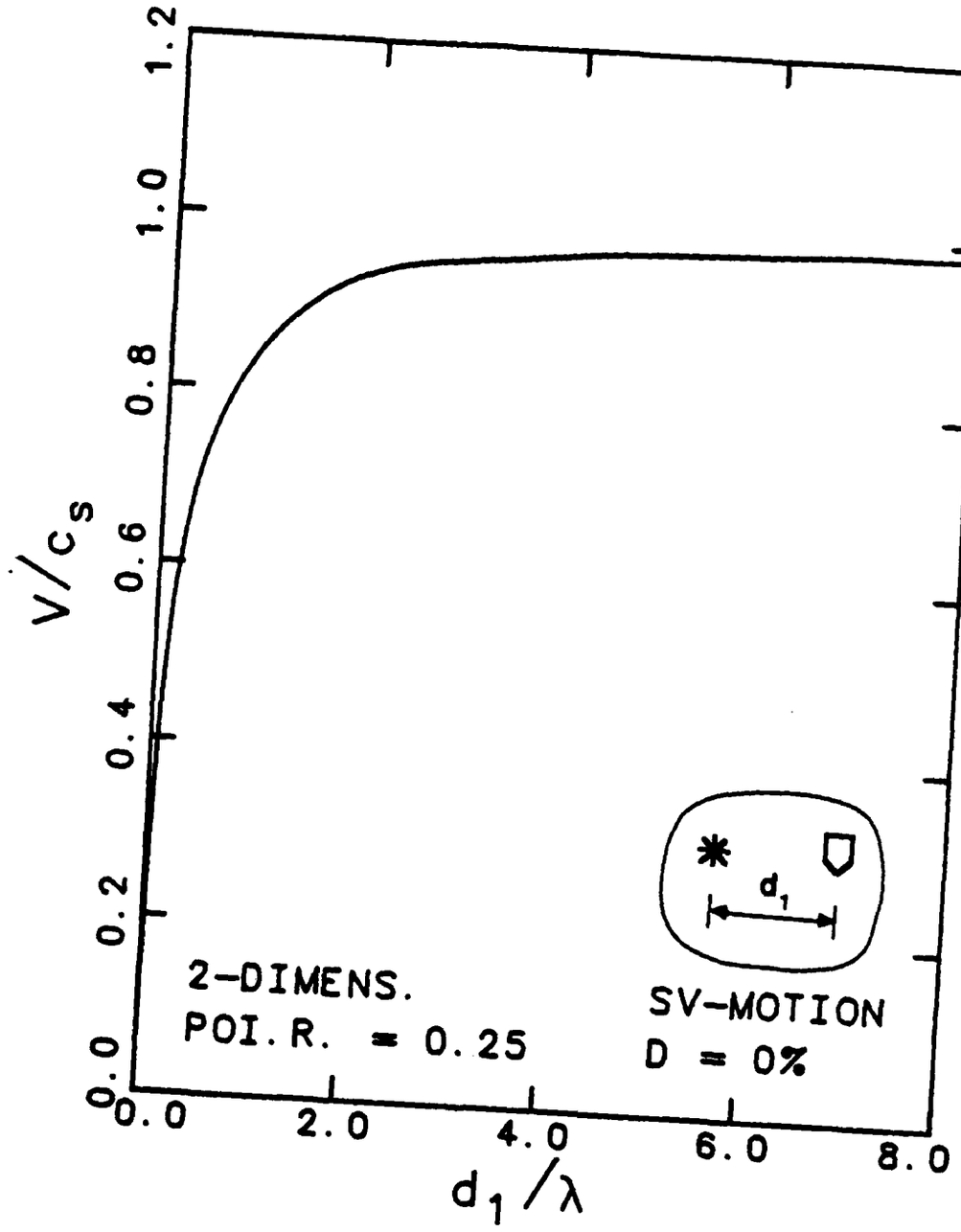

Fig. 4.36 - Dispersion curve obtained from the phase of the transfer function for two-dimensional in-plane shear motion in a medium with no damping and Poisson's ratio = 0.25.

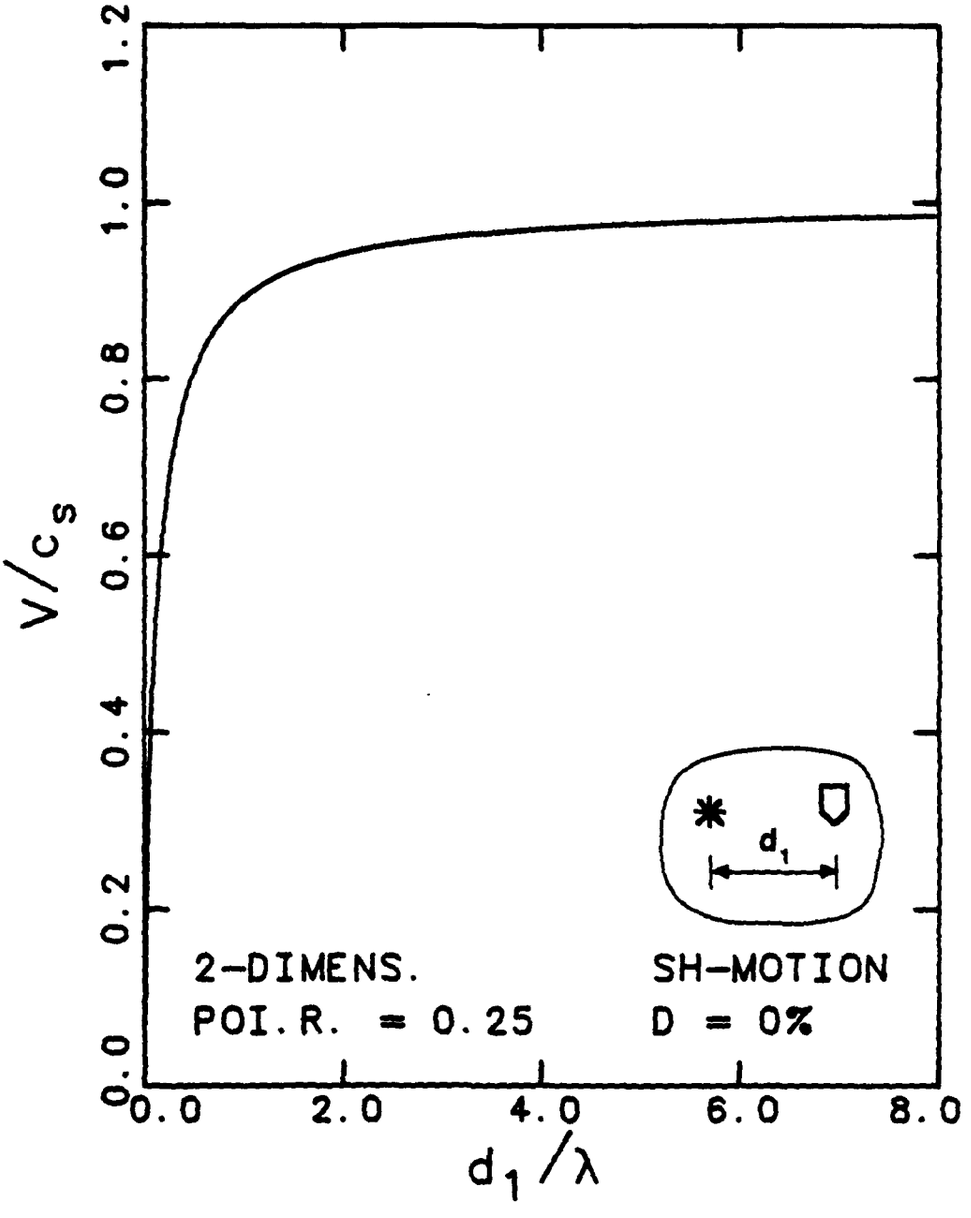

Fig. 4.37 - Dispersion curve obtained from the phase of the transfer function for two-dimensional antiplane shear motion in a medium with no damping and Poisson's ratio = 0.25.

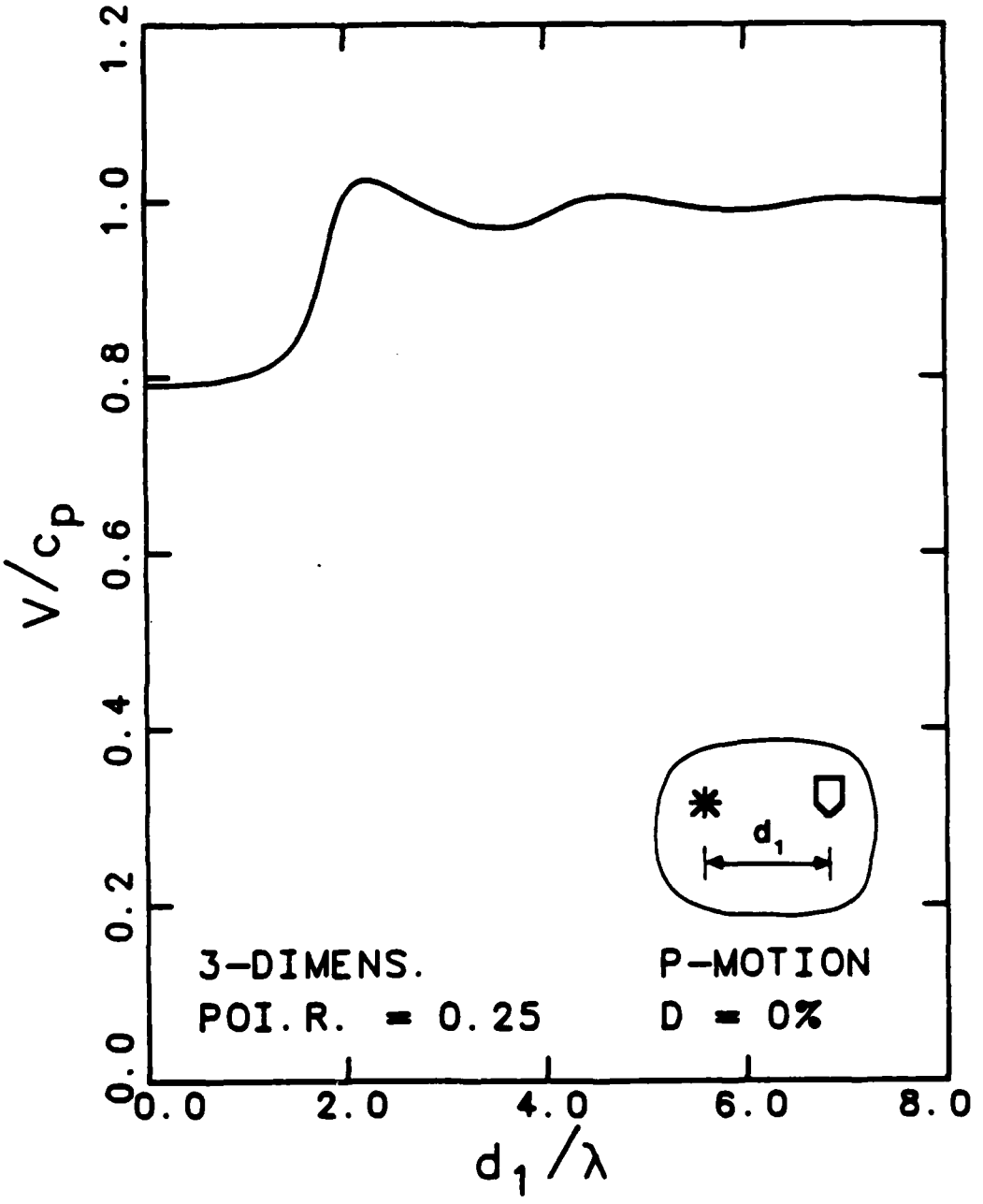

Fig. 4.38 - Dispersion curve obtained from the phase of the transfer function for Three-dimensional longitudinal motion in a medium with no damping and Poisson's ratio = 0.25.

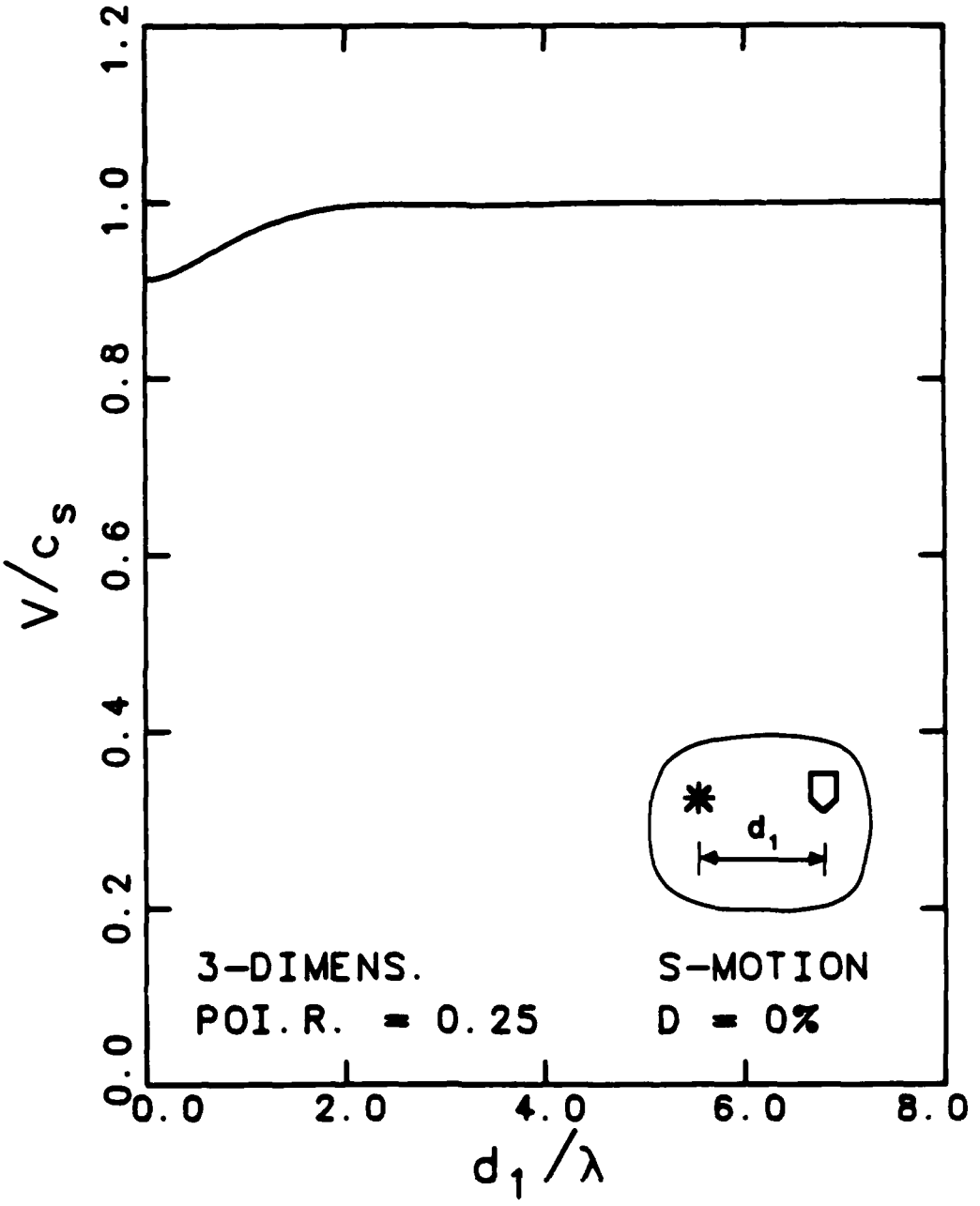

Fig. 4.39 - Dispersion curve obtained from the phase of the transfer function for three-dimensional shear motion in a medium with no damping and Poisson's ratio = 0.25.

elastic velocities by a few percent (about five percent), but at low values of d_1/λ (less than two), the velocities are significantly underestimated.

Dispersion curves based on three-dimensional wave motions (Figs. 4.38 and 4.39), however, give better estimates. At values of $d_1/\lambda > 2$, the velocities obtained are accurate predictions of the elastic velocities. At short values of d_1/λ, say one, the transfer function gives apparent velocities that are closer to the elastic velocities than the velocities obtained from using the cross spectrum information at two receivers, Figs. 4.27 through 4.30, (especially for low values of d_2/d_1).

In Appendix D are included the dispersion curves derived from the transfer function approach for materials with five percent damping and 0.25 for Poisson's ratio and zero damping and a Poisson's ratio of 0.4, Figs. D.21 through D.25 and Figs. D.26 through D.30, respectively. The first set of curves is almost identical to the ones with no damping (Figs. 4.35 through 4.39) and the same comments apply. The curves corresponding to a value of 0.4 for Poisson's ratio (Figs. D.26 through D.30) did not present any special advantages when compared to the curves obtained from the cross spectrum information. The poorest comparisons between apparent wave velocities and elastic velocities occurred for three-dimensional P-motion in mediums with high values of Poisson's ratio. In this case it seems better to use the phase of the cross spectrum at two receivers with a high d_2/d_1 ratio than to use the phase of the transfer function at one receiver.

4.6 SUMMARY

Several methods to calculate body wave velocities from seismic records have been reviewed in this chapter. The methods include those based on the visual estimation of the time of arrival at one receiver (direct times), those based on the visual estimation of interval times between two receivers, those based on the cross-correlation function, and those based on dispersion curves obtained from the phase of the cross spectrum or transfer function.

Visual determinations of various times of arrival of waves are the most common methods to calculate wave velocities. Velocities obtained from direct travel times are slightly higher than those corresponding to the elastic constants (c_s and c_p). Many times the differences depend on the individual reducing the field data and on the amplification applied to the time signals. These small errors can partially be reduced if interval times from first arrivals are used, but the choice of an arrival time is still a personal matter. This subjective evaluation of interval times can be avoided if interval times are calculated from first peaks, first troughs or zero crossings. The use of interval times also eliminates possible triggering errors.

The use of the cross-correlation function to calculate wave velocities seems to be a very valuable method. Velocities obtained by this method were accurate representations of the elastic wave velocities for most cases analyzed. The only erroneous results were those corresponding to P-wave velocities obtained from longitudinal-motion records at receivers in the near-field ($d_1/\lambda < 2$, with d_1 being the distance from the source to the first receiver and λ the predominant shear wavelength of the time record)

of a medium with a high value of Poisson's ratio (greater than about 0.4, Fig. C.9) . A very important advantage of the use of the cross-correlation function is that calculations of wave velocities can be easily automated with the use of a computer. However, for the successful use of this technique in the field, one still has to generate and record only one predominate wave type.

The use of dispersion curves of apparent wave velocity also turned out to be an excellent tool for evaluation of elastic wave velocities. Apparent velocities at high values of d_1/L (values in general greater than 2) were equal to elastic wave velocities of the material (with L being the wavelength corresponding to the apparent wave velocity). When dispersion curves were calculated from the cross spectrum of the signals at two receivers, it is better to have a source-receiver configuration with high values of d_2/d_1 (for a fixed value of d_1 and with d_2 being the distance from the source to the second receiver). For a typical crosshole setup ($d_2/d_1 = 2$), the frequencies should be filtered so as to eliminate any frequencies that give values of $d_1/L < 1$. For cases involving materials with high values of Poisson's ratio (say 0.4) and when measuring P-wave velocities from longitudinal-motion records, the filtering criteria should be more strict, and values of $d_1/L > 2$ should be used.

Wave velocities can also be evaluated from the transfer function as discussed in Section 4.5.3. However, dispersion curves obtained from the phase of the transfer function do not present any particular benefit when compared to dispersion curves obtained from the phase information of the cross spectrum for two-dimensional cases (line sources). For point sources (three-dimensional motions), apparent wave velocities obtained from the transfer function were good estimates of elastic wave velocities when values

of d_1/L were greater than one, for all the cases but for three-dimensional longitudinal motion in a medium with a high value of Poisson's ratio. The principal advantage of using the transfer function is that only one receiver is needed.

CHAPTER FIVE
EVALUATION OF BODY WAVE ATTENUATION

5.1 INTRODUCTION

Most uses of seismic methods in engineering applications have been to determine wave velocities. Very little effort has been applied to the study of techniques to obtain damping values. The main emphasis of this report is on wave velocities. However, a preliminary analytical investigation on damping has been carried out. A brief theoretical background of wave amplitude attenuation along with the description of a technique to evaluate material damping is presented in this chapter.

5.2 THEORETICAL BACKGROUND

The amplitudes of seismic waves decrease as the waves propagate through a medium. This attenuation of wave amplitude is caused by two mechanisms: 1) spreading of wave energy from a source, generally called geometrical or radiational damping, and 2) dissipation of energy due to mainly frictional losses in the material itself, commonly known as attenuation, material or internal damping.

There are several measures of energy losses in a dissipative medium. For a plane harmonic wave, assuming that all energy losses

are due to frictional forces (case of a plane wave front), the decay in wave amplitude can be defined as

$$u_2/u_1 = e^{-\alpha(d_2-d_1)} \tag{5.1}$$

where,

u_1 is the amplitude of the displacement at a distance d_1 from the source,

u_2 is the amplitude of the displacement at a distance d_2 from the source,

α is the attenuation coefficient, and

e is the base of natural logarithms.

Eq. 5.1 can be derived from the solution to the plane wave equation by assuming that there is a phase shift between stresses and strains (White, 1983; Toksöz and Johnston, 1981; Gordon and Davis, 1968). The attenuation coefficient is not necessarily the same for different types of waves. Shear waves generally present different attenuation characteristics than longitudinal waves.

The natural logarithm of the ratio of the amplitudes at two successive points spaced apart by a distance equal to one wavelength of the harmonic wave (L) is defined as the logarithmic decrement, δ, and is used as another measure of frictional losses. Logarithmic decrement can be expressed as

$$\delta = \ln[u_1(d=d_1)/u_2(d=d_1+L)] \tag{5.2}$$

The relationship between the logarithmic decrement and the coefficient of attenuation is easily found to be

$$\delta = \alpha L \tag{5.3}$$

Another parameter that measures energy dissipation is the "damping capacity" factor (or specific damping capacity). Damping capacity, Ψ, is defined as the energy dissipated in one stress cycle divided by the elastic strain energy stored when the strain is a maximum and is expressed as

$$\Psi = \Delta W/W \tag{5.4}$$

where,

ΔW is the energy dissipated per stress cycle, and

W is the elastic strain energy stored when the strain is a maximum.

Equation 5.4 is based on the assumption of a hysteretic type of behavior. The damping capacity has been found to be frequency independent but strain dependent. At very low strains, however, (like those associated with most wave propagation phenomena in engineering applications, strains below 10^{-6}) the damping capacity appears to be independent of strain amplitude.

A similar measure of internal friction is obtained with the material damping coefficient (or hysteretic damping ratio), D, which is defined as

$$D = \Psi/4\pi = \Delta W/(4\pi W) \tag{5.5}$$

In a material with small damping, the hysteretic damping ratio can be defined as half of the ratio of the imaginary to the real part of a complex elastic modulus, as mentioned in Section 2.2

and used through out this study. If the complex shear modulus, for instance, is defined as

$$G^* = G + iG_I \tag{5.6}$$

then the damping ratio in shear is

$$D = G_I/2G \tag{5.7}$$

where G is the real shear modulus and G_I is the imaginary part of the complex shear modulus.

5.3 MATERIAL DAMPING CALCULATED FROM SEISMIC RECORDS

Special interest and effort have been devoted in the past to determination of attenuation parameters from field measurements The field procedure itself presents several problems, such as 1 precise calibration of the receivers is necessary, 2) interference of reflected and refracted waves adversely affects the measurements; 3) electrical or mechanical noise can adversely affect the results; 4) perfect coupling between the boreholes and the receivers is necessary; 5) the three-dimensional orientation of the receivers must be accurately controlled, and 6) coupling between near- and far-field components has to be considered

Several procedures to obtain damping or attenuation parameters have been proposed in the past (Hoar, 1982; Redpath et al, 1982) and an extensive review of seismic wave attenuation has been compiled by Toksoz and Johnston (1981). A procedure

calculate damping ratio, based on spectral analysis techniques is suggested in the following paragraphs.

For a medium with a linear stress-strain relation, wave amplitude, u, is proportional to the square root of the energy, $W^{1/2}$. Hence, Eq. 5.5 can be expressed as

$$D = \Delta u/(2\pi u) \tag{5.8}$$

where Δu is the amplitude decay per cycle. Therefore, damping ratio can be expressed as

$$D = -[(L/2\pi u)(du/dr)] \tag{5.9}$$

where r is the distance in the direction of propagation. Upon integrating Eq. 5.9 one finds that

$$\ln(u/u_o) = -[2\pi D/L](r-r_o) \tag{5.10}$$

where u_o is the amplitude at a reference point r_o.

The relation between damping ratio, D, and the attenuation coefficient, α, can be obtained directly from Eq. 5.10 as

$$\alpha = 2\pi D/L \tag{5.11}$$

The phase velocity of a plane wave, v, is related to the wavelength, L, by: $v = L\omega/2\pi$. Therefore damping ratio can be defined from Eq. 5.10 as

$$D = -[\omega \cdot \ln(u/u_0)]/[\omega \cdot (r-r_0)] \qquad (5.12)$$

where,

ω is frequency in rad/sec. The damping ratio obtained by Eq. 5.12 is constant with frequency.

A convenient way to calculate phase velocities, v, from apparent velocities, V, is described in Section 4.5. If one uses apparent velocities instead of phase velocity in Eq. 5.12 results in

$$D(\omega) = -[V(\omega) \cdot \ln(u/u_0)]/[\omega \cdot (r-r_0)] \qquad (5.13)$$

where $D(\omega)$ represents an apparent damping ratio.

In Eq. 5.13, dissipation of energy occurs only from internal friction in the material and no dissipation of energy arises from geometrical spreading (plane waves have been considered). If the seismic waves originate from a point source (as usually happens), a correction must be applied to Eq. 5.13 to account for energy losses due to geometrical spreading. It is shown in Chapter Three that wave amplitude decay due to radiational damping is proportional to the square root of distance for two-dimensional motion (cylindrical fronts) and is proportional to the distance for three-dimensional motion (spherical fronts). The relations are valid for the far field, but they can be considered good approximations for a wide range of frequencies (or distances). If one assumes that the relations are valid for any frequency range, the expression for apparent damping ratio becomes

$$D(\omega) = - \frac{V(\omega)\cdot \ln [(u/u_o)(r/r_o)^{1/2}]}{\omega(r-r_o)} \qquad (5.14)$$

for two-dimensional motion, and

$$D(\omega) = - \frac{V(\omega)\cdot \ln [(u/u_o)(r/r_o)]}{\omega(r-r_o)} \qquad (5.15)$$

for three-dimensional motion.

The expressions derived so far apply to steady-state harmonic motion. Any other motion has to be decomposed into its different harmonics by applying a Fourier transform. Then, by using the notation introduced in Section 4.5.2 and Eqs. 4.3 and 4.4, the equation for the apparent damping ratio becomes

$$D(f) = - \frac{\ln[\frac{U_2(f)}{U_1(f)} \cdot (\frac{d_2}{d_1})^{\frac{1}{2}}]}{\phi(f)} \qquad (5.16)$$

for two-dimensional motion, and

$$D(f) = - \frac{\ln[\frac{U_2(f)}{U_1(f)} \cdot \frac{d_2}{d_1}]}{\phi(f)} \qquad (5.17)$$

for three-dimensional motion.

In the development of Eqs. 5.16 and 5.17, it has been assumed that the response of a medium to an impulse has been

decomposed into its harmonics by means of a Fourier transform. In these equations

D(f) is apparent damping ratio,

f is frequency in Hz,

$\phi(f)$ is phase of cross spectrum in radians (or difference between the linear spectrum phases),

$U_1(f)$ is amplitude of the linear spectrum at the first receiver,

$U_2(f)$ is amplitude of the linear spectrum at the second receiver, and

d_1 and d_2 are distances from the source to the first and second receivers, respectively.

Equations 5.16 and 5.17 can be written in terms of the auto spectrum, A, instead of the linear spectrum as

$$D(f) = - \frac{\ln[\frac{A_2(f)}{A_1(f)} \cdot \frac{d_2}{d_1}]^{\frac{1}{2}}}{\phi(f)} \qquad (5.18)$$

and

$$D(f) = - \frac{\ln\{[\frac{A_2(f)}{A_1(f)}]^{\frac{1}{2}} \cdot \frac{d_2}{d_1}\}}{\phi(f)} \qquad (5.19)$$

for two- and three-dimensional motions, respectively,

5.4 CURVES OF APPARENT DAMPING RATIO

Apparent damping ratios for two and three-dimensional motions have been calculated for two materials. In the first case, the apparent damping ratio is determined for a medium with no material damping and Poisson's ratio of 0.25. In the second case, a medium with 5 percent material damping and Poisson's ratio of 0.25 is considered.

Figures 5.1 through 5.10 show the curves of apparent damping ratio versus d_1/λ for a medium with D = 0% (λ is wavelength of the shear wave). These curves were obtained using the same spacings between the receivers as those used to study the velocity dispersion curves. The behavior (fluctuations with d_1/λ and d_2/d_1) of these curves is similar to that found for the velocity dispersion curves. For the two-dimensional SH-motion (Figs 5.5 and 5.6), the apparent damping ratio coincides precisely with the material damping ratio. (The disagreement at low frequencies or low d_1/λ is similar to that obtained for the velocity dispersion curves and the reasons for this behavior are not totally known). For the cases with coupled motions (two-dimensional P- and SV-motions and three-dimensional P- and S-motions), apparent damping ratio presents fluctuations around the actual damping ratio of the material. These fluctuations are large for low values of d_1/λ and for low values of d_2/d_1, but in the far field (large spacings and/or high frequencies), the value of the apparent damping ratio rapidly approaches the actual material damping ratio. It is also interesting to note that the fluctuations are much larger for P-SV motions than for S-motions (note the different scales).

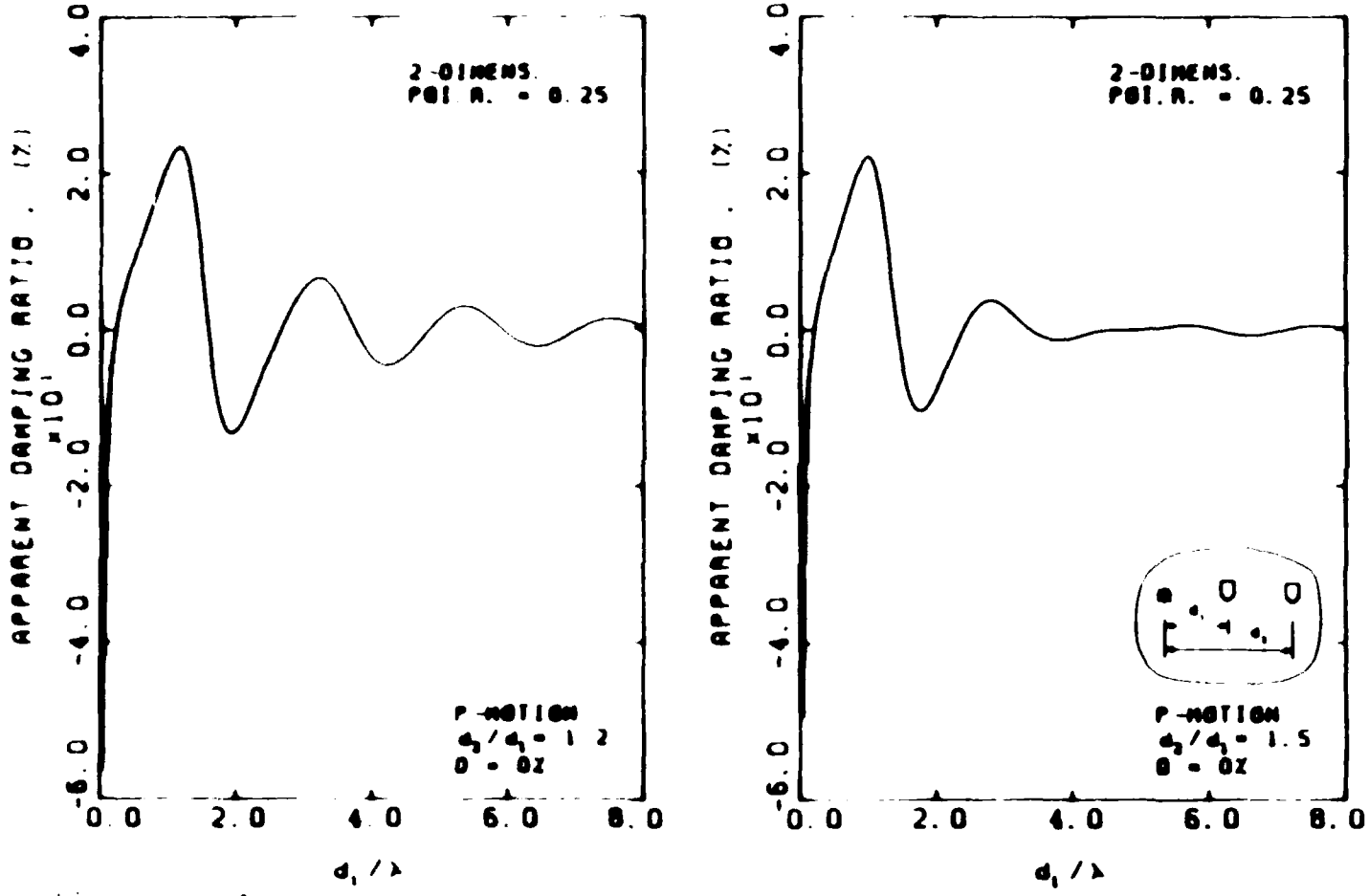

Fig. Apparent damping ratio for in-plane longitudinal motion in a medium with no damping and Poisson's ratio = 0.25 Small spacing between receivers

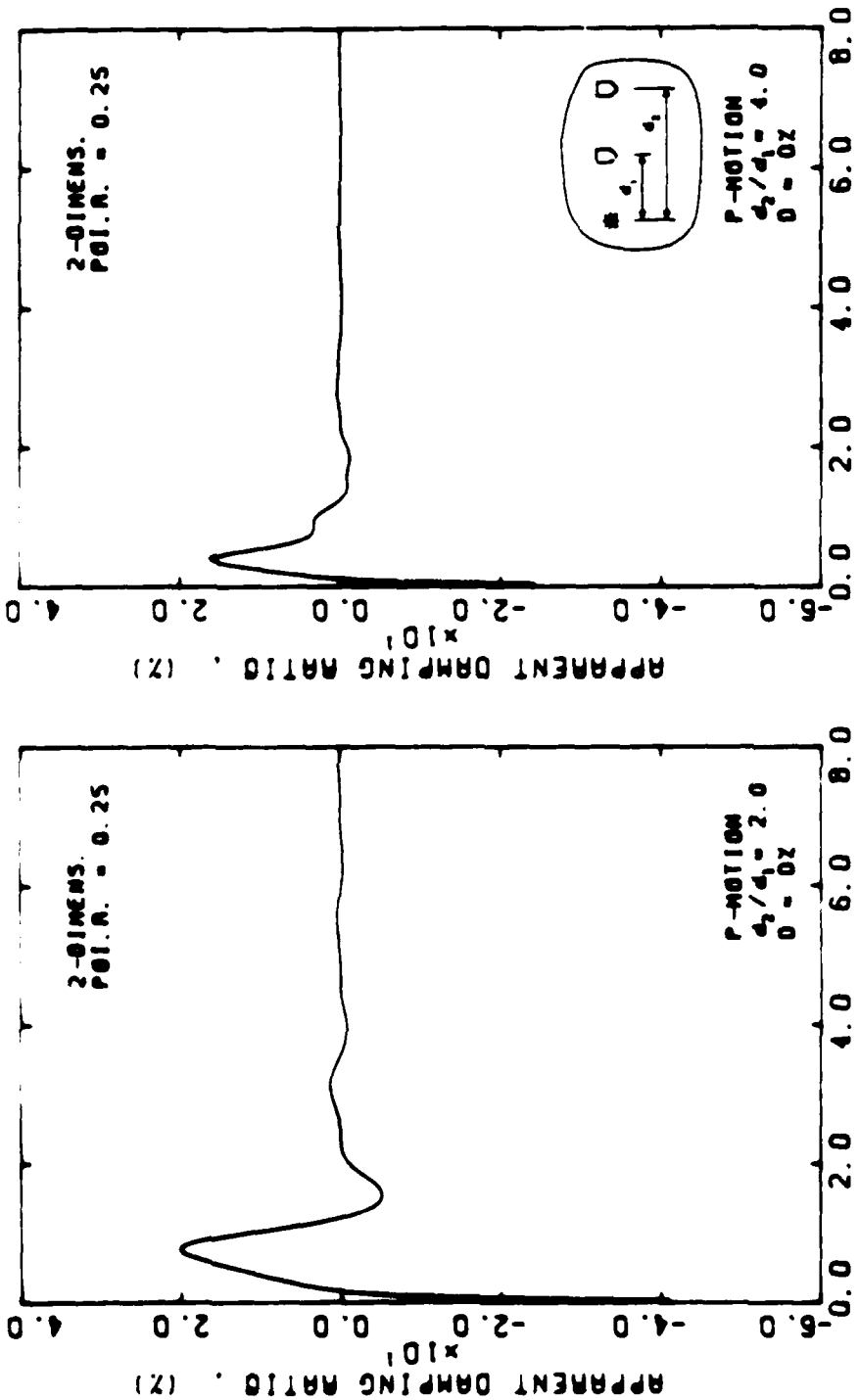

Fig. 5.4 - Apparent damping ratio for in-plane longitudinal motion in a medium with no damping and Poisson's ratio = 0.25. Large spacing between receivers.

Fig. 5.3 - Apparent damping ratio for in-plane shear motion in a medium with no damping and Poisson's ratio = 0.25. Small spacing between receivers.

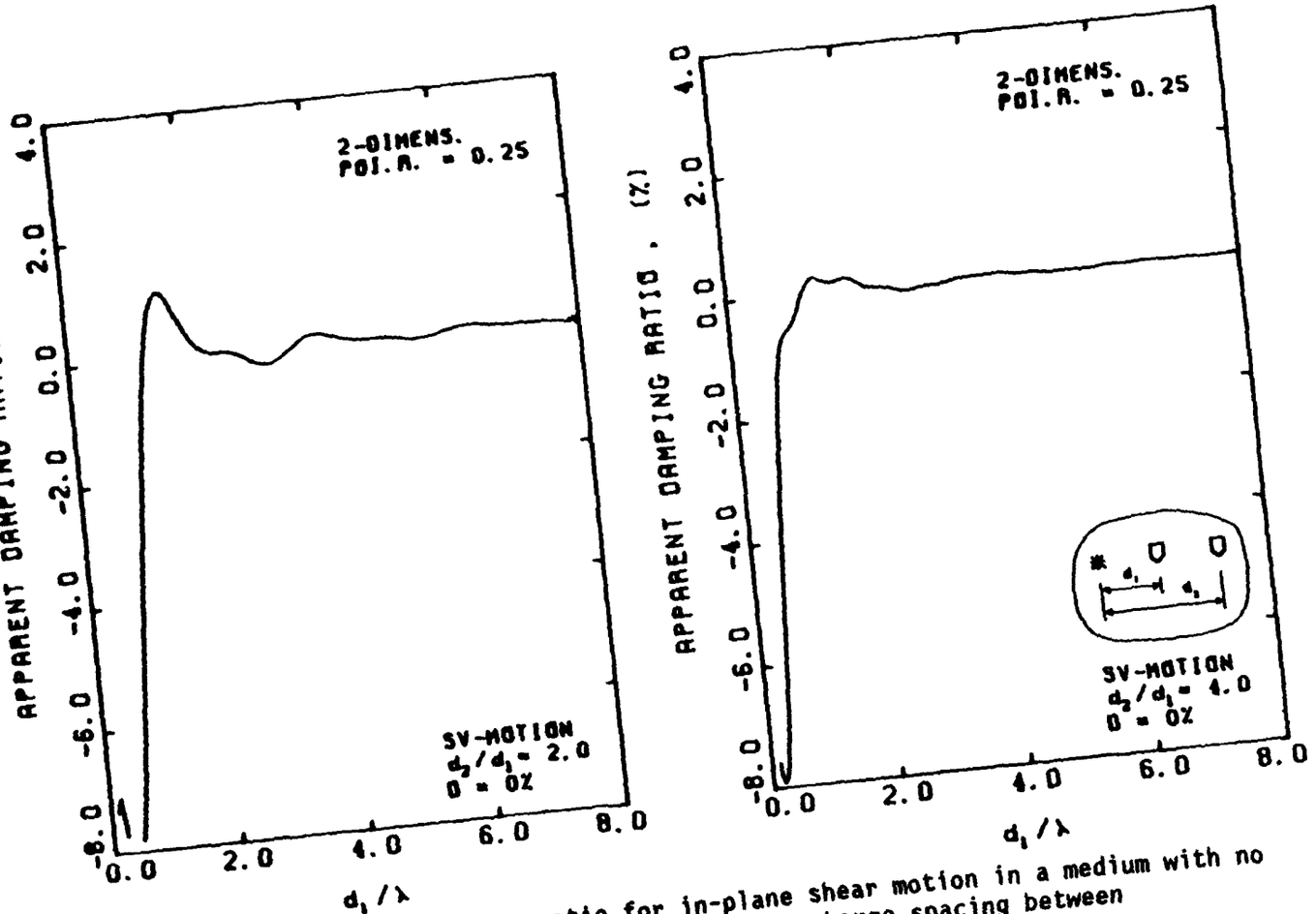

Fig. 5.4 - Apparent damping ratio for in-plane shear motion in a medium with no damping and Poisson's ratio = 0.25. Large spacing between receivers.

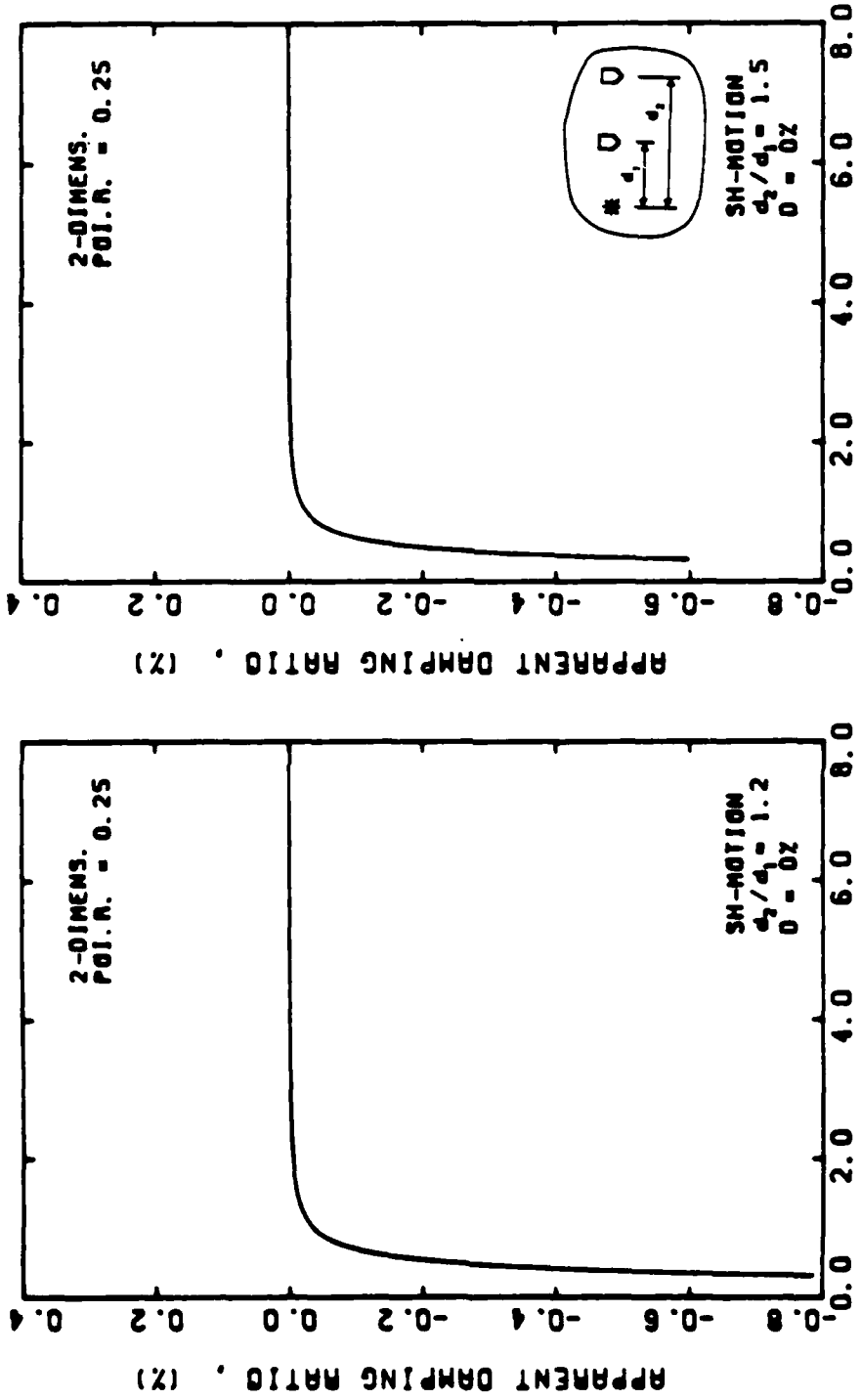

Fig. 5.5 - Apparent damping ratio for antiplane shear motion in a medium with no damping and Poisson's ratio = 0.25. Small spacing between receivers.

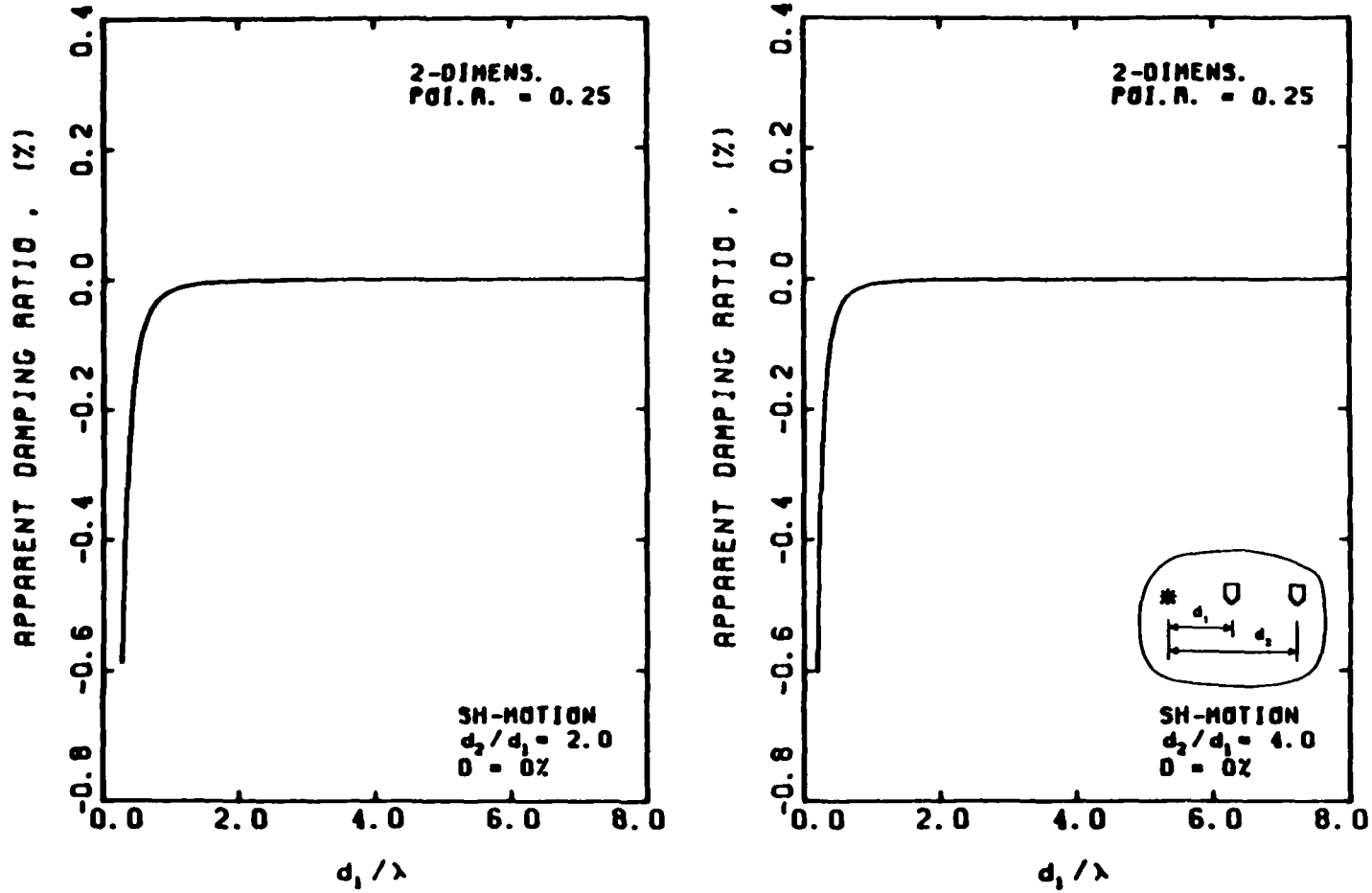

Fig. 5.6 - Apparent damping ratio for antiplane shear motion in a medium with no damping and Poisson's ratio = 0.25. Large spacing between receivers.

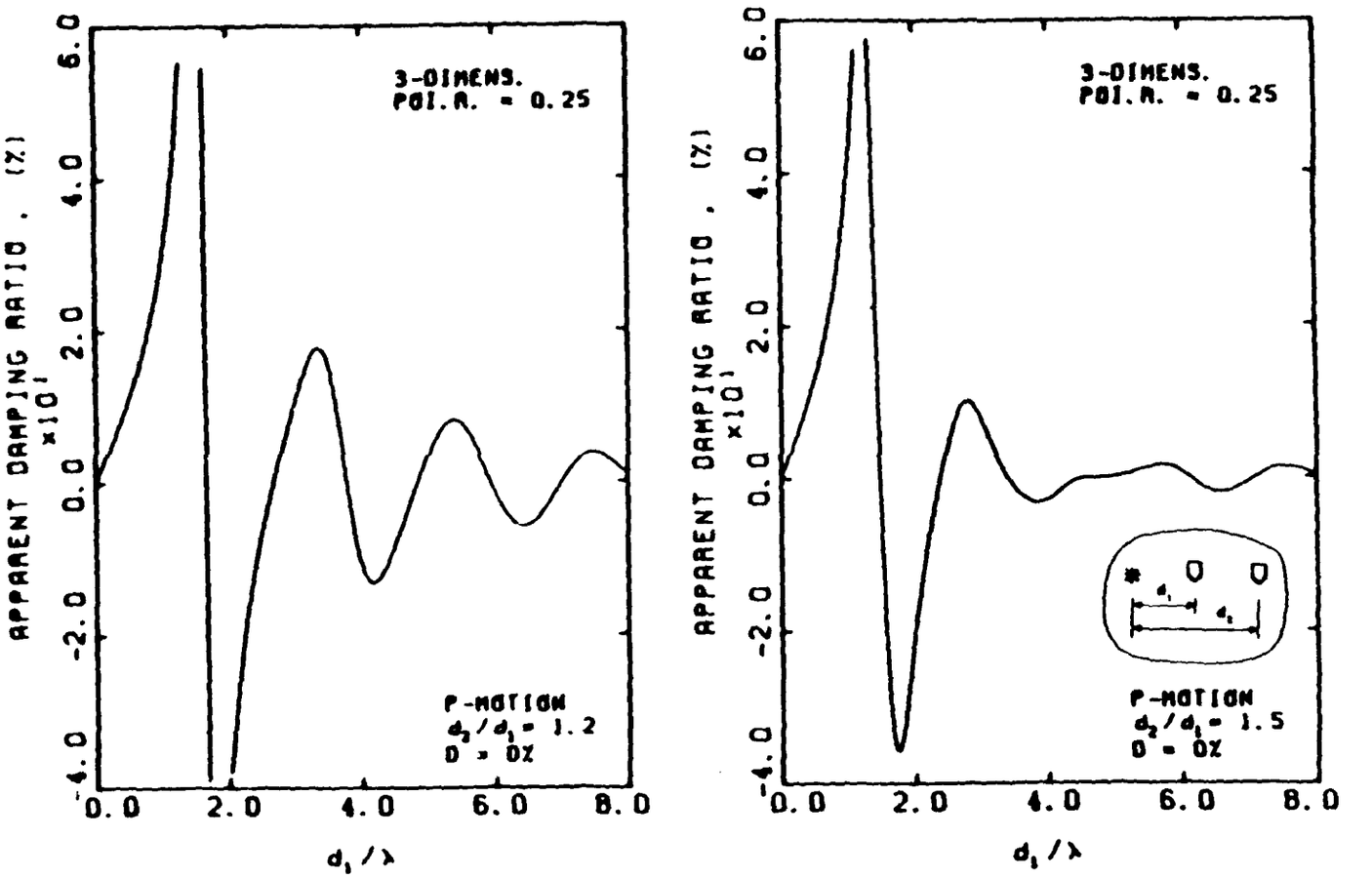

Fig. 5.7 - Apparent damping ratio for three-dimensional longitudinal motion in a medium with no damping and Poisson's ratio = 0.25. Small spacing between receivers.

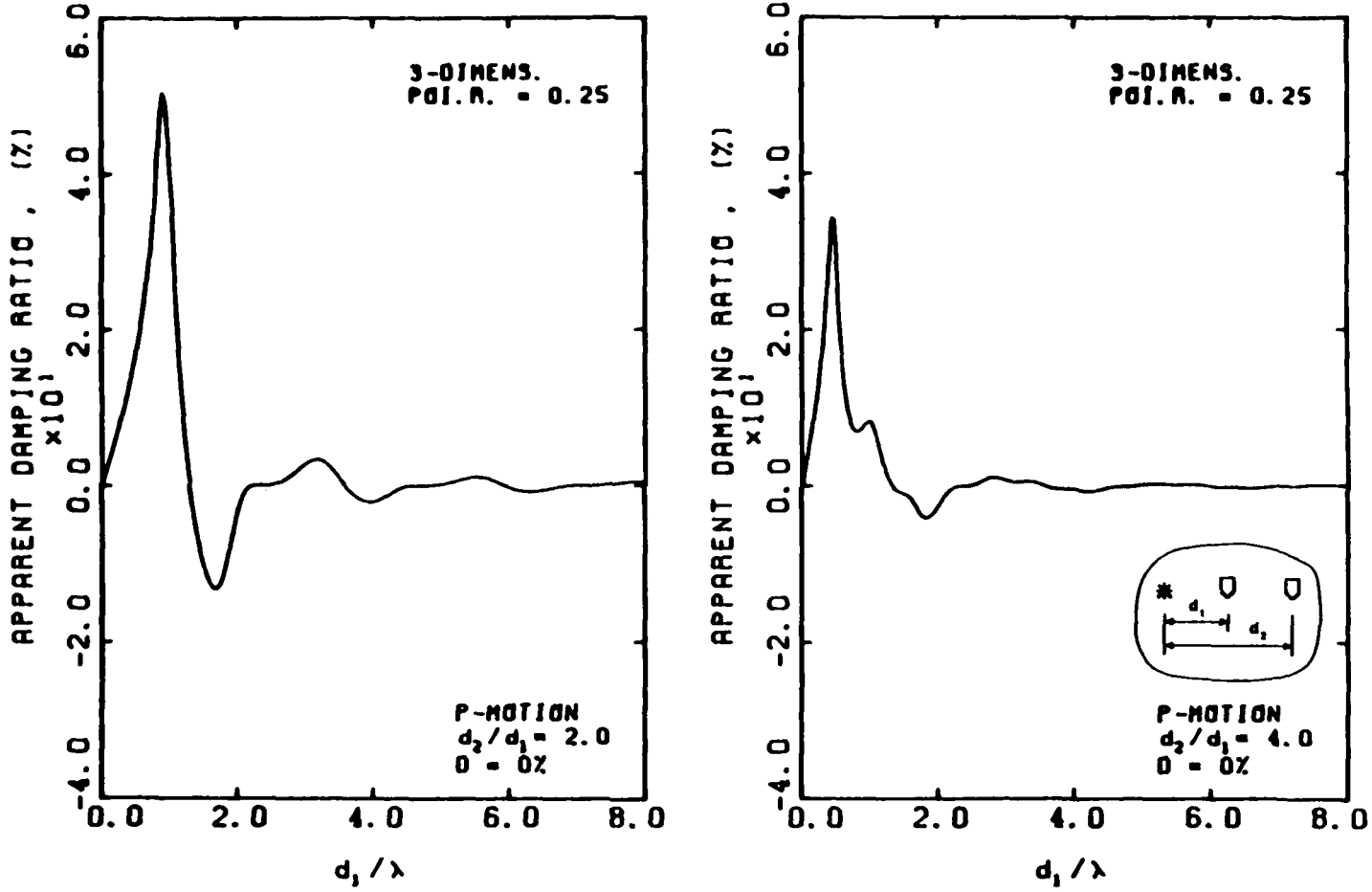

Fig. 5.8 - Apparent damping ratio for three-dimensional longitudinal motion in a medium with no damping and Poisson's ratio = 0.25. Large spacing between receivers.

3-DIMENS.
POI.R. = 0.25
APPARENT DAMPING RATIO , (%)
4.0
2.0
0.0
-2.0
-4.0
3-DIMENS.
POI.R. = 0.25
APPARENT DAMPING RATIO , (%)
4.0
2.0
0.0
-2.0
-4.0

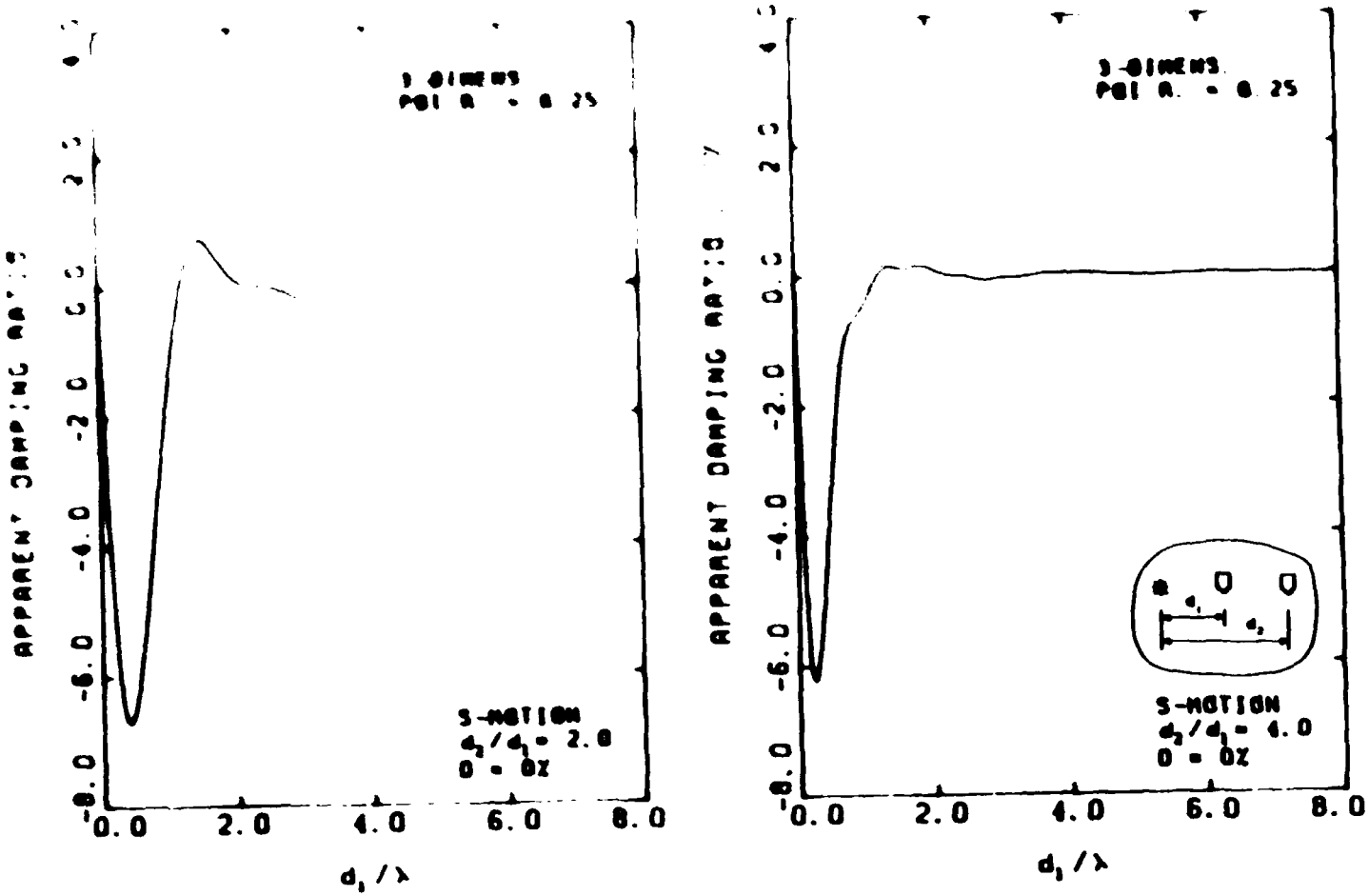

Fig. 5.10 - Apparent damping ratio for three-dimensional shear motion in a medium with no damping and Poisson's ratio = 0.25. Large spacing between receivers.

For the cases where the material damping ratio was 5 percent rather than zero (Figs. 5.11 through 5.20), the tendency is the same as when D = 0 percent.

For typical field measurements where d_2/d_1 has a value of the order of 2 (such as in crosshole measurements), apparent damping ratio can be assumed to equal the actual material damping ratio at a value of $d_1/\lambda = 2$. The apparent damping ratio could be used, therefore, to calculate material damping in the field.

Although only one unique value of damping has been used for both shear and longitudinal motions, different values could have been used as well. In a field experiment, the value of damping obtained from longitudinal motion records would be that associated with the constrained modulus while the value obtained from transverse motion records would be that associated with the shear modulus.

5.5 SUMMARY

A brief theoretical background of wave amplitude attenuation is presented in this chapter. A method to calculate damping ratios from seismic records is also presented . The method is based on spectral analysis techniques and requires calculation of the auto spectrum at two different receivers. For configurations such that d_2/d_1 is equal to two (typical of crosshole seismic testing), the method seems to give values of apparent damping ratio that are good approximations of the actual damping ratio for values of d_1/L greater than one. As in the case of apparent wave velocities, for a fixed value of d_1, the best values of damping ratio are obtained for higher ratios of d_2/d_1. Although good from a theoretical point

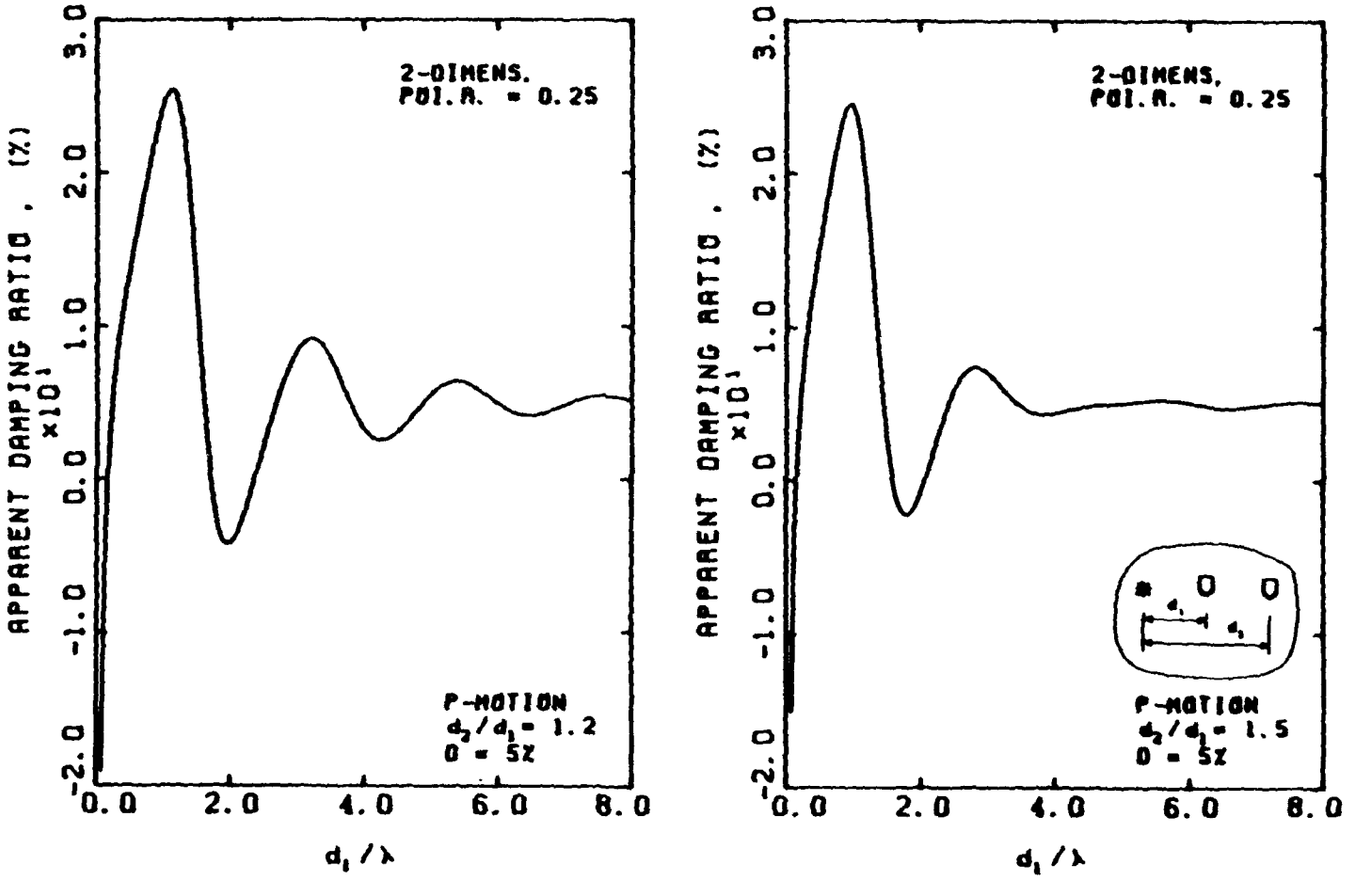

Fig. 5.11 - Apparent damping ratio for in-plane longitudinal motion in a medium with five percent damping and Poisson's ratio = 0.25. Small spacing between receivers.

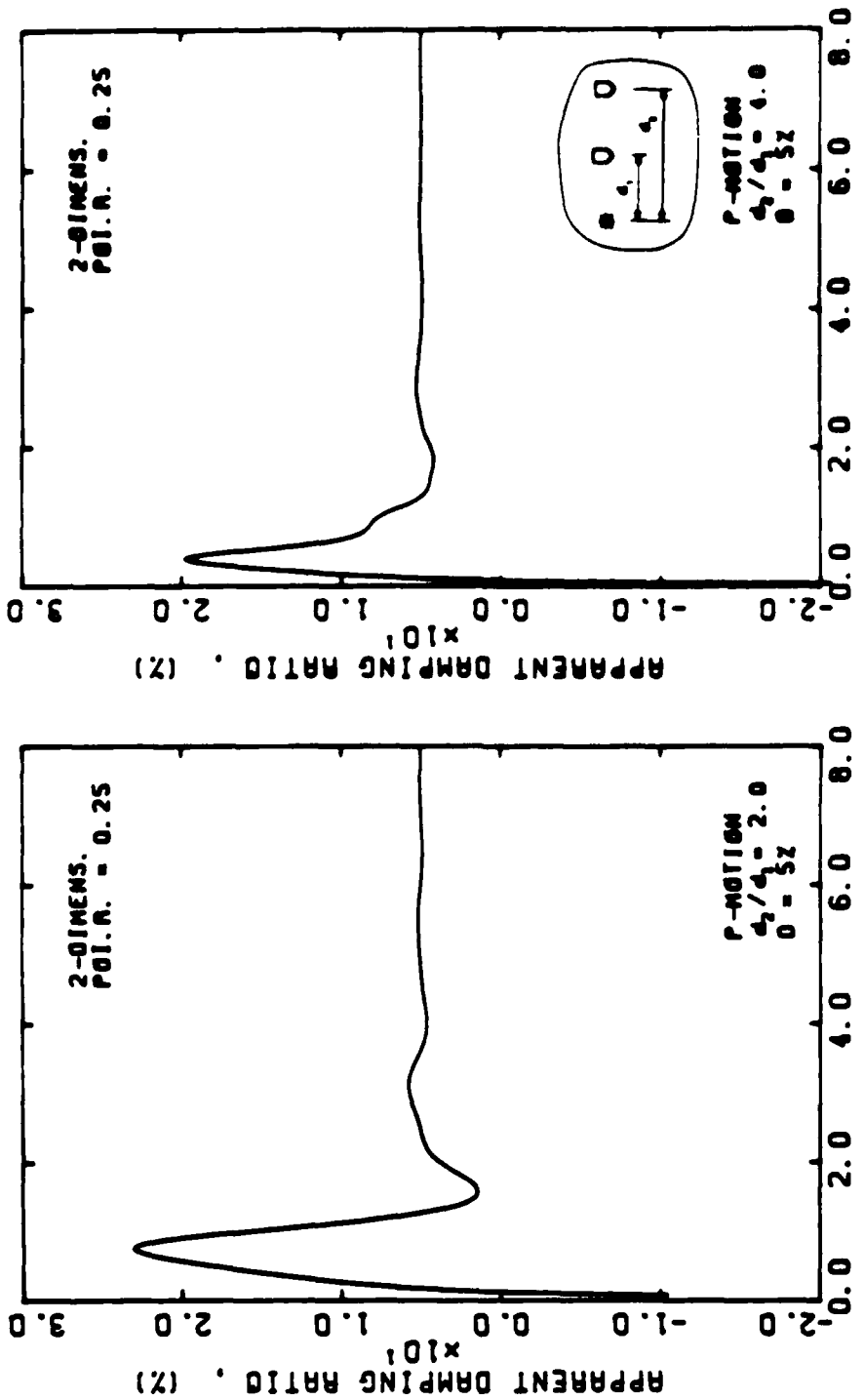

Fig. 5.12 - Apparent damping ratio for in-plane longitudinal motion in a medium with five percent damping and Poisson's ratio = 0.25. Large spacing between receivers.

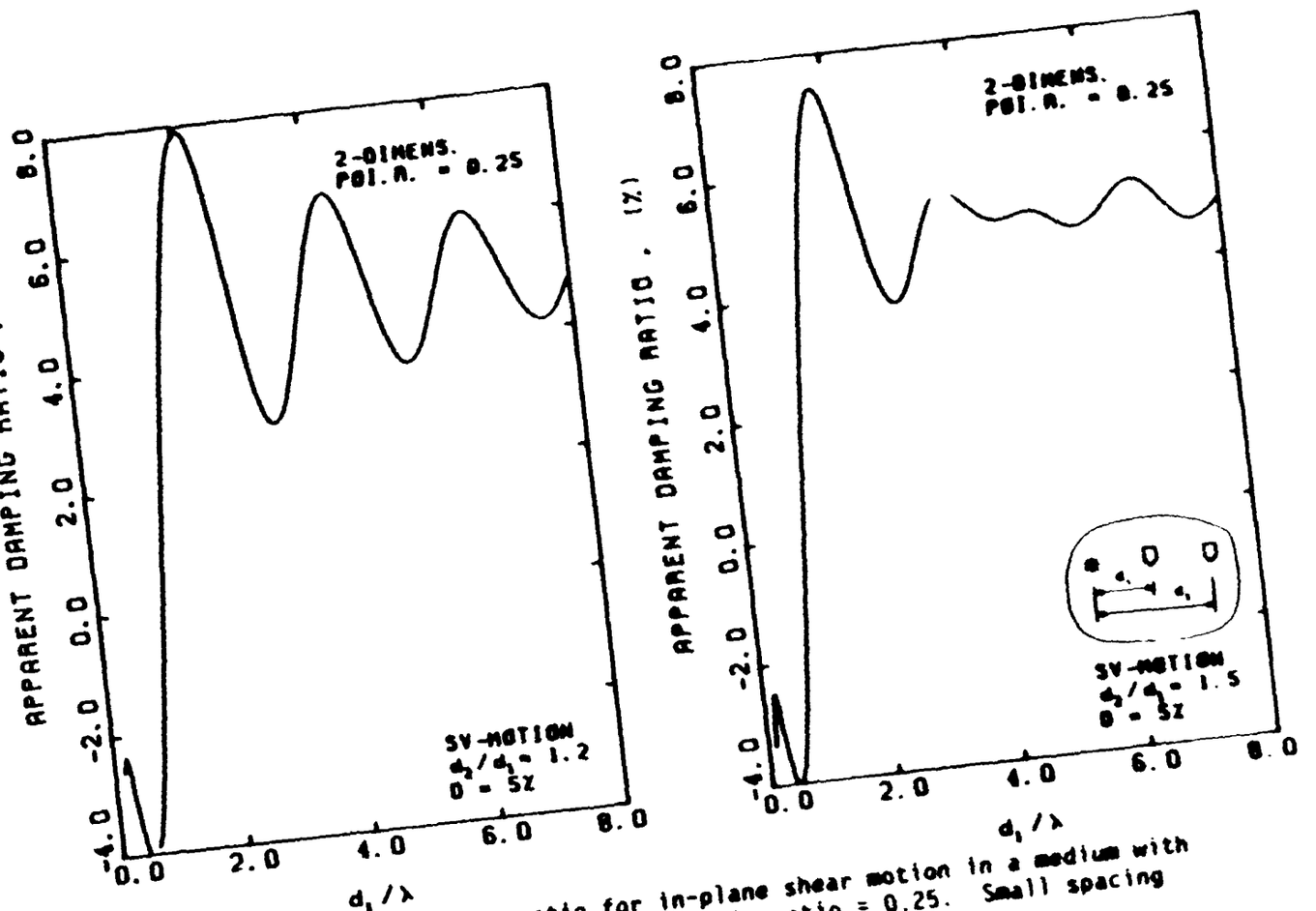

Fig. 5.13 - Apparent damping ratio for in-plane shear motion in a medium with five percent damping and Poisson's ratio = 0.25. Small spacing between receivers.

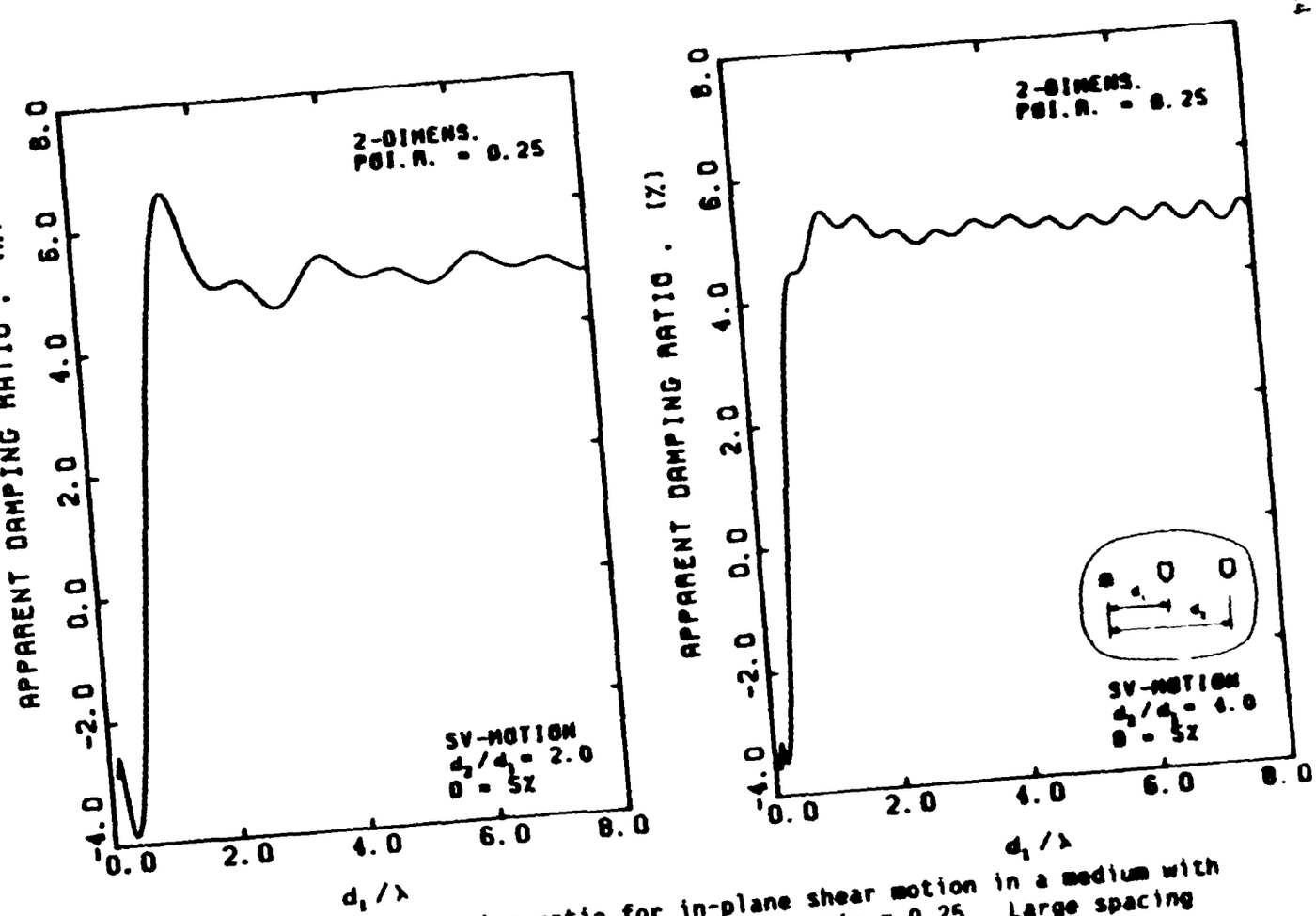

Fig. 5.14 - Apparent damping ratio for in-plane shear motion in a medium with five percent damping and Poisson's ratio = 0.25. Large spacing between receivers.

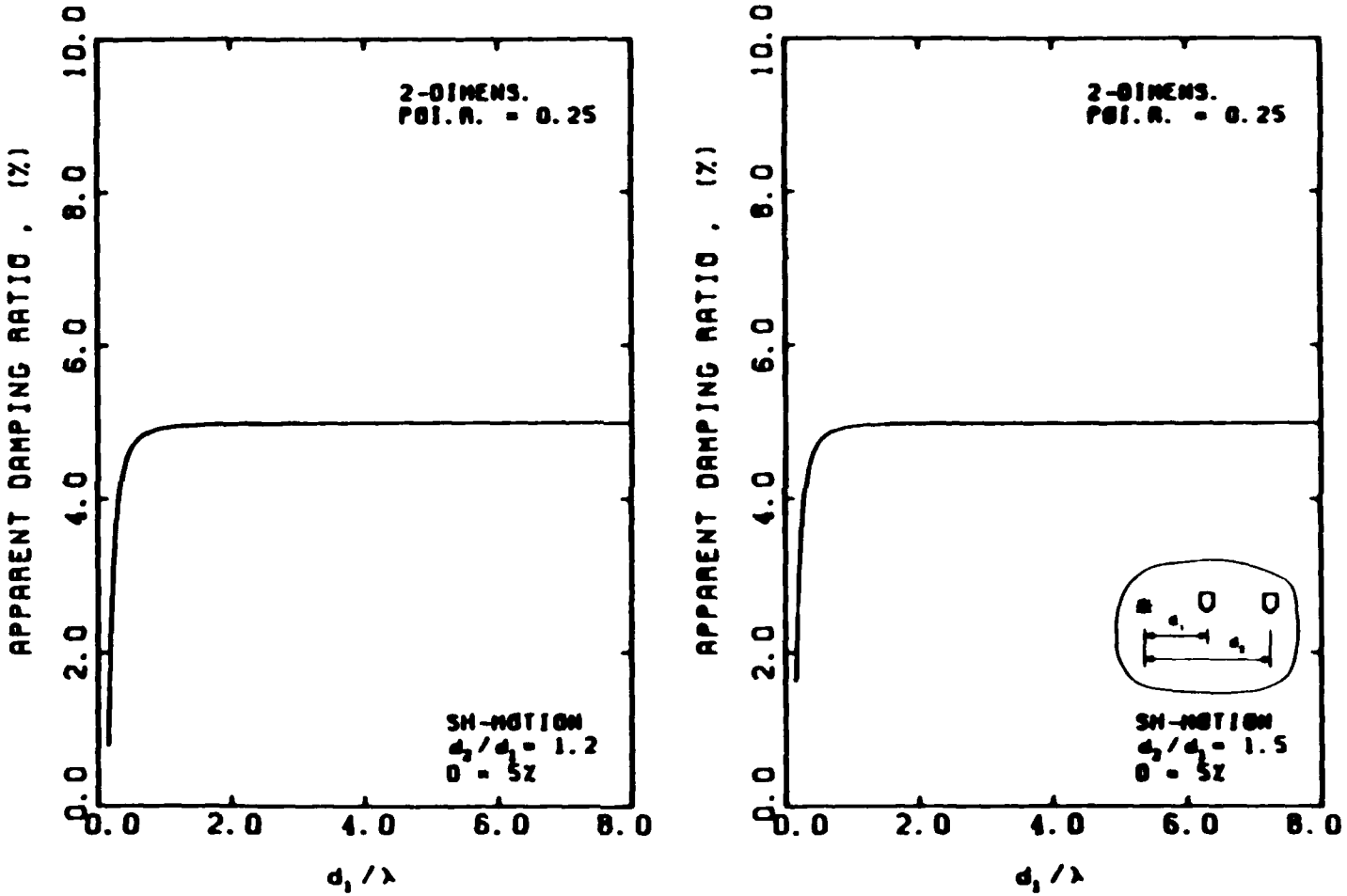

Fig. 5.15 - Apparent damping ratio for antiplane shear motion in a medium with five percent damping and Poisson's ratio = 0.25. Small spacing between receivers.

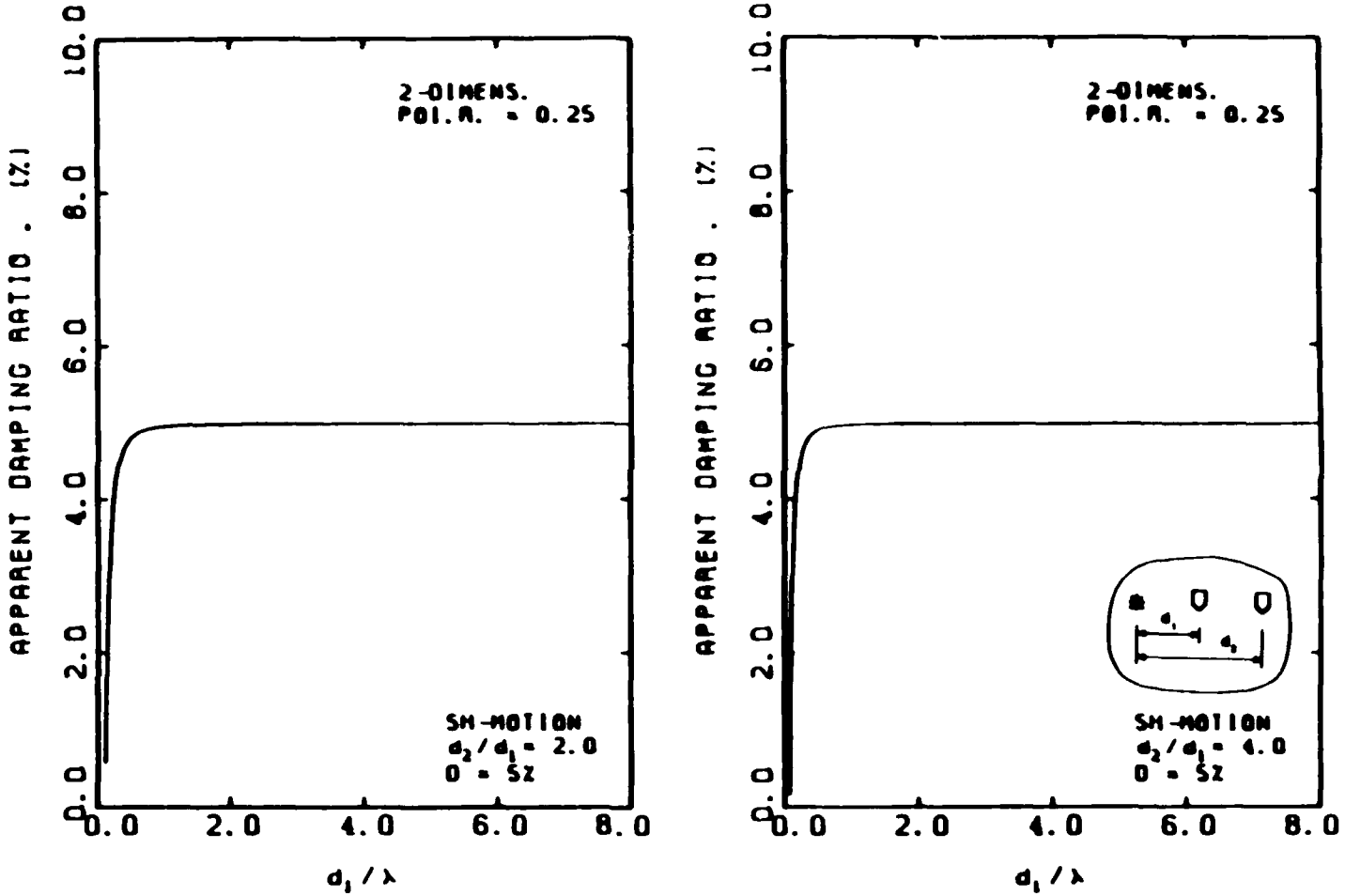

Fig. 5.16 - Apparent damping ratio for antiplane shear motion in a medium with five percent damping and Poisson's ratio = 0.25. Large spacing between receivers.

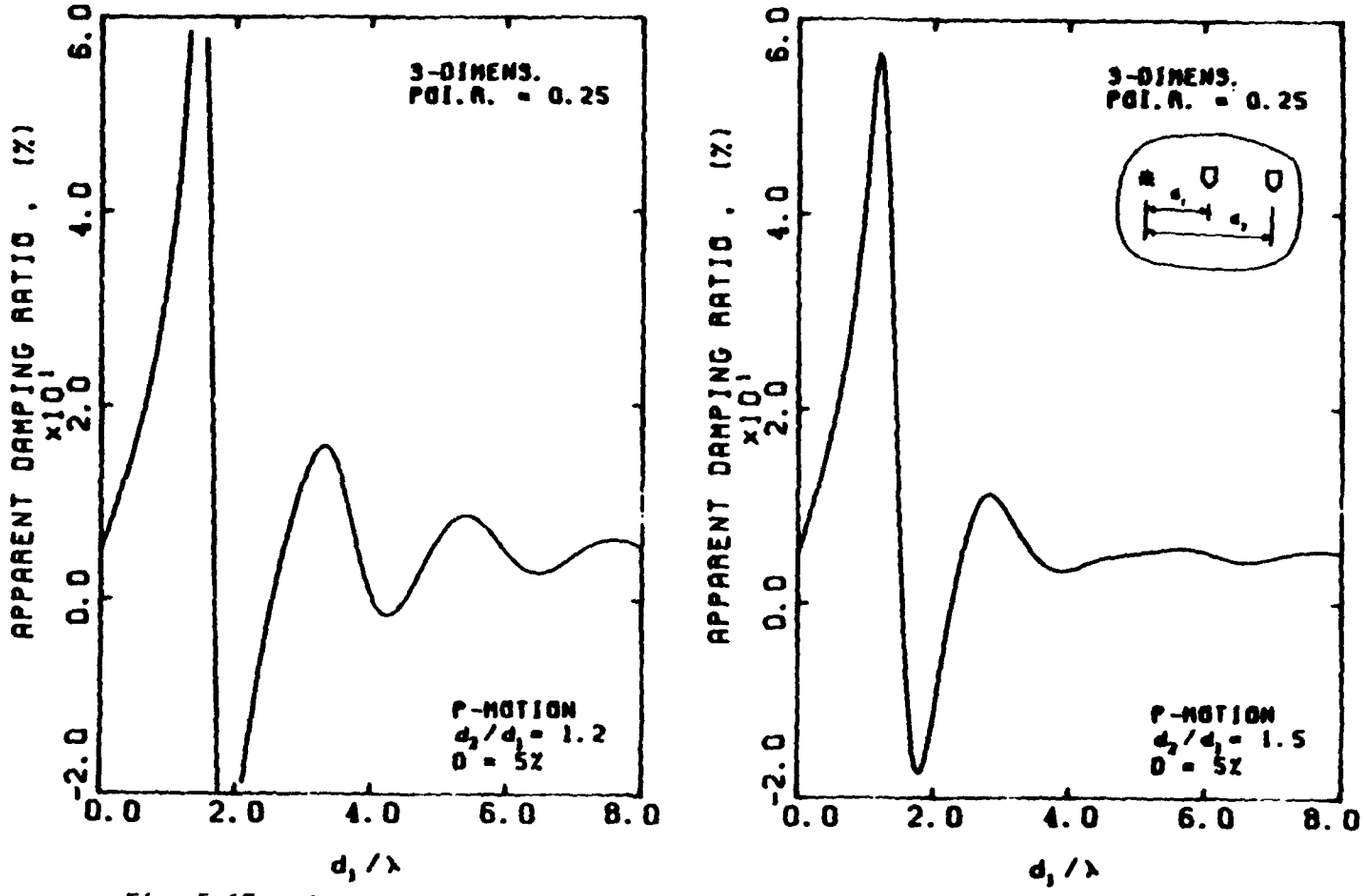

Fig. 5.17 - Apparent damping ratio for three-dimensional longitudinal motion in a medium with five percent damping and Poisson's ratio = 0.25. Small spacing between receivers.

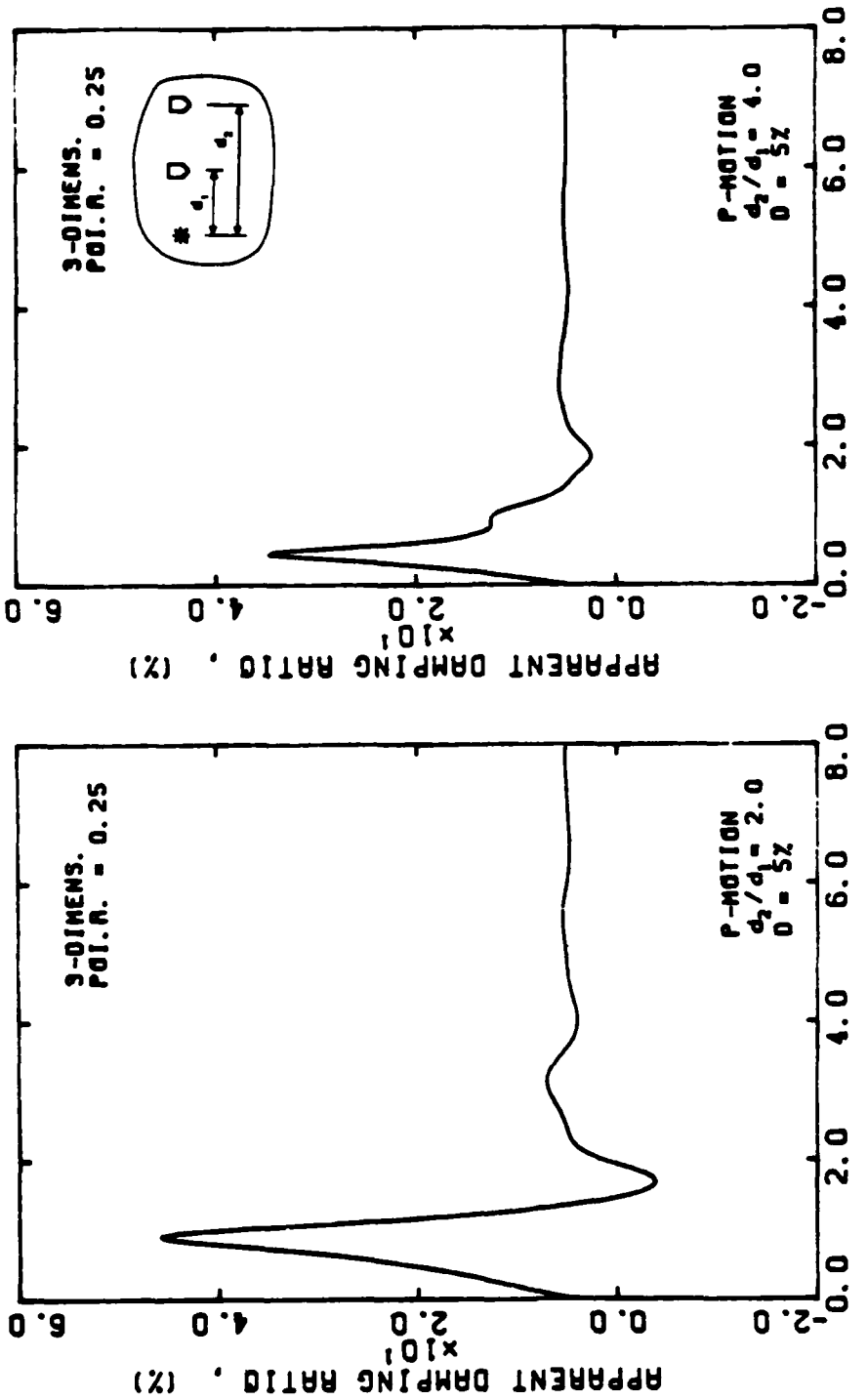

Fig. 5.18 - Apparent damping ratio for three-dimensional longitudinal motion in a medium with five percent damping and Poisson's ratio = 0.25. Large spacing between receivers.

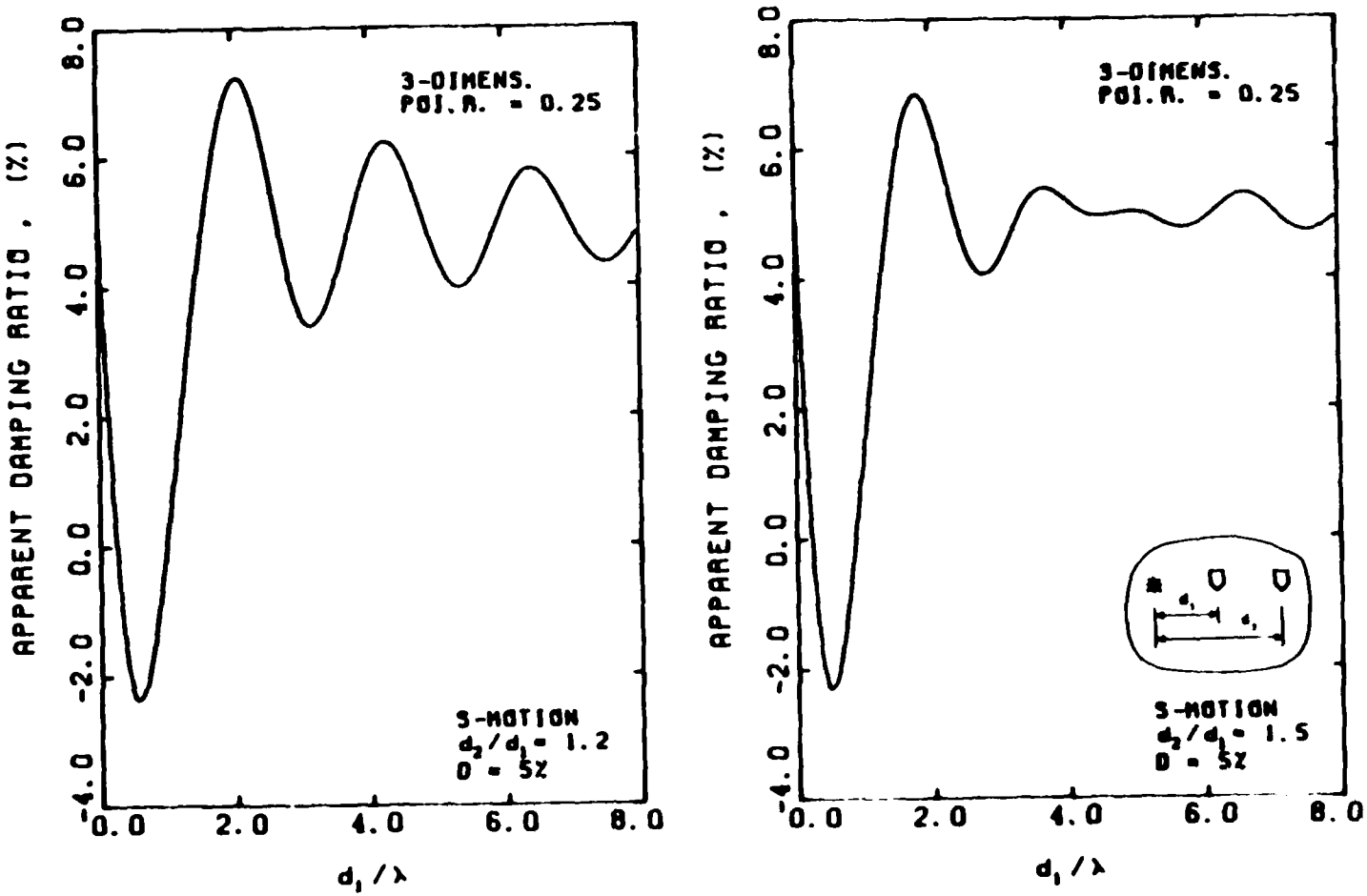

Fig. 5.19 - Apparent damping ratio for three-dimensional shear motion in a medium with five percent damping and Poisson's ratio = 0.25. Small spacing between receivers.

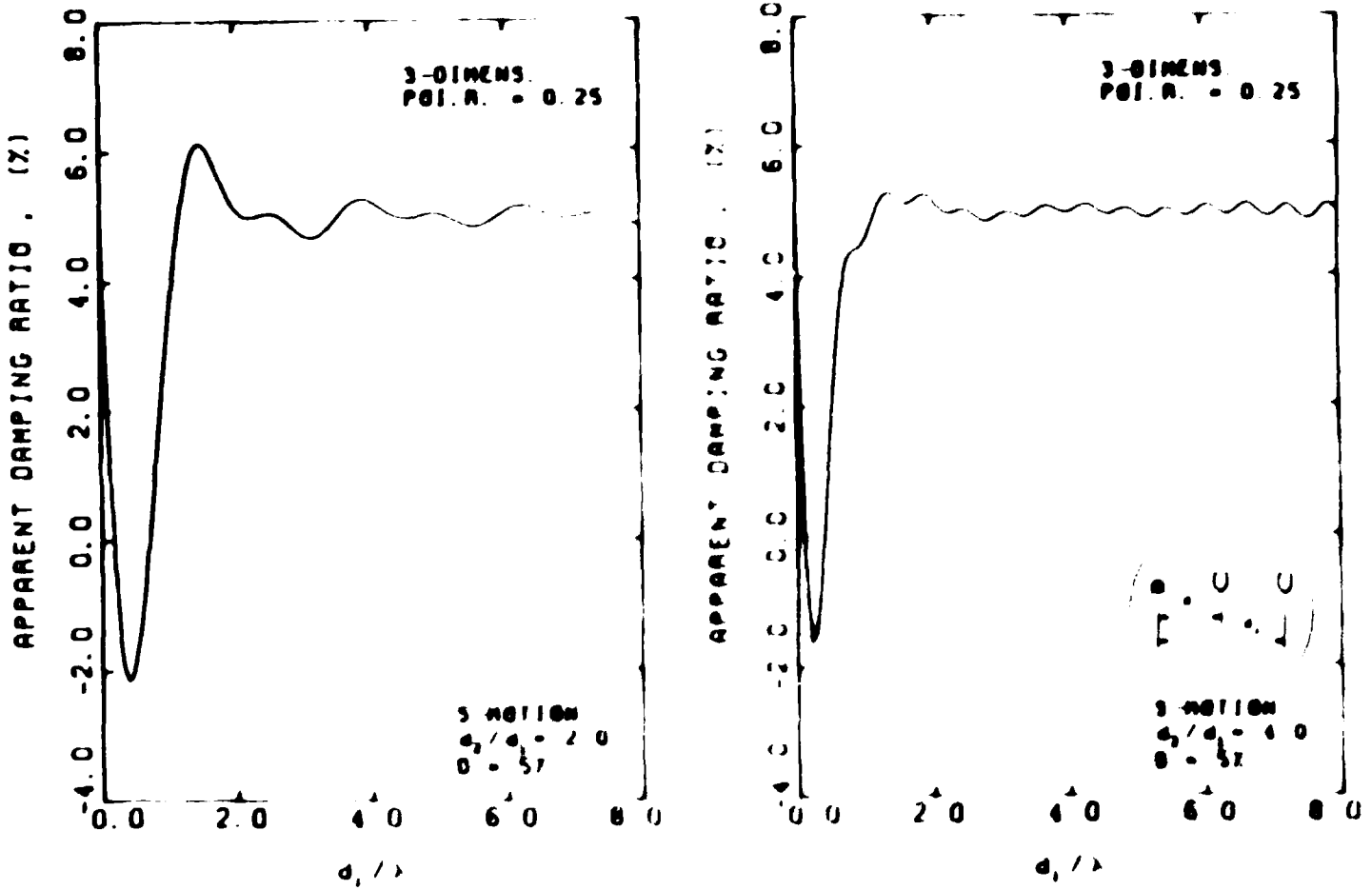

Fig. 5.20 Apparent damping ratio for three dimensional shear motion in a medium with five percent damping and Poisson's ratio = 0.25. Large spacing between receivers.

of view, values of $d_2/d_1 >> 4$ will probably present complications in the field since there will be very little energy arriving at the second receiver. In this respect it is recommended that some experimental studies be carried out to determine the best source-receiver configuration.

CHAPTER SIX

SUMMARY, CONCLUSIONS AND RECOMMENDATIONS

6.1 INTRODUCTION

Seismic methods are used in engineering to determine the elastic properties and damping characteristics of materials at low strains (strains less than o.ool percent for most geotechnical materials). Seismic methods employ both body and surface waves. Body waves are compression and shear waves. These waves are typically used to sample within the interior of solid media (such as geotechnical sites). In this study, body waves are investigated analytically to improve the understanding and uses of them. The use of seismic methods in engineering applications presents many advantages. For instance, seismic methods: 1. reduce sampling disturbance; 2. model properly in situ stress conditions; 3. test large or small representative zones of interest; and 4. are based on sound theoretical principles.

In most engineering applications of seismic methods using body waves, the receivers typically have to be placed very close to the points of excitation. This configuration creates several complications that do not occur in most geophysical applications. In addition, the use of information provided by the seismic records has been routinely limited to the first arrival of the waves. Therefore, an analytical investigation was undertaken to better understand and use seismic methods in engineering. Results,

conclusions and recommendations from this study are summarized in the following paragraphs.

6.2 BODY WAVE CHARACTERISTICS

An analytical formulation to generate synthetic wave forms of body waves created by point or line sources and propagating in a full space was explained. The fact that body waves spread from point source in a spherical fashion and from line sources in a cylindrical manner can be an important factor in using these seismic waves in engineering applications. At long distances from the sources, spherical wave fronts can be considered plane, and the classical theory of plane wave propagation is valid. This case is the most common for geophysical applications where distances from the source to the closest receivers are of the order of hundreds of meters. Distances that are involved in most engineering applications, however, are a few meters. The characteristics of body waves at these short distances was studied, and an understanding of the limitations of using the theory of plane wave propagation was developed.

The behavior of spherical or cylindrical body waves at close distances to the source was found to be in some cases quite different from plane wave behavior. An analysis of the characteristics of generated wave records from point or line sources was performed. From these waveforms, it was found that, in wave propagation records of longitudinal motion, there is a first wave (denoted by L_P) propagating at the compressional wave velocity and a second wave (denoted by L_S) that exhibits longitudinal motion but propagates at the shear wave velocity. The amplitude of the second wave (L_S) decreases at a much faster rate than that of the

primary wave (L_P). Even though the contribution of the L_S wave at distances near the source is quite important, at distances far from the source the L_S wave is almost insignificant compared with the primary wave (L_P). For these reasons, the primary wave in a longitudinal-motion record is called the far-field wave (because it lasts even in the far field), and it is the wave typically referred to in the literature as the P-wave. The L_S wave is called the near-field wave, the near-field effect, the additional near-field wave or the additional near-field effect because it only "exists" in the near field.

Similar conclusions were found for transverse motion records. In this case, however, the near-field wave (denoted as T_P) propagates at the compressional wave velocity, and the far-field wave (denoted as T_S) propagates at the shear wave velocity.

All of these observations apply to three-dimensional (point sources) and two-dimensional in-plane motions (line sources). For two-dimensional antiplane motion (sometimes called SH-motion), only one wave propagating at the shear wave velocity appears, and there are no near-field terms.

For time domain records, near-field and far-field distances have been defined as those distances from the source, d, such that the value d/λ is smaller or greater than two, respectively, for transverse motions (with λ being the shear wavelength). Near- and far-field field distances are defined as those distances such that d/λ is smaller or greater than about ten for longitudinal motions (λ is again the shear wavelength).

Some of the polarity reversals in the wave forms encountered in the field when the direction of the source is reversed were

found to be explained by the behavior of the near-field waves. In addition, receiver cross-sensitivity and imperfect alignment contribute to the lack of polarity reversal in the P-wave train.

6.3 BODY WAVE VELOCITIES

Techniques to evaluate body wave velocities were studied in Chapter Four. The effects that frequency and strain independent material damping of the hysteretic type have on wave records and resulting wave velocities were also investigated. Waves propagating in this type of material arrive at an earlier time than that predicted by the compressional and shear speeds, $c_p = [(\lambda + 2G)/\rho]^{\frac{1}{2}}$ and $c_s = (G/\rho)^{\frac{1}{2}}$, respectively. To obtain a good estimate of the elastic properties, it is convenient to pick arrival times of the wave from the source to the receiver a little after the actual arrival of the wave. It is concluded that the best results are obtained when interval times from first peaks or first troughs are used. The results are always better when the receivers are located in the far field.

The cross-correlation technique to determine interval times is found to be an appropriate method to calculate wave velocities. This technique has the advantage with respect to the other time-domain methods that it can be easily automated. The results were found to be accurate and reliable for all cases analyzed, except for the case when compressional wave velocities were determined from longitudinal-motion records in media with high values of Poisson's ratio, values on the order of 0.4 or greater. (This case of high Poisson's ratios also presented problems for some of the other techniques.)

Spectral analysis techniques to calculate wave velocities from the phase of the cross spectrum of two time records, or from the phase of the transfer function of one record, are effective tools to calculate elastic moduli. It is shown that, when two receivers are used and the cross spectrum phase is employed, the best values of elastic wave velocities are obtained when:

1. for a fixed d_1, the ratio of the distances from the source to the second and first receivers, d_2/d_1, is of the order of four or higher.
2. For a fixed value of d_2/d_1, the best comparisons are obtained at high values of d_1/λ.

For a typical crosshole setup, where d_2/d_1 is equal to two, apparent velocities are equal to the plane wave phase velocities at values of d_1/L greater than one. Both procedures, using the cross spectrum and using the transfer function present the advantage that they can be easily automated. The only significant advantage that the use of the transfer function seems to have with respect to the use of the cross spectrum is of an economical nature since the number of receivers needed is only one.

6.4 WAVE ATTENUATION AND MATERIAL DAMPING

Wave records at several distances from the source and plots of wave amplitude attenuation with distance are presented in Chapter Three. It was found that, for point sources, the amplitude decay due to only geometrical damping is inversely proportional to the distance from the source at distances that are far from the source ($d/\lambda > 2$). In the very near-field range ($d/\lambda < 0.5$), the decay is also inversely proportional to the distance. Only in a small range of distances ($0.5 < d/\lambda < 2$ for transverse motions and

$0.5 < d/\lambda < 10$ for longitudinal motions) is this relation not valid. For line sources, the amplitude reduction due to geometrical damping is in proportion to the square root of the distance only in the far-field. In the very near-field ($d/\lambda < 0.5$), the amplitudes decay at a smaller rate. When material damping is included, wave amplitudes decay at much faster rates than those corresponding to only geometrical damping for distances greater than L (with L being the wavelength of the propagating wave). At distances smaller than L, the decay is practically equal to that corresponding to geometrical damping.

A technique to estimate damping ratios from seismic records that is based on spectral analysis techniques is suggested in Chapter Five. Apparent damping ratios calculated by this method, fluctuated around the correct value of material damping ratio, but at large values of d_1/L, the fluctuations were minimal. The analytical results indicate that this method can give a good prediction of damping ratio if the two receivers are spaced at a ratio $d_2/d_1 > 2$ and the apparent damping ratios used to calculate the actual damping are taken for frequencies such that d_1/L is greater than one. Like the other spectral analysis techniques to calculate velocities, the method to compute damping can be easily automated.

APPENDIX A

TIME DOMAIN RECORDS

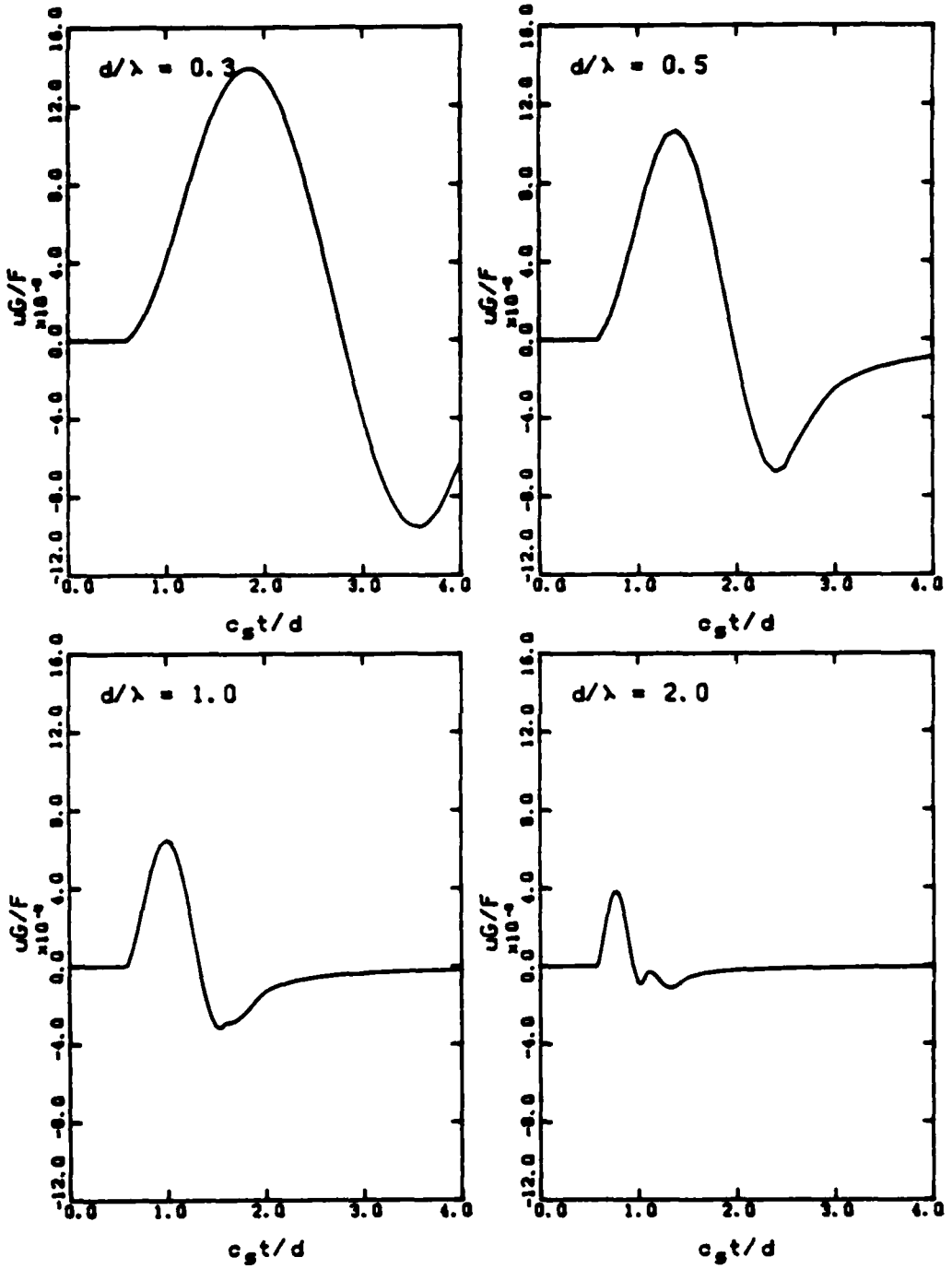

Fig. A.1 - Amplitude decay with distance (short distances) for two-dimensional longitudinal motion in a medium with no damping and Poisson's ratio = 0.25.

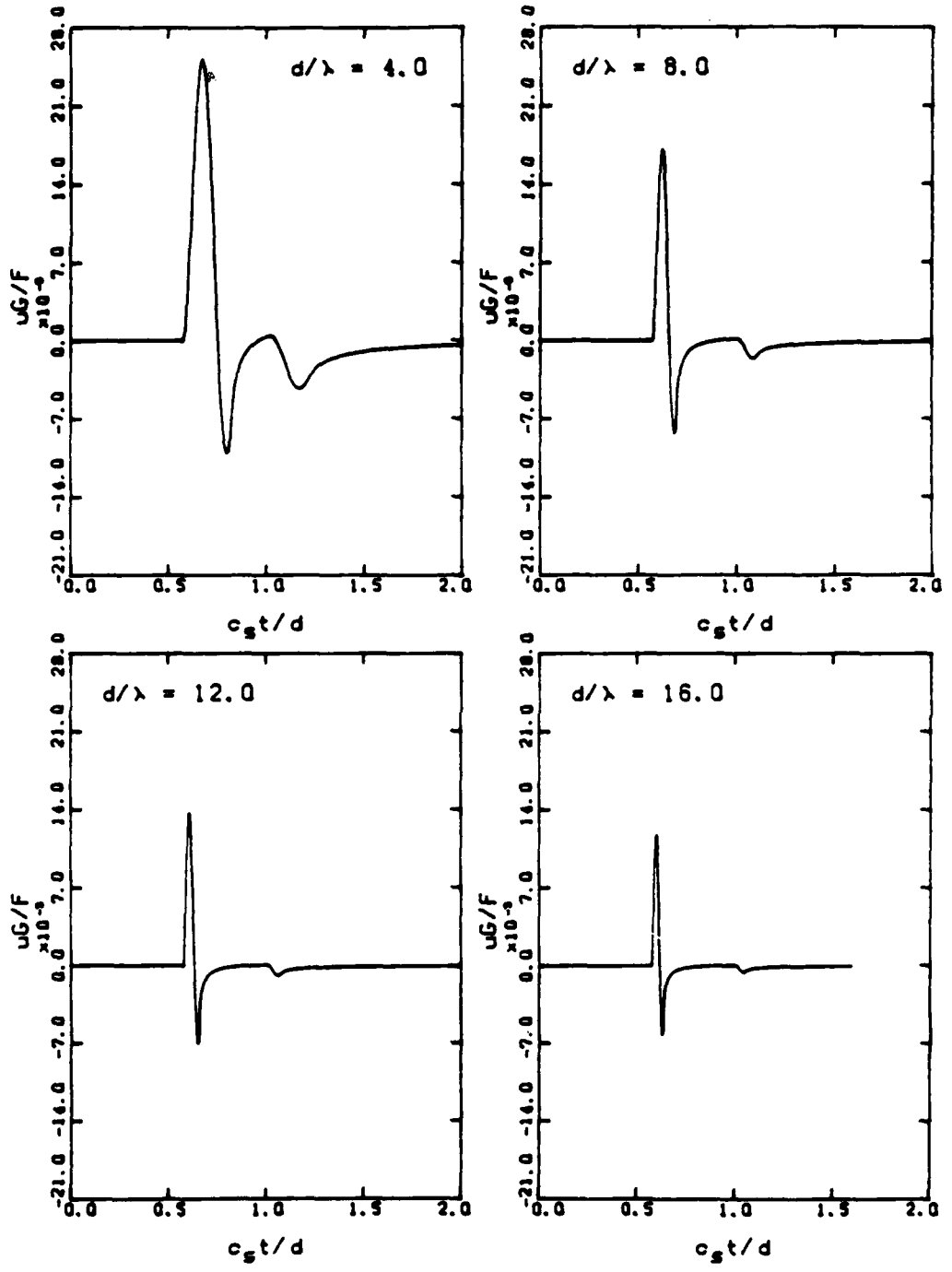

Fig. A.2 - Amplitude decay with distance (long distances) for two-dimensional longitudinal motion in a medium with no damping and Poisson's ratio = 0.25.

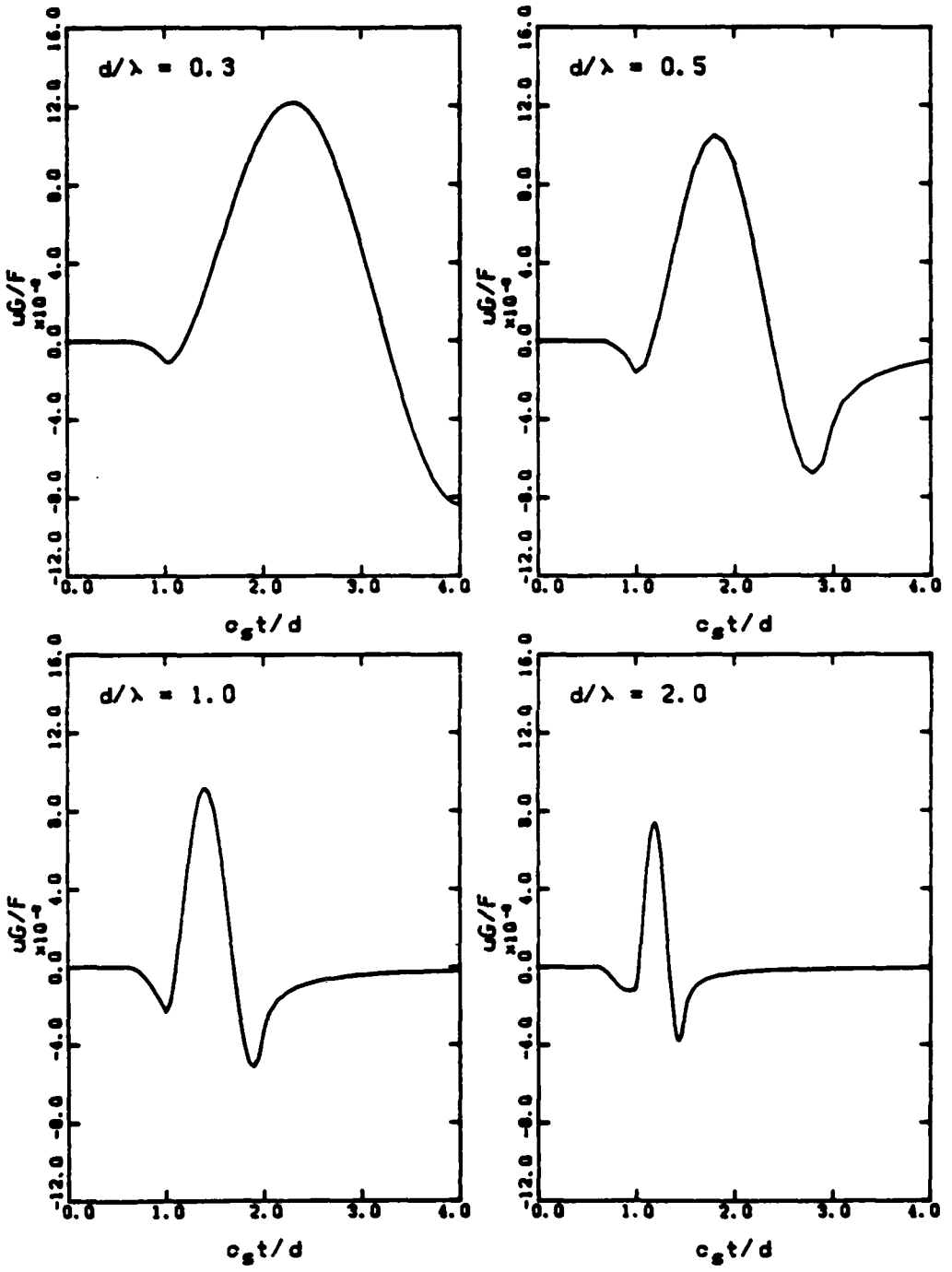

Fig. A.3 - Amplitude decay with distance (short distances) for in-plane shear motion in a medium with no damping and Poisson's ratio = 0.25.

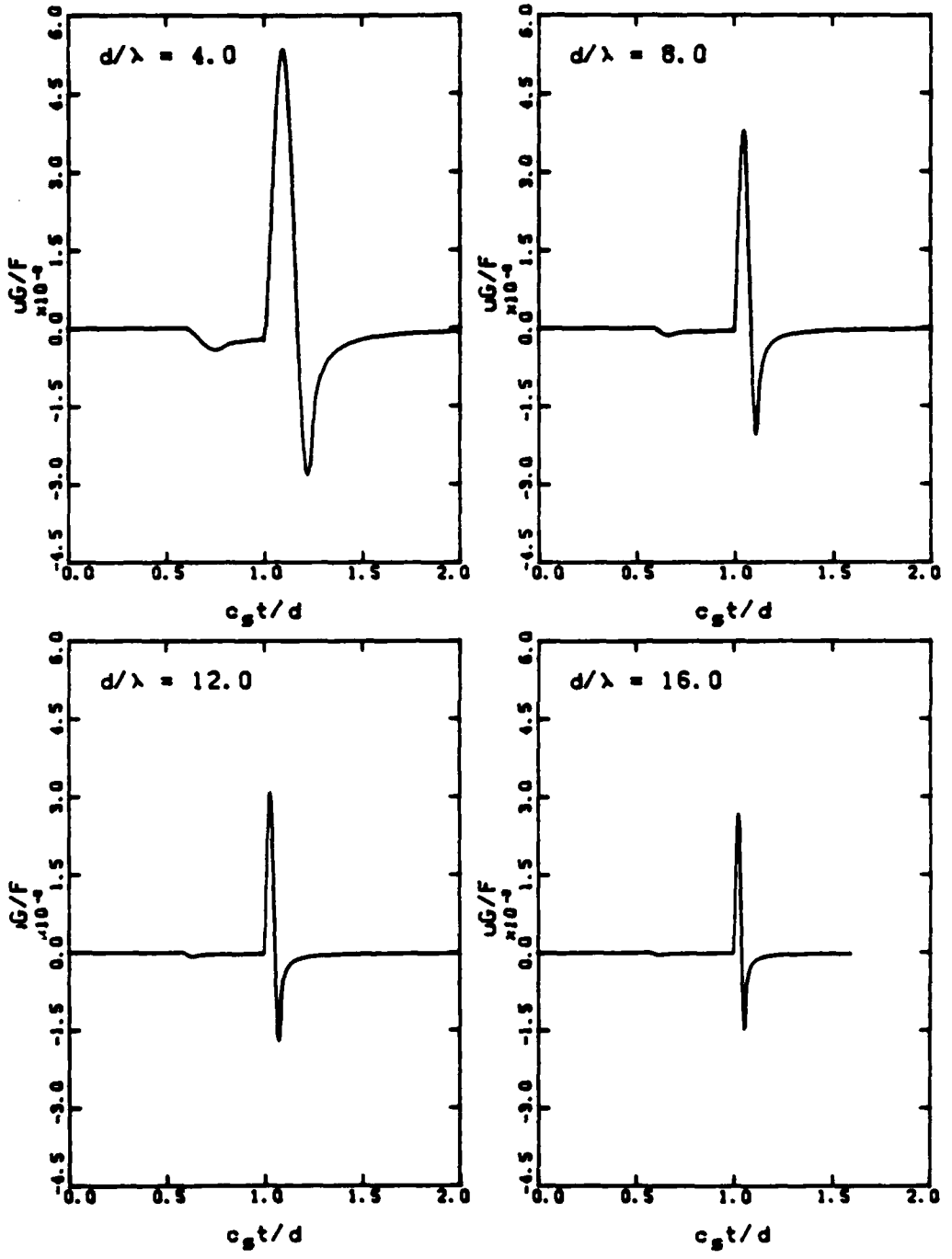

Fig. A.4 - Amplitude decay with distance (long distances) for in-plane shear motion in a medium with no damping and Poisson's ratio = 0.25.

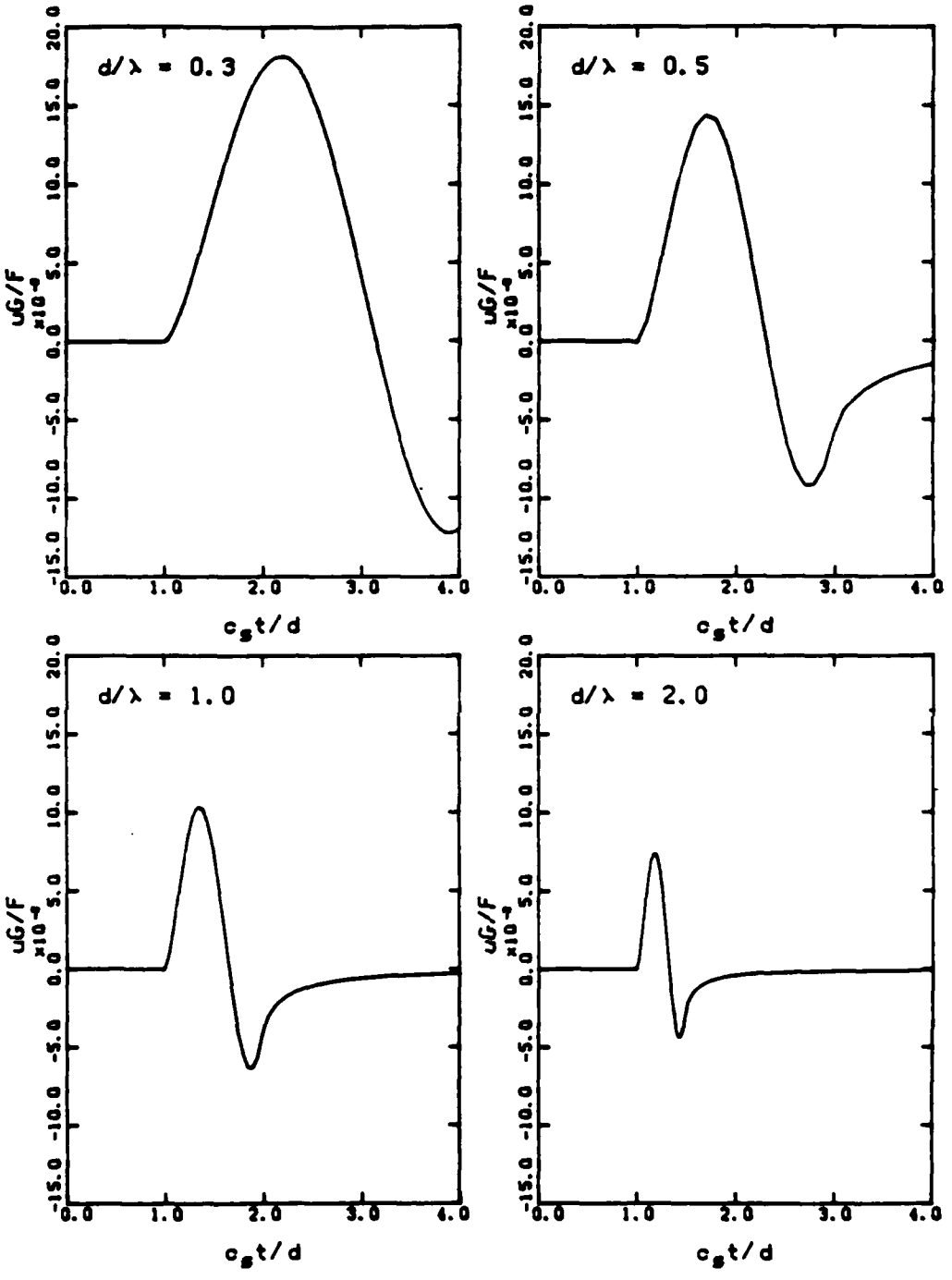

Fig. A.5 - Amplitude decay with distance (short distances) for antiplane shear motion in a medium with no damping and Poisson's ratio = 0.25.

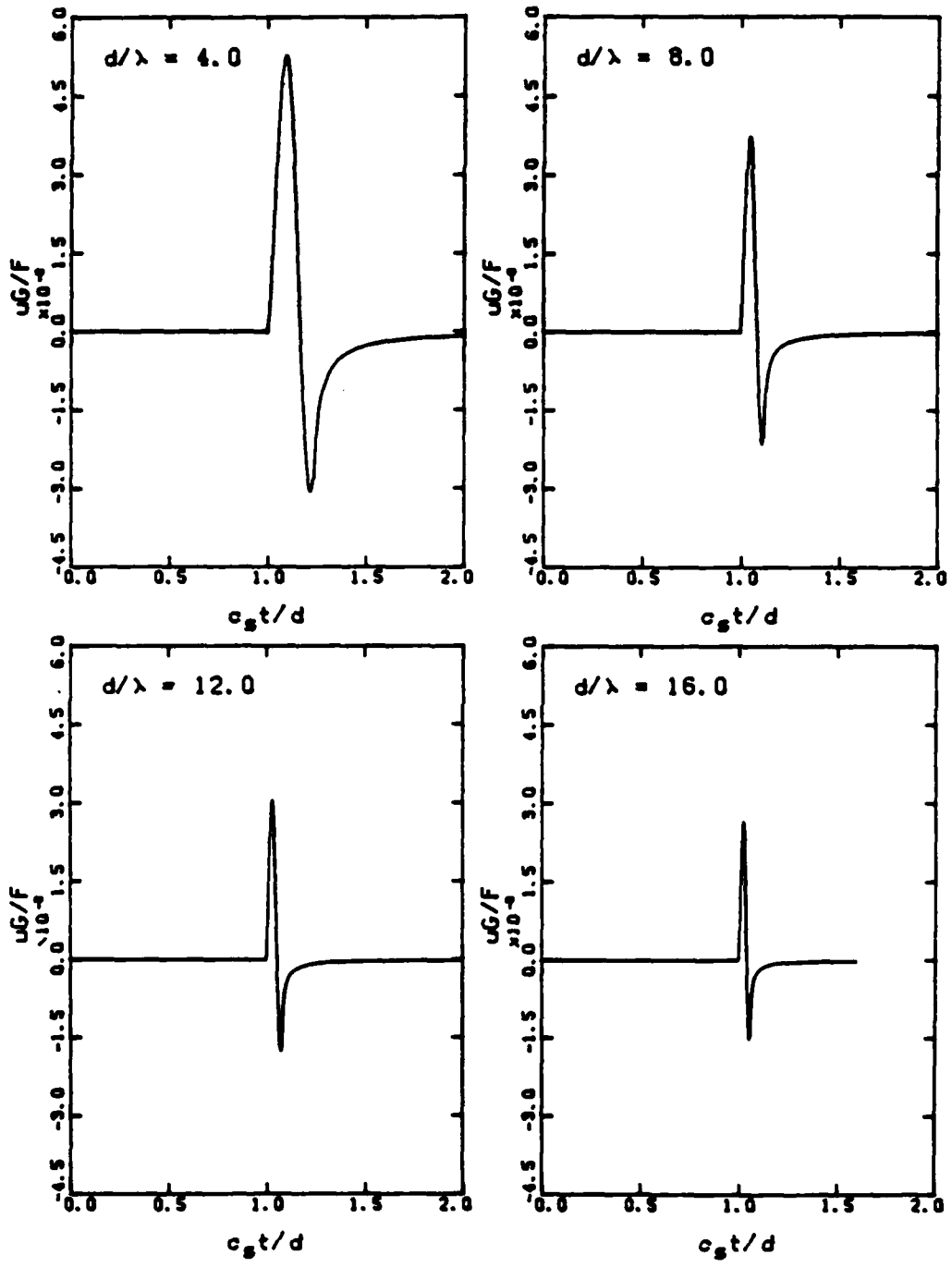

Fig. A.6 - Amplitude decay with distance (long distances) for antiplane shear motion in a medium with no damping and Poisson's ratio = 0.25.

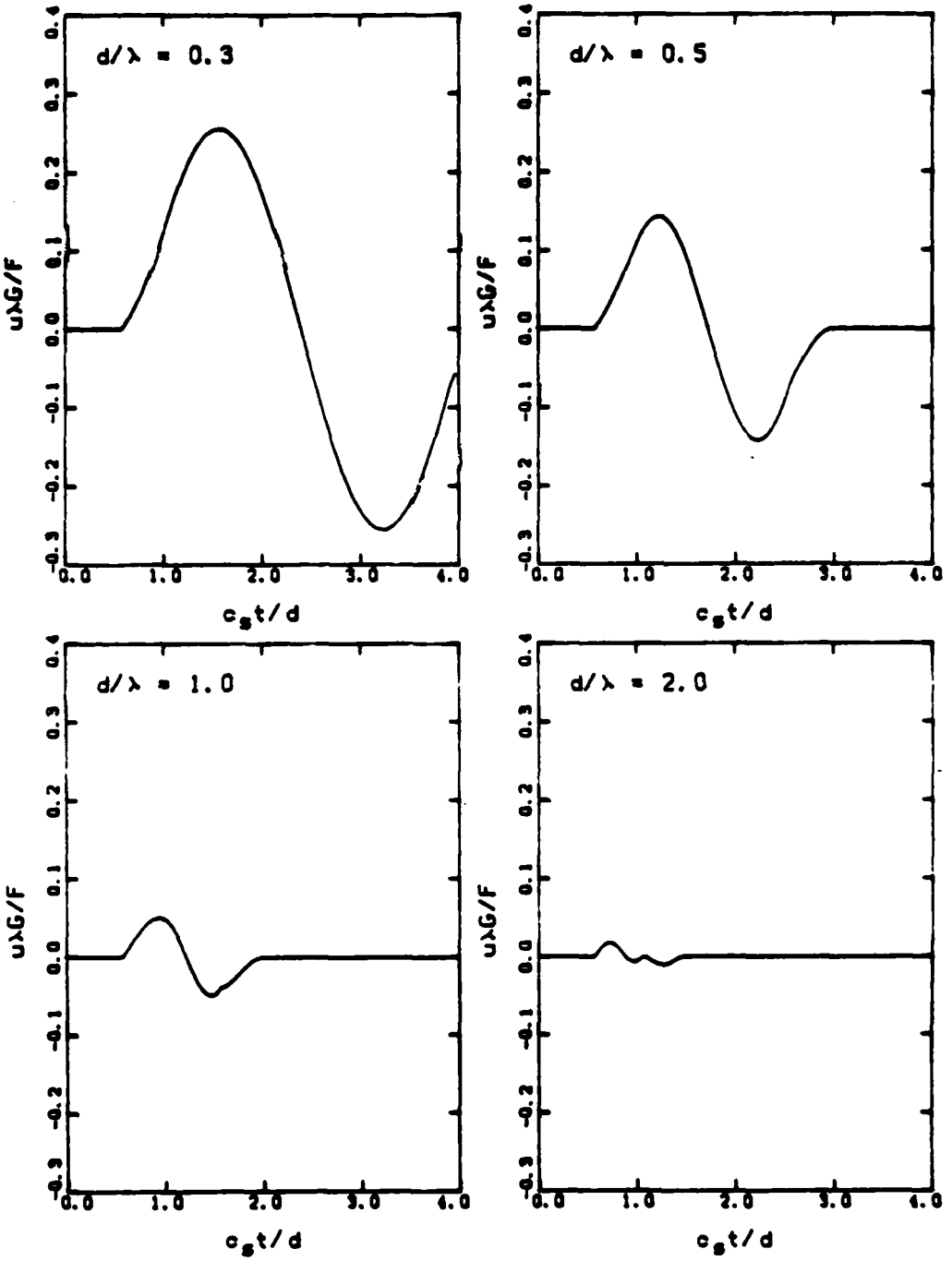

Fig. A.7 - Amplitude decay with distance (short distances) for three-dimensional longitudinal motion in a medium with no damping and Poisson's ratio = 0.25.

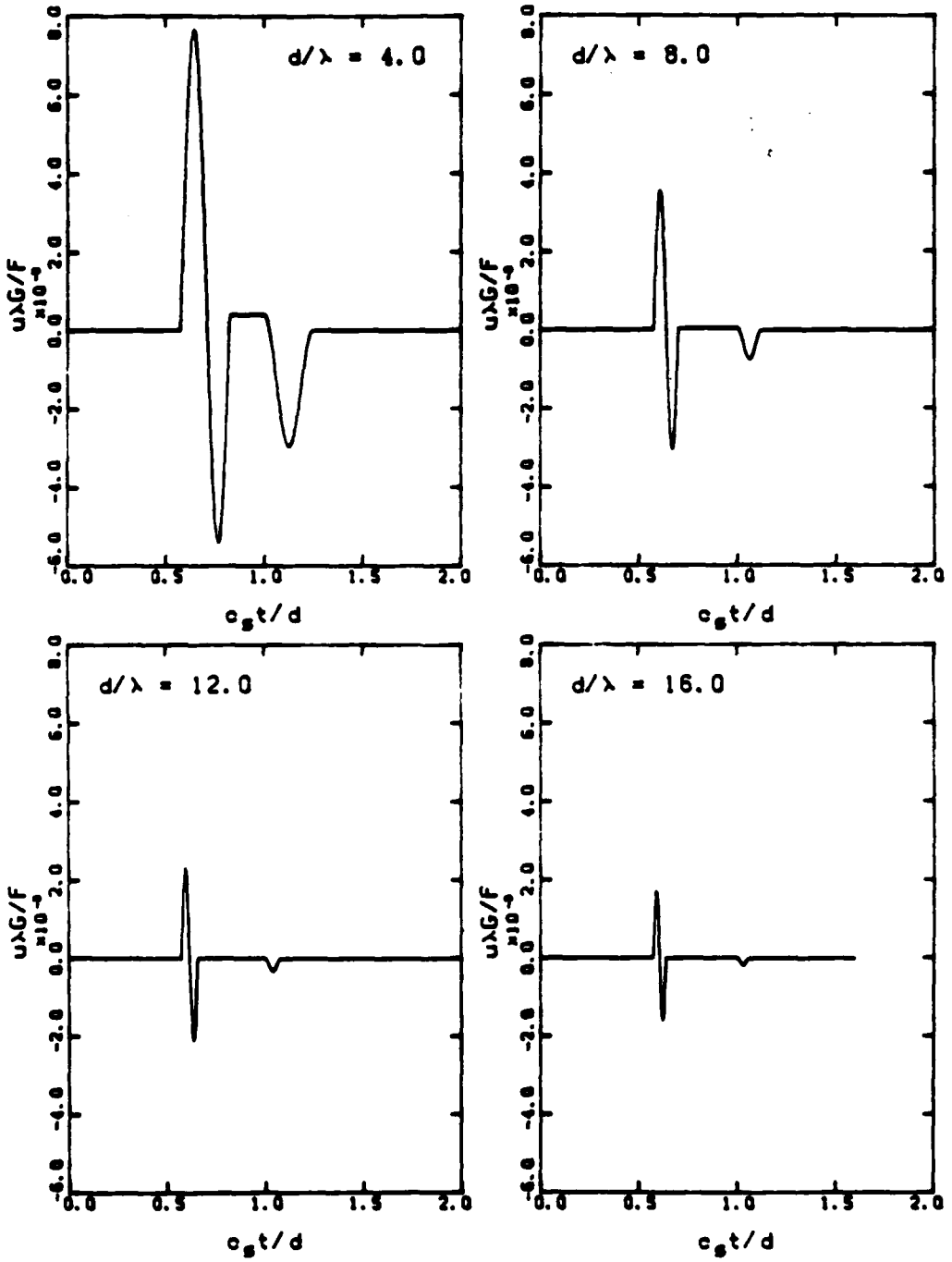

Fig. A.8 - Amplitude decay with distance (long distances) for three-dimensional longitudinal motion in a medium with no damping and Poisson's ratio = 0.25.

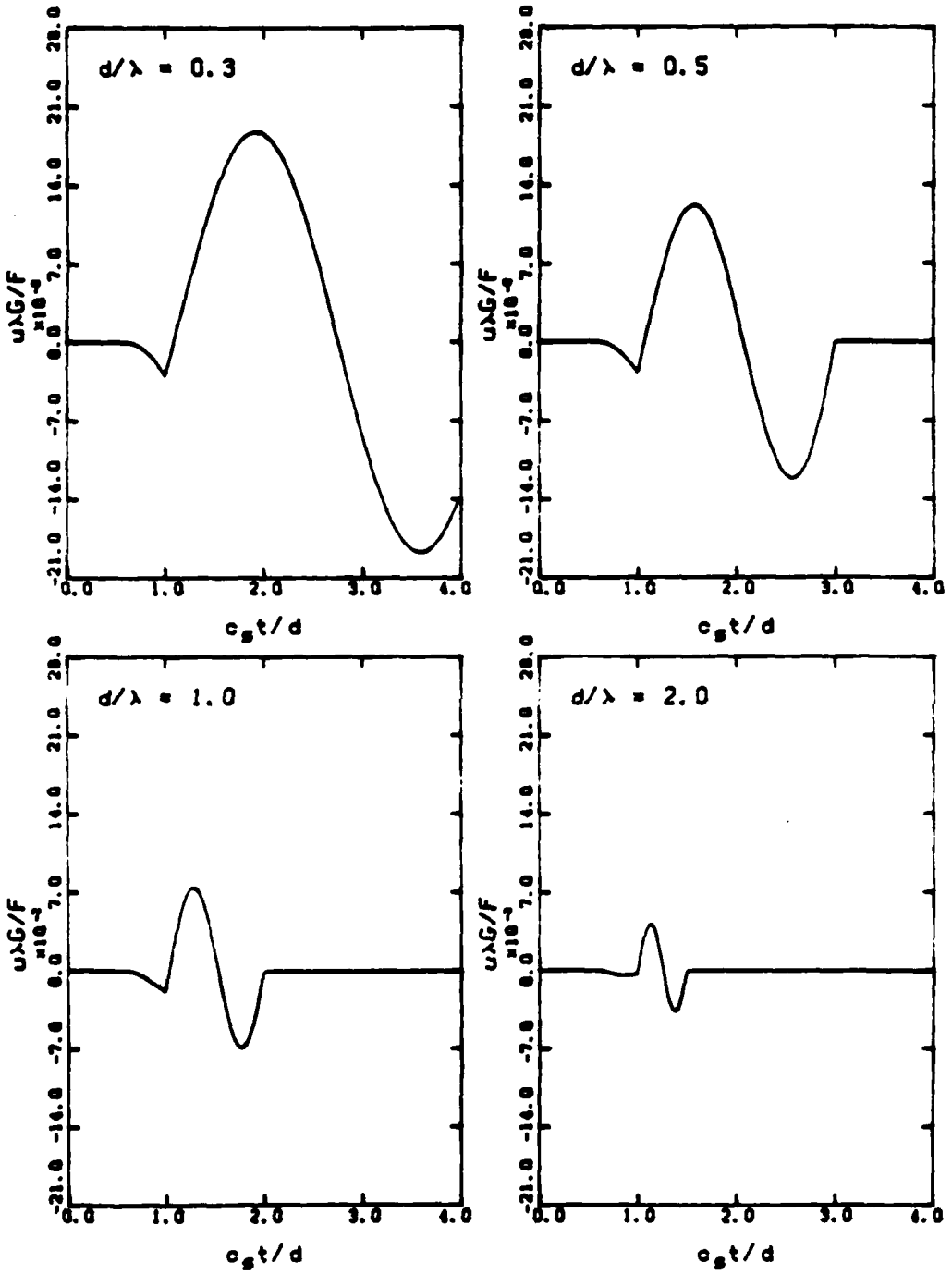

Fig. A.9 - Amplitude decay with distance (short distances) for three-dimensional shear motion in a medium with no damping and Poisson's ratio = 0.25.

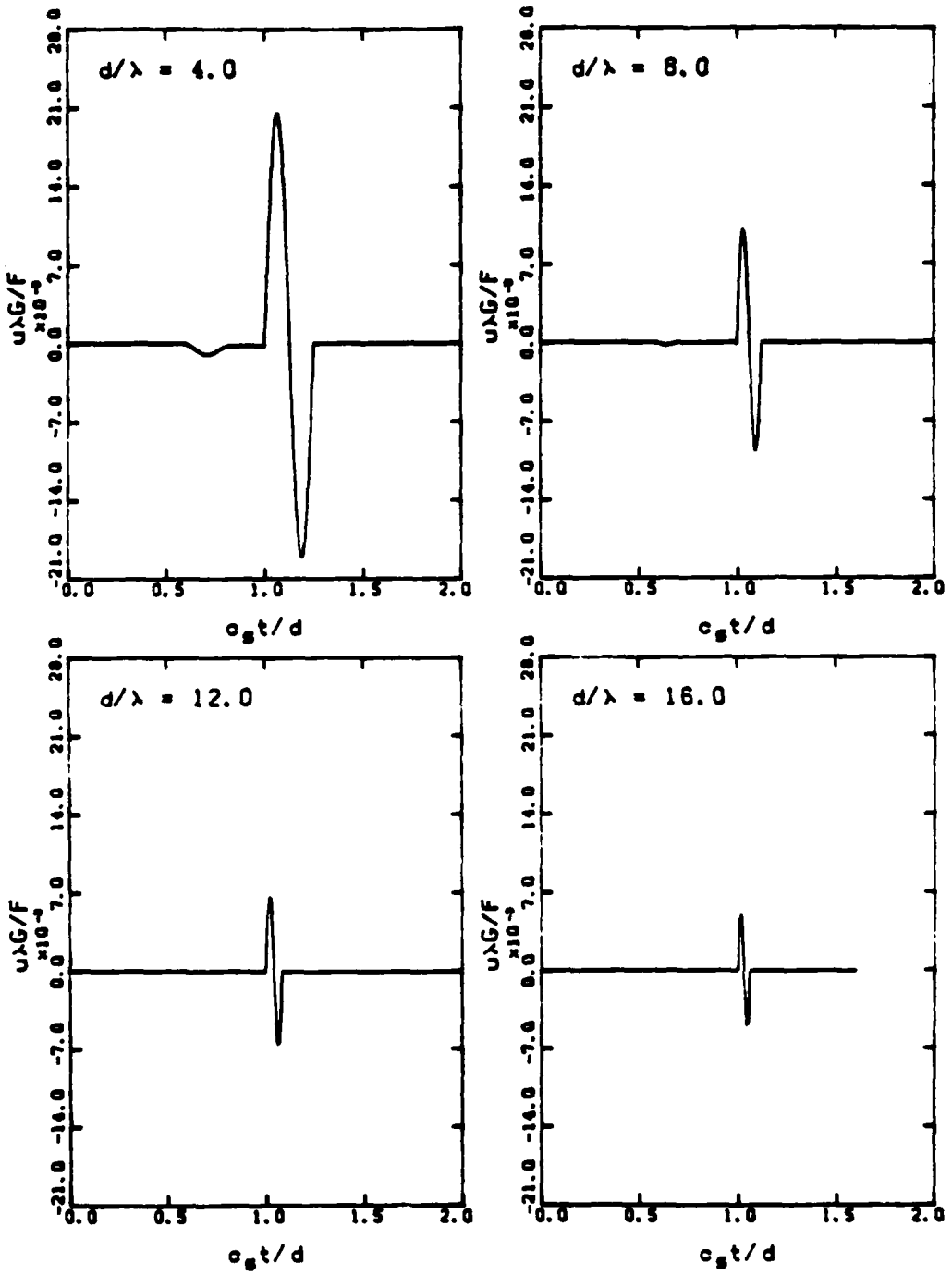

Fig. A.10 - Amplitude decay with distance (long distances) for three-dimensional shear motion in a medium with no damping and Poisson's ratio = 0.25.

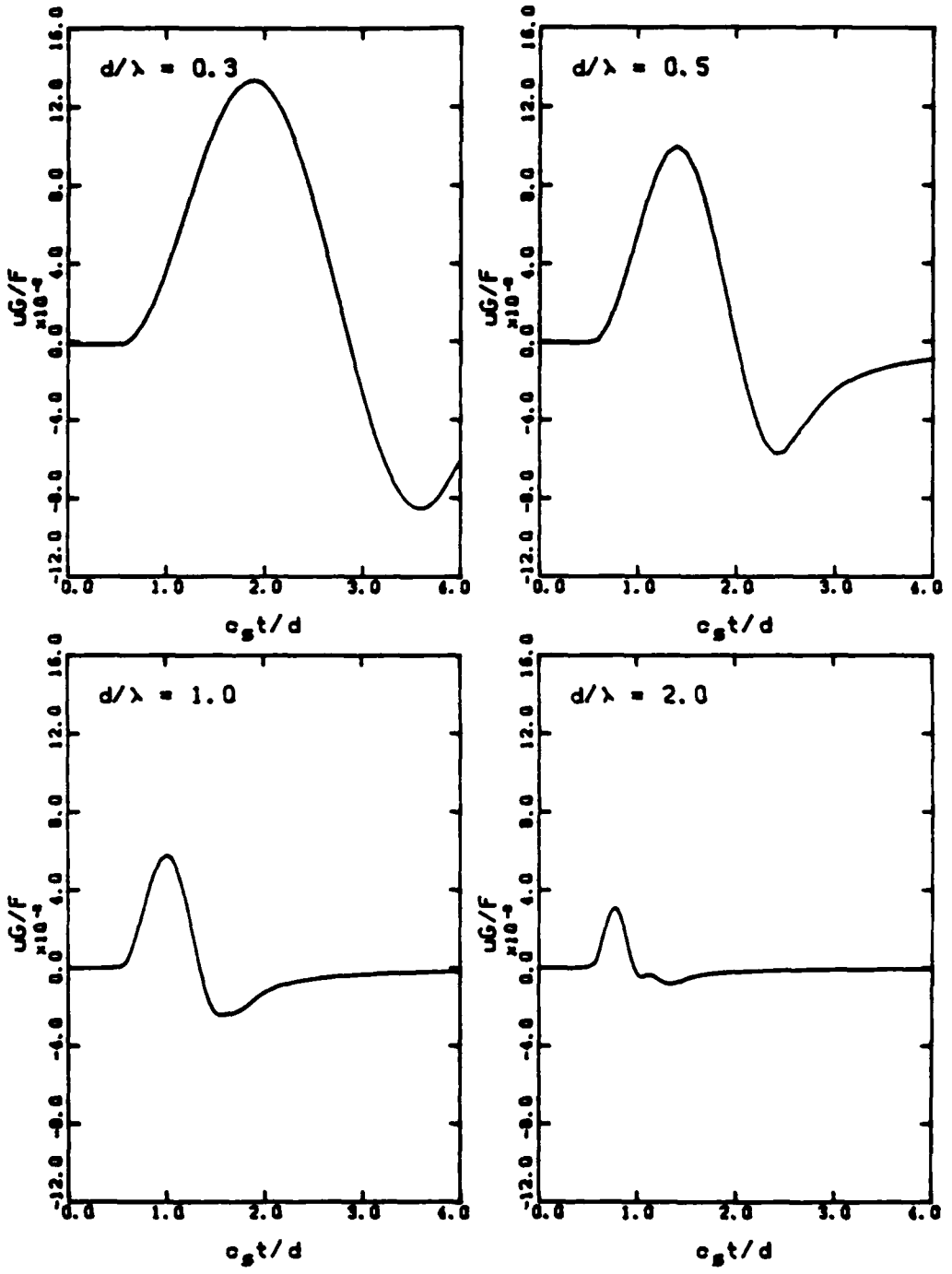

Fig. A.11 - Amplitude decay with distance (short distances) for two-dimensional longitudinal motion in a medium with five percent damping and Poisson's ratio = 0.25.

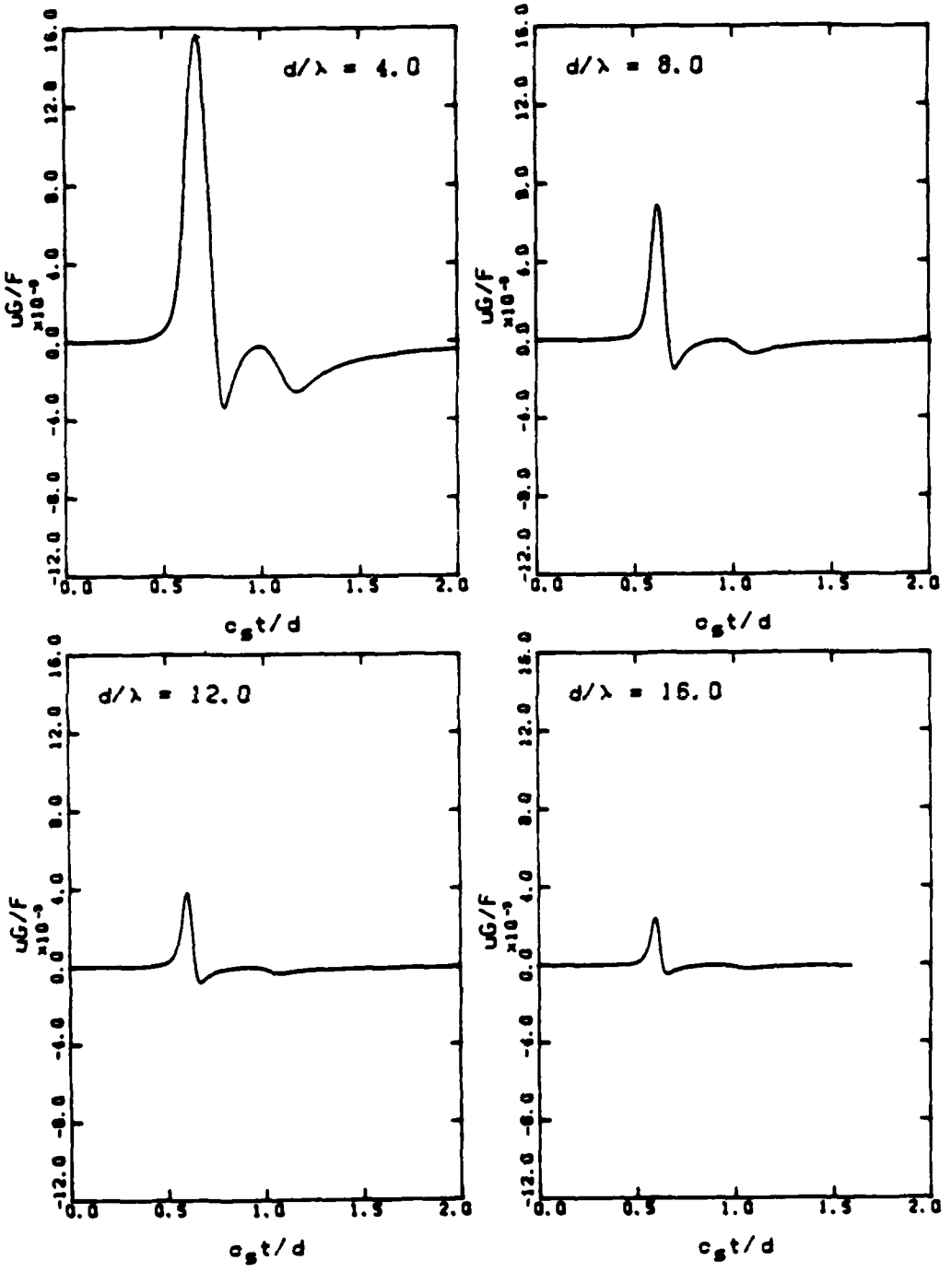

Fig. A.12 - Amplitude decay with distance (long distances) for two-dimensional longitudinal motion in a medium with five percent damping and Poisson's ratio = 0.25.

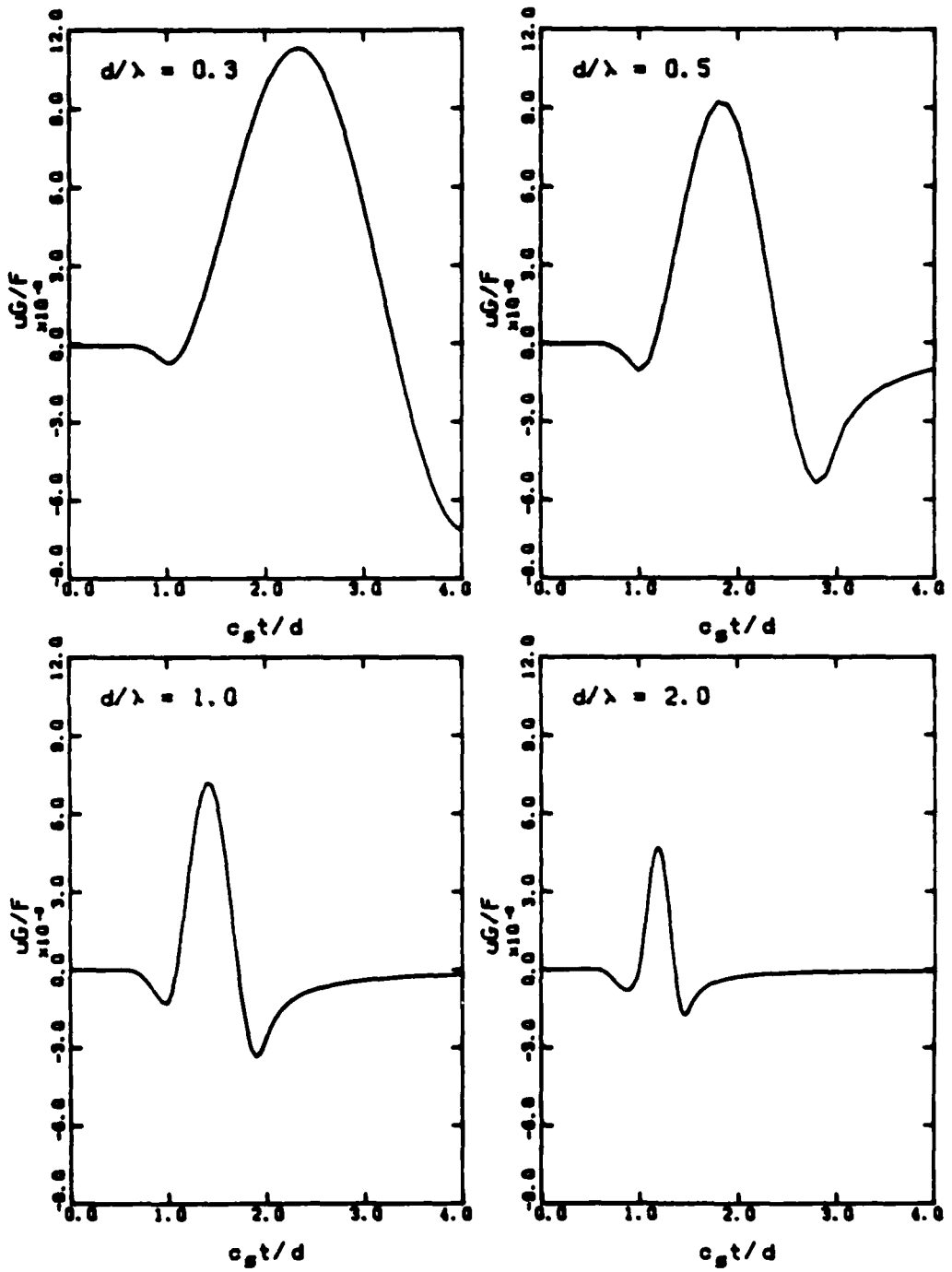

Fig. A.13 - Amplitude decay with distance (short distances) for in-plane shear motion in a medium with five percent damping and Poisson's ratio = 0.25.

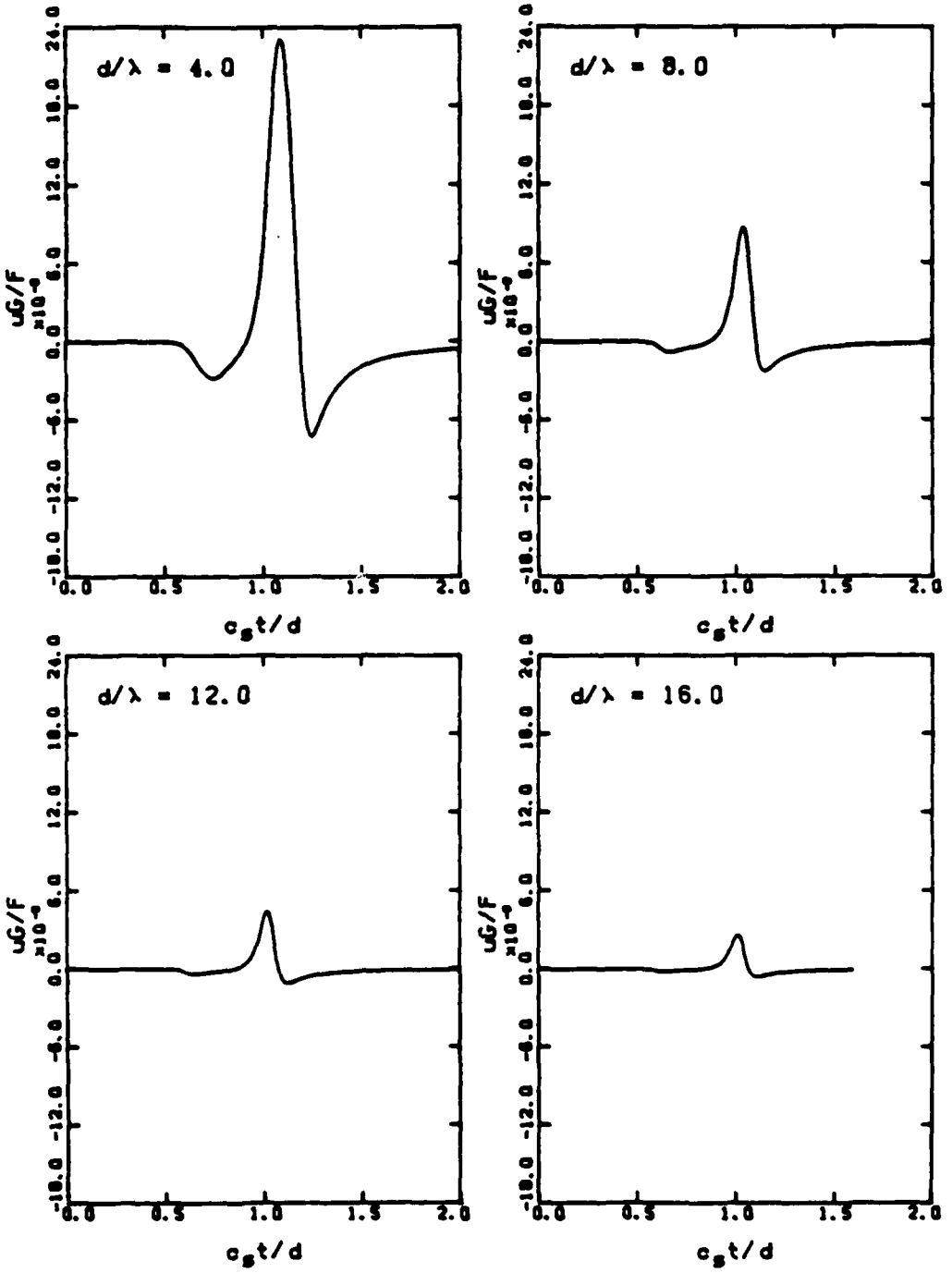

Fig. A.14 - Amplitude decay with distance (long distances) for in-plane shear motion in a medium with five percent damping and Poisson's ratio = 0.25.

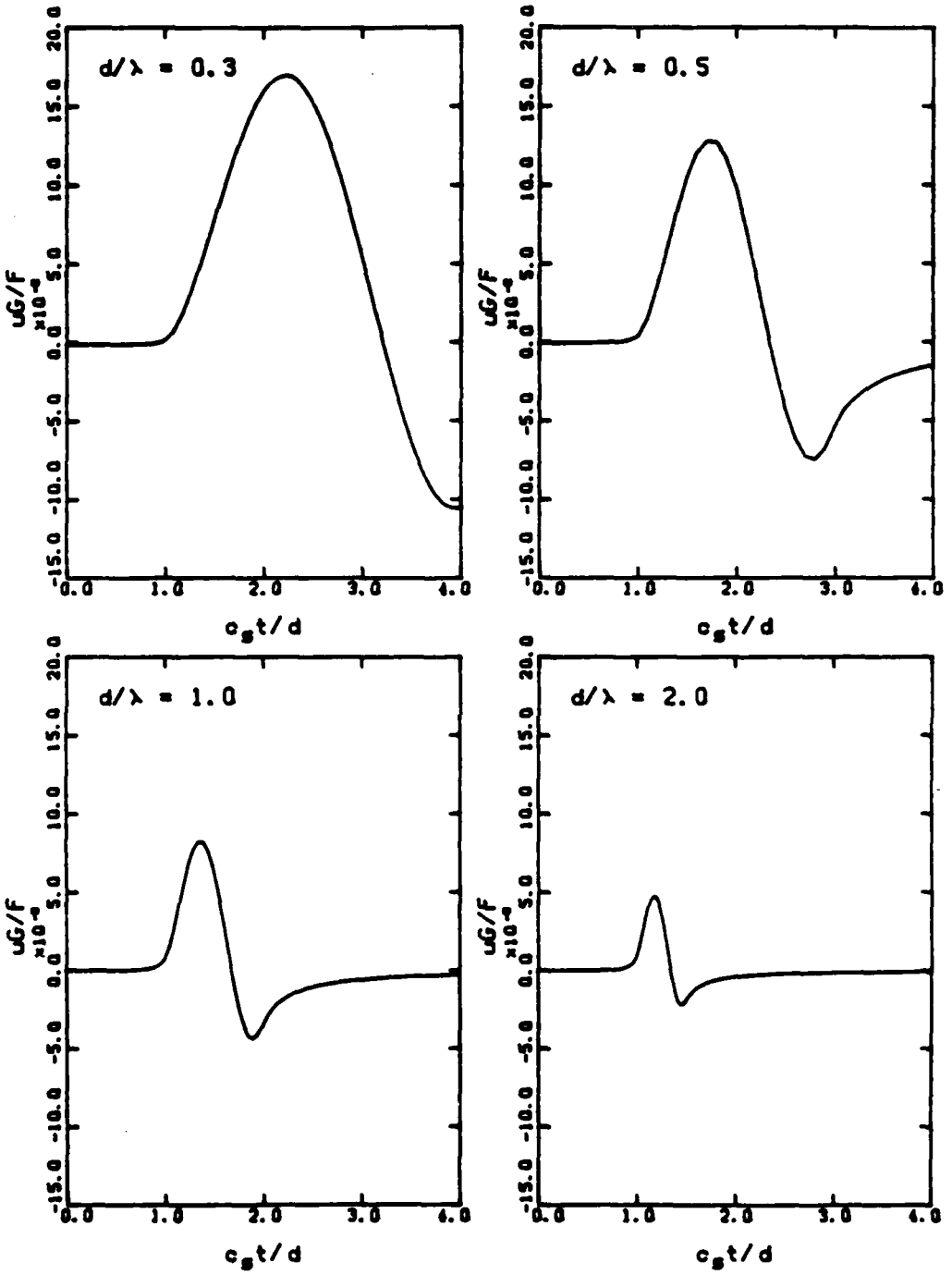

Fig. A.15 - Amplitude decay with distance (short distances) for antiplane shear motion in a medium with five percent damping and Poisson's ratio = 0.25.

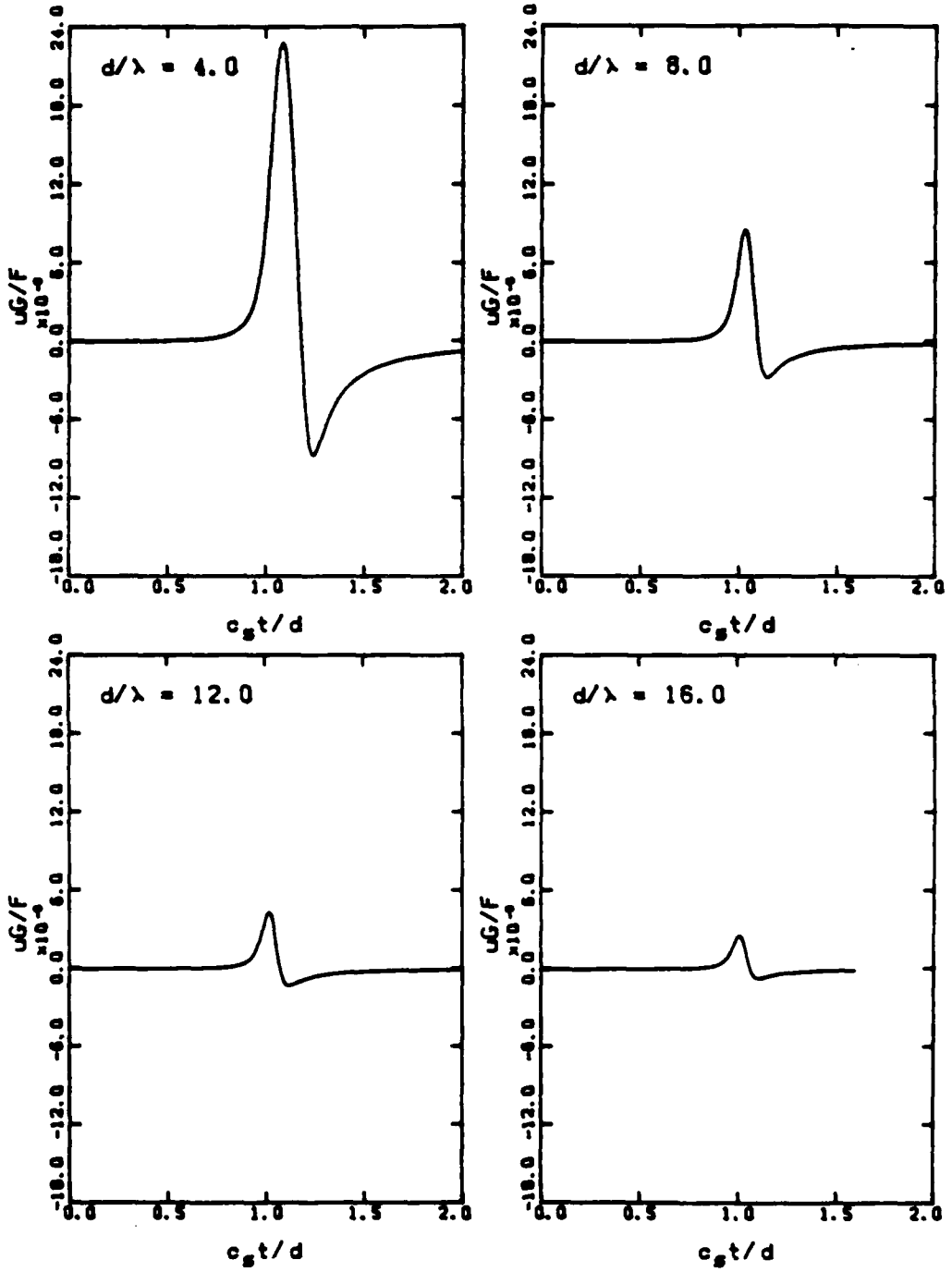

Fig. A.16 - Amplitude decay with distance (long distances) for antiplane shear motion in a medium with five percent damping and Poisson's ratio = 0.25.

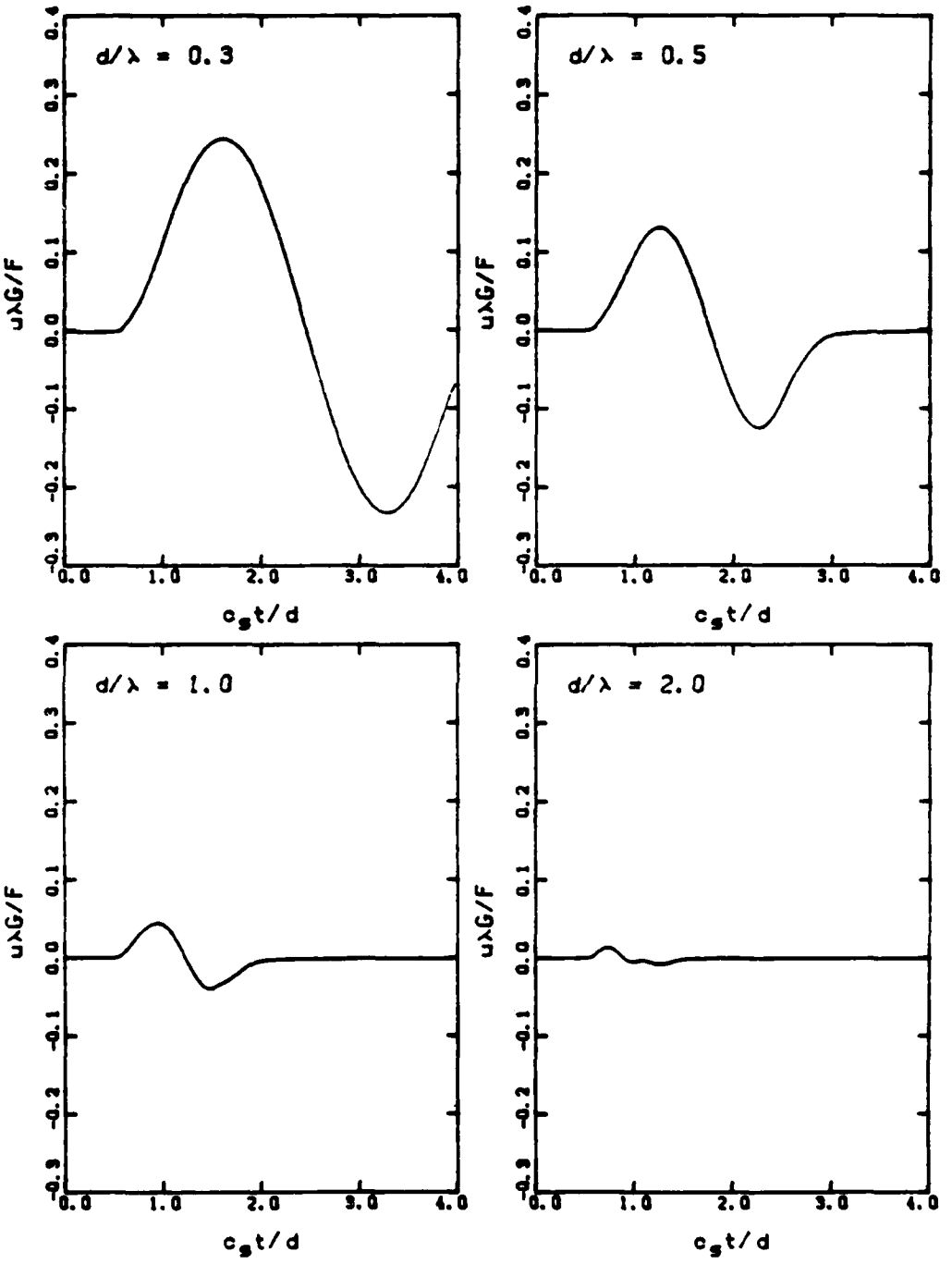

Fig. A.17 - Amplitude decay with distance (short distances) for three-dimensional longitudinal motion in a medium with five percent damping and Poisson's ratio = 0.25.

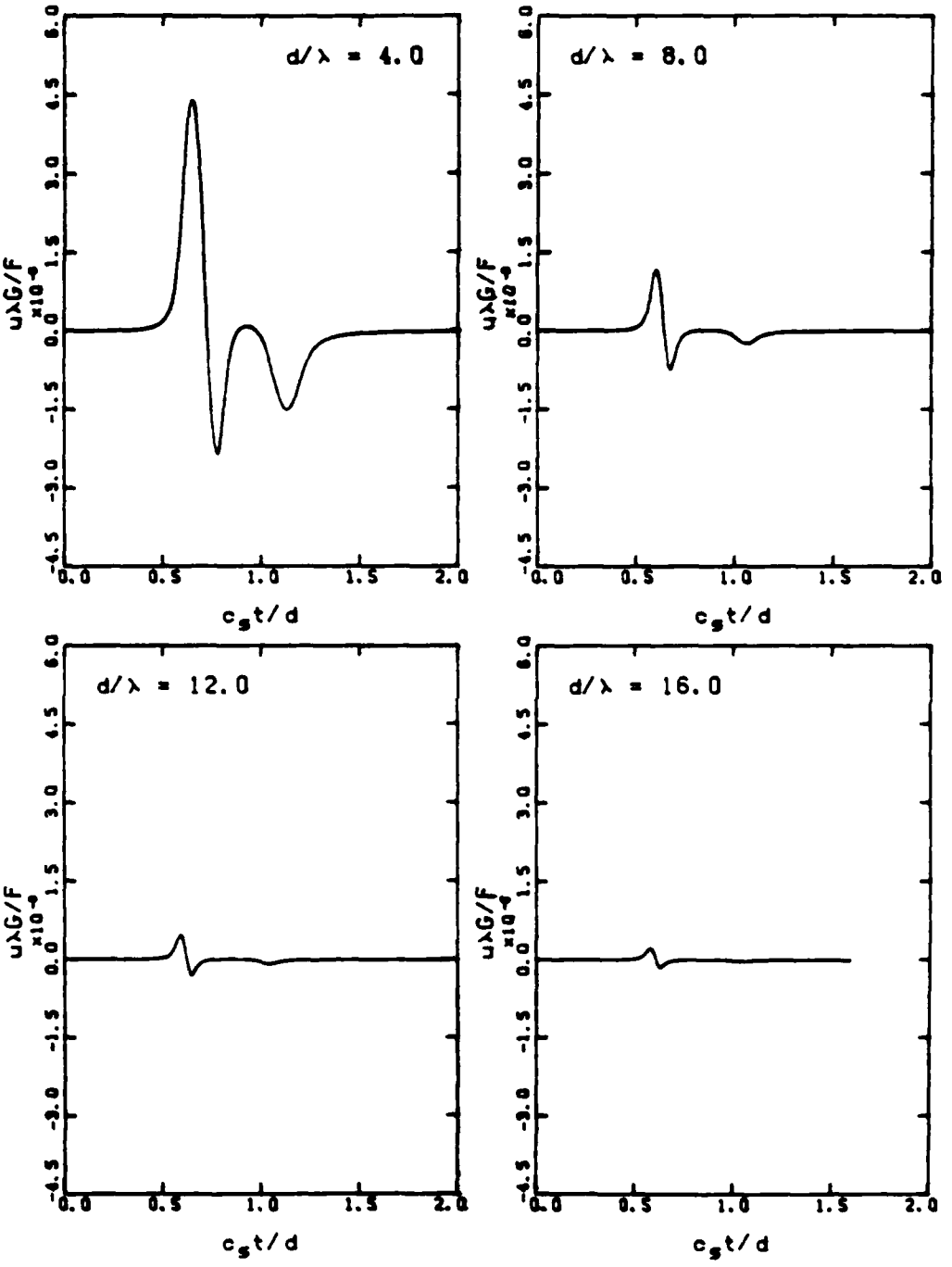

Fig. A.18 - Amplitude decay with distance (long distances) for three-dimensional longitudinal motion in a medium with five percent damping and Poisson's ratio = 0.25.

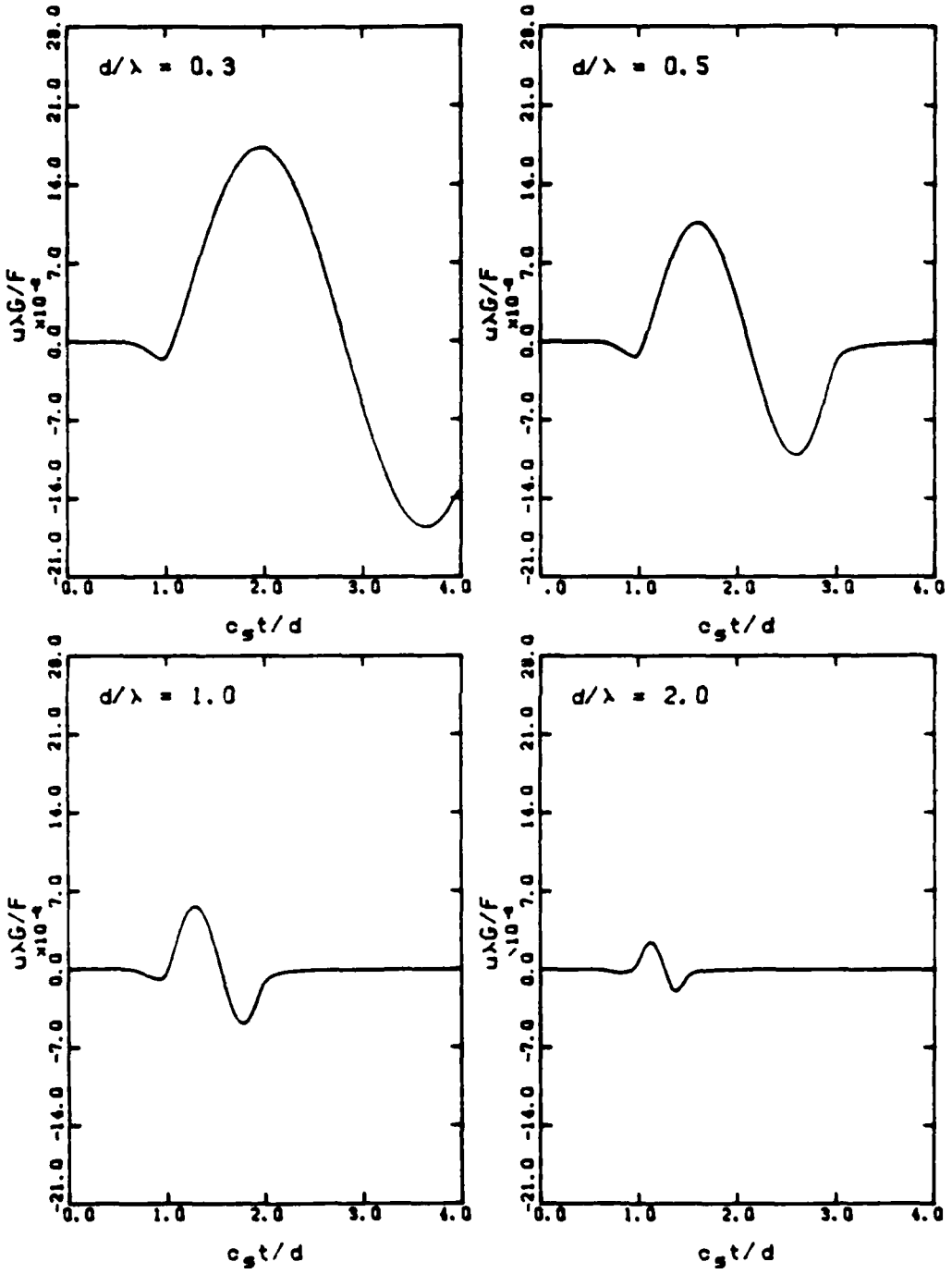

Fig. A.19 - Amplitude decay with distance (short distances) for three-dimensional shear motion in a medium with five percent damping and Poisson's ratio = 0.25.

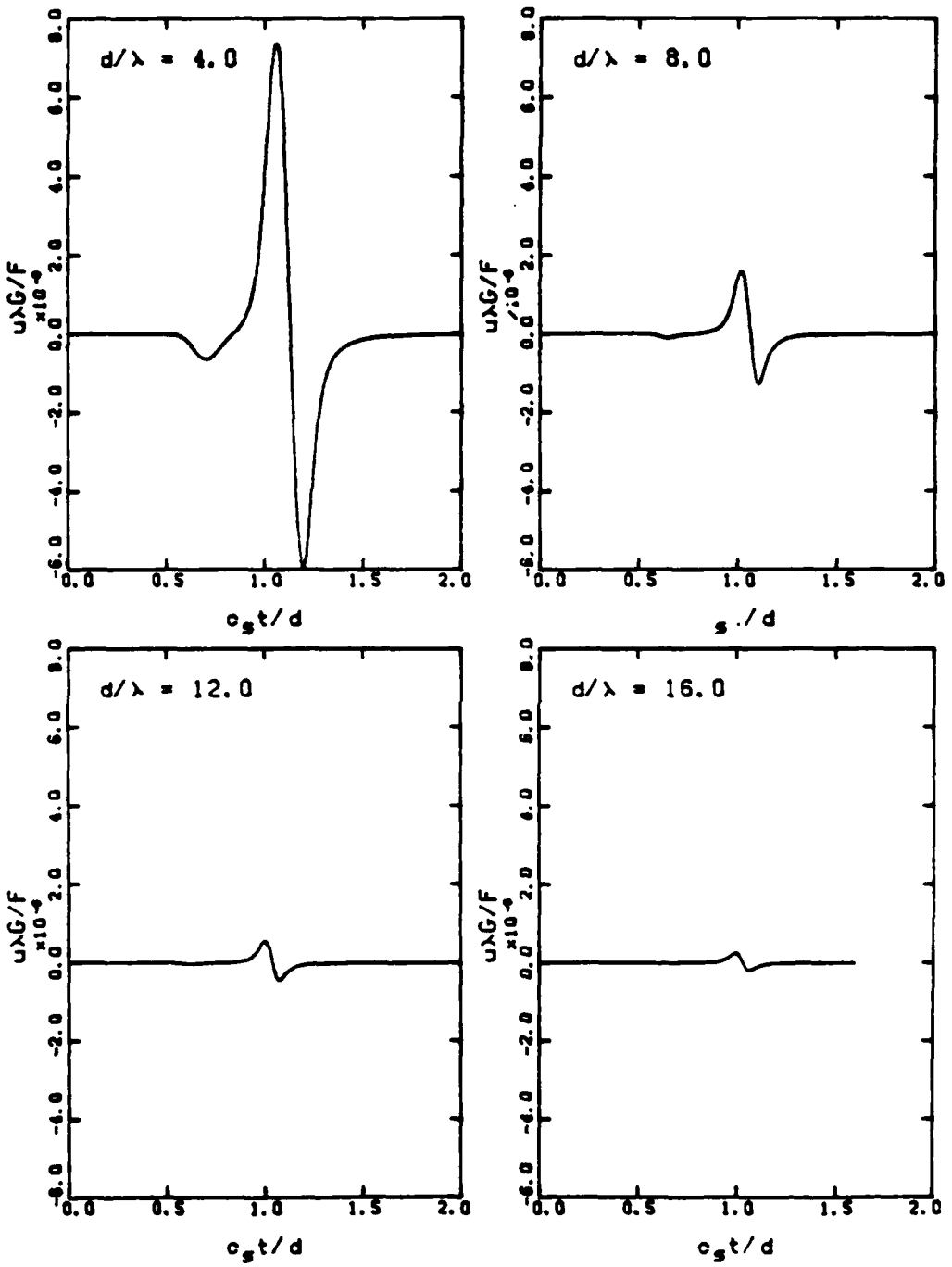

Fig. A.20 - Amplitude decay with distance (long distances) for three-dimensional shear motion in a medium with five percent damping and Poisson's ratio = 0.25.

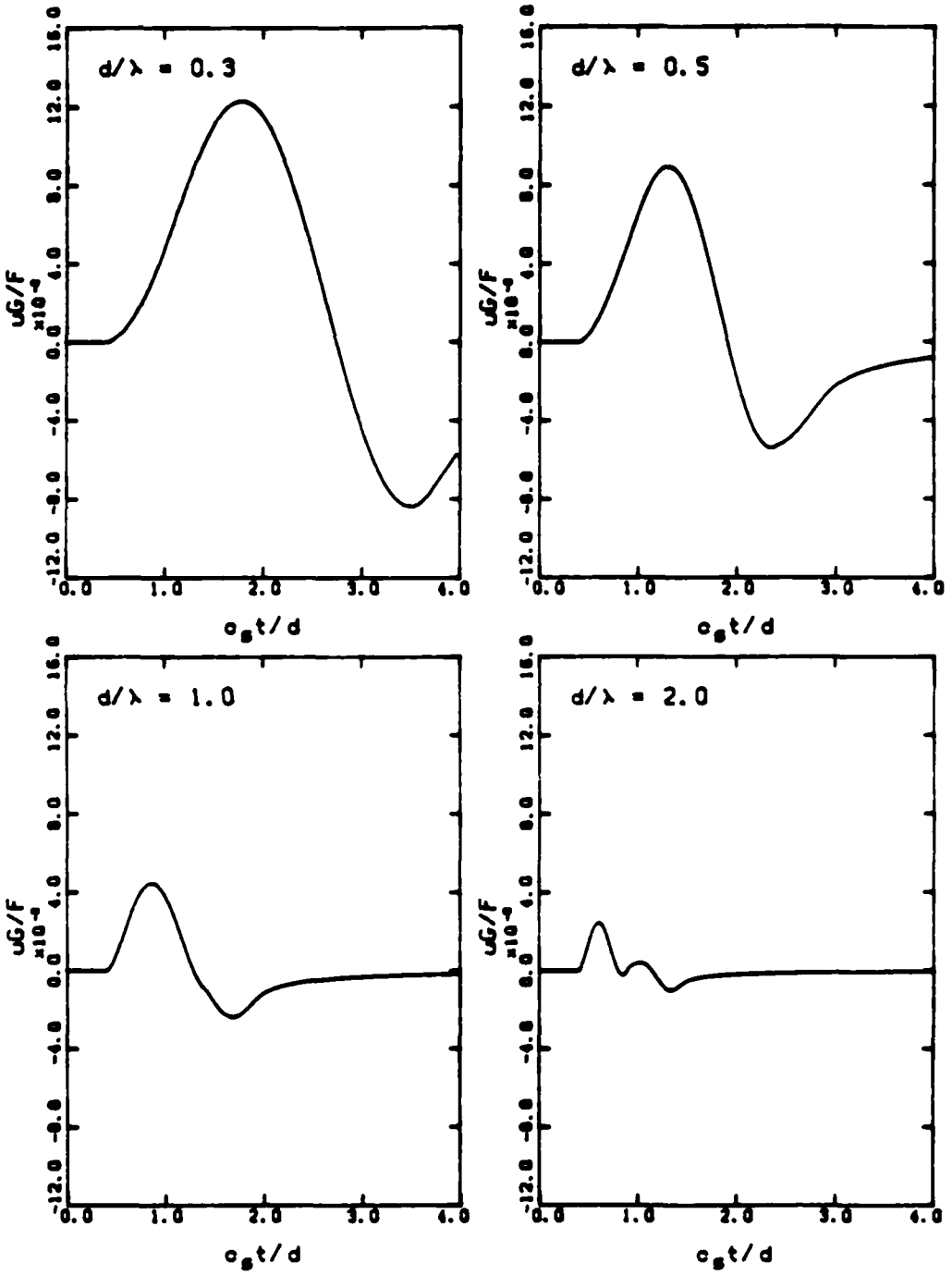

Fig. A.21 - Amplitude decay with distance (short distances) for two-dimensional longitudinal motion in a medium with no damping and Poisson's ratio = 0.4.

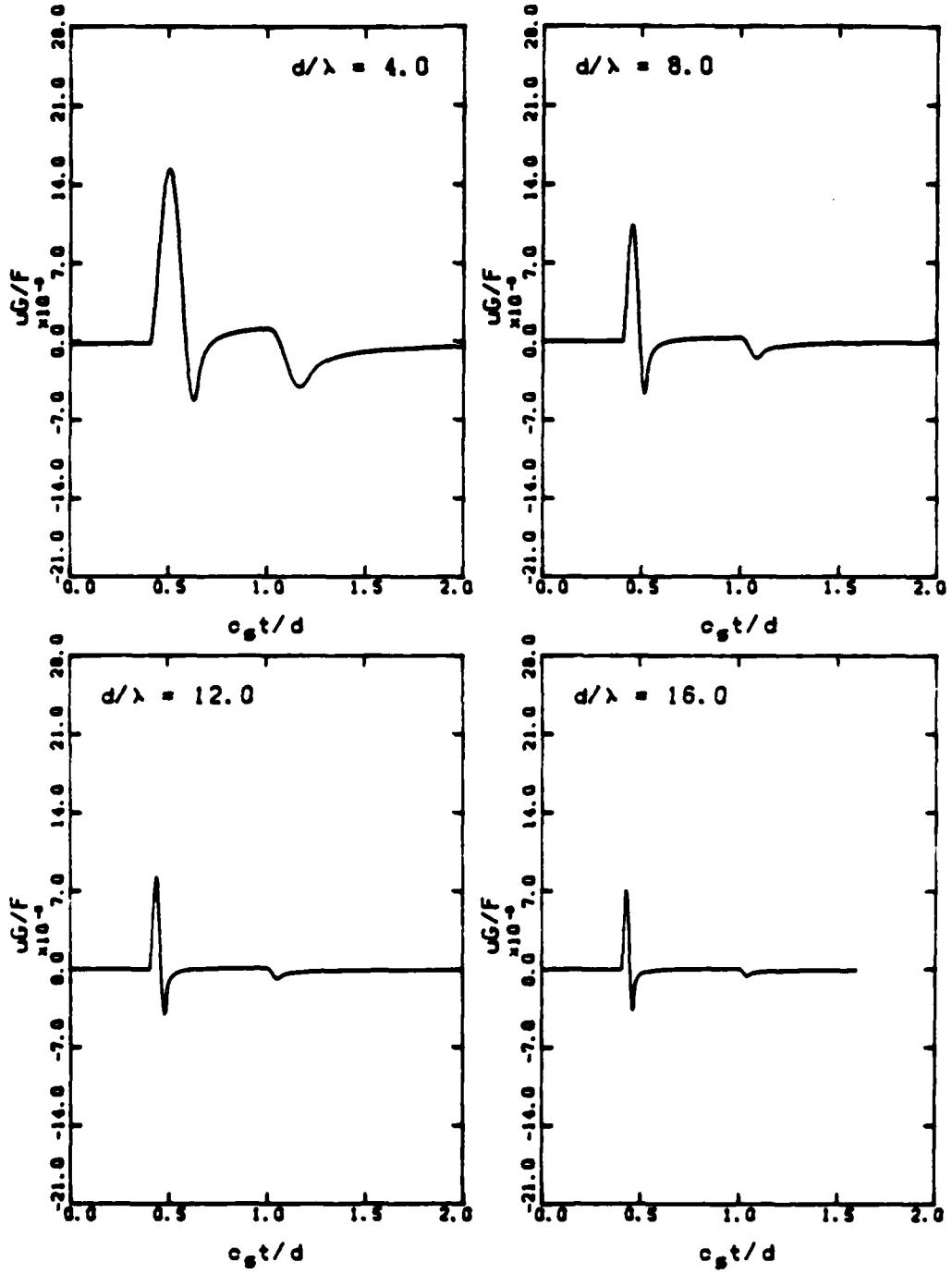

Fig. A.22 - Amplitude decay with distance (long distances) for two-dimensional longitudinal motion in a medium with no damping and Poisson's ratio = 0.4.

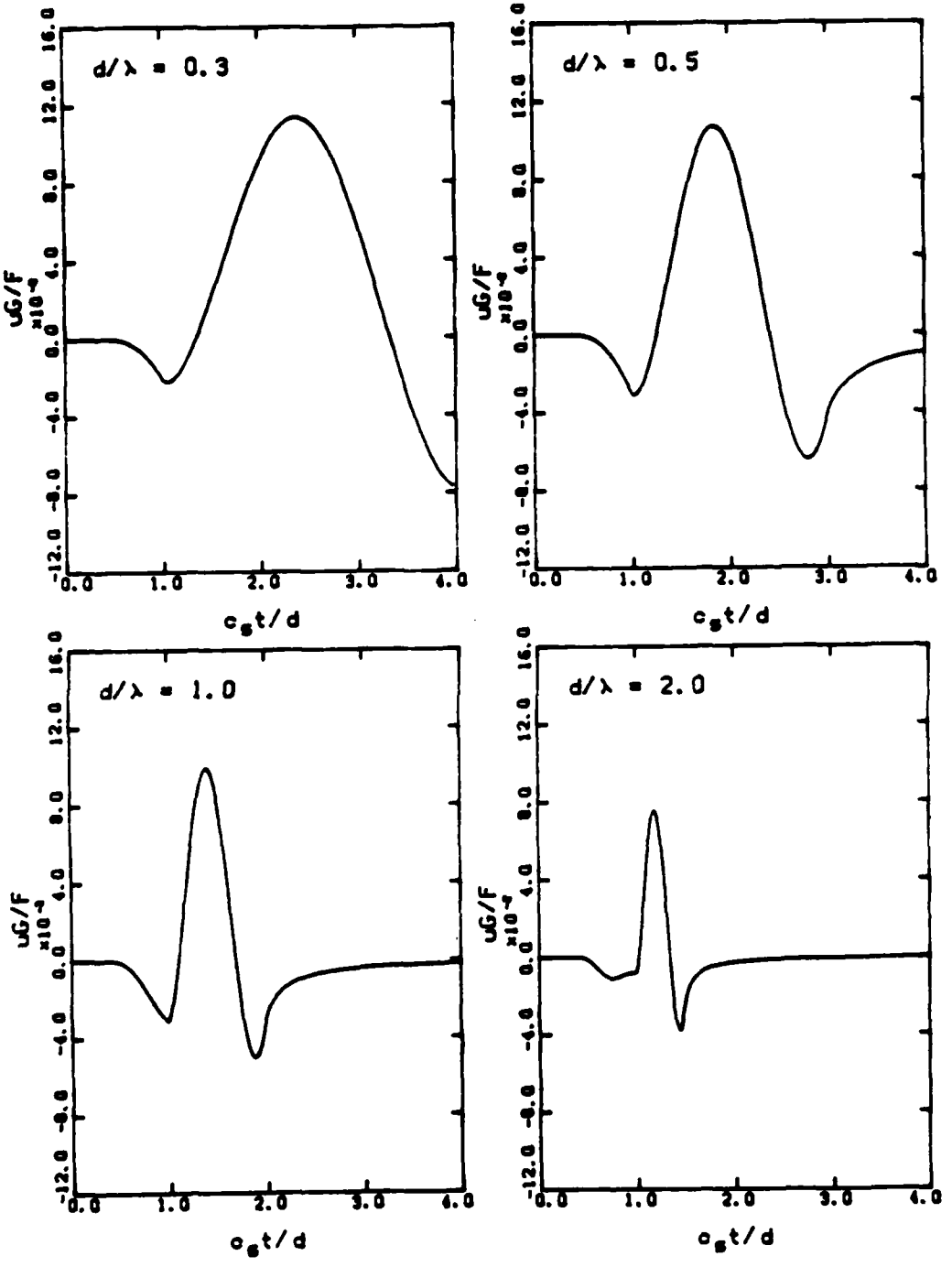

Fig. A.23 - Amplitude decay with distance (short distances) for in-plane shear motion in a medium with no damping and Poisson's ratio = 0.4.

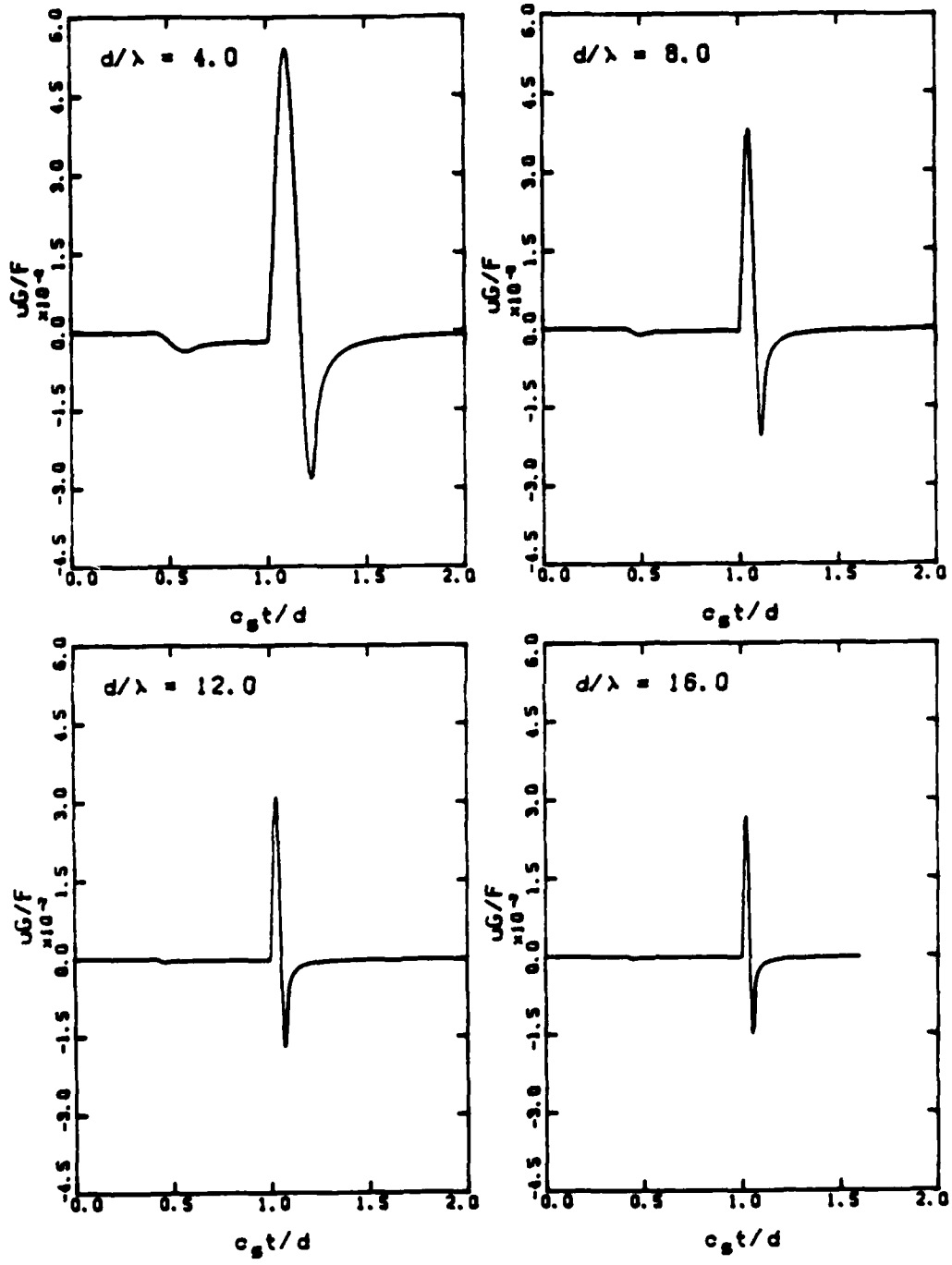

Fig. A.24 - Amplitude decay with distance (long distances) for in-plane shear motion in a medium with no damping and Poisson's ratio = 0.4.

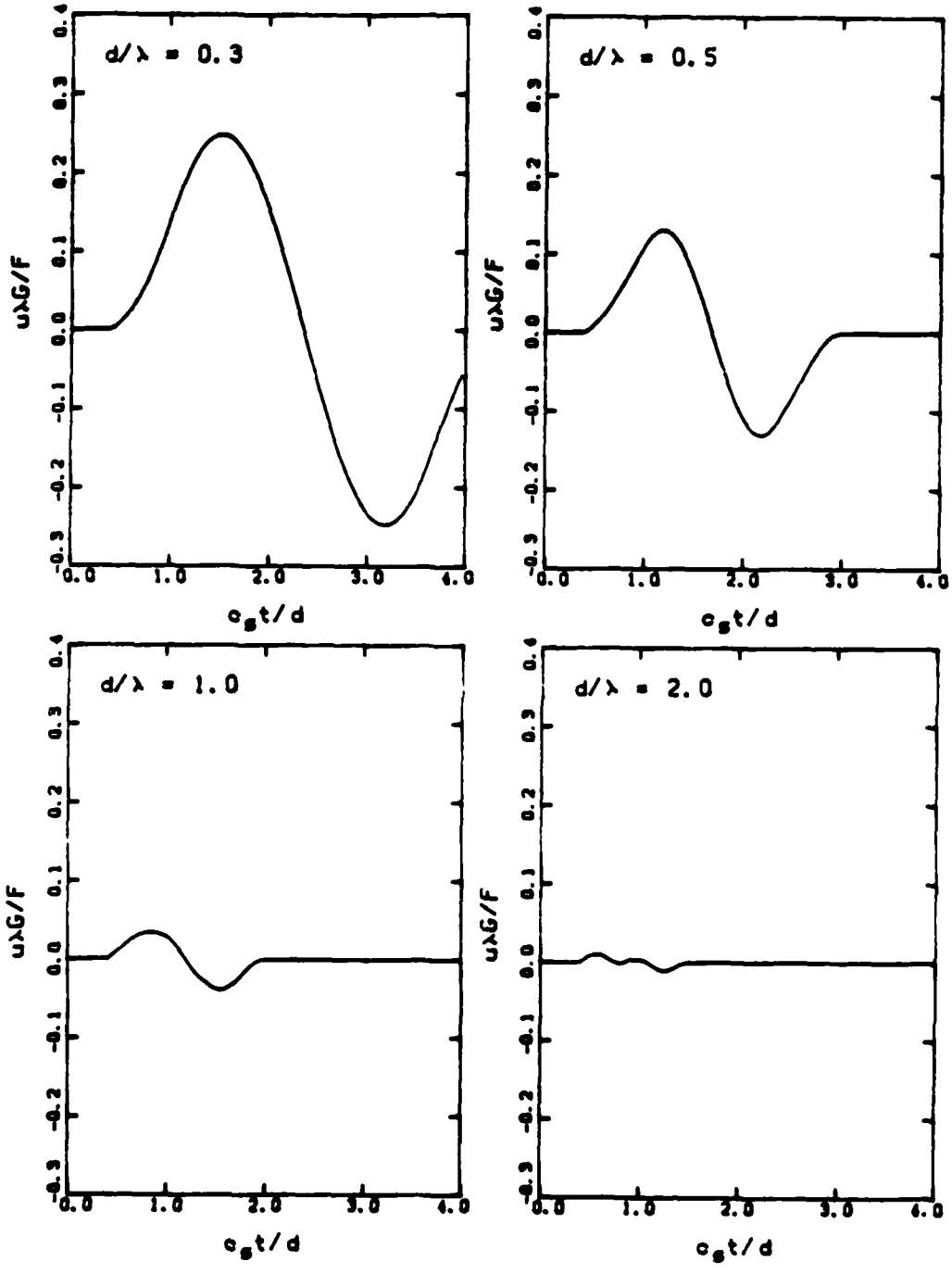

Fig. A.25 - Amplitude decay with distance (short distances) for three-dimensional longitudinal motion in a medium with no damping and Poisson's ratio = 0.4.

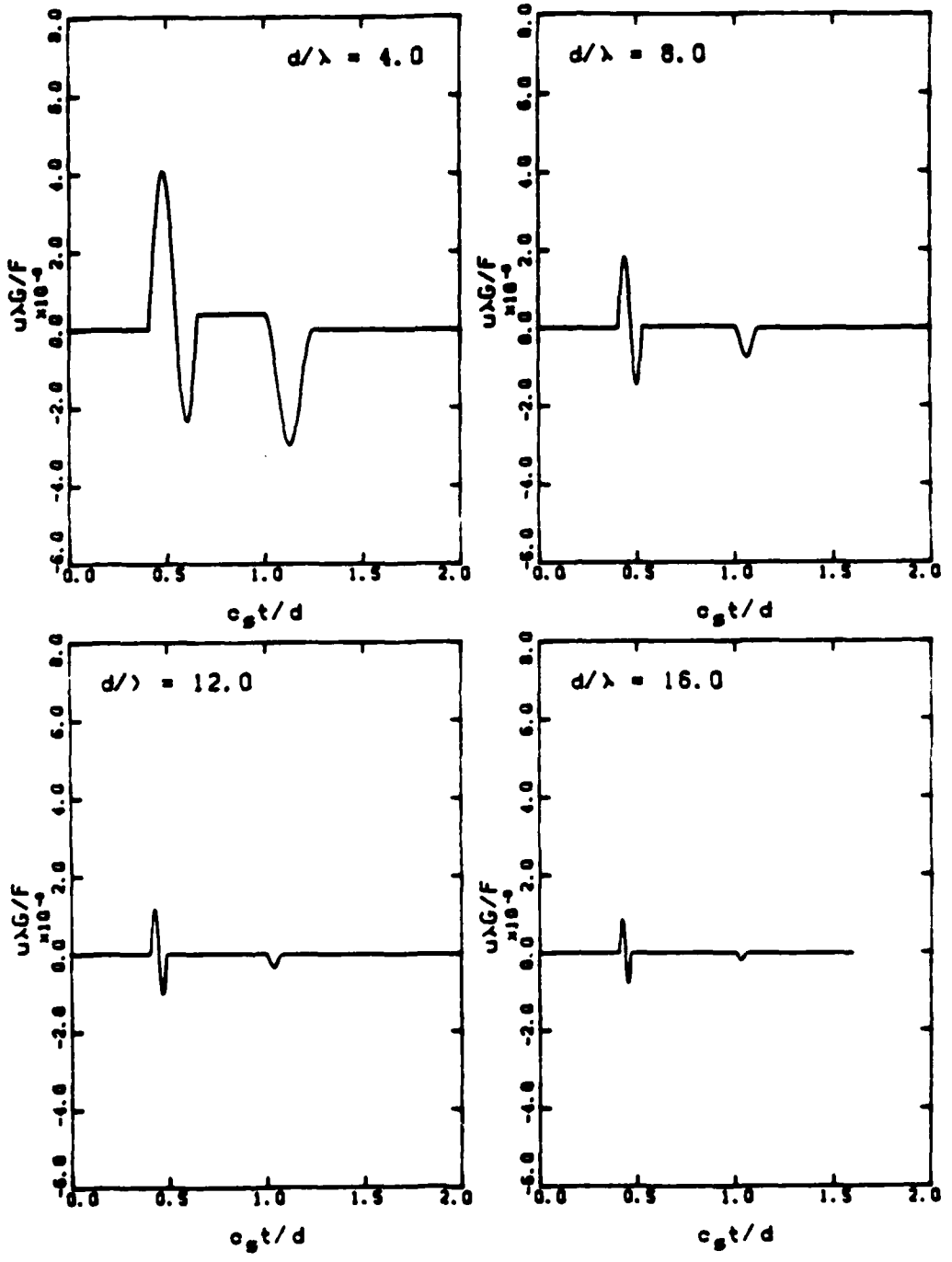

Fig. A.26 - Amplitude decay with distance (long distances) for three-dimensional longitudinal motion in a medium with no damping and Poisson's ratio = 0.4.

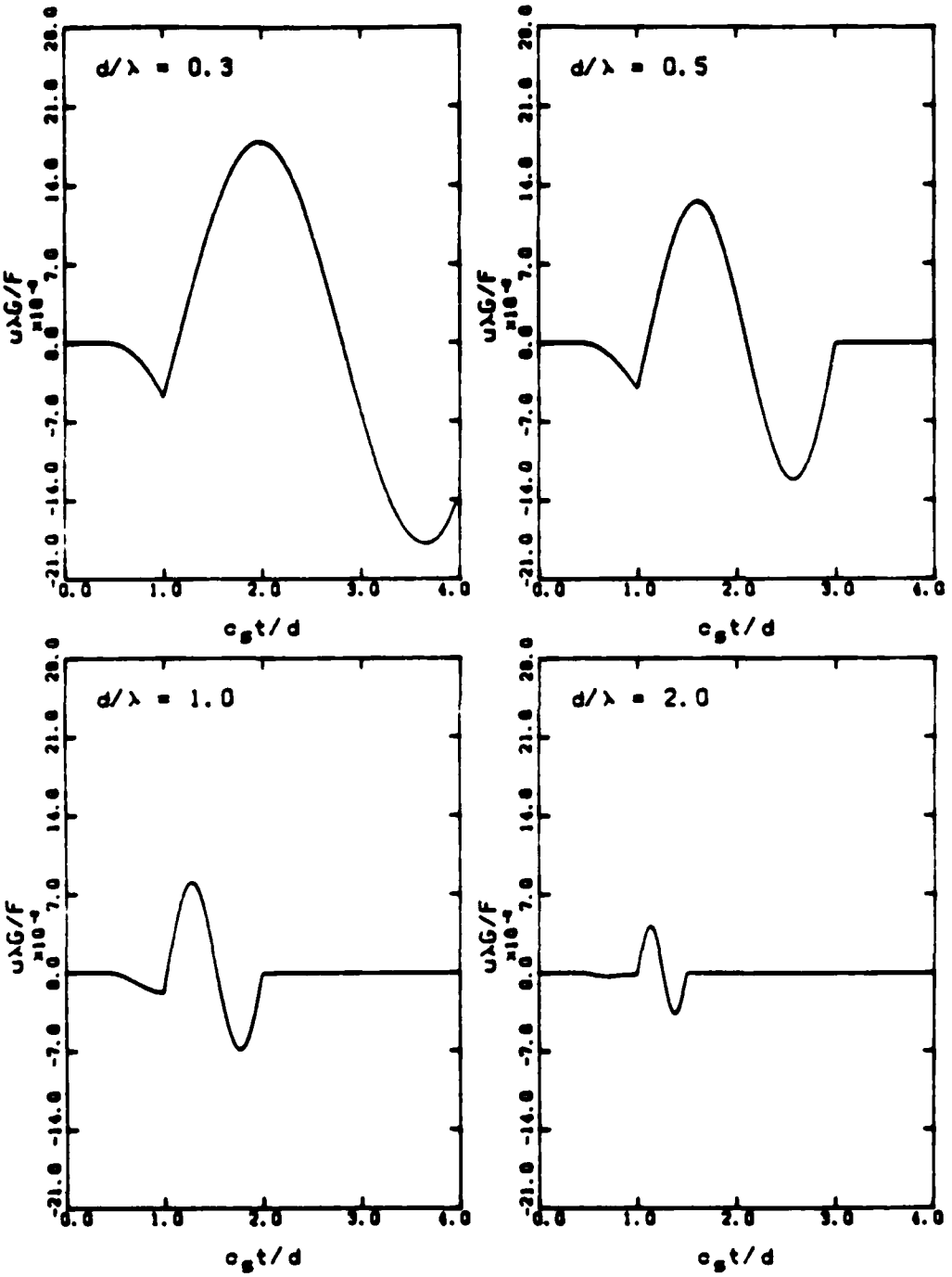

Fig. A.27 - Amplitude decay with distance (short distances) for three-dimensional shear motion in a medium with no damping and Poisson's ratio = 0.4.

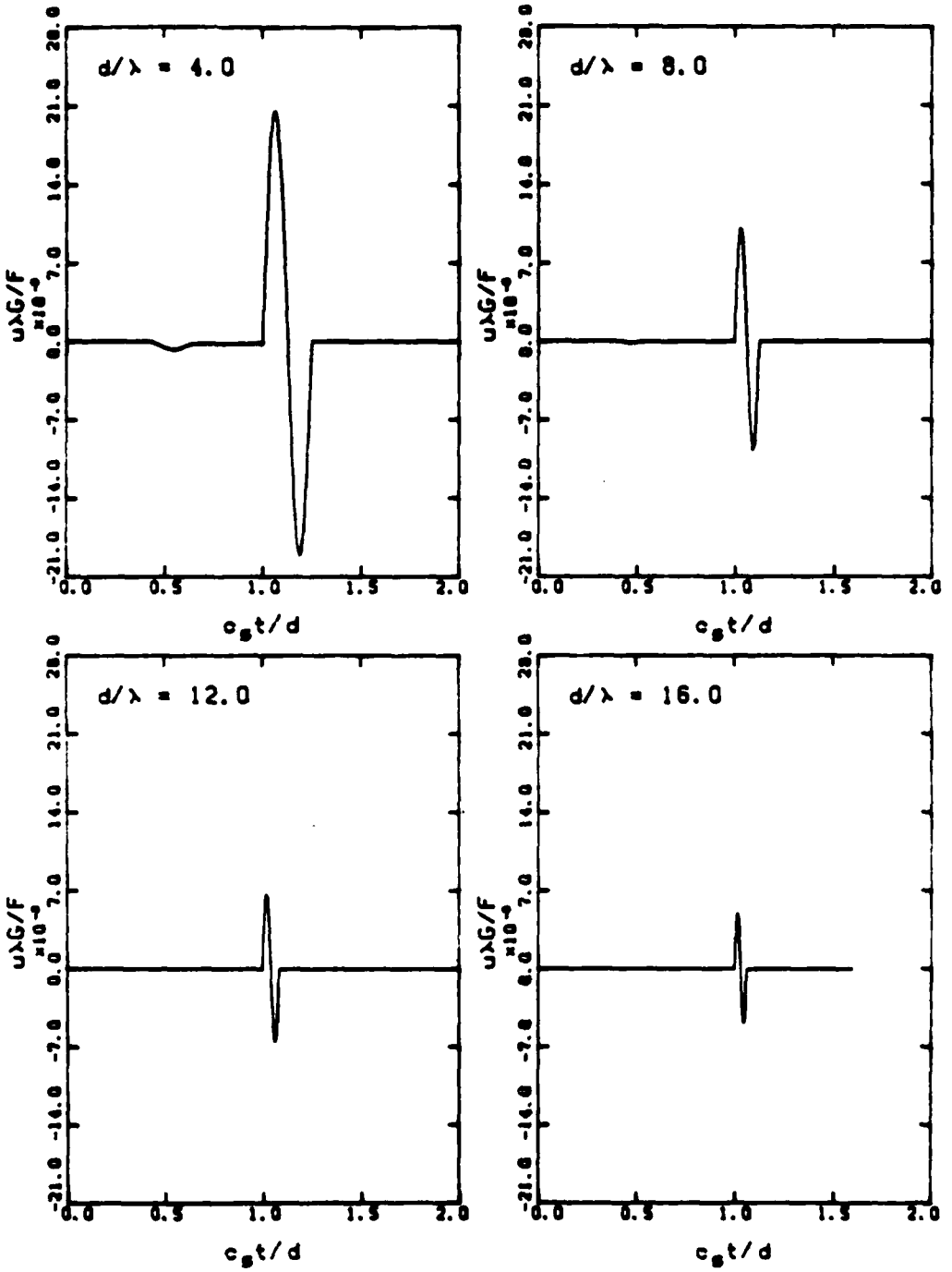

Fig. A.28 - Amplitude decay with distance (long distances) for three-dimensional shear motion in a medium with no damping and Poisson's ratio = 0.4.

APPENDIX B

RELATIONSHIP BETWEEN ELASTIC AND DAMPED BODY WAVE VELOCITIES AND MODULI

Material damping ratio is presented in Chapter Five as a convenient way to account for energy losses due to frictional forces. The definition of a frequency and strain independent damping ratio is given in Eq. 5.5. A convenient way to express material damping ratio, for small values of damping, is by the use of complex moduli. The damping ratio is then defined as one half of the ratio of the imaginary part of the complex modulus by its real part. For a material in which energy losses in shear are different than in compression-extension types of motion, it is preferable to define two damping ratios, one for shear and another for compression-extension. Therefore, the damping ratio in shear, D_S, is defined as

$$D_S = G_I/2G \tag{B.1}$$

and the damping ratio in compression, D_P, as

$$D_P = M_I/2M \tag{B.2}$$

where

G and G_I are the real and imaginary parts of the shear modulus, and

M and M_I are the real and imaginary parts of the constrained modulus.

In this way the complex shear modulus, G^*, and complex constrained modulus, M^*, are given by

$$G^* = G + iG_I = G(1 + 2iD_S) \tag{B.3}$$

and

$$M^* = M + iM_I = M(1 + 2iD_P) \tag{B.4}$$

If one uses shear and compressional wave velocities as the parameters to define the stiffness of the material, then the energy loses associated with material damping are more easily accounted for by using complex wave velocities. The counterparts to Eqs. B.3 and B.4, in terms of complex shear and compression wave velocities, (c_s^* and c_p^*, respectively) are

$$c_s^* = c_s + ic_{sI} = c_s(1 + iD_S) \tag{B.5}$$

and

$$c_p^* = c_p + ic_{pI} = c_p(1 + iD_P) \tag{B.6}$$

where

c_s and c_{sI} are the real and imaginary parts of the shear wave velocity, and

c_p and c_{pI} are the real and imaginary parts of the compressional wave velocity, respectively.

Equations B.5 and B.6 are good approximations of Eqs. B.3 and B.4 for small values of damping (as usually happens for the small strain amplitudes encountered in most seismic engineering applications). In other words one can define the complex shear modulus as

$$G^* = \rho c_s^{*2} = \rho c_s^2(1 + 2iD_s - D_S^2) \simeq$$

$$\simeq \rho c_s^2(1 + 2iD_S) =$$

$$\simeq G(1 + 2iD_S) \qquad (B.7)$$

which is a good approximation of Eq. B.3 for small values of the damping ratio, D_S. A parallel reasoning can be used for constrained modulus and compressional wave velocities.

It should be noted that these complex velocities do not represent propagation velocities but are approximate mathematical tools to account for energy dissipation. In this respect, consider a plane harmonic wave of the form

$$\exp[i\omega(t - x/c)] \qquad (B.8)$$

This wave propagates parallel to the x-axis of a non-dissipative medium with a propagation velocity represented by the variable c (the phase velocity). If the phase velocity is considered complex to account for energy losses, then the wave will be of the form

$$\exp[i\omega(t - x/c^*)] =$$

$$\exp\{i\omega[t - x/(c + ic_I)]\} =$$

$$\exp[-\omega c_I x/(c^2 + c_I{}^2)] \cdot \exp\{i\omega[t - cx/(c^2 + c_I{}^2)]\} \qquad (B.9)$$

Equation B.9 represents a plane wave that propagates along the x-axis with a velocity, c^D, the damped wave propagation velocity, which has a value of

$$c^D = (c^2 + c_I{}^2)/c \qquad (B.10)$$

and whose amplitude attenuates with distance with a coefficient of attenuation, α of

$$\alpha = \omega c_I/(c^2 + c_I{}^2) \qquad (B.11)$$

By expressing Eqs. B.10 and B.11 in terms of the damping ratio, the damped velocity of propagation is given by

$$c^D = c\cdot(1 + D^2) \qquad (B.12)$$

and the coefficient of attenuation is given by

$$\alpha = \omega\cdot D/[c(1 + D^2)] \simeq$$

$$\simeq \omega\cdot D/c = 2\pi D/L \qquad (B.13)$$

where L is the wavelength, ($L = 2\pi c/\omega$).

It can be observed from Eq. B.12 that a damped wave propagates at a velocity which is practically the same as that of

the undamped wave. For instance, if D = 5 % the damped wave velocity is only 0.25 percent higher than the undamped elastic velocity, and if D = 20 % (very high value) the damped velocity is still only 4 percent higher than the undamped elastic velocity.

APPENDIX C

CROSS-CORRELATION RECORDS

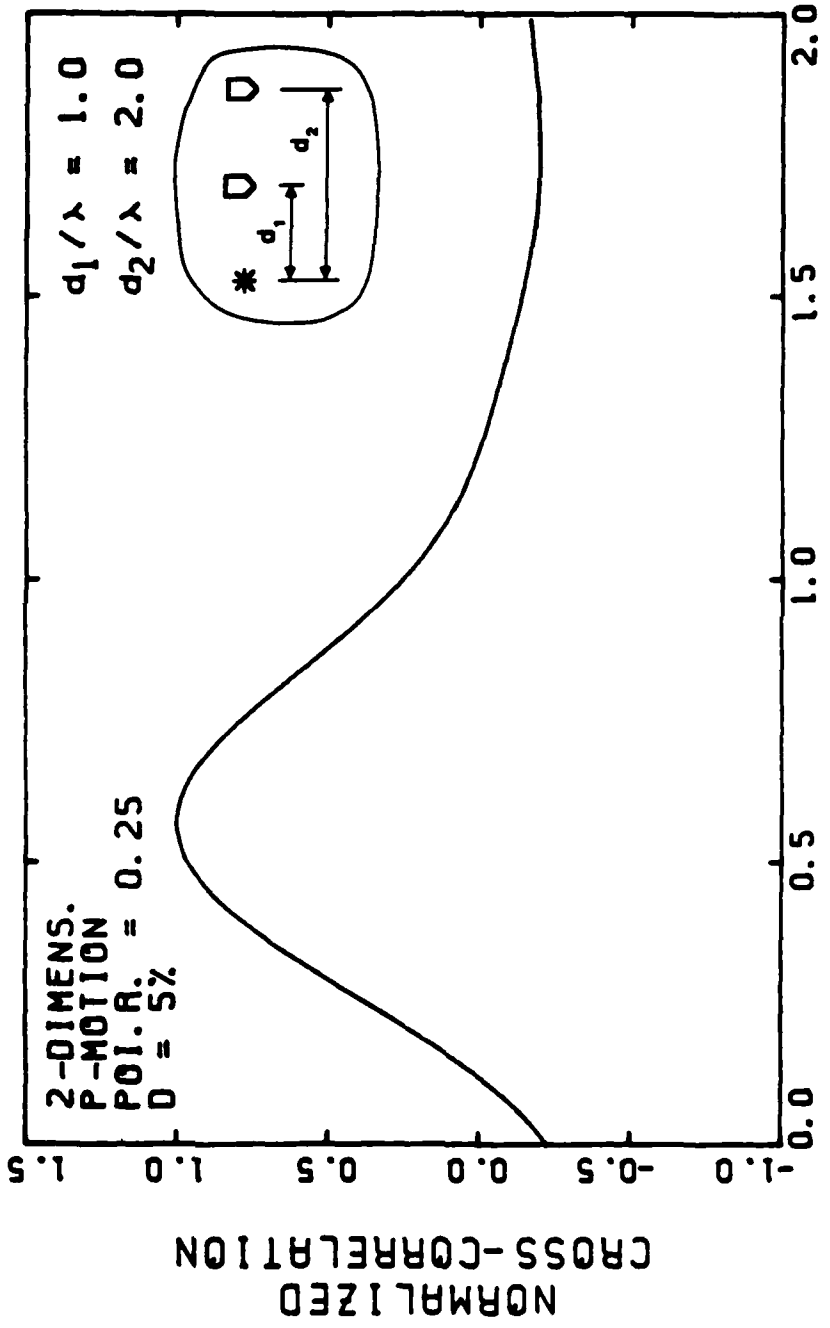

Fig. C.1 - Cross-correlation function of two-dimensional P-motion records obtained in the near field. Poisson's ratio = 0.25 and damping = 5 %.

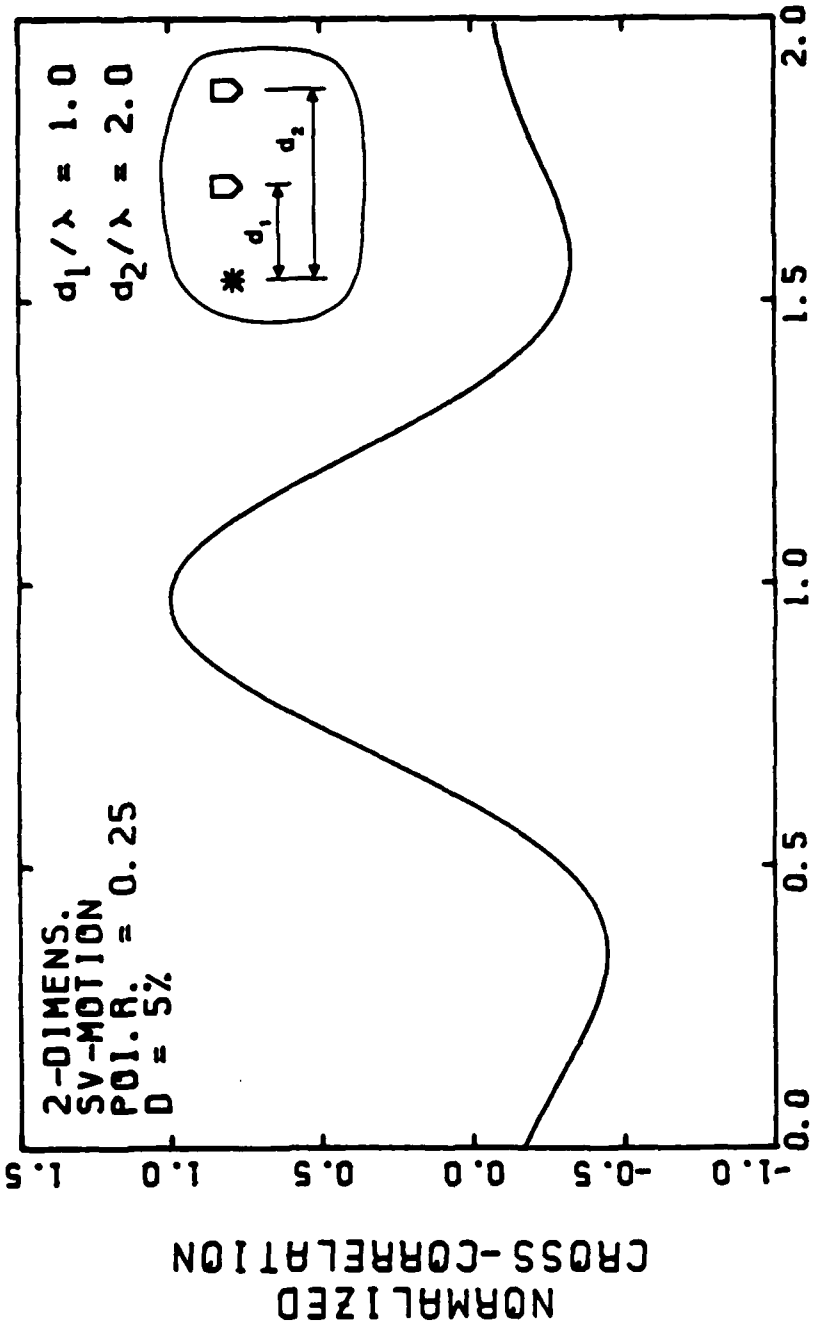

Fig. C.2 - Cross-correlation function of two-dimensional SV-motion records obtained in the near field. Poisson's ratio = 0.25 and damping = 5 %.

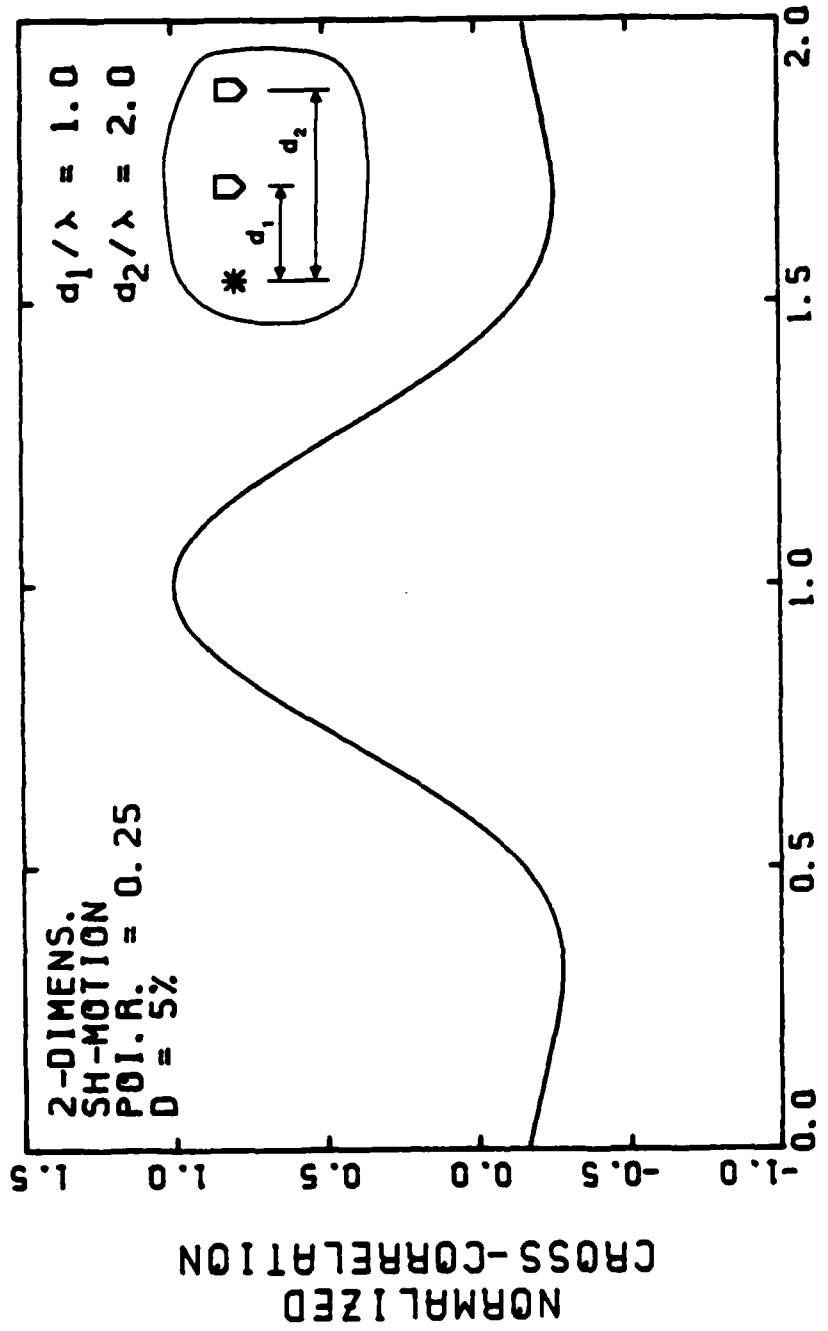

Fig. C.3 - Cross-correlation function of two-dimensional SH-motion records obtained in the near field. Poisson's ratio = 0.25 and damping = 5 %.

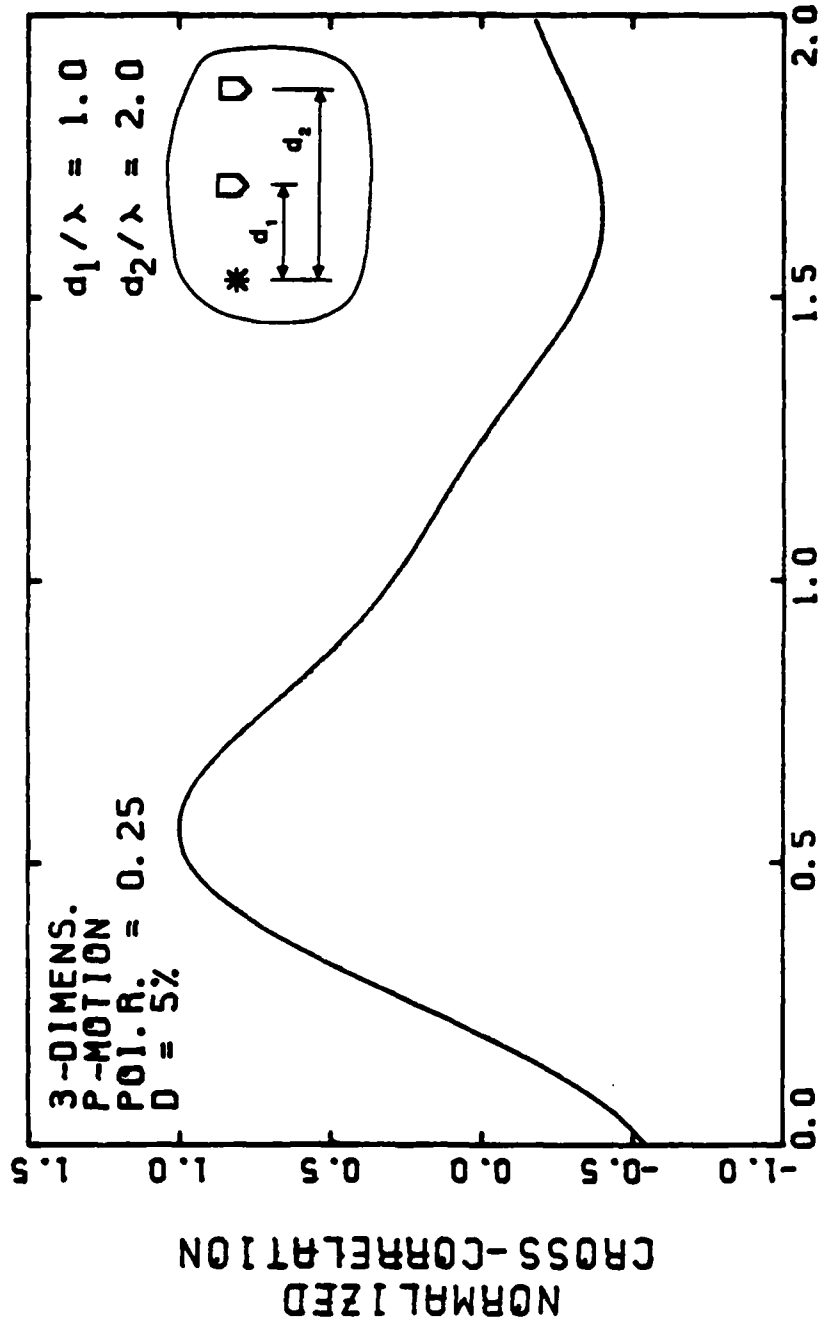

Fig. C.4 - Cross-correlation function of three-dimensional P-motion records obtained in the near field. Poisson's ratio = 0.25 and damping = 5 %.

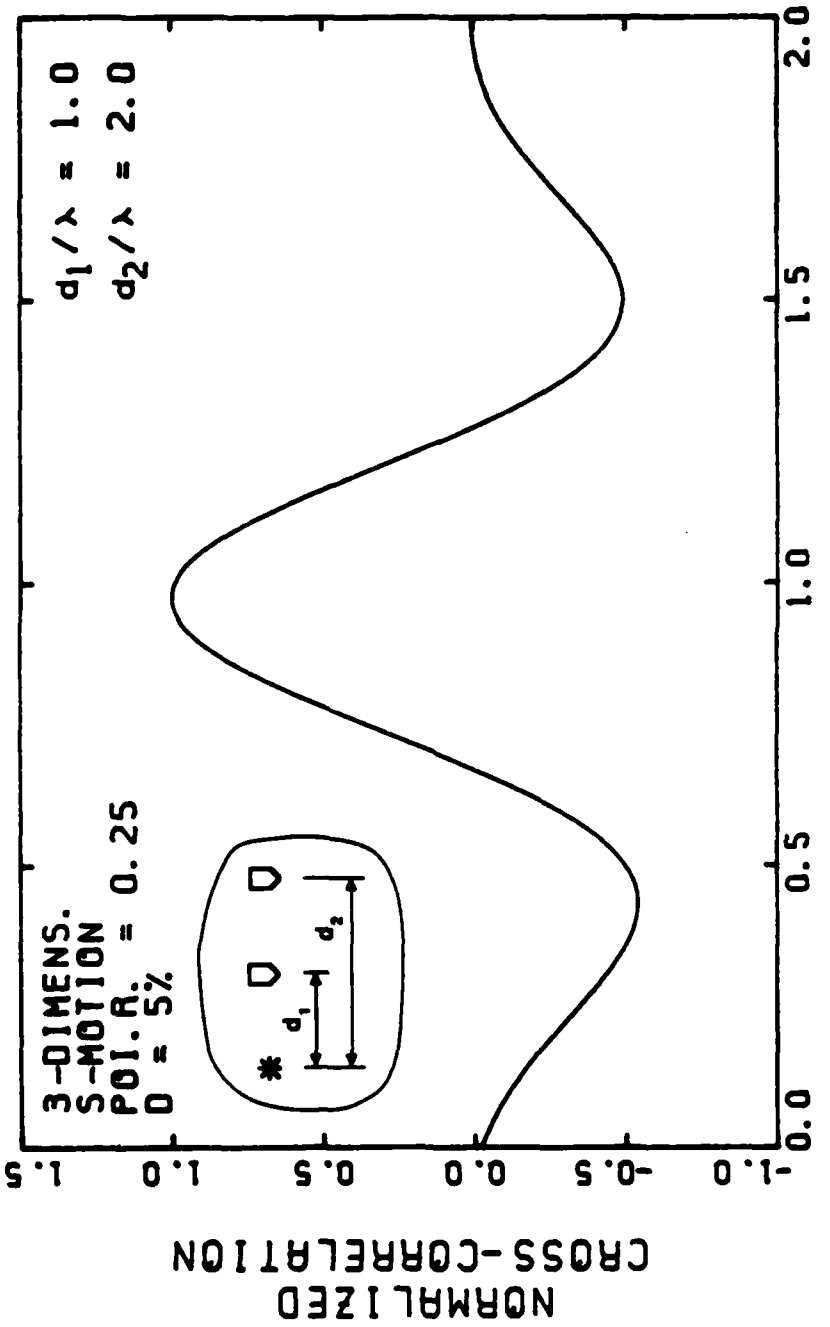

Fig. C.5 - Cross-correlation function of three-dimensional S-motion records obtained in the near field. Poisson's ratio = 0.25 and damping = 5 %.

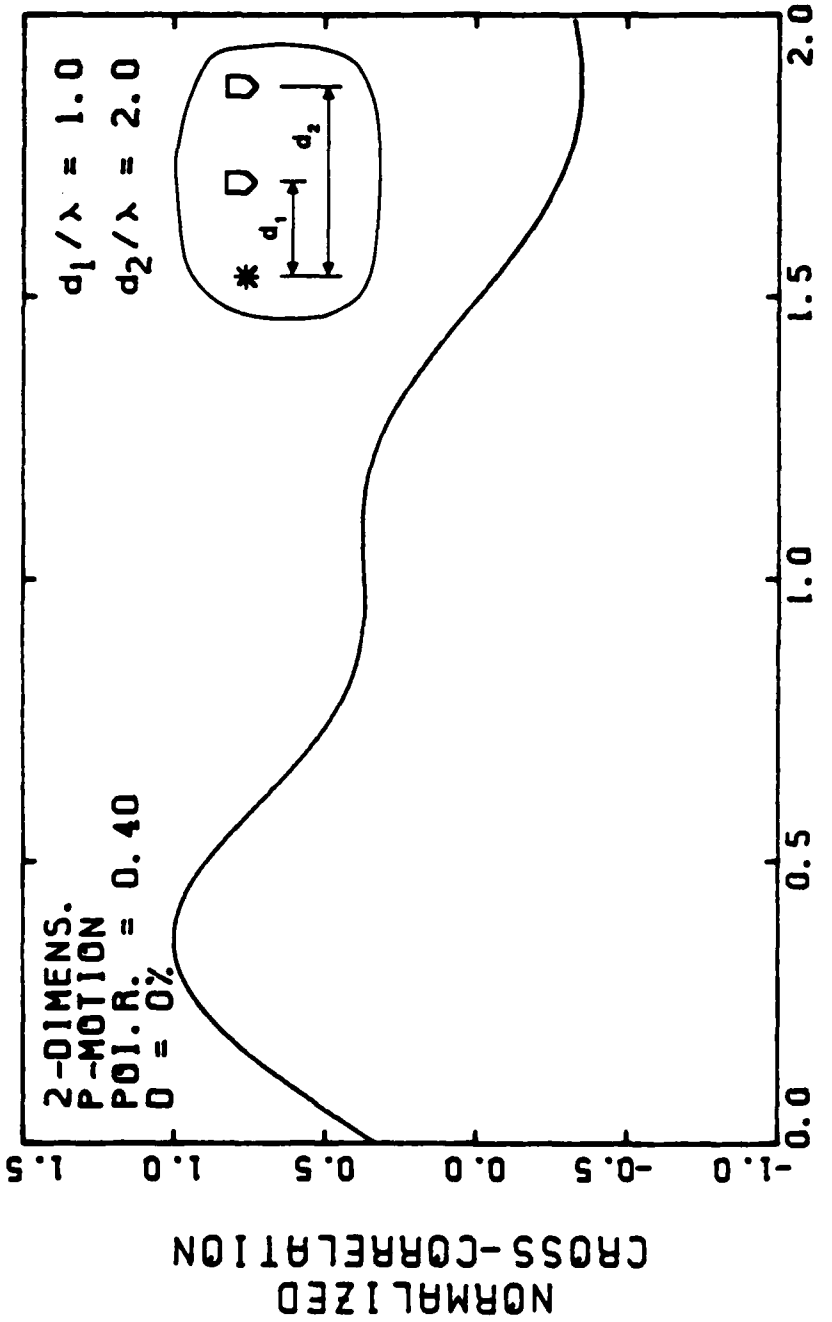

Fig. C.6 - Cross-correlation function of two-dimensional P-motion records obtained in the near field. Poisson's ratio = 0.4, Damping = 0 %.

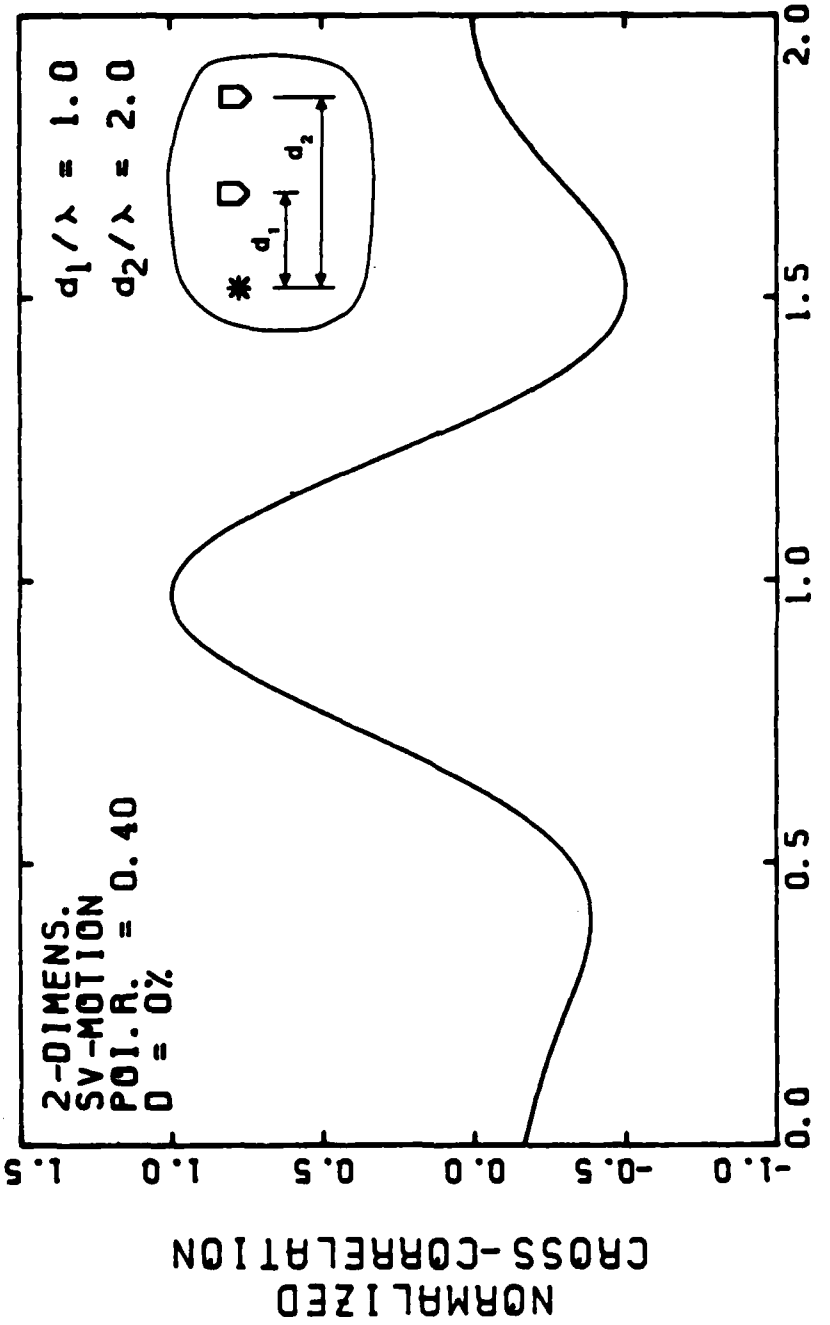

Fig. C.7 - Cross-correlation function of two-dimensional SV-motion records obtained in the near field. Poisson's ratio = 0.4, Damping = 0 %.

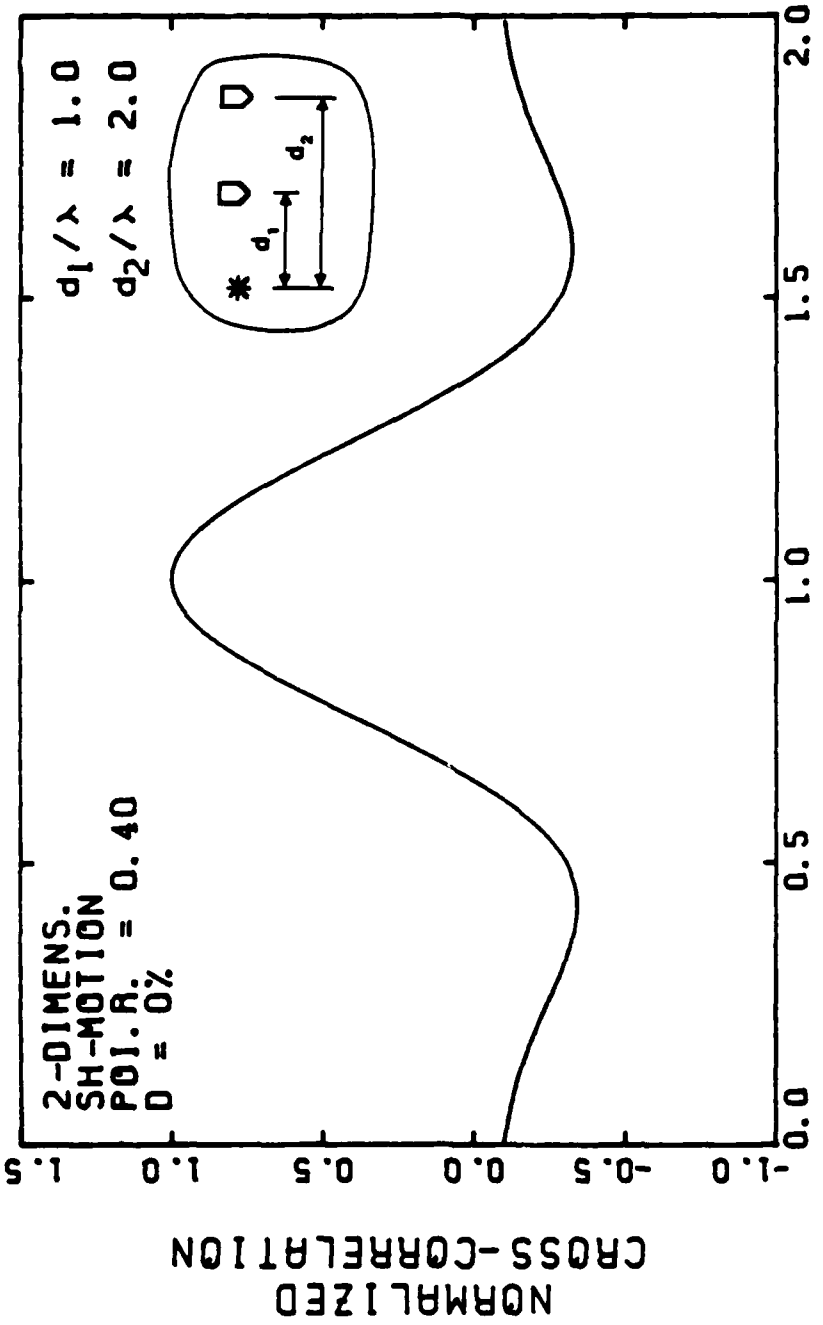

Fig. C.8 - Cross-correlation function of two-dimensional SH-motion records obtained in the near field. Poisson's ratio = 0.4, Damping = 0 %.

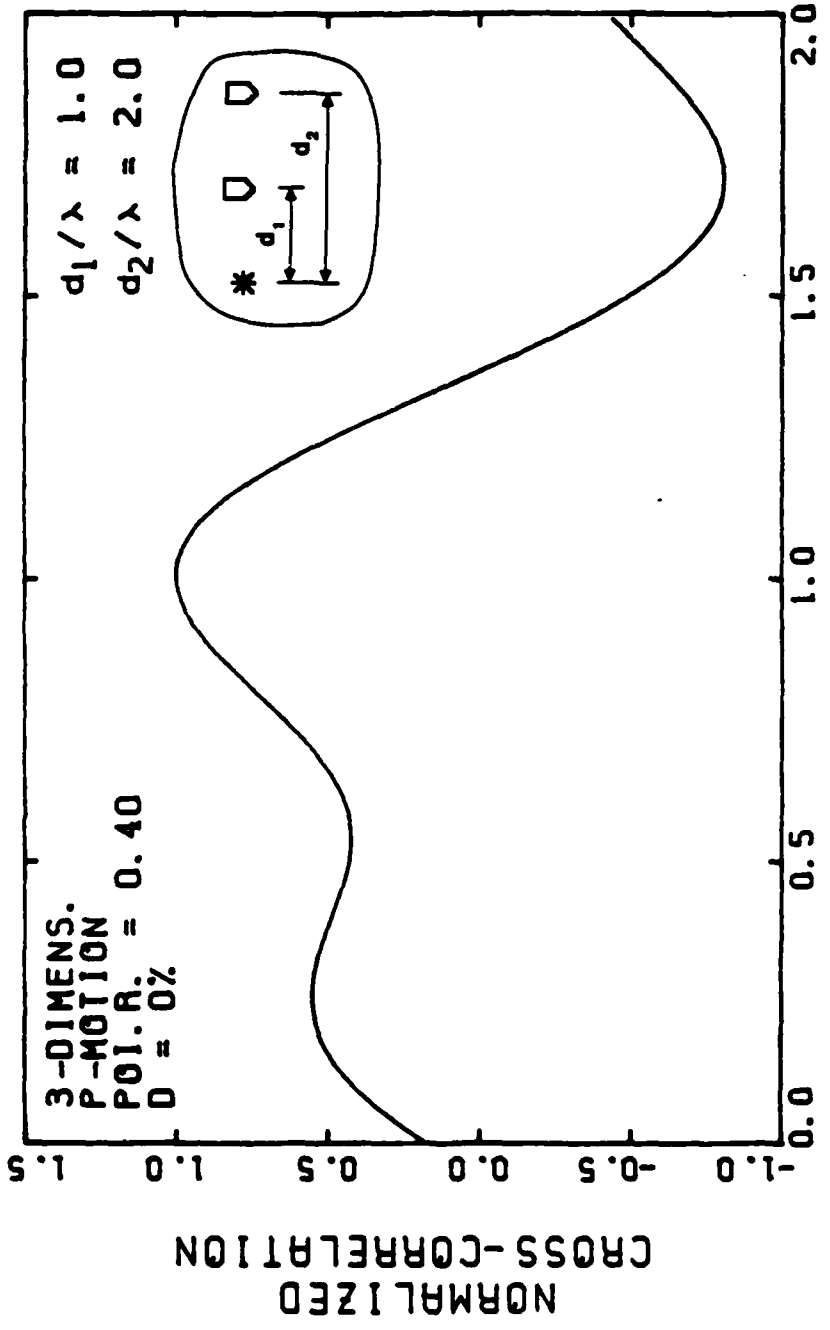

Fig. C.9 - Cross-correlation function of three-dimensional P-motion records obtained in the near field. Poisson's ratio = 0.4, Damping = 0 %.

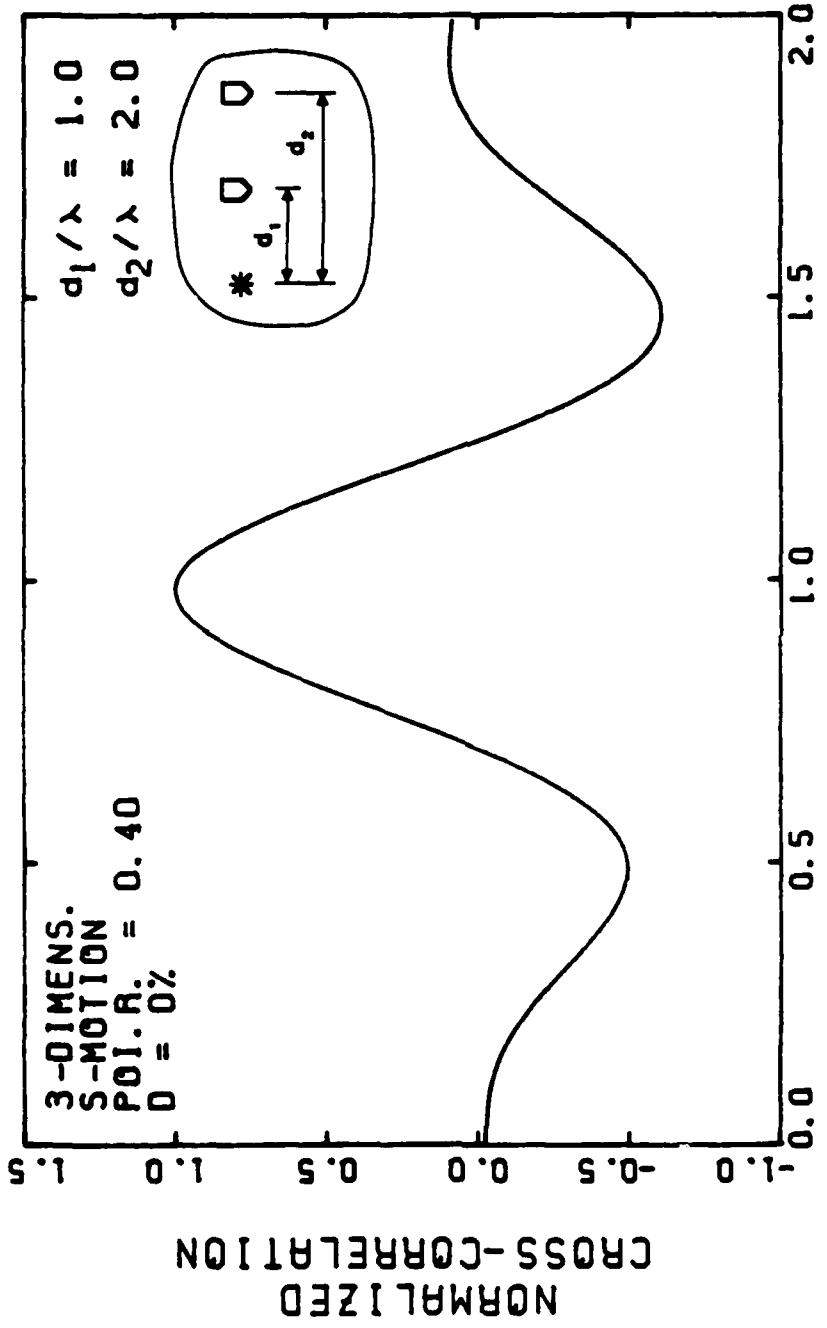

Fig. C.10 - Cross-correlation function of three-dimensional S-motion records obtained in the near field. Poisson's ratio = 0.4, Damping = 0 %.

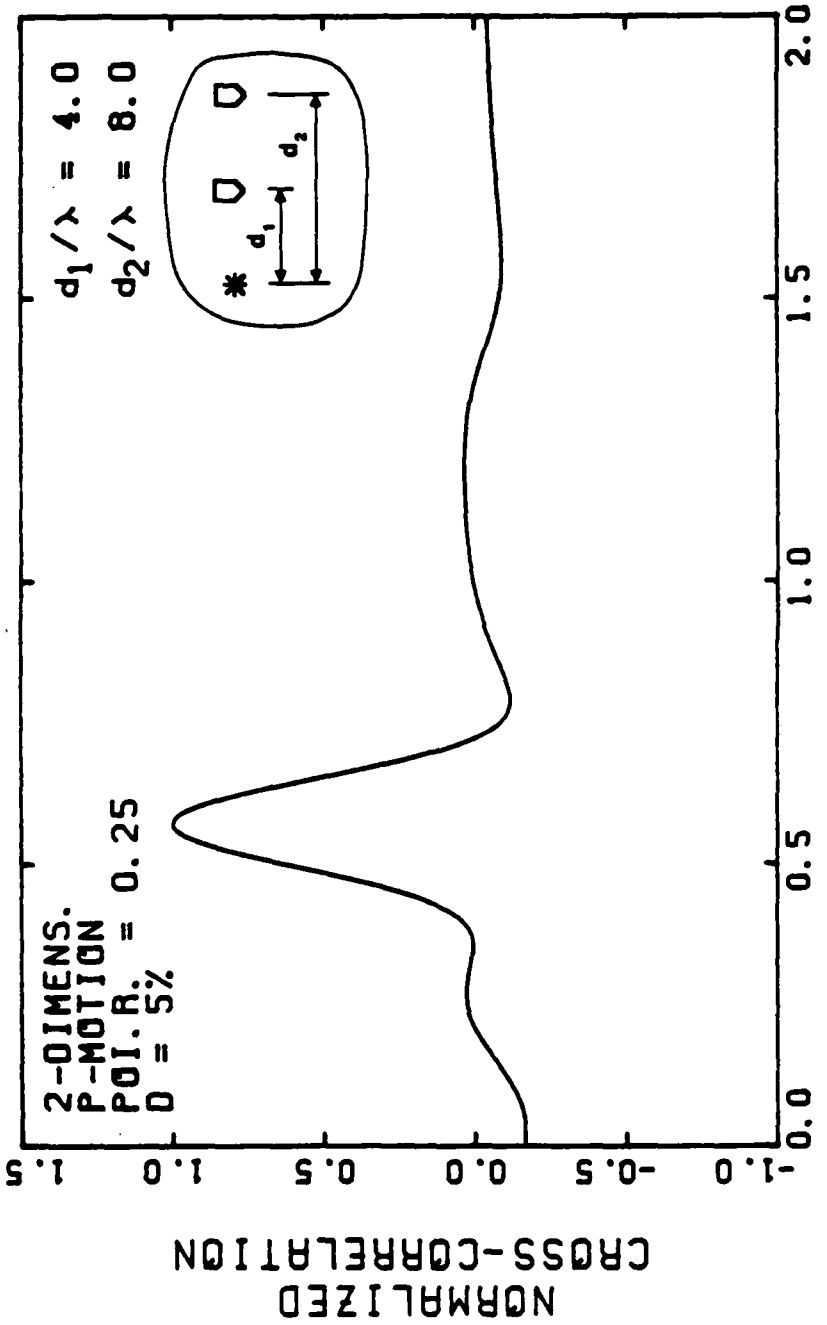

Fig. C.11 - Cross-correlation function of two-dimensional P-motion records obtained in the far field. Poisson's ratio = 0.25 and damping = 5 %.

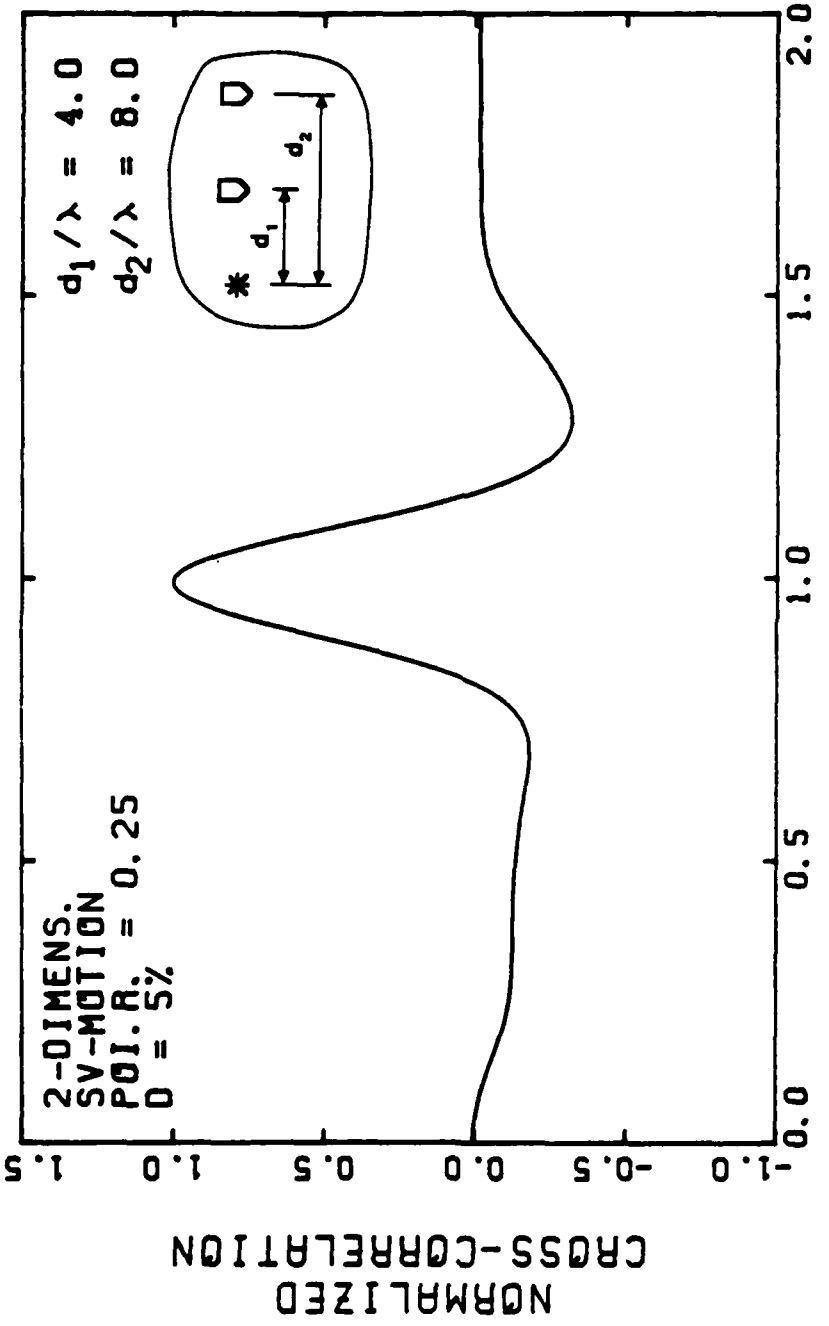

Fig. C.12 - Cross-correlation function of two-dimensional SV-motion records obtained in the far field. Poisson's ratio = 0.25 and damping = 5 %.

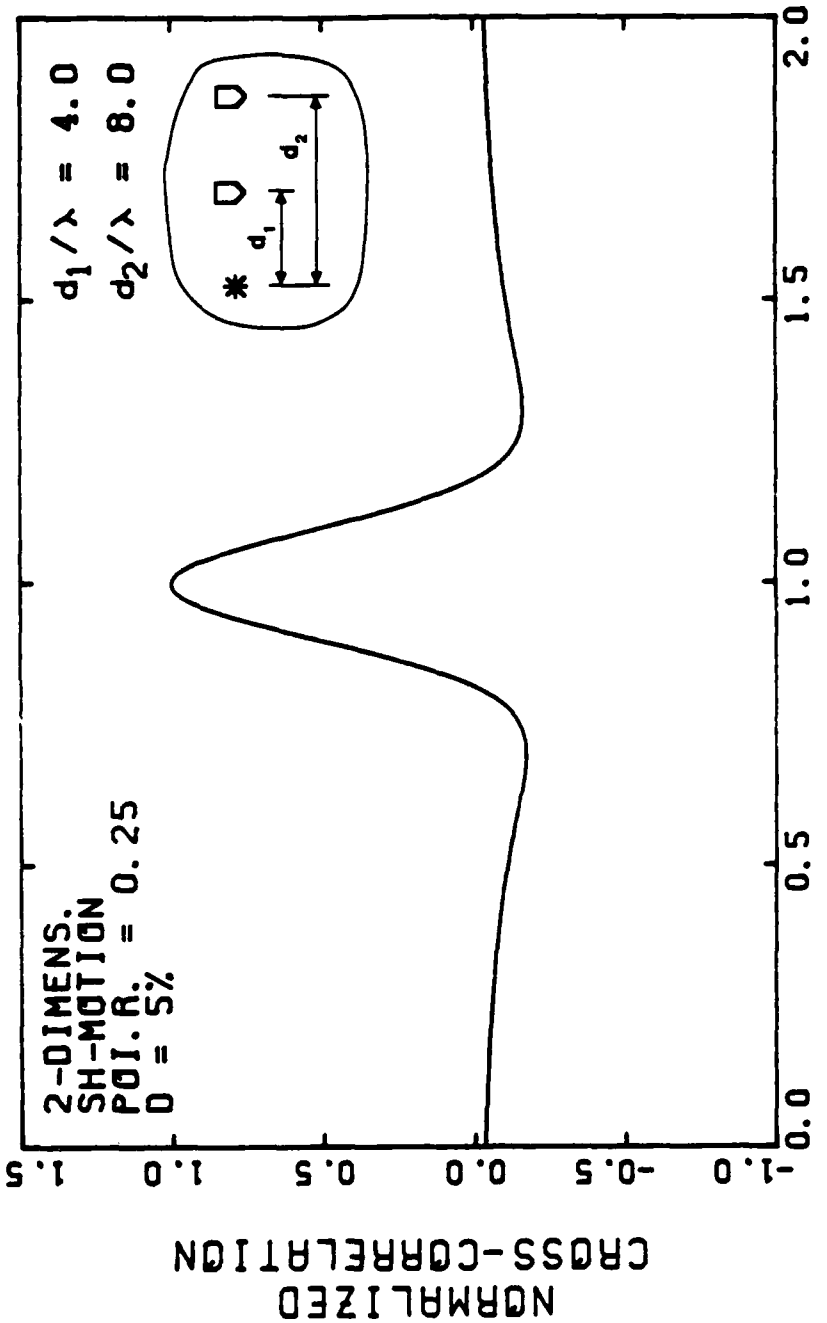

Fig. C.13 Cross-correlation function of two-dimensional SH-motion records obtained in the far field. Poisson's ratio = 0.25 and damping = 5 %.

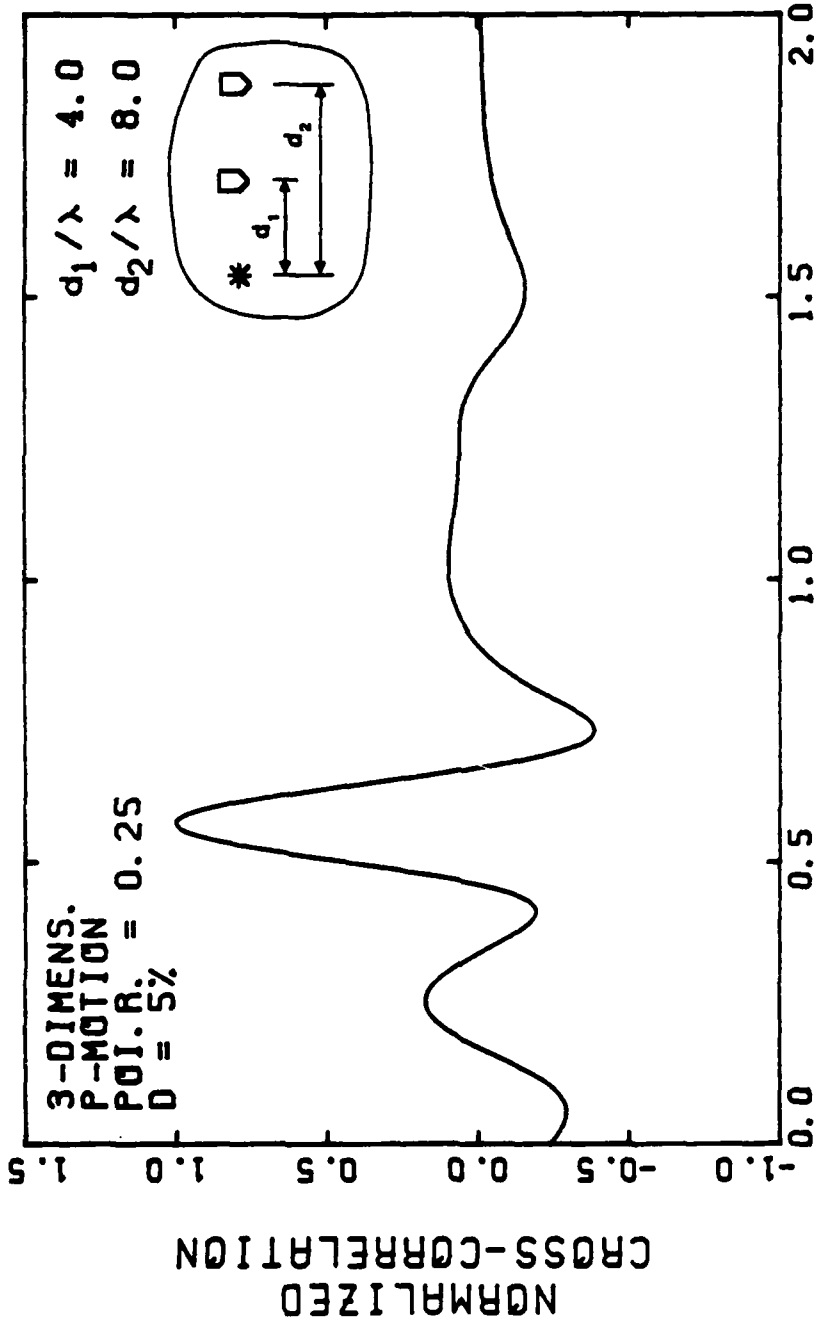

Fig. C.14 - Cross-correlation function of three-dimensional P-motion records obtained in the far field. Poisson's ratio = 0.25 and damping = 5 %.

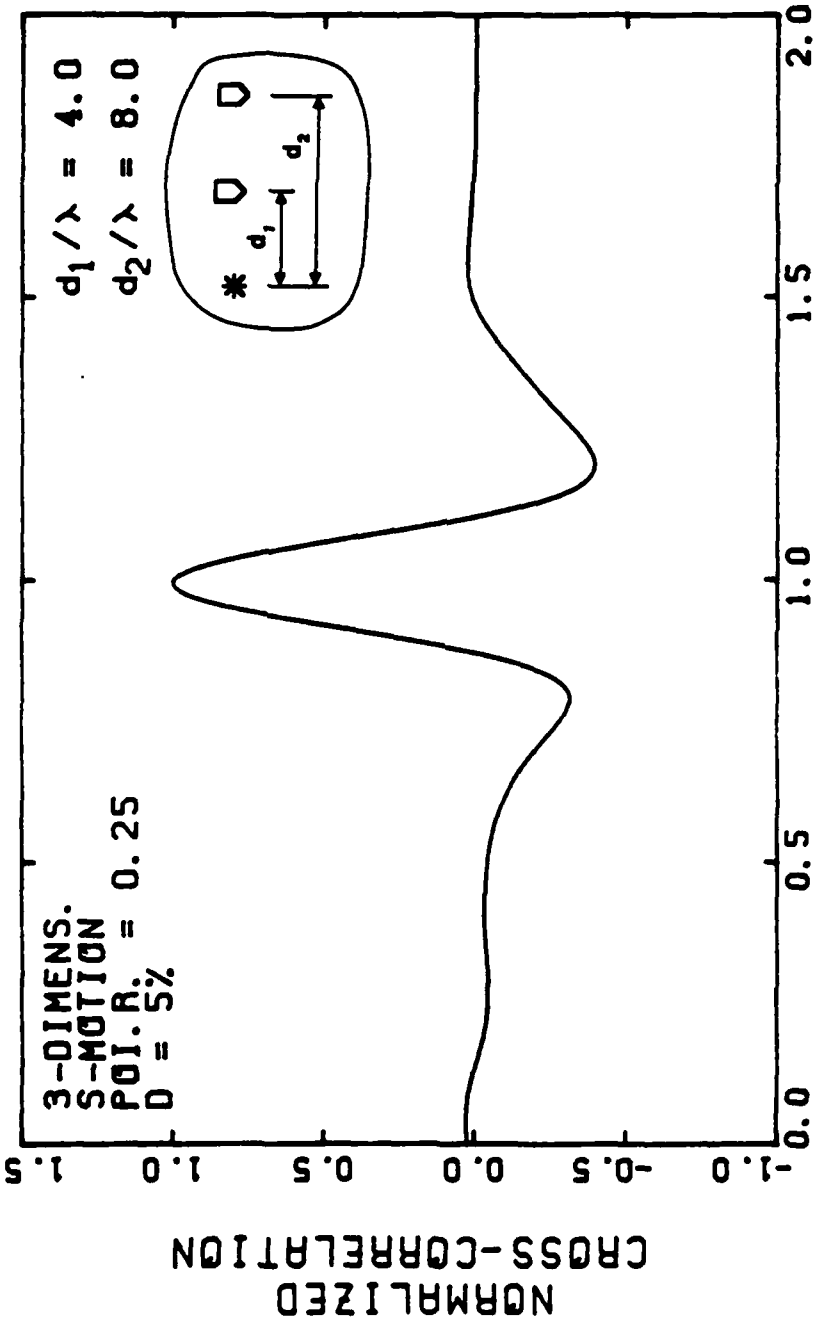

Fig. C.15 - Cross-correlation function of three-dimensional S-motion records obtained in the far field. Poisson's ratio = 0.25 and damping = 5 %.

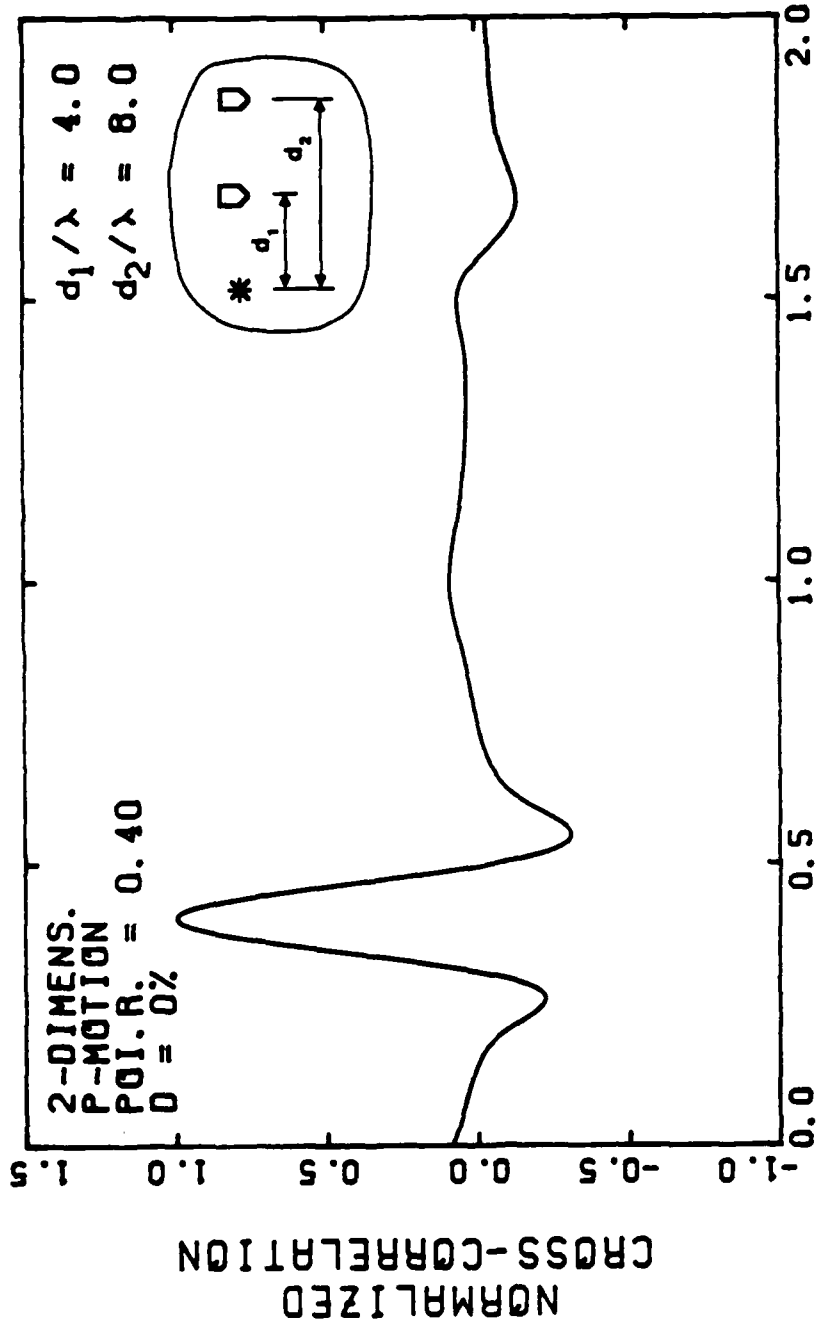

Fig. C.16 - Cross-correlation function of two-dimensional P-motion records obtained in the far field. Poisson's ratio = 0.4 and damping = 0 %.

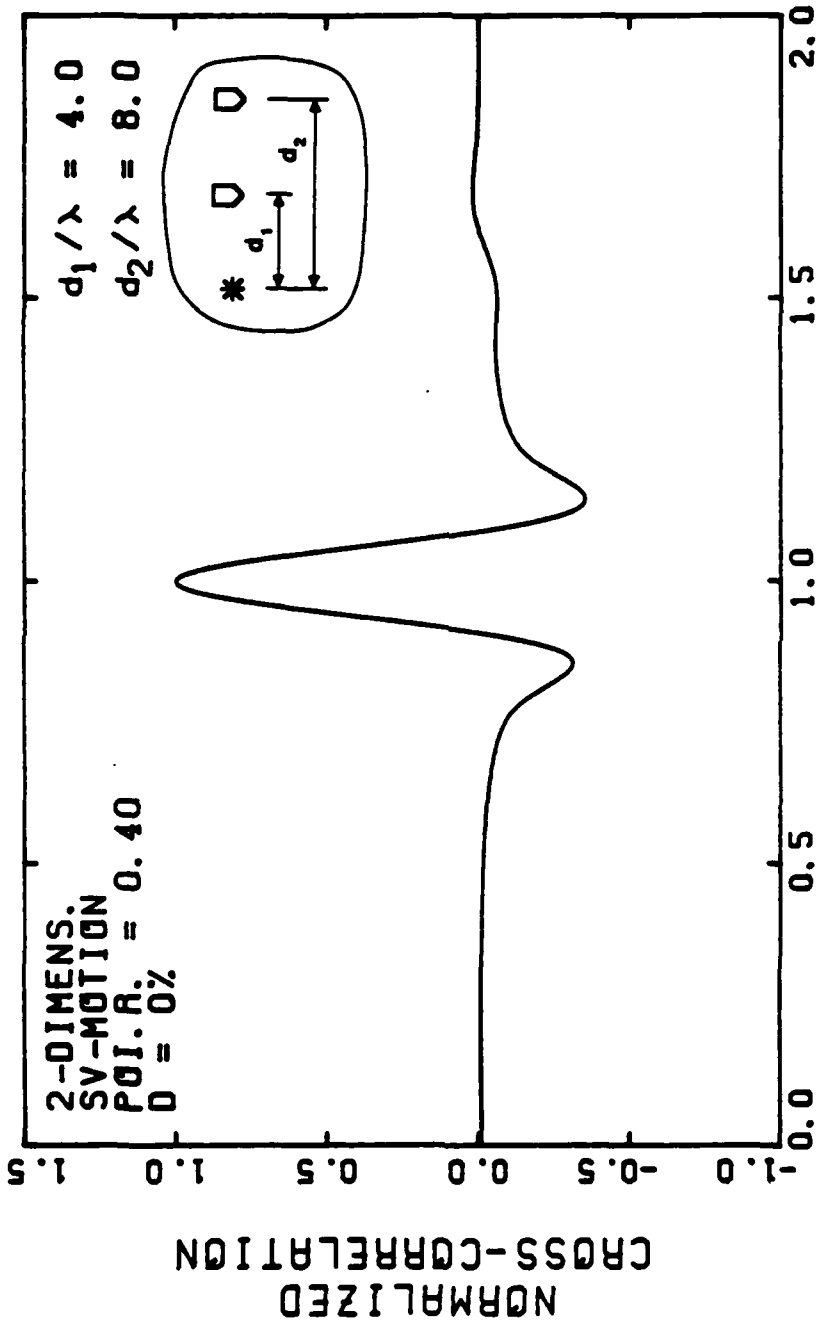

Fig. C.17 - Cross-correlation function of two-dimensional SV-motion records obtained in the far field. Poisson's ratio = 0.4 and damping = 0 %.

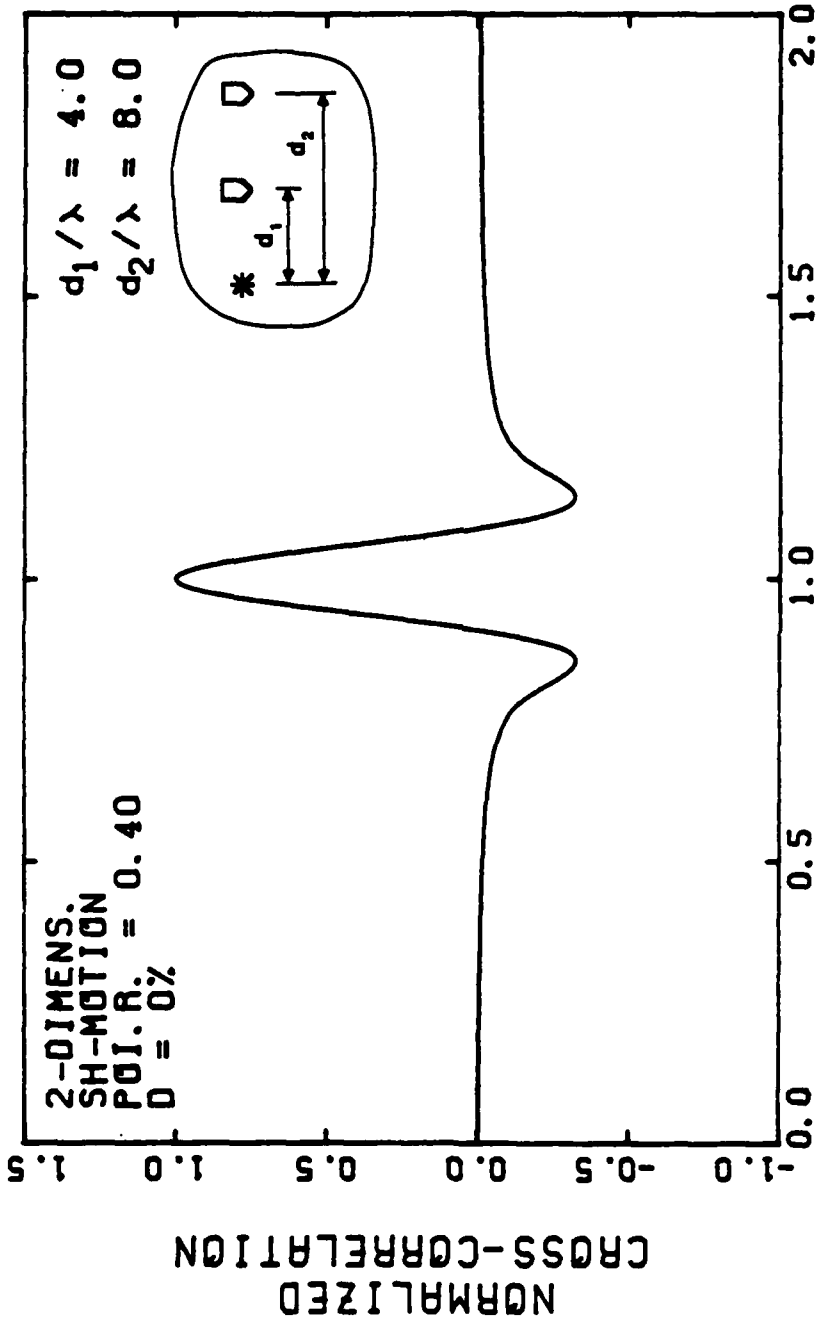

Fig. C.18 - Cross-correlation function of two-dimensional SH-motion records obtained in the far field. Poisson's ratio = 0.4 and damping = 0 %.

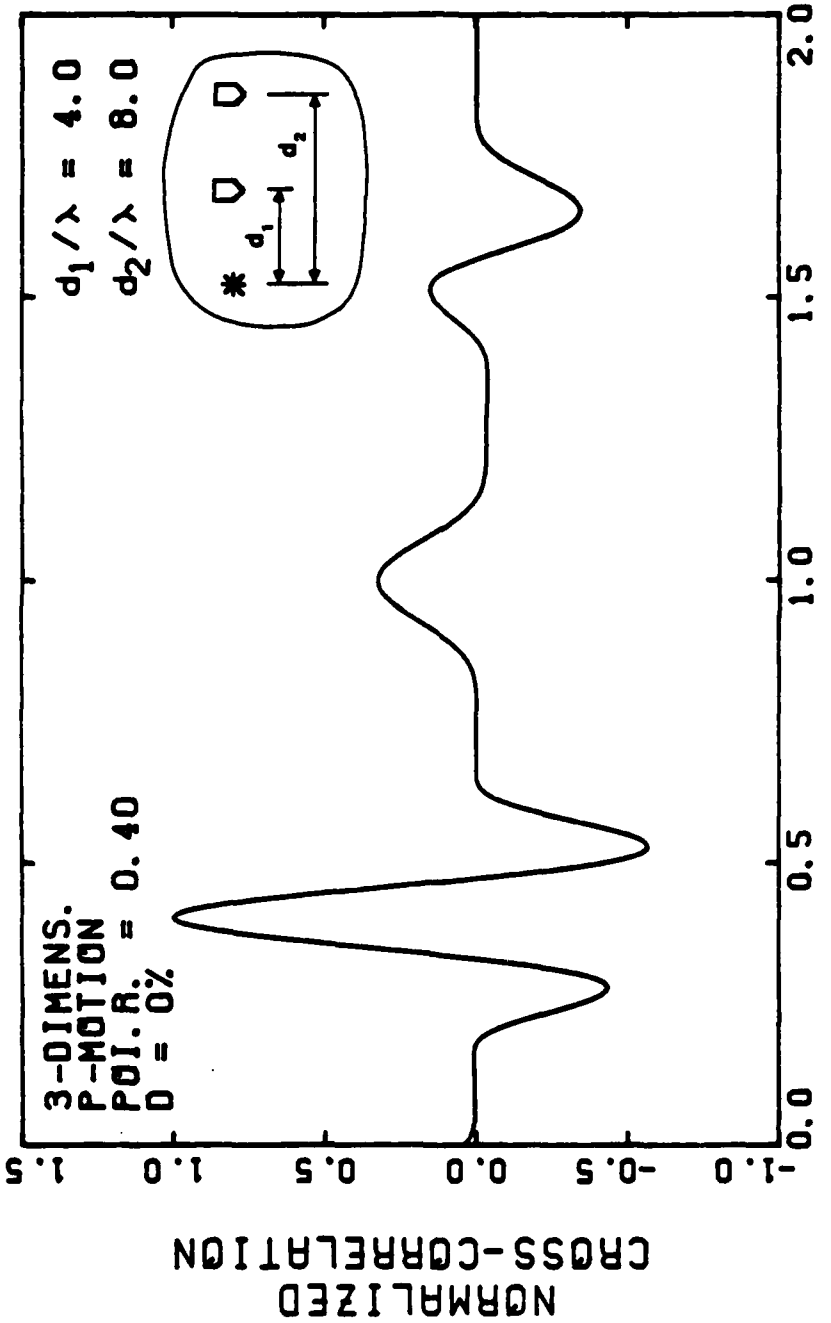

Fig. C.19 - Cross-correlation function of three-dimensional P-motion records obtained in the far field. Poisson's ratio = 0.4 and damping = 0 %.

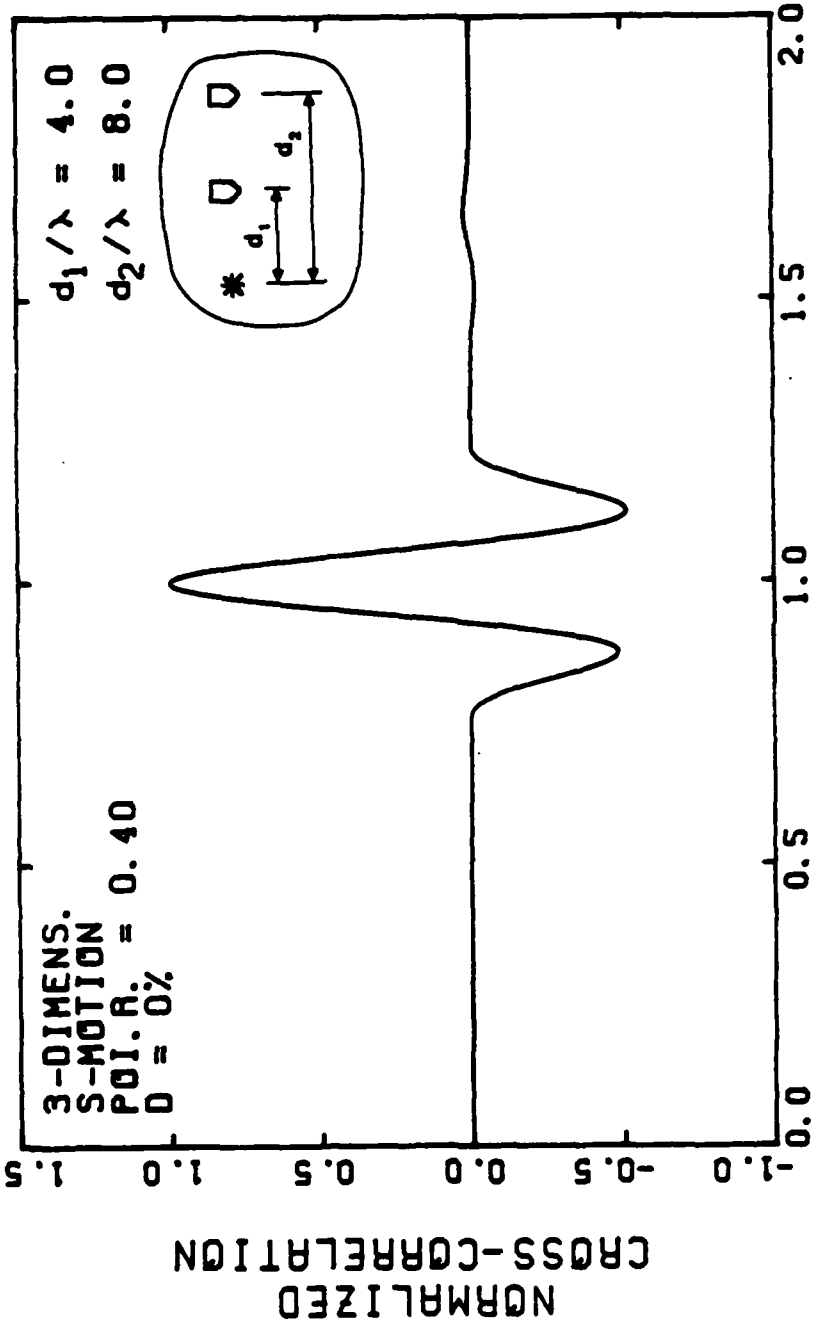

Fig. C.20 - Cross-correlation function of three-dimensional S-motion records obtained in the far field. Poisson's ratio = 0.4 and damping = 0 %.

APPENDIX D

BODY WAVE DISPERSION CURVES

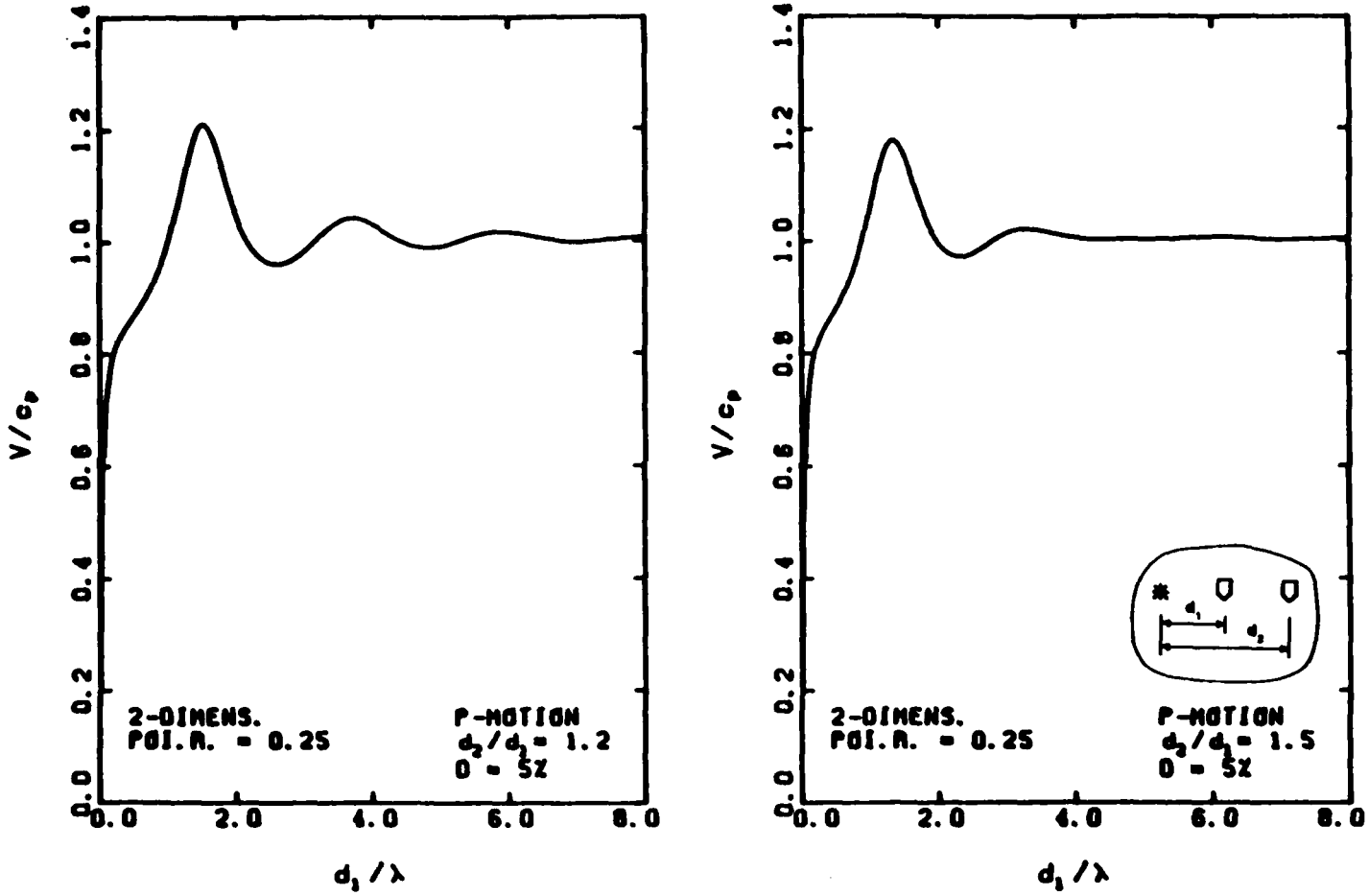

Fig. D.1 - Dispersion curves for two-dimensional in-plane longitudinal motion in a medium with five percent damping and Poisson's ratio = 0.25. Small spacing between receivers.

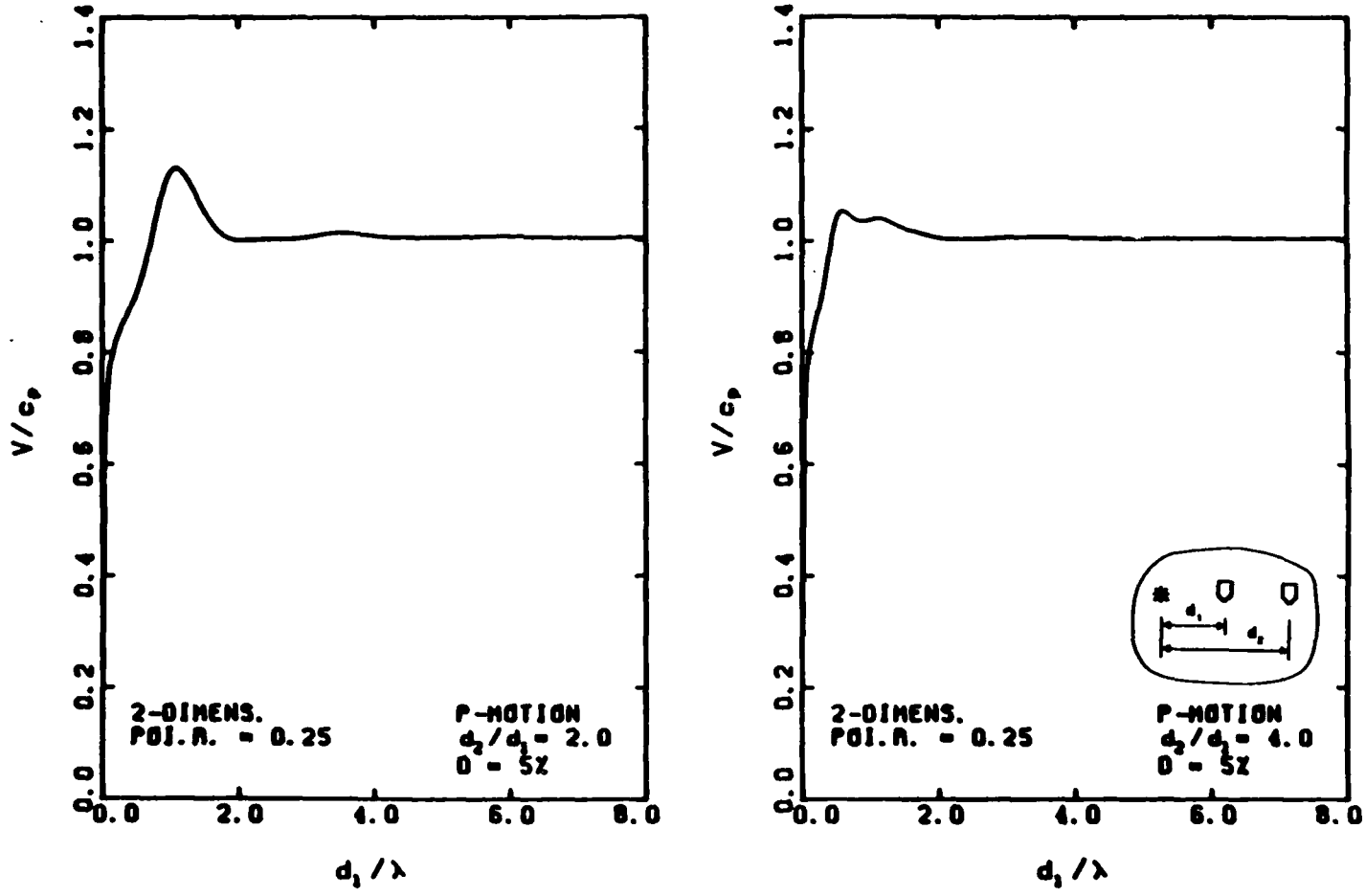

Fig. D.2 - Dispersion curves for two-dimensional in-plane longitudinal motion in a medium with five percent damping and Poisson's ratio = 0.25. Large spacing between receivers.

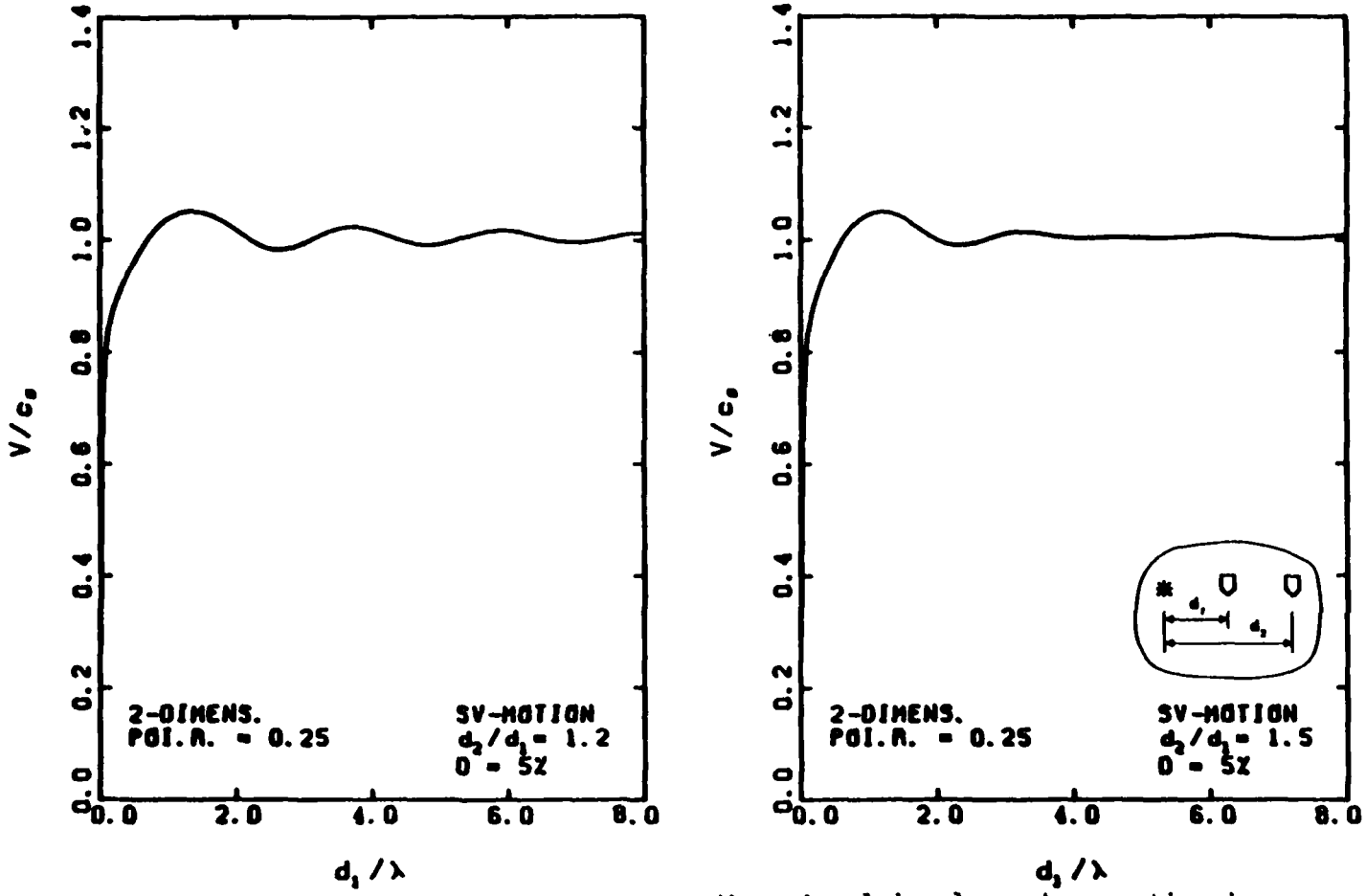

Fig. D.3 - Dispersion curves for two-dimensional in-plane shear motion in a medium with five percent damping and Poisson's ratio = 0.25. Small spacing between receivers.

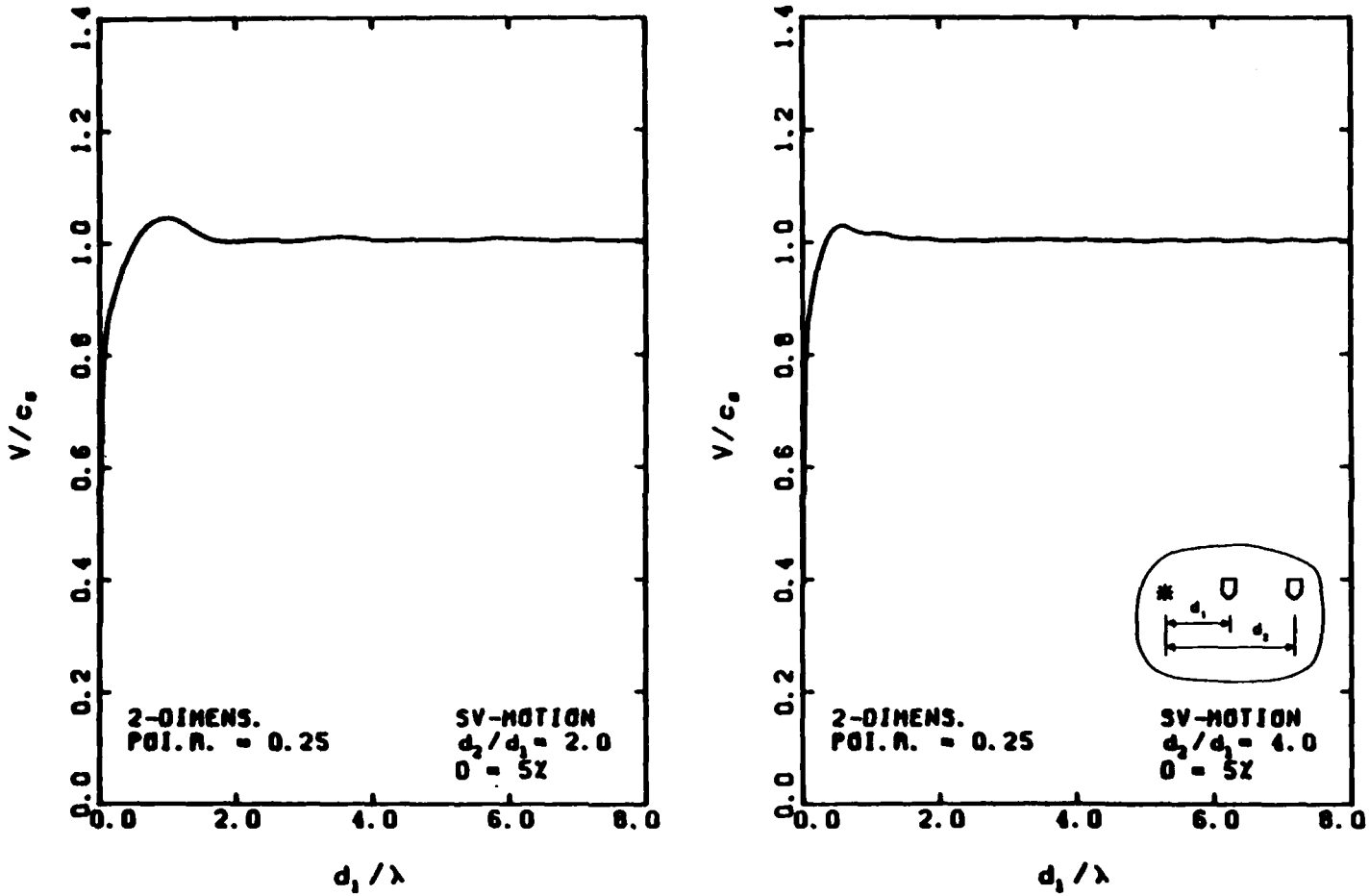

Fig. D.4 - Dispersion curves for two-dimensional in-plane shear motion in a medium with five percent damping and Poisson's ratio = 0.25. Large spacing between receivers.

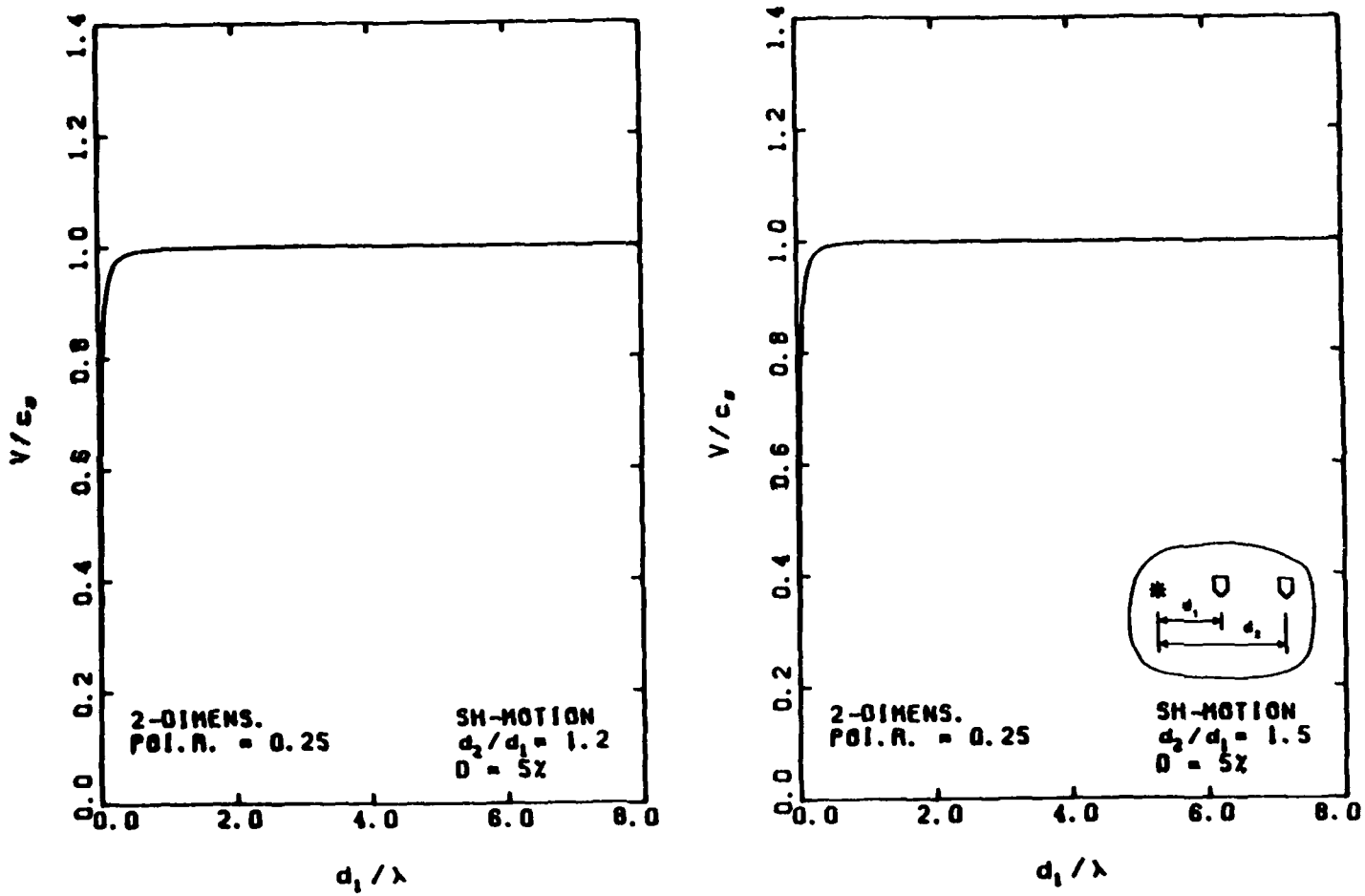

Fig. D.5 - Dispersion curves for two-dimensional antiplane shear motion in a medium with five percent damping and Poisson's ratio = 0.25. Small spacing between receivers.

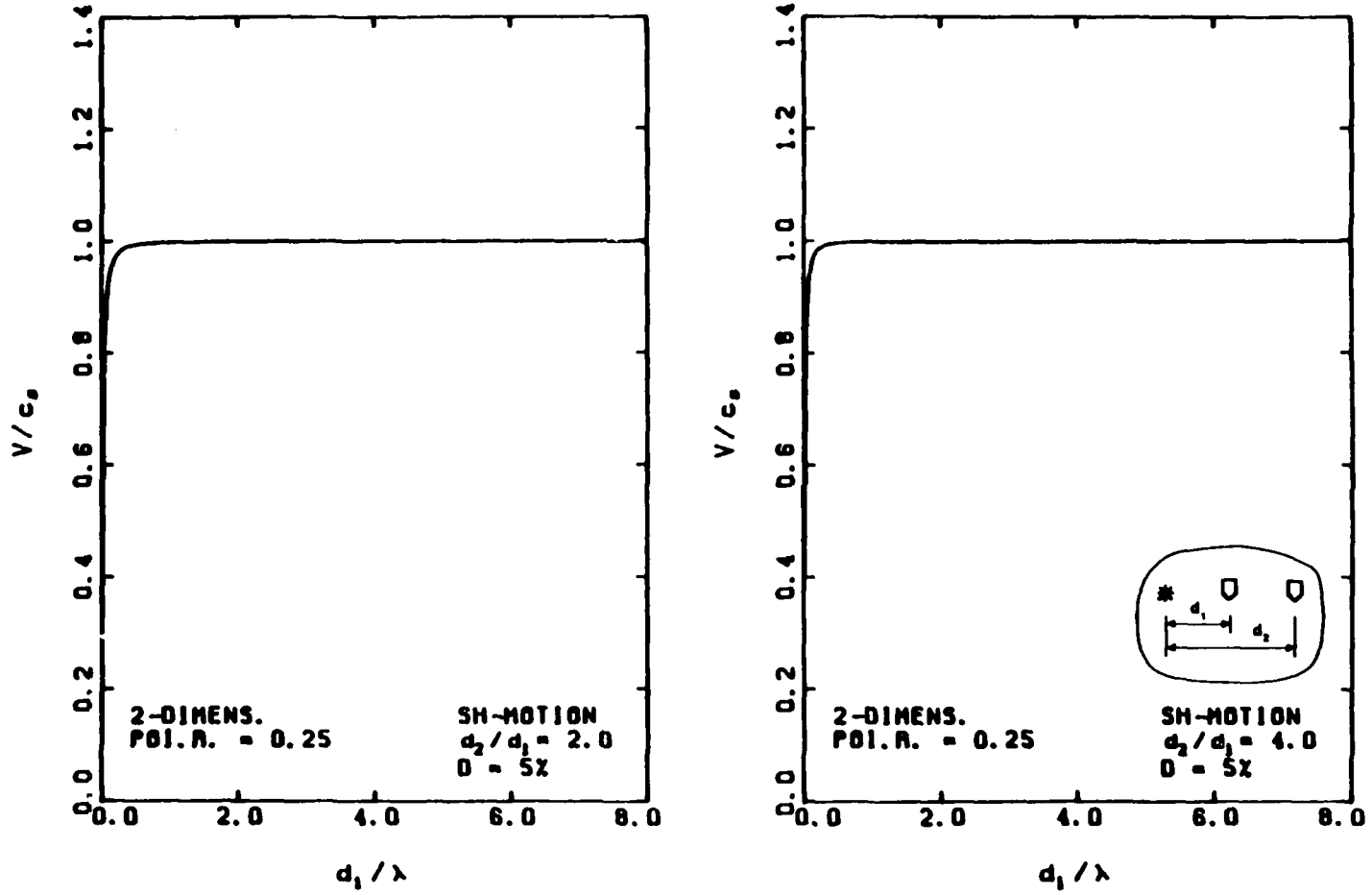

Fig. D.6 - Dispersion curves for two-dimensional antiplane shear motion in a medium with five percent damping and Poisson's ratio = 0.25. Large spacing between receivers.

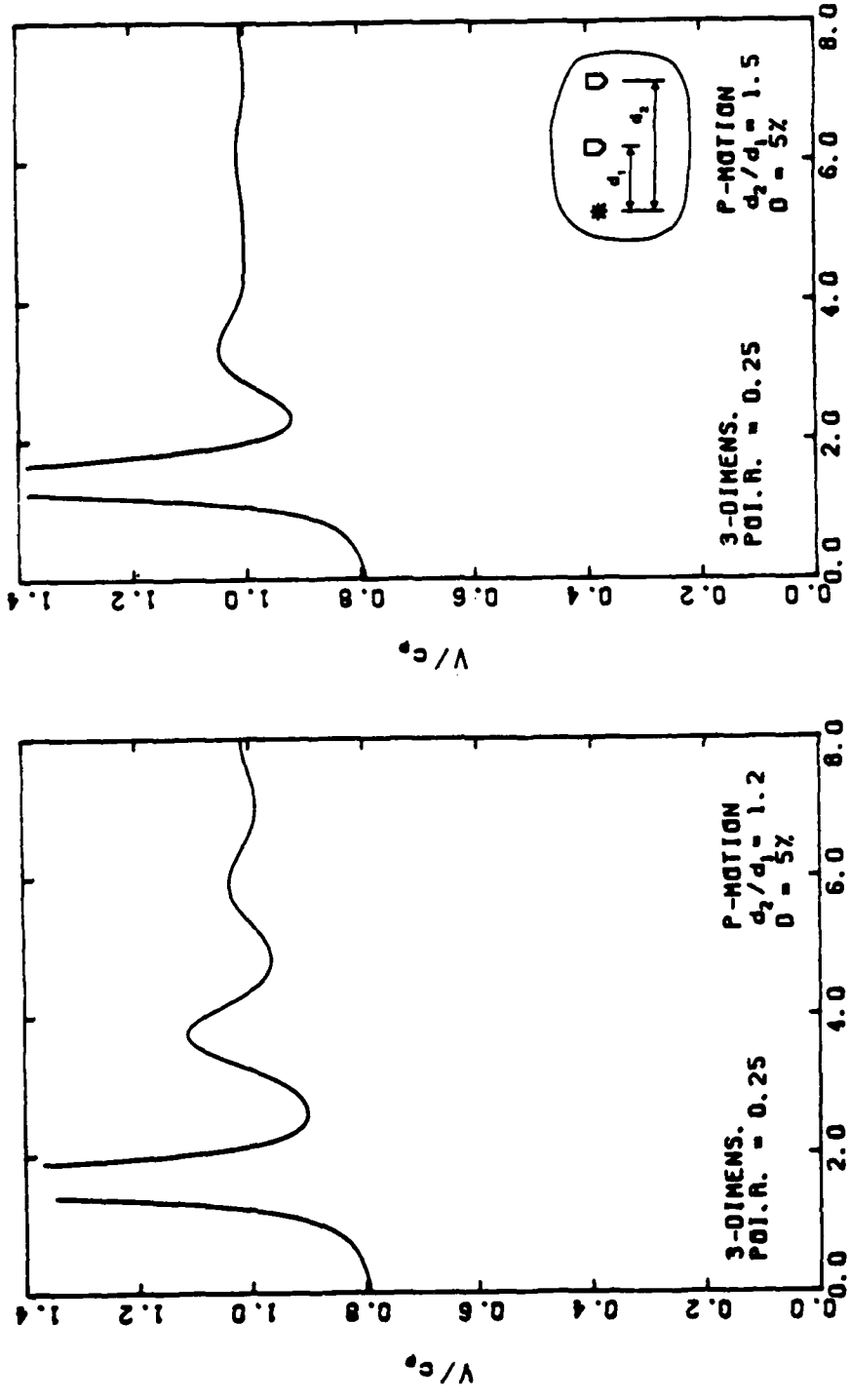

Fig. D.7 - Dispersion curves for three-dimensional longitudinal motion in a medium with five percent damping and Poisson's ratio = 0.25. Small spacing between receivers.

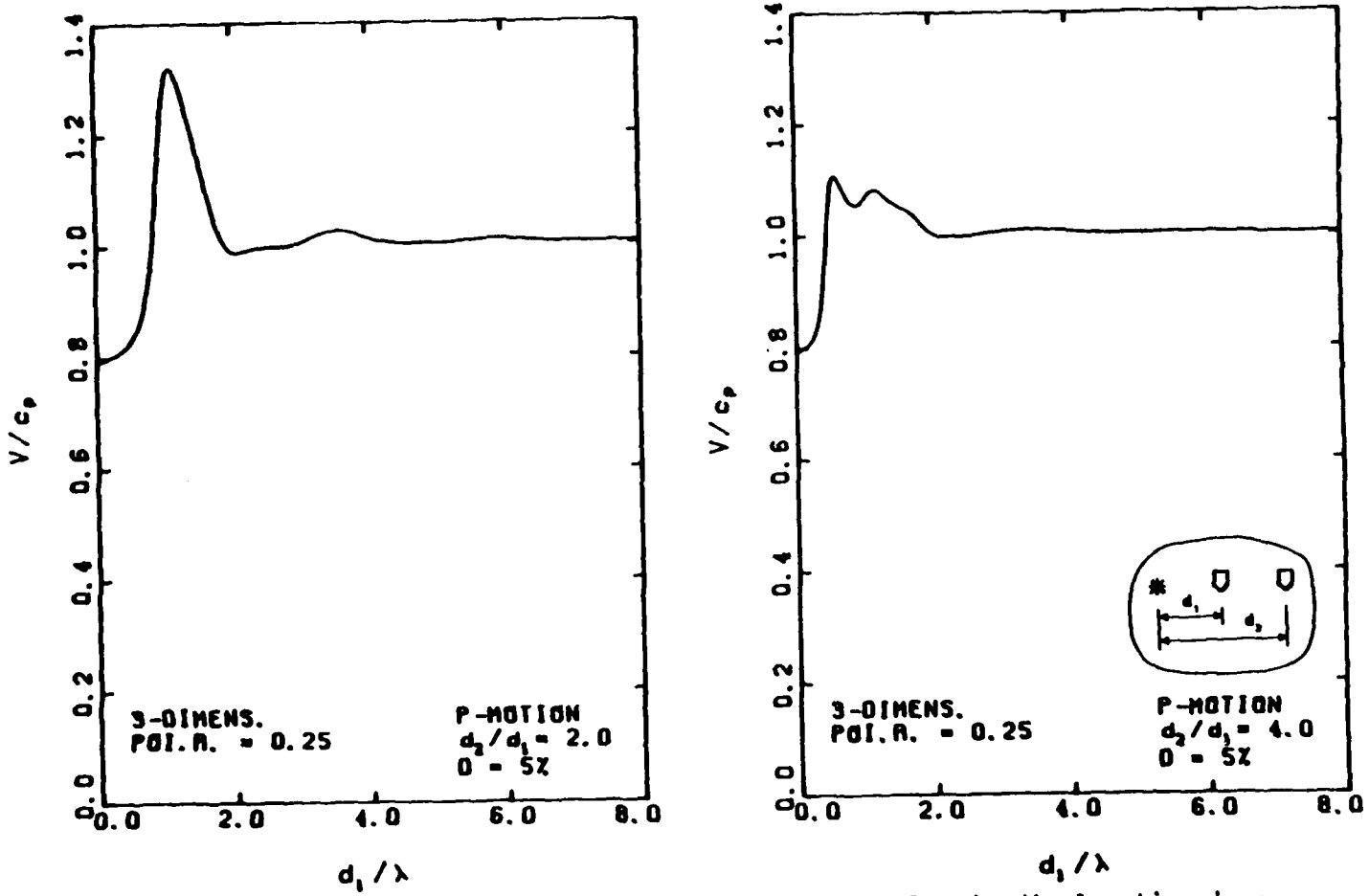

Fig. D.8 - Dispersion curves for three-dimensional longitudinal motion in a medium with five percent damping and Poisson's ratio = 0.25. Large spacing between receivers.

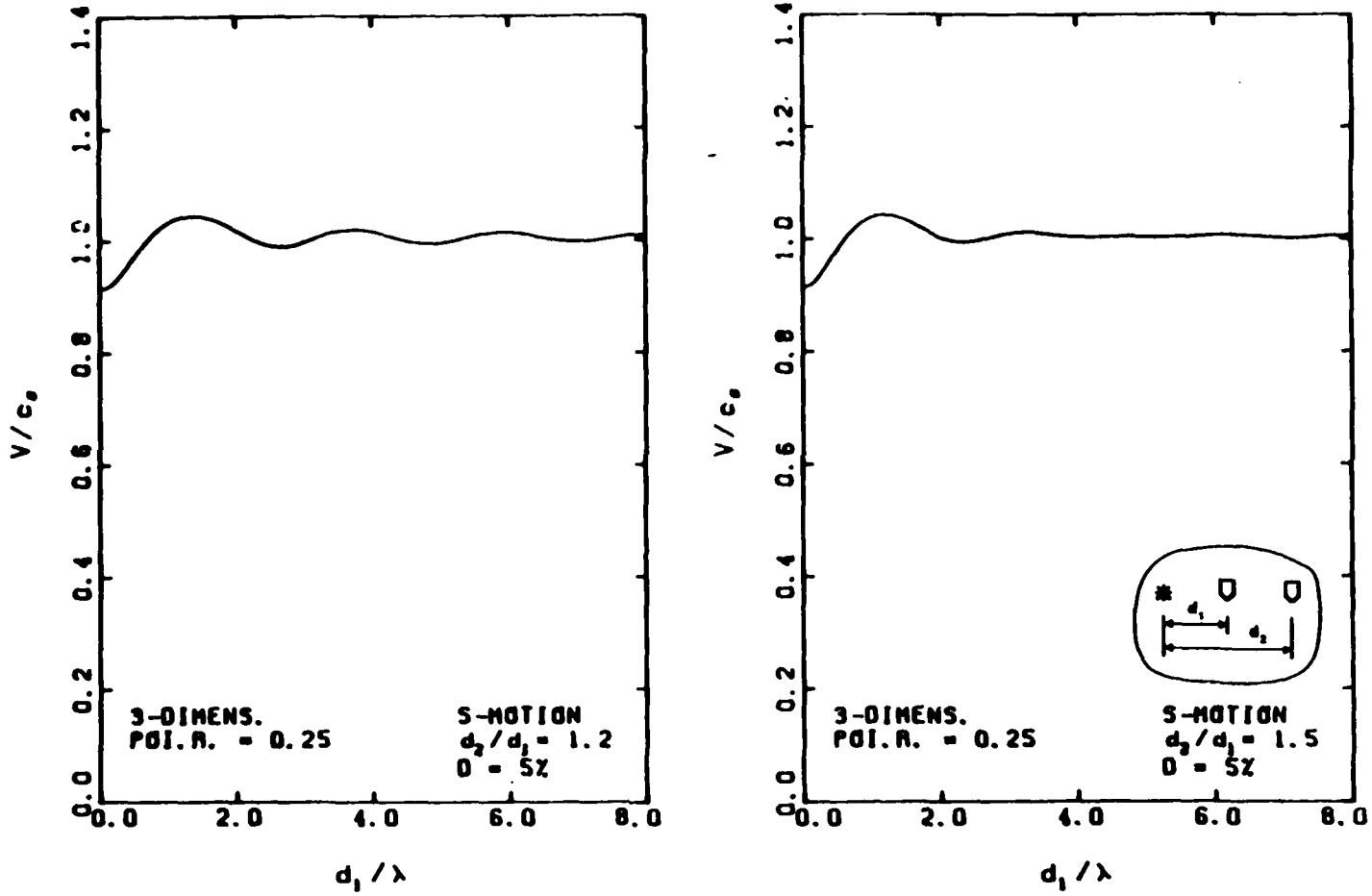

Fig. D.9 - Dispersion curves for three-dimensional shear motion in a medium with five percent damping and Poisson's ratio = 0.25. Small spacing between receivers.

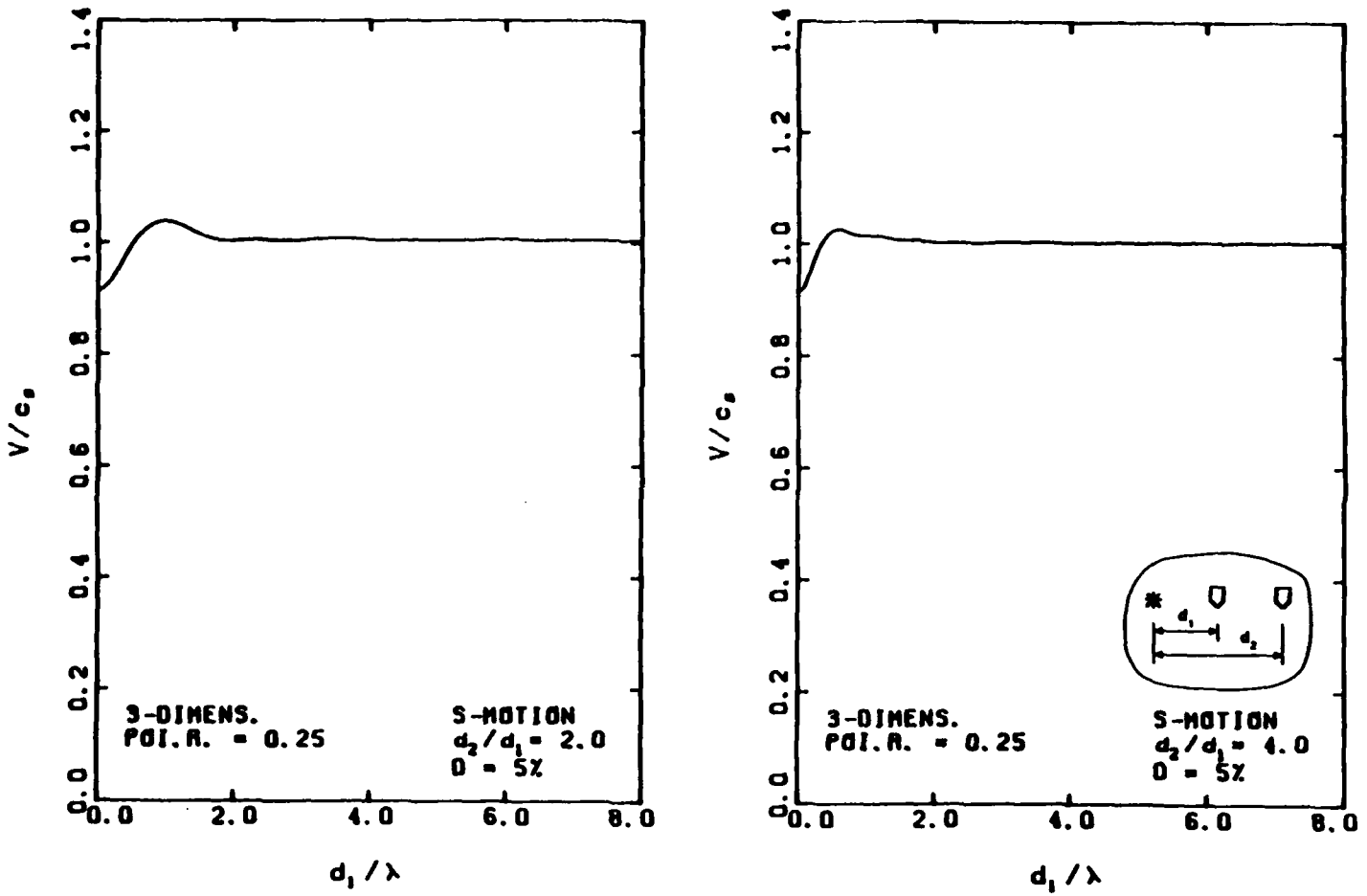

Fig. D.10 - Dispersion curves for three-dimensional shear motion in a medium with five percent damping and Poisson's ratio = 0.25. Large spacing between receivers.

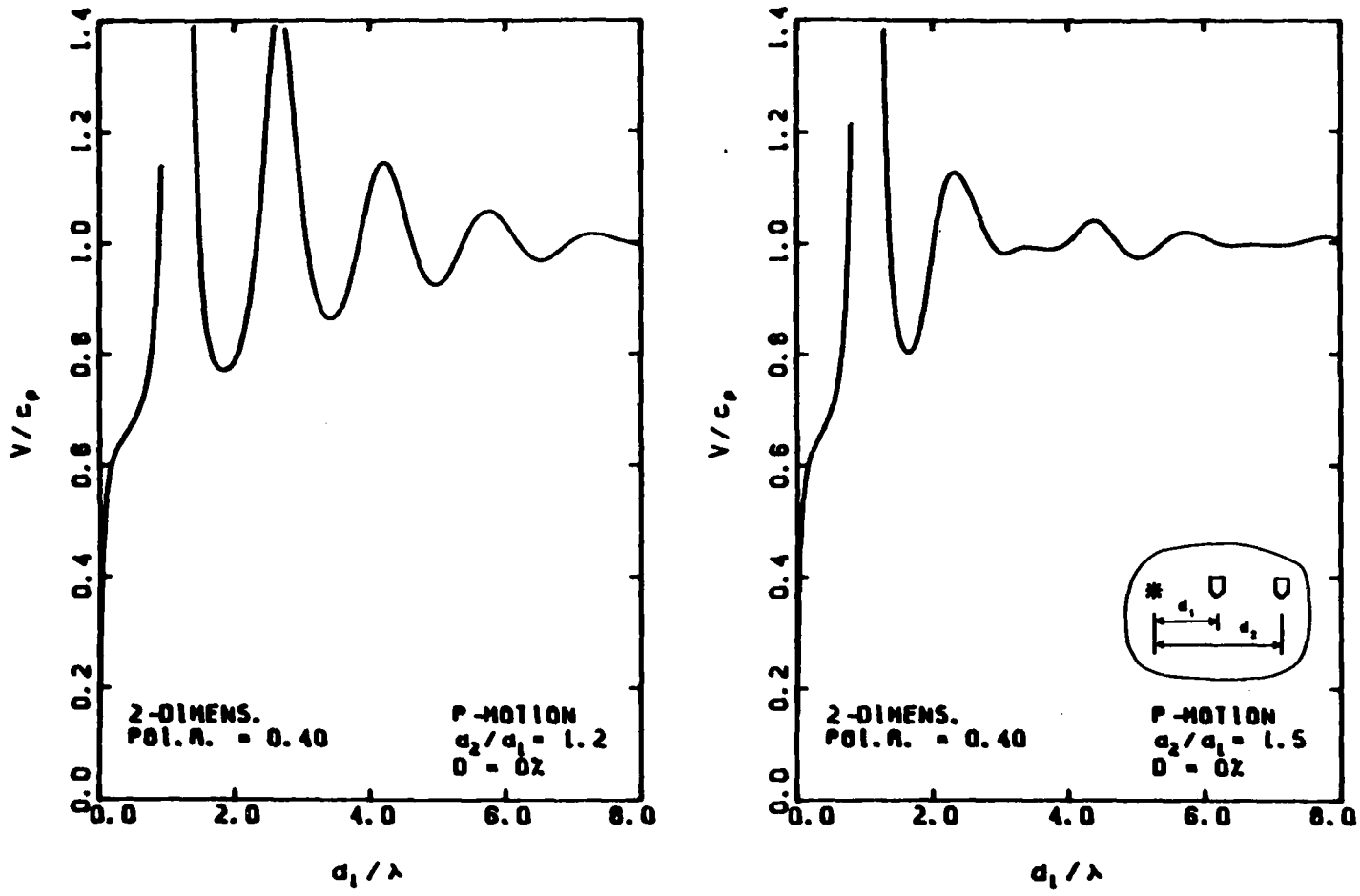

Fig. D.11 - Dispersion curves for two-dimensional in-plane longitudinal motion in a medium with no damping and Poisson's ratio = 0.4. Small spacing between receivers.

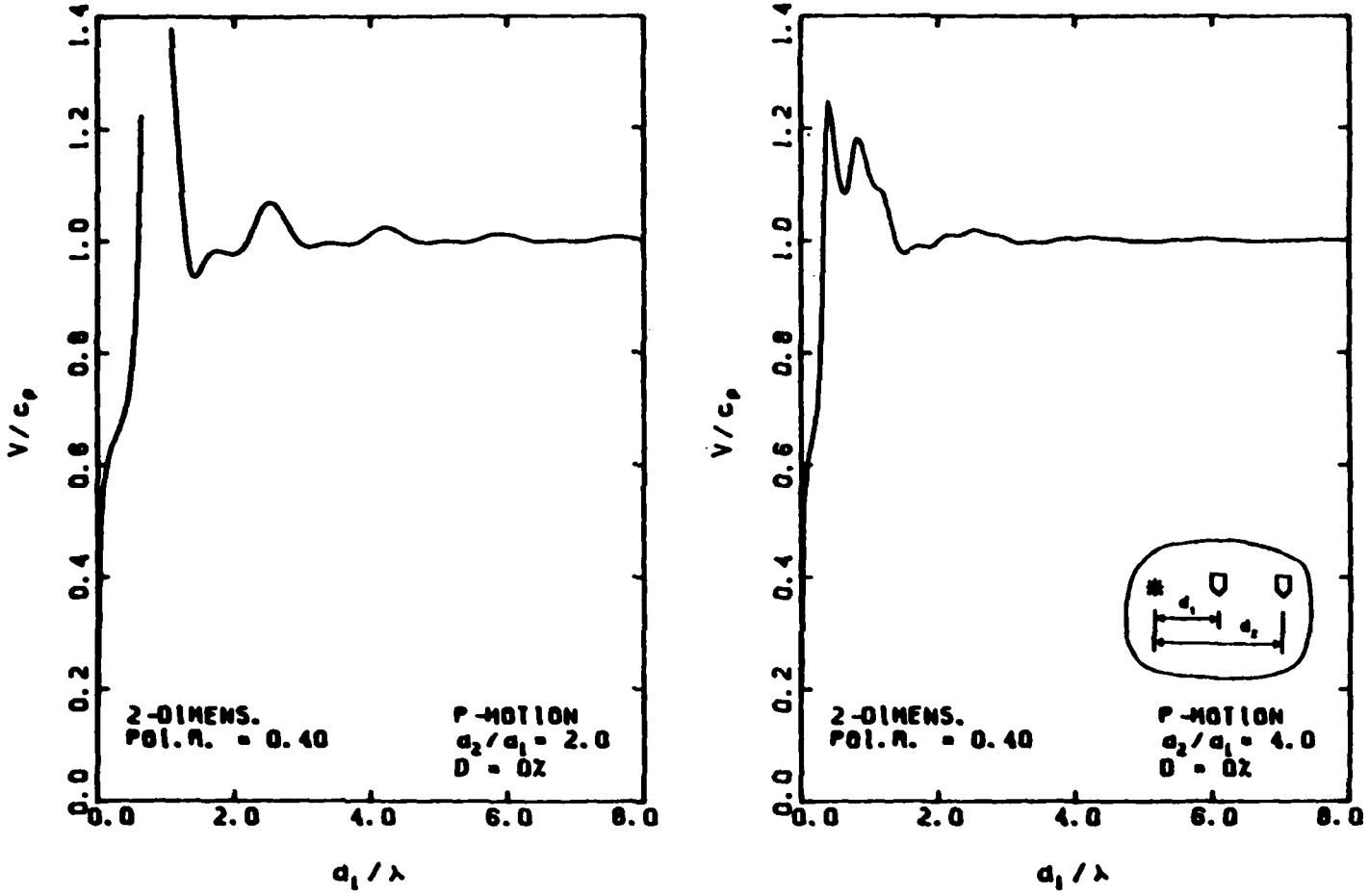

Fig. D.12 - Dispersion curves for two-dimensional in-plane longitudinal motion in a medium with no damping and Poisson's ratio = 0.4. Large spacing between receivers.

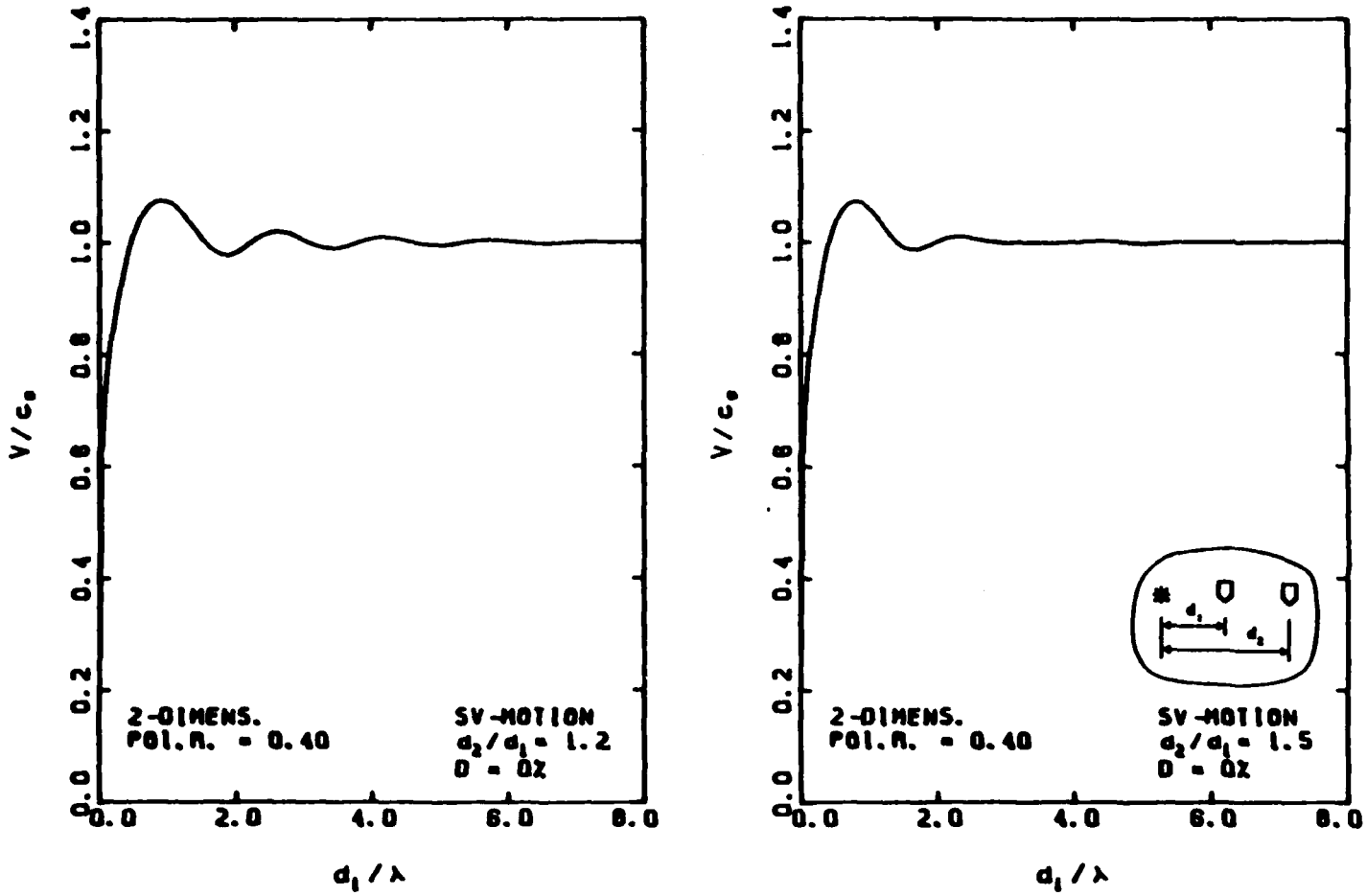

Fig. D.13 - Dispersion curves for two-dimensional in-plane shear motion in a medium with no damping and Poisson's ratio = 0.4. Small spacing between receivers.

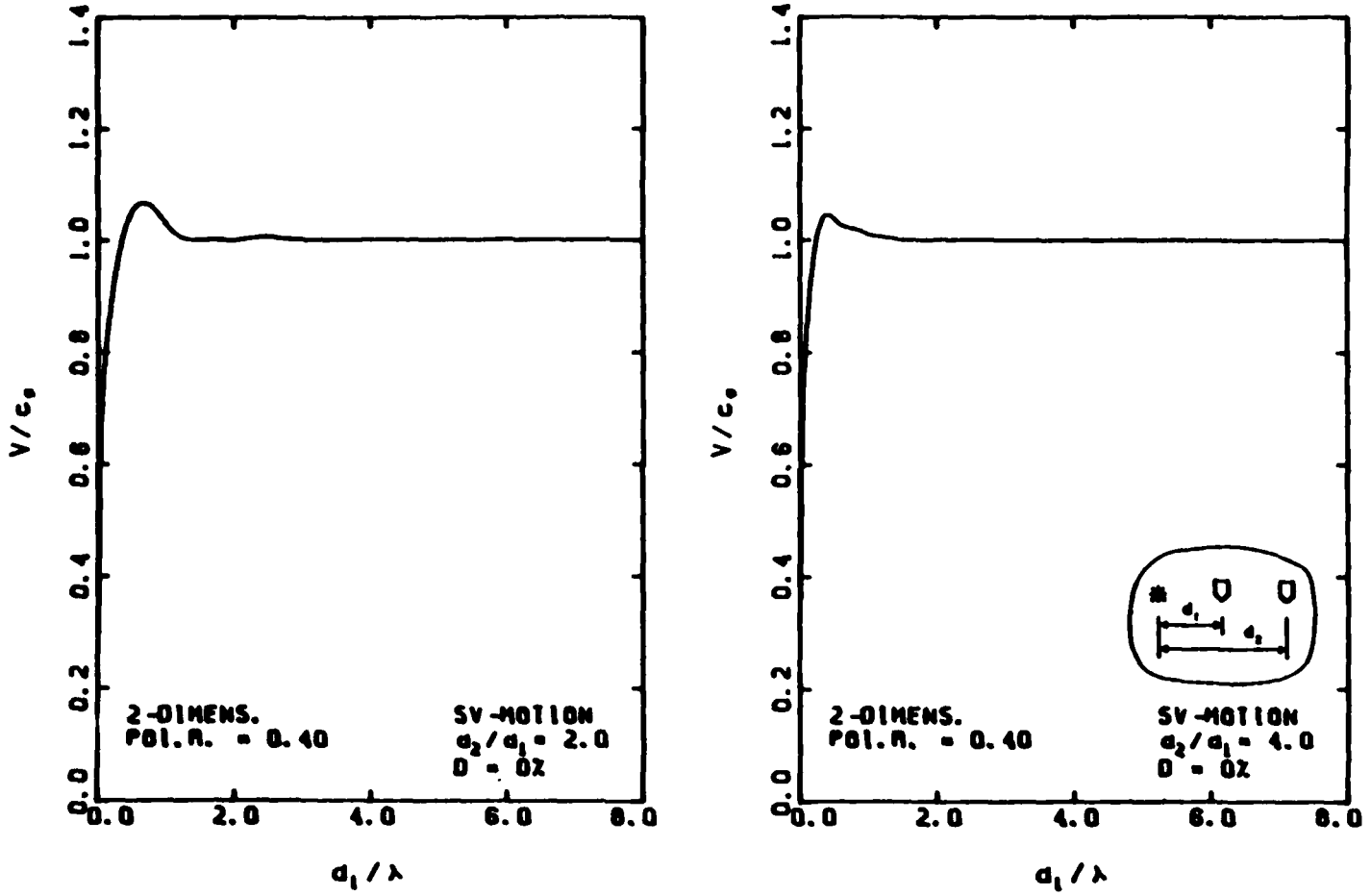

Fig. D.14 - Dispersion curves for two-dimensional in-plane shear motion in a medium with no damping and Poisson's ratio = 0.4. Large spacing between receivers.

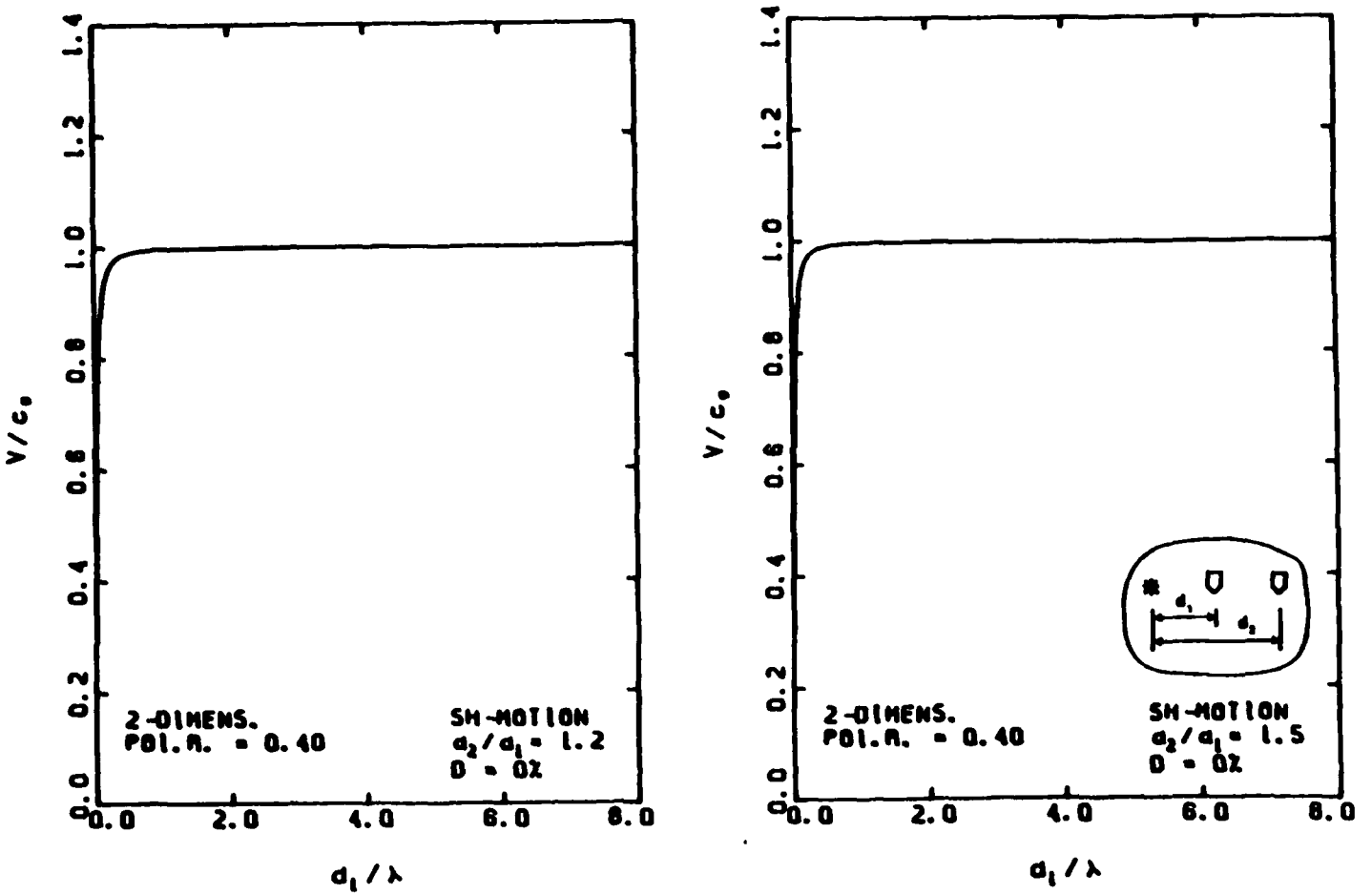

Fig. D.15 - Dispersion curves for two-dimensional antiplane shear motion in a medium with no damping and Poisson's ratio = 0.4. Small spacing between receivers.

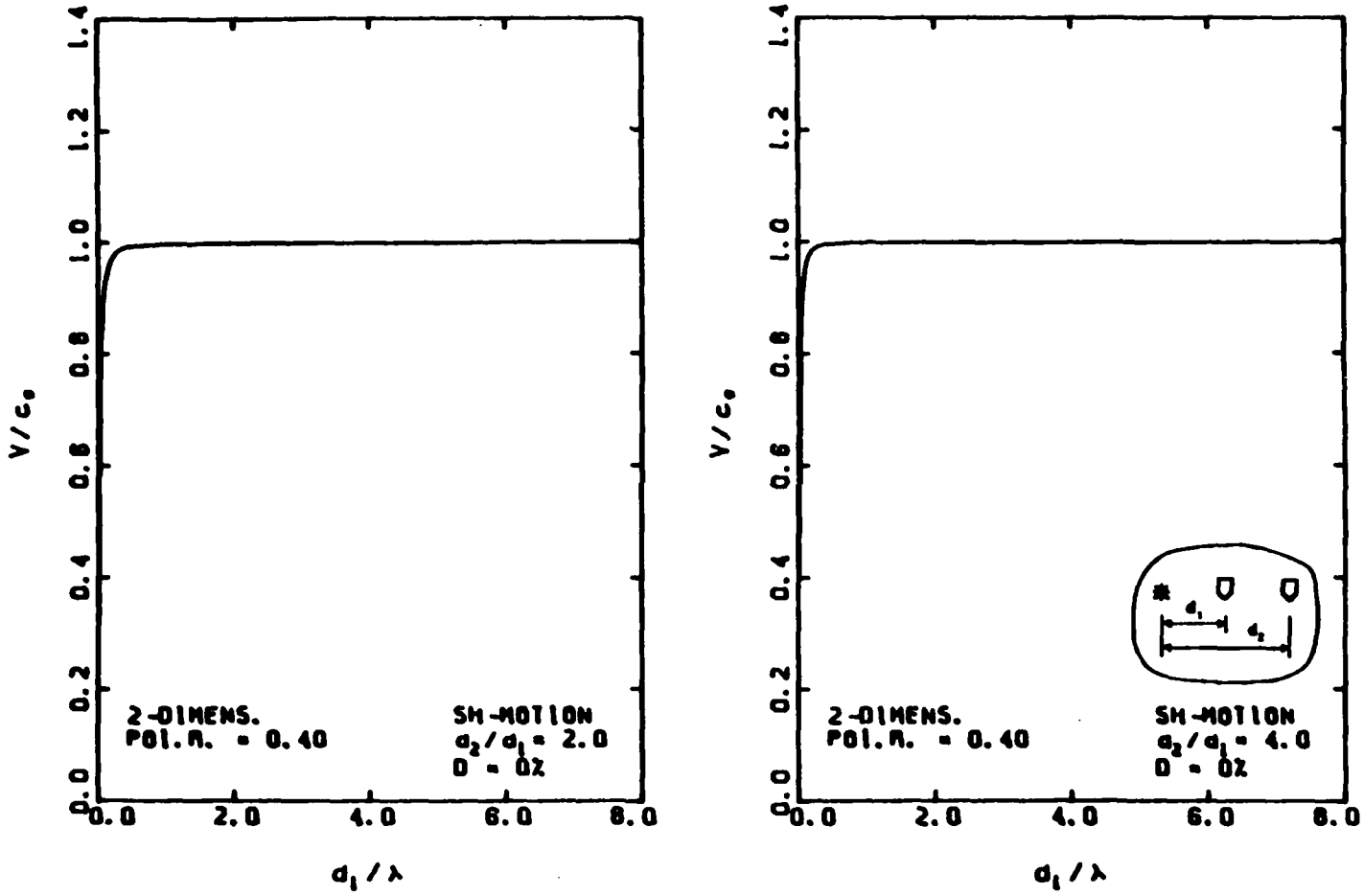

Fig. D.16 - Dispersion curves for two-dimensional antiplane shear motion in a medium with no damping and Poisson's ratio = 0.4. Large spacing between receivers.

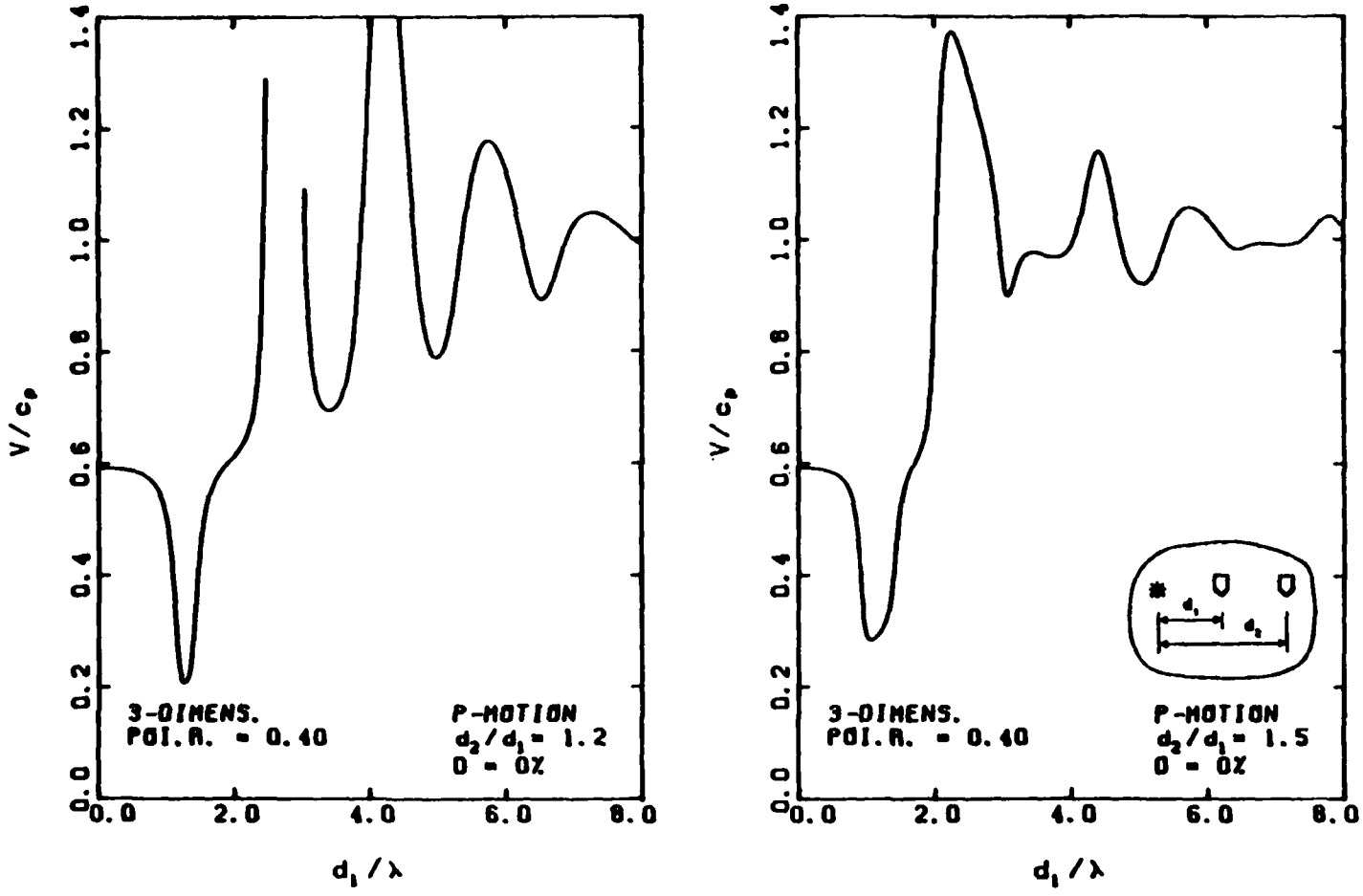

Fig. D.17 - Dispersion curves for three-dimensional longitudinal motion in a medium with no damping and Poisson's ratio = 0.4. Small spacing between receivers.

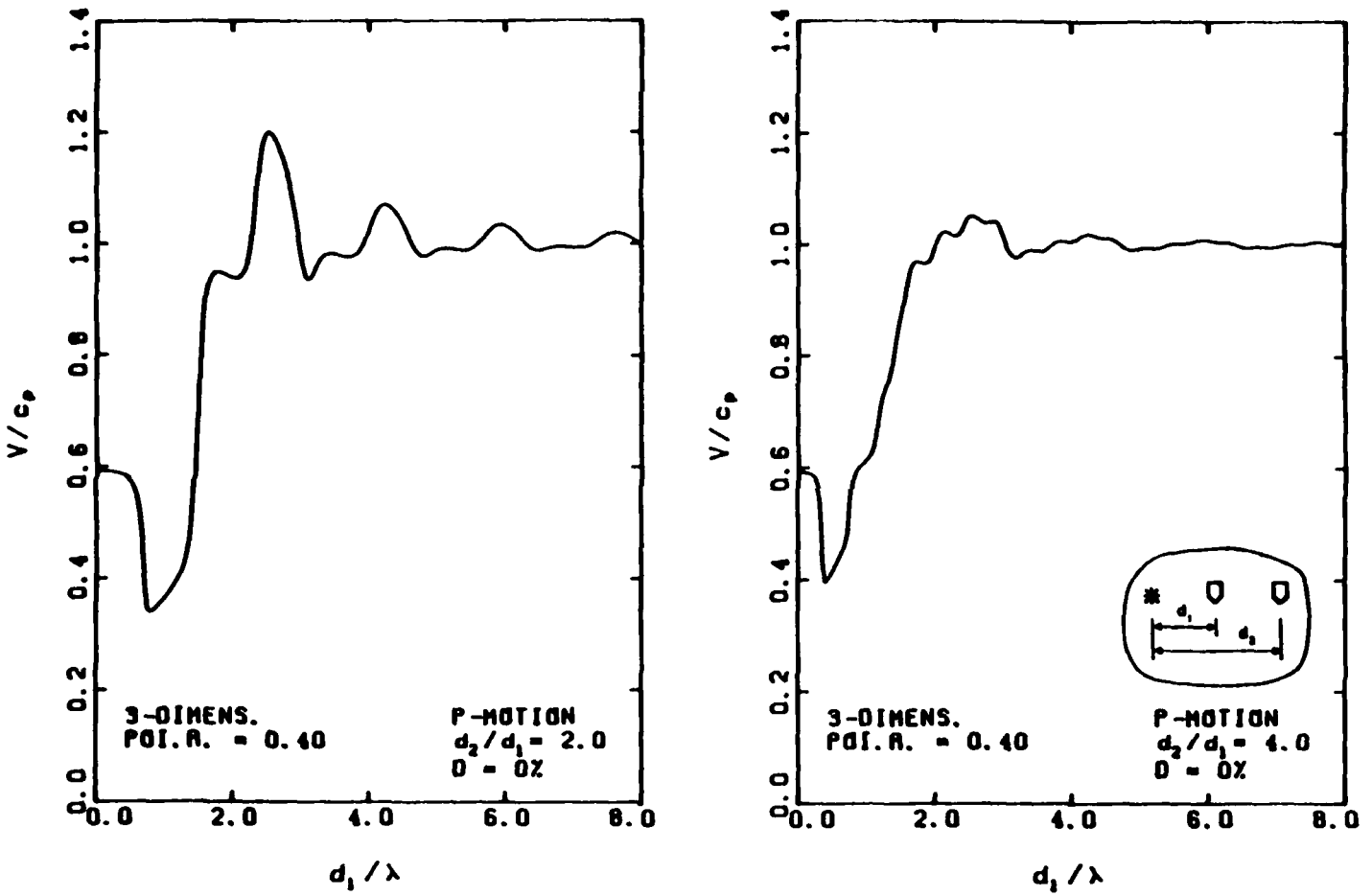

Fig. D.18 - Dispersion curves for three-dimensional longitudinal motion in a medium with no damping and Poisson's ratio = 0.4. Large spacing between receivers.

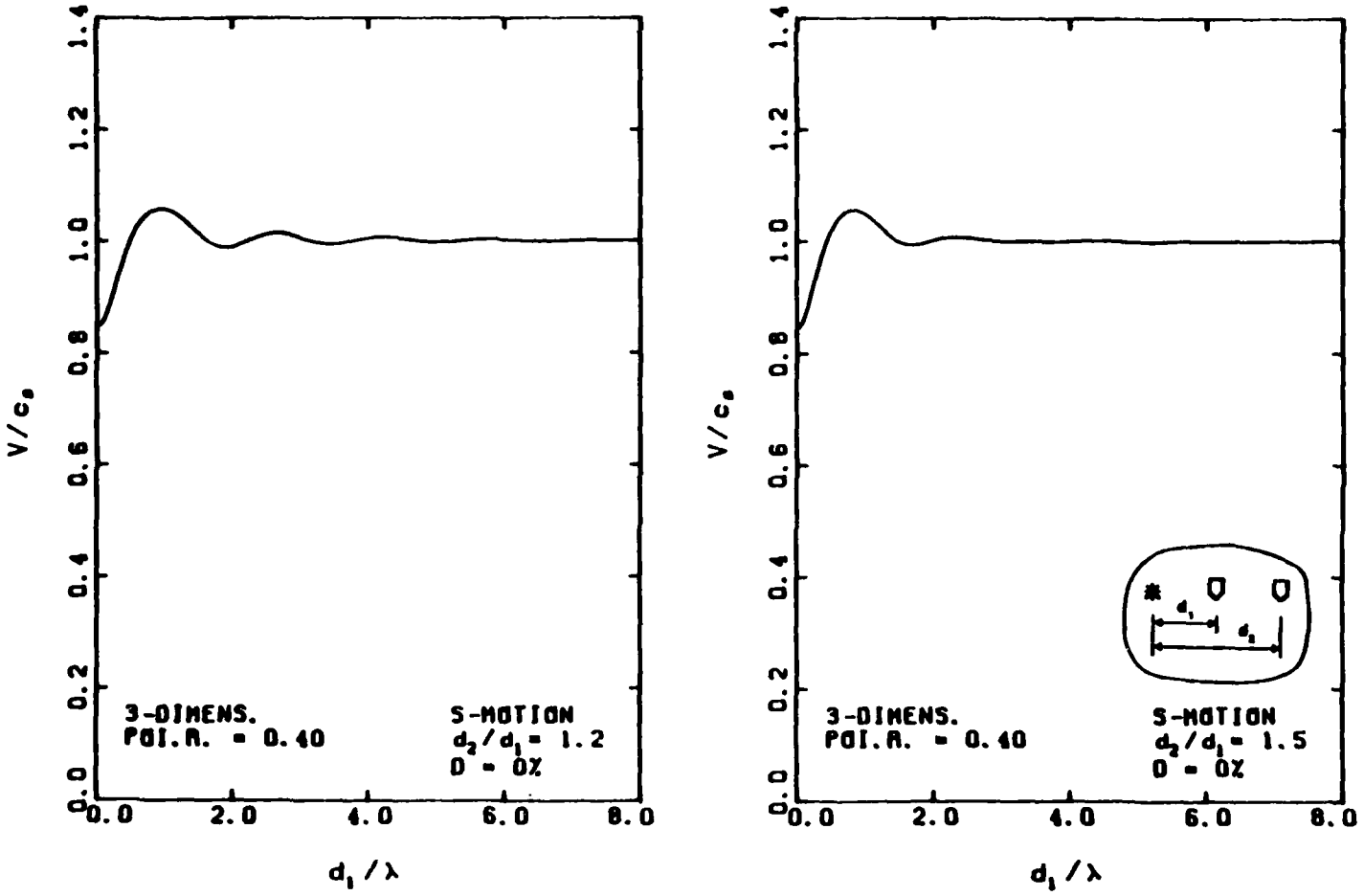

Fig. D.19 - Dispersion curves for three-dimensional shear motion in a medium with no damping and Poisson's ratio = 0.4. Small spacing between receivers.

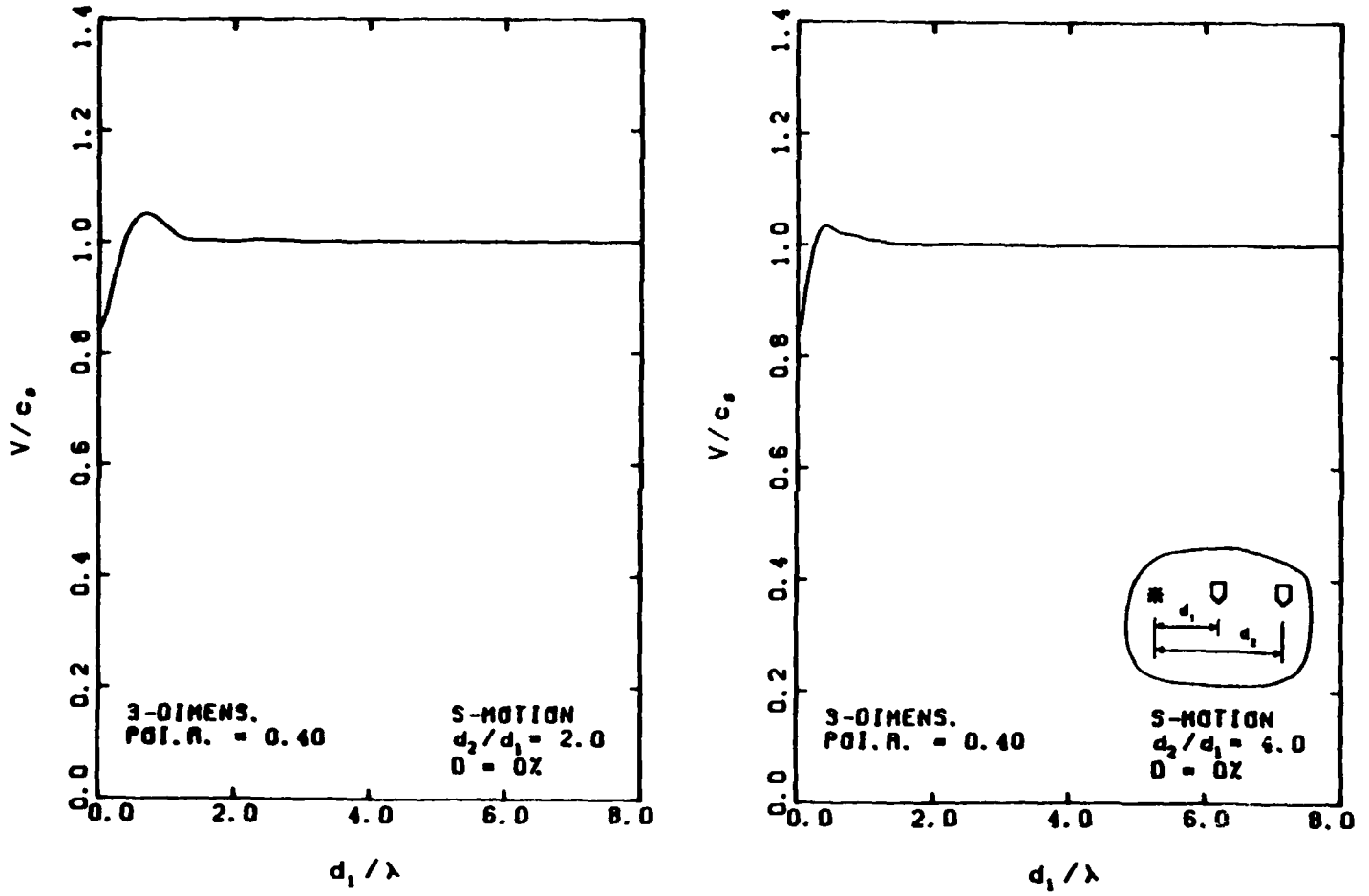

Fig. D.20 - Dispersion curves for three-dimensional shear motion in a medium with no damping and Poisson's ratio = 0.4. Large spacing between receivers.

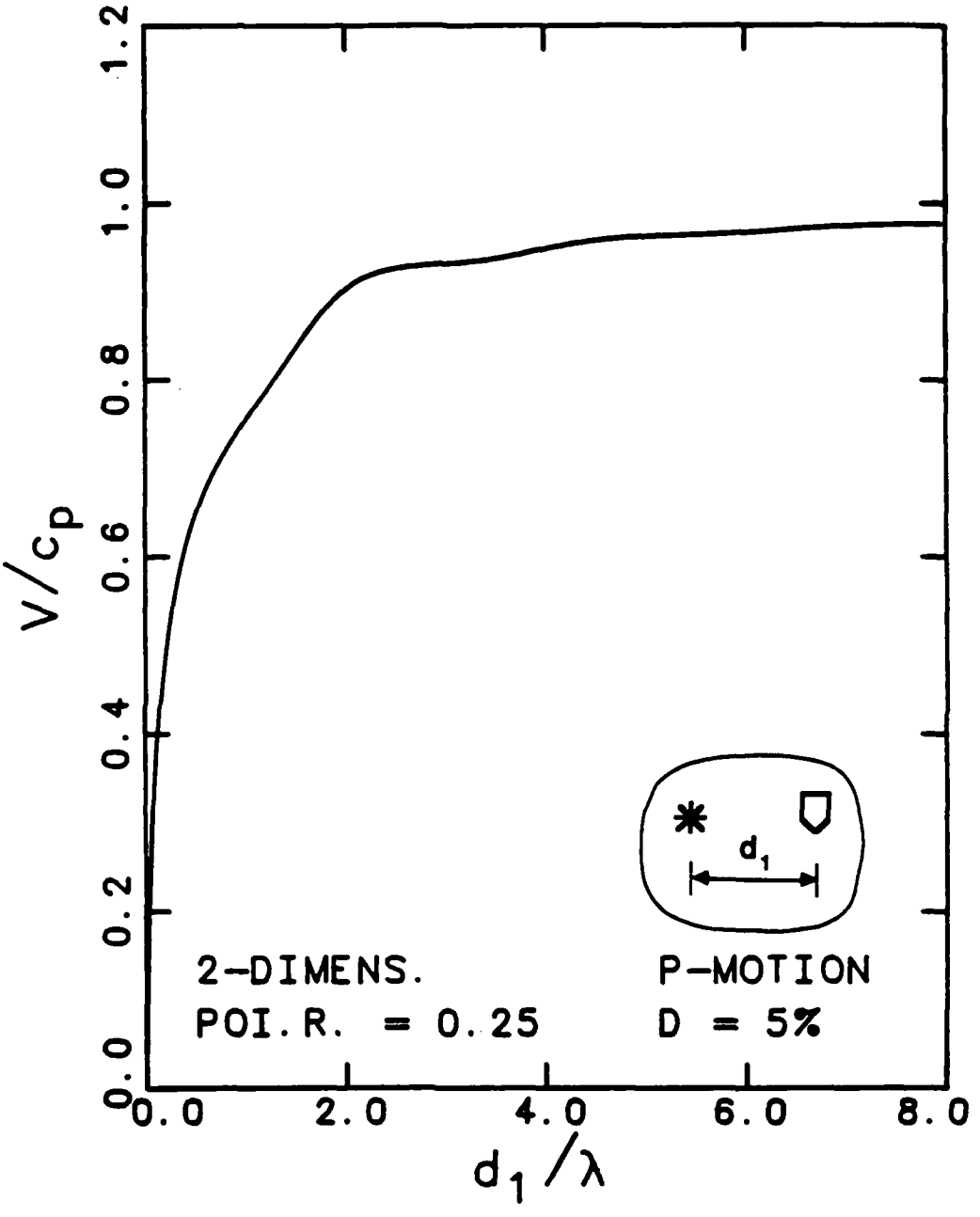

Fig. D.21 - Dispersion curves obtained from the phase of the transfer function for two-dimensional longitudinal motion in a medium with five percent damping and Poisson's ratio = 0.25.

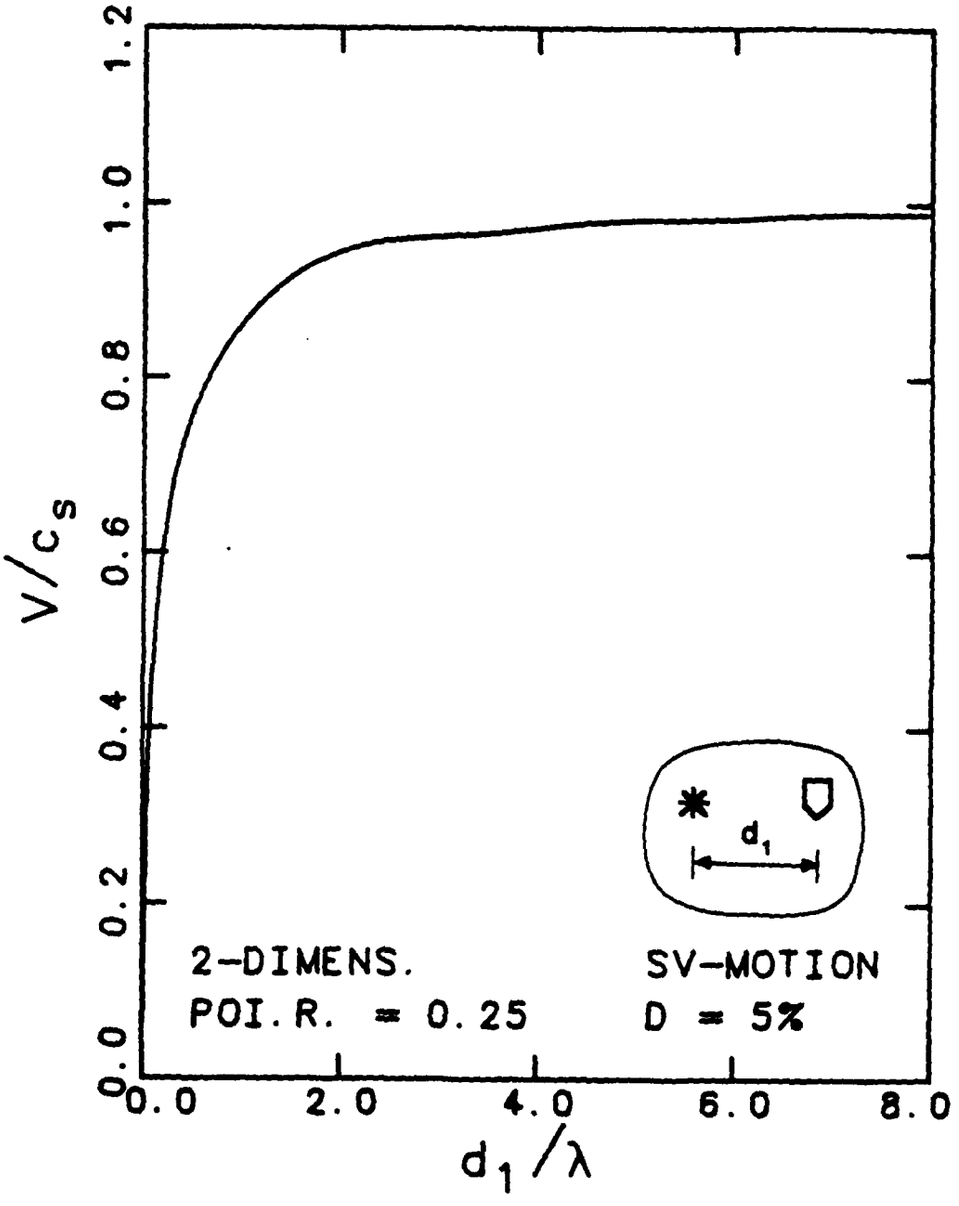

Fig. D.22 - Dispersion curves obtained from the phase of the transfer function for two-dimensional in-plane shear motion in a medium with five percent damping and Poisson's ratio = 0.25.

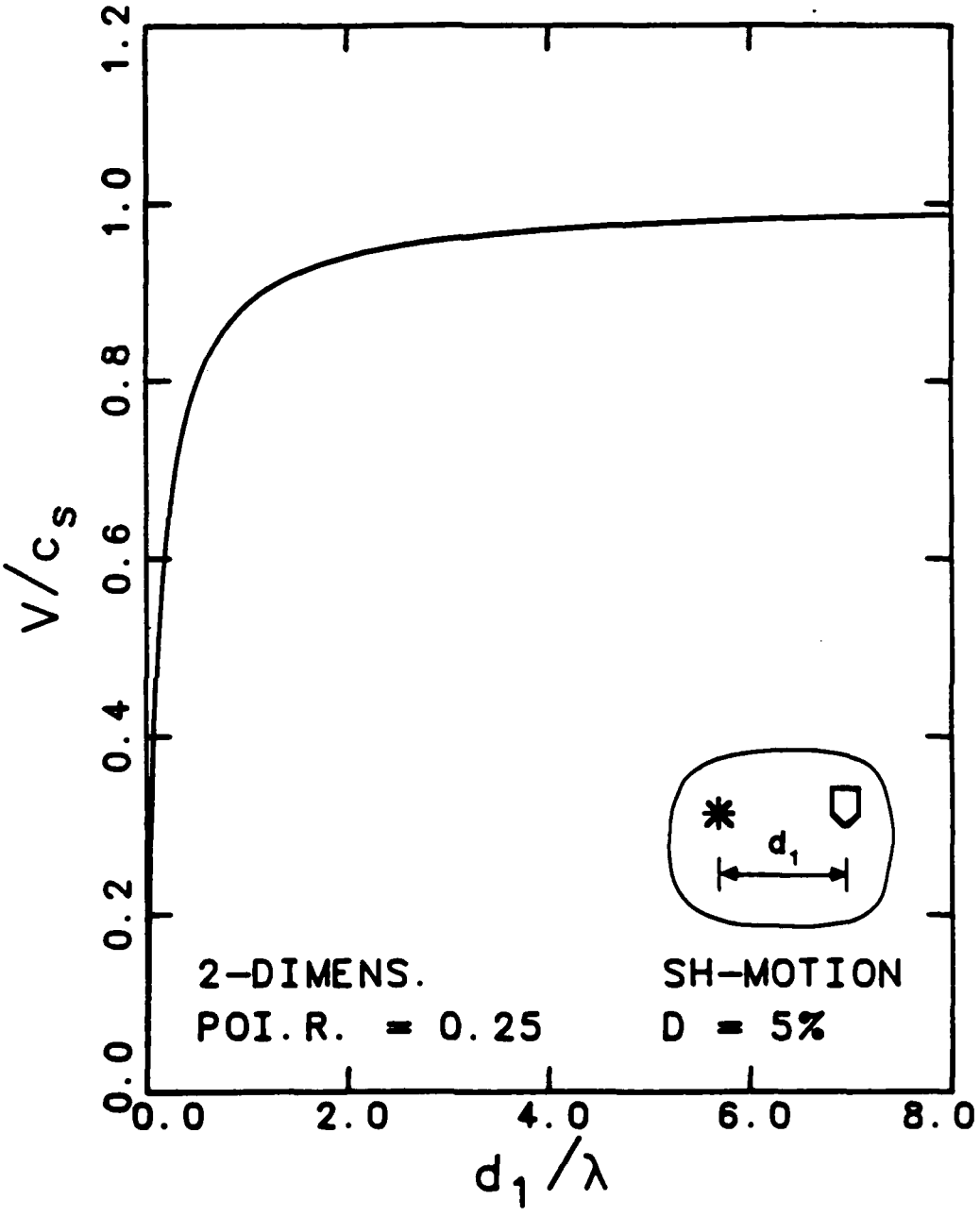

Fig. D.23 - Dispersion curves obtained from the phase of the transfer function for two-dimensional antiplane shear motion in a medium with five percent damping and Poisson's ratio = 0.25.

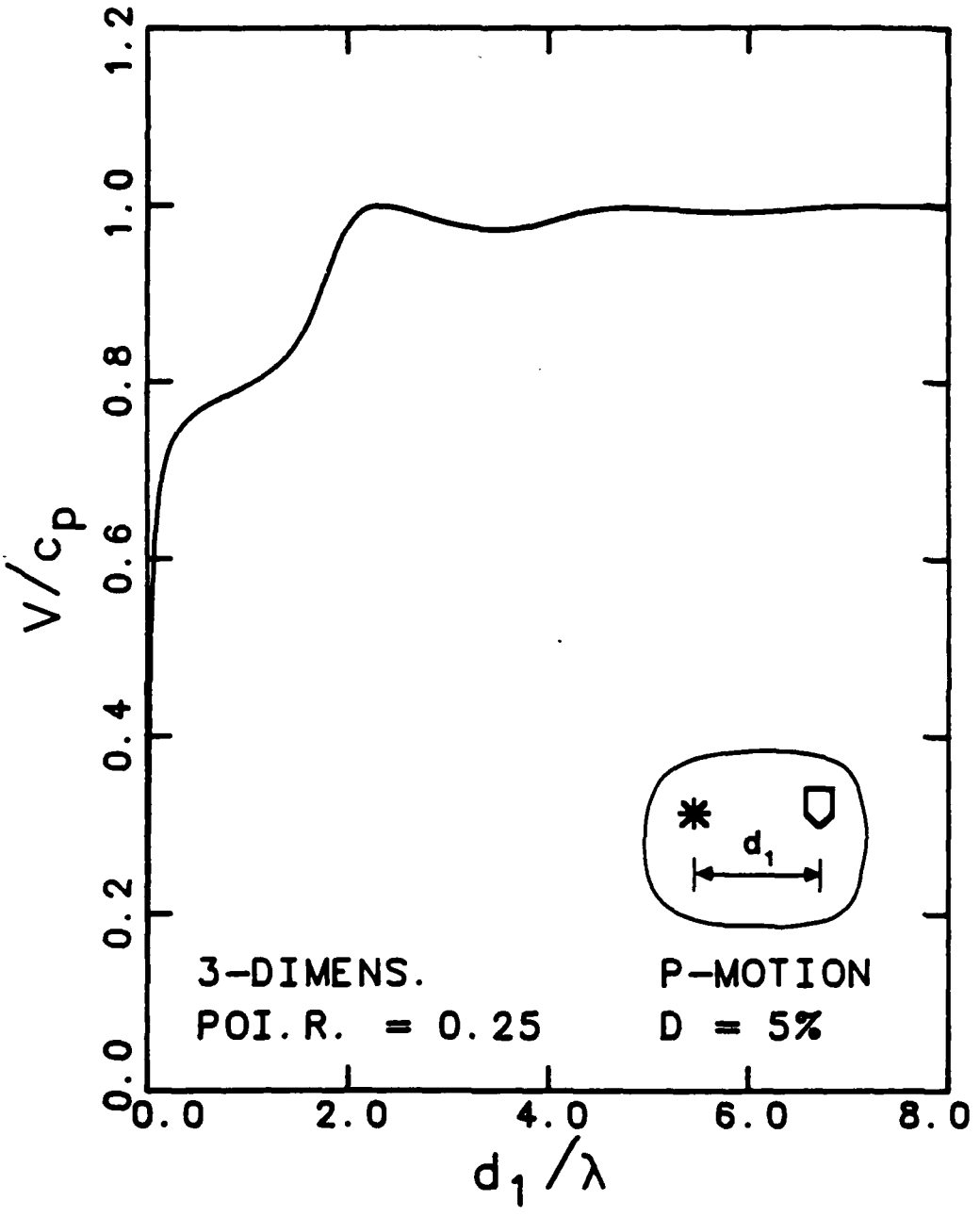

Fig. D.24 - Dispersion curves obtained from the phase of the transfer function for Three-dimensional longitudinal motion in a medium with five percent damping and Poisson's ratio = 0.25.

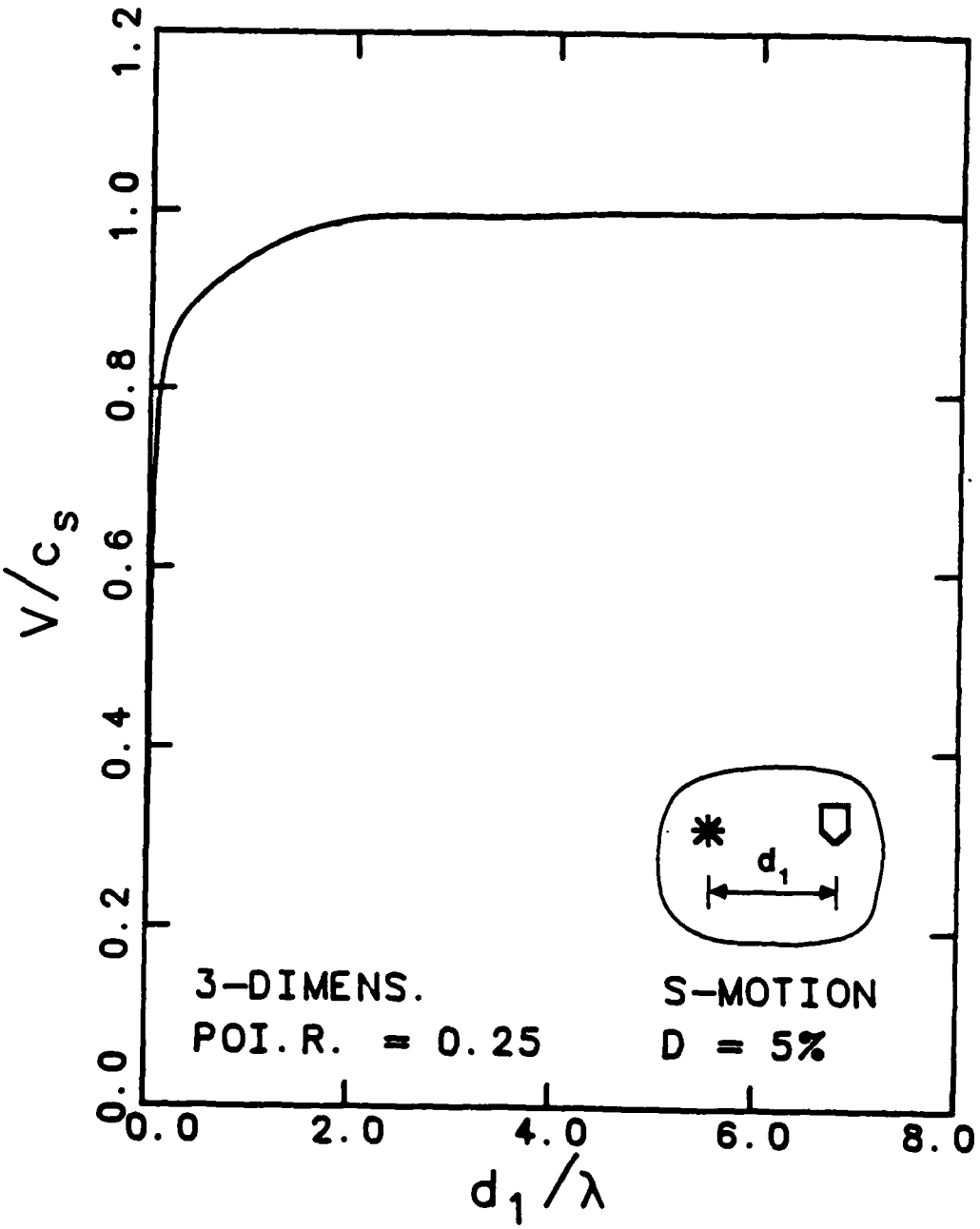

Fig. D.25 - Dispersion curves obtained from the phase of the transfer function for three-dimensional shear motion in a medium with five percent damping and Poisson's ratio = 0.25.

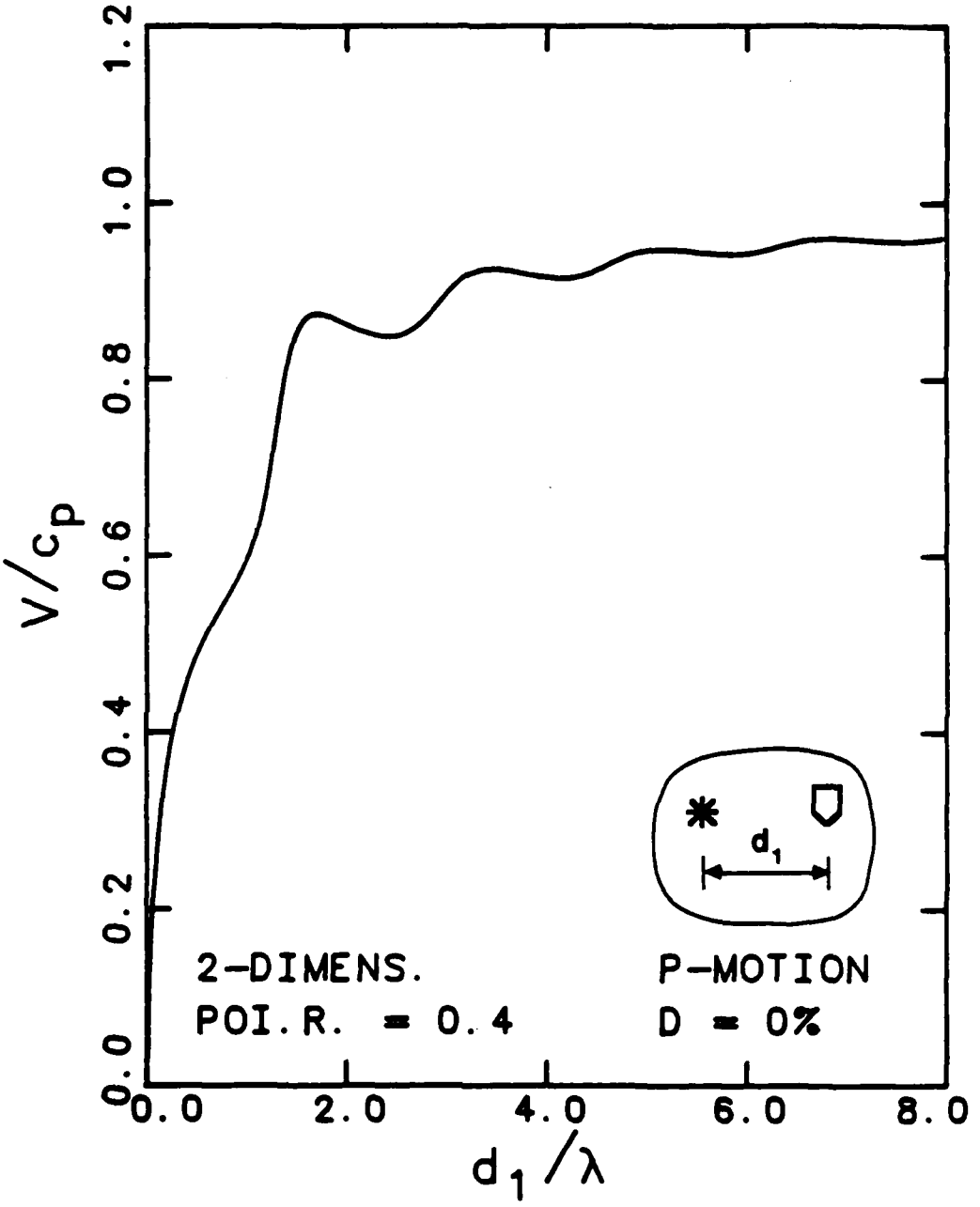

Fig. D.26 - Dispersion curves obtained from the phase of the transfer function for two-dimensional longitudinal motion in a medium with no damping and Poisson's ratio = 0.4.

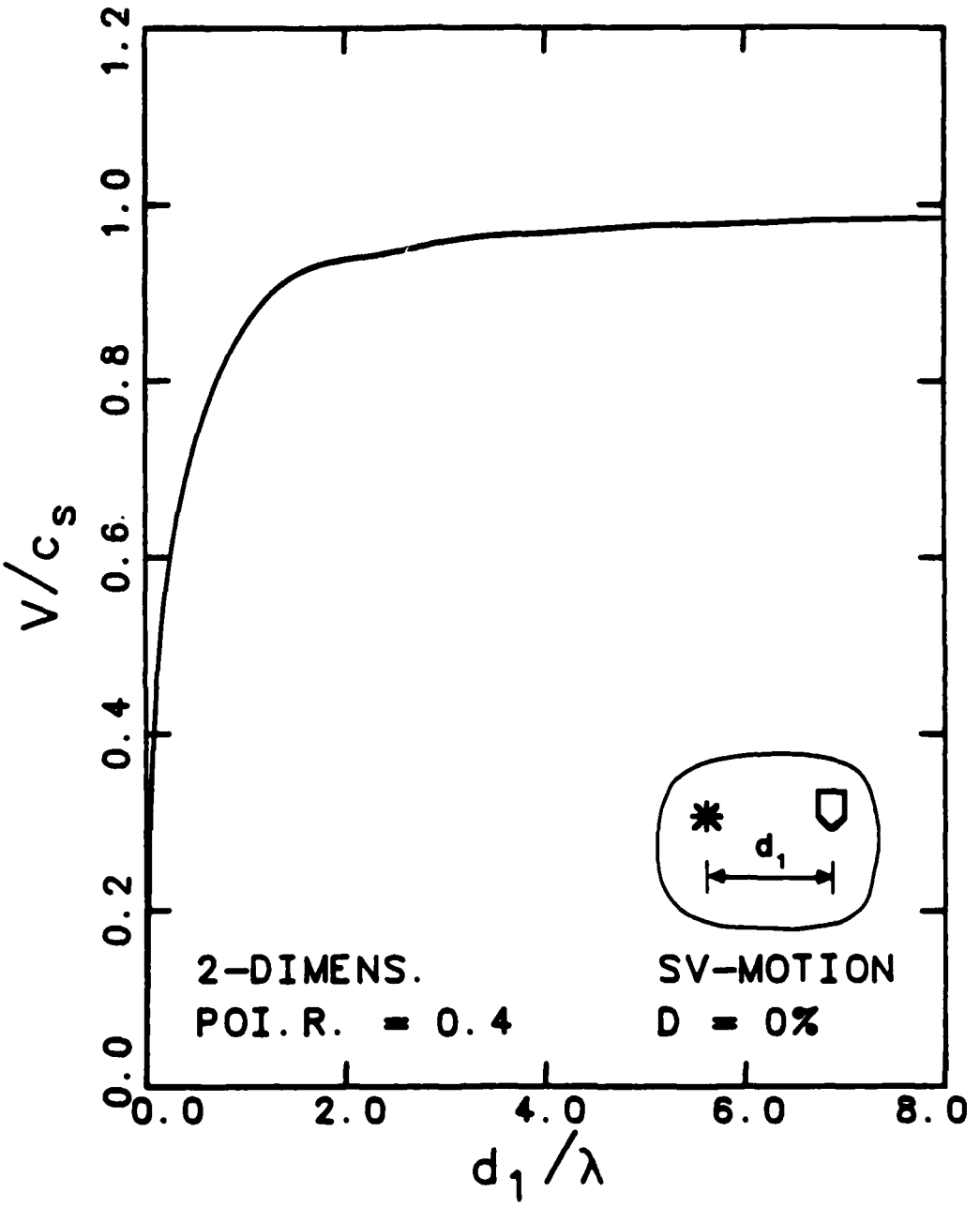

Fig. D.27 - Dispersion curves obtained from the phase of the transfer function for two-dimensional in-plane shear motion in a medium with no damping and Poisson's ratio = 0.4.

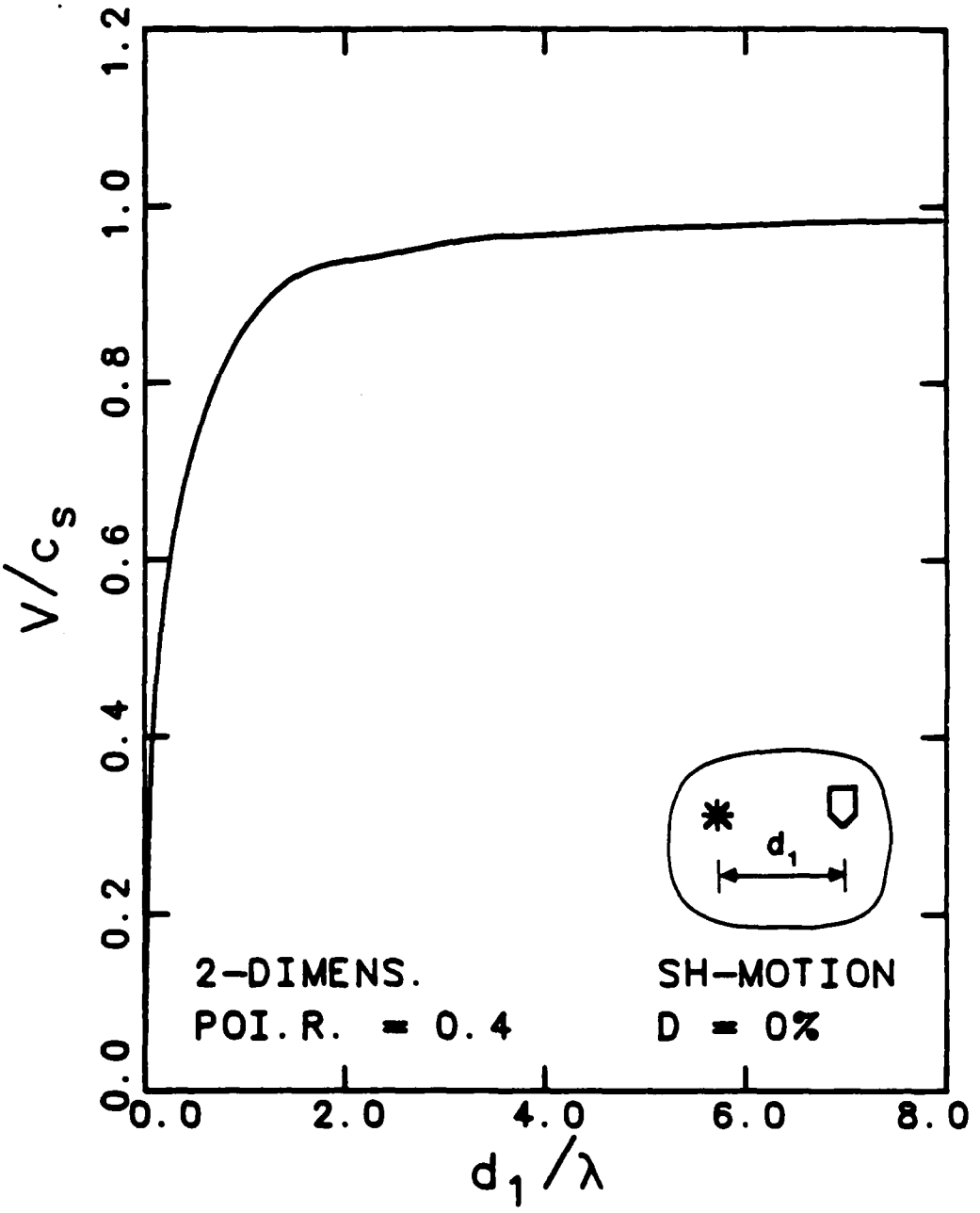

Fig. D.28 - Dispersion curves obtained from the phase of the transfer function for two-dimensional antiplane shear motion in a medium with no damping and Poisson's ratio = 0.4.

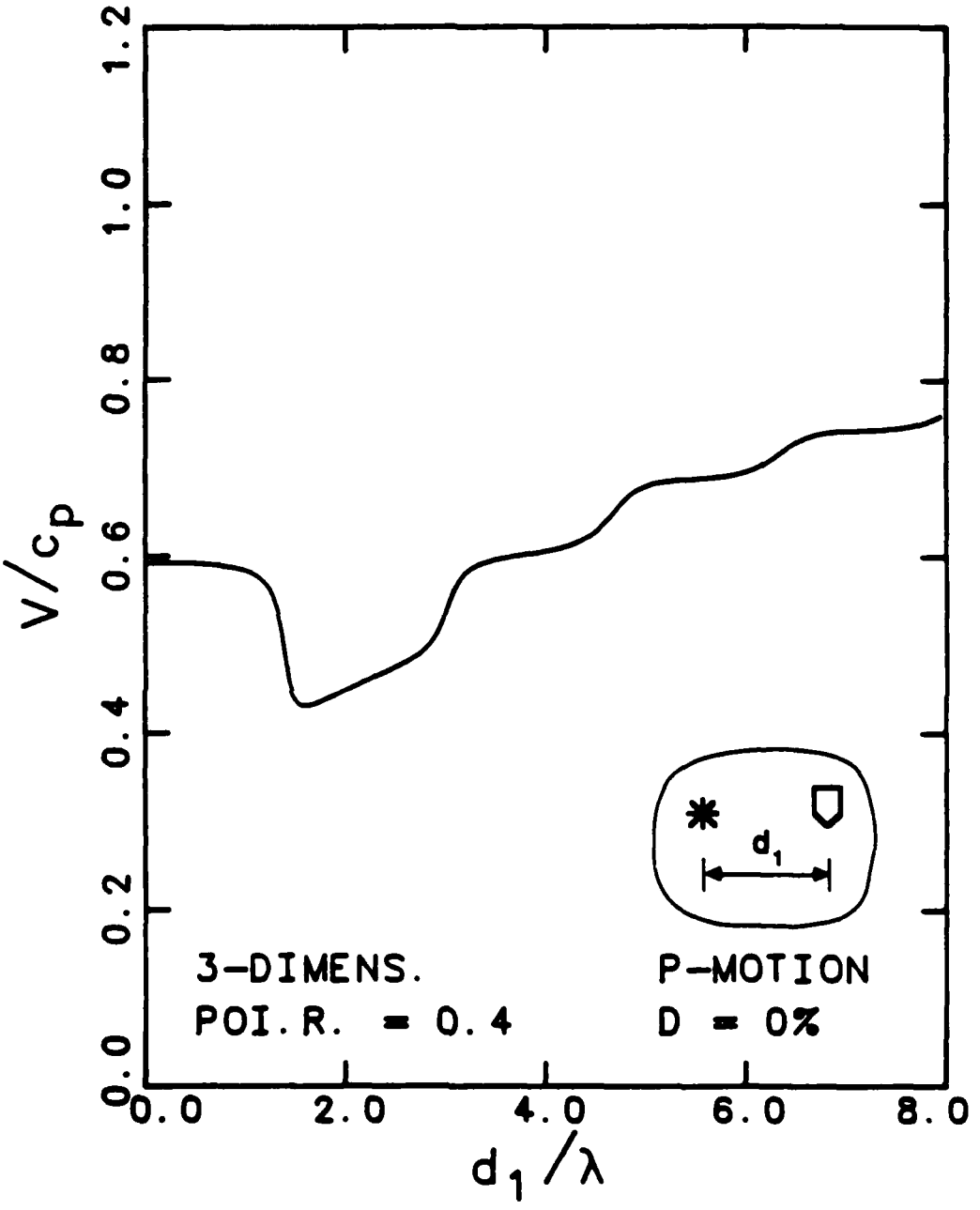

Fig. D.29 - Dispersion curves obtained from the phase of the transfer function for Three-dimensional longitudinal motion in a medium with no damping and Poisson's ratio = 0.4.

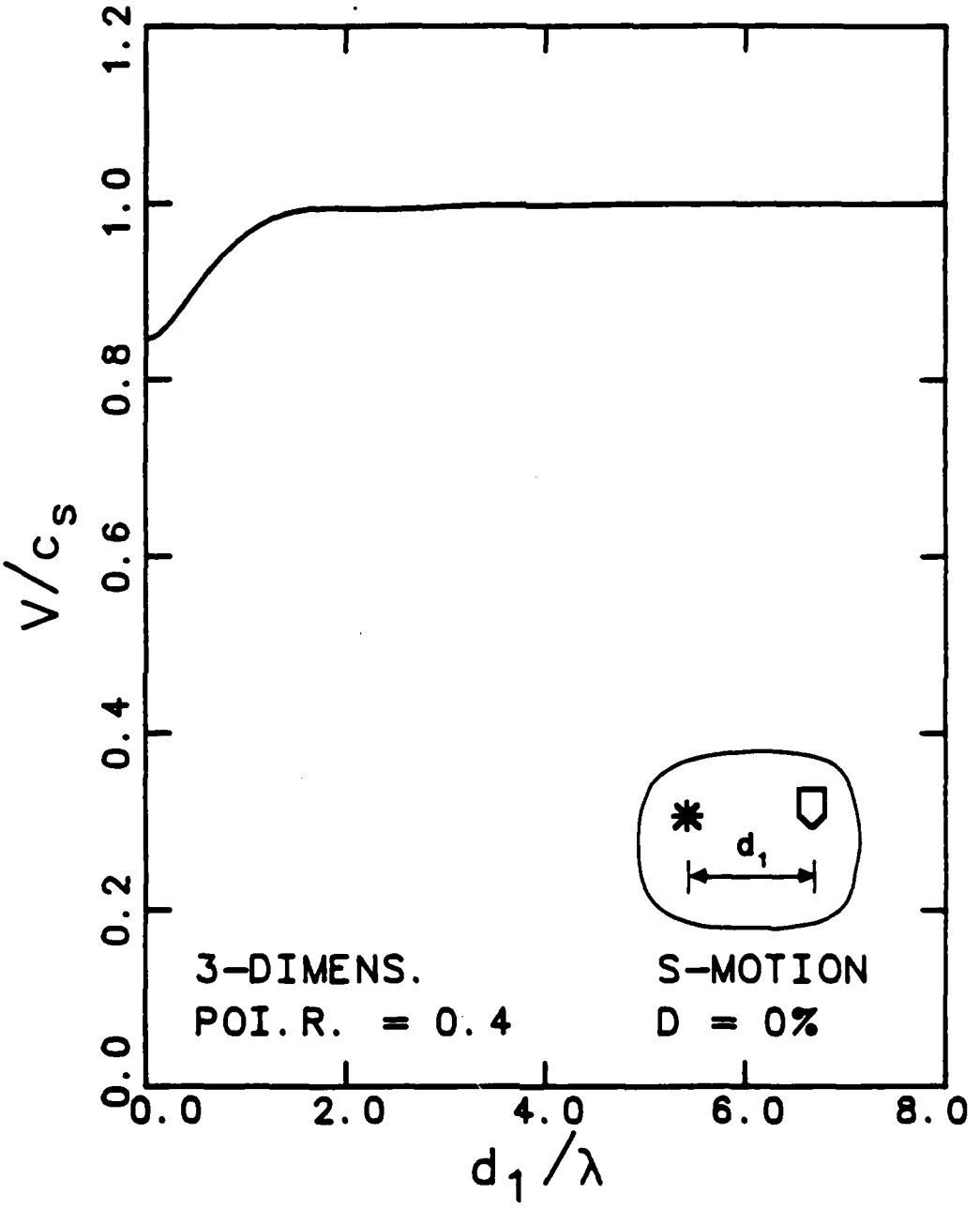

Fig. D.30 - Dispersion curves obtained from the phase of the transfer function for three-dimensional shear motion in a medium with no damping and Poisson's ratio = 0.4.

BIBLIOGRAPHY

1. Achenbach, J. D. (1973); Wave Propagation in Elastic Solids, North-Holland.

2. Aki, K. and Richards, P. G. (1980); Quantitative Seismology, Theory and Methods, Freeman and Company, San Francisco.

3. American Society of Testing Materials (1985); "Crosshole Seismic Testing", Standard Test Method D 4428/D 4428 M-84, 1985 Annual Book of ASTM Standards, Vol. 04.08, Soil and Rock; Building Stones, ASTM, Philadelphia, Pennsylvania.

4. Bracewell, R. N. (1965); The Fourier Transform and its Applications, McGraw-Hill Book Company.

5. Brigham, E. O. (1974); The Fast Fourier Transform, Prentice-Hall Inc., New Jersey.

6. Cruse, T. A. and Rizzo, F. J. (1968); "A Direct Formulation and Numerical Solution of the General Transient Elastodynamic Problem. I", Journal of Mathematical Analysis and Applications, Vol. 22, pp. 244-259.

7. Engineer Manual 1110-1-1802 (1979); Geophysical Exploration, Department of the Army, Corps of Engineers, U.S.A.

8. Gordon, R. B. and Davis, L. A. (1968); "Velocity and Attenuation of Seismic Waves in Imperfectly Elastic Rock", Journal of Geophysical Research, Vol. 73, pp. 3917-3935.

9. Hoar, R. (1982); "Field Measurement of Seismic Wave Velocity and Attenuation", Ph.D. Thesis, The University of Texas at Austin, Austin, Texas.

10. Hoar, R. J. and Stokoe, K. H., II (1978); "Generation and Measurements of Shear Waves in Situ", Dynamic Geotechnical Testing, ASTM STP 654, American Society for Testing and Materials, pp. 3-29.

11. Johnston, D. H., Toksöz, M. N. and Timur, A. (1979); "Attenuation of Seismic Waves in Dry and Saturated Rocks: II. Mechanisms", Geophysics, Vol. 44, pp. 691-711.

12. Lee, S. H. and Stokoe, K. H., II (1986); "Investigation of Low-Amplitude Shear Wave Velocity in Anisotropic Material", Geotechnical Engineering Report, GR86-6, Civil Engineering Department, University of Texas at Austin, August.

13. Newland, D. E. (1975); An Introduction to Random Vibrations and Spectral Analysis, Longman.

14. Patel, N. S. (1981); "Generation and Attenuation of Seismic Waves in Downhole Testing", Master's Thesis, The University of Texas at Austin, Austin, Texas.

15. Redpath, B. B., Edwards, R. B., Hale, R. J., and Kintzer, F. Z. (1982), "Development of Field Techniques to

Measure Damping Values for Near-Surface Rocks and Soils", URS/John A. Blume and Associates Report, San Francisco, California.

16. Richart, F. E., Jr., Hall J. R., Jr. and Woods, R. D. (1970); Vibrations of Soils and Foundations, Prentice-Hall, Inc., New Jersey.

17. Ricker, N. (1953); "The forms and Laws of Propagation of Seismic Wavelets", Geophysics, Vol.18, No.1., pp. 10-40.

18. Stokoe, K. H.,II and Hoar, R. J. (1978); "Variables Affecting In Situ Seismic Measurements", Proceedings of the Conference on Earthquake Engineering and Soil Dynamics, ASCE Geotechnical Engineering Division, Pasadena, California, Vol. II, pp. 919-939

19. Stokoe, K. H., II, Sanchez-Salinero, I. and Mok, Y. J. (1985); "Evaluation of Shear Wave Velocity Profiles at O'Neill Forebay, San Luis and Contra Loma Dams, California", Geotechnical Engineering Report, GR85-2, The University of Texas at Austin, Austin, Texas.

20. Stokoe, K. H., II and Woods, R. D. (1972); "In Situ Shear Wave Velocity by Cross-Hole Method", Journal of the Soil Mechanics and Foundations Division, ASCE, Vol. 98, No SM5, pp. 443-460.

21. Toksöz, M. N. and Johnston, D. H. (1981): Editors, Seismic Wave Attenuation, Society of Exploration Geophysicists Geophysics Reprint Series No. 2, Tulsa, Oklahoma

22. Toksöz, M. N., Johnston, D. H. and Timur, A. (1979); "Attenuation of Seismic Waves in Dry and Saturated Rocks: I. Laboratory Measurements", Geophysics, Vol. 44, pp. 681-690.

23. White, J. E. (1983); Underground Sound, Application of Seismic Waves, Elsevier.

24. Woods, R. D. (1968); "Screening of Surface Waves in Soils", Journal of Soil Mechanics and Foundation Division, ASCE, Vol. 94, No. SM 4, July, pp. 951-979.

25. Woods, R. D. (1978); "Measurement of Dynamic Soil Properties", Proceedings of the Conference on Earthquake Engineering and Soil Dynamics, ASCE Geotechnical Engineering Division, Vol. I, Pasadena, California, pp. 91-178.

END

5-87

DTIC